Drivers of Landscape-scale Nutrient Export Detected from Satellite Remote Sensing and Imaging Spectroscopy

By

Aditya Singh

A dissertation submitted in partial fulfillment of

the requirements for the degree of

Doctor of Philosophy

(Forestry)

at the

UNIVERSITY OF WISCONSIN-MADISON

2014

Date of final oral examination: 08/15/2013

The dissertation is approved by the following members of the Final Oral Committee:

Eric Kruger, Professor, Forest and Wildlife Ecology

Steven P. Loheide-II, Associate Professor, Civil and Environmental Engineering

Mutlu Ozdogan, Assistant Professor, Forest Ecology and Environmental Studies

Emily Stanley, Professor, Department of Zoology and Center for Limnology

Philip A. Townsend, Professor, Forest and Wildlife Ecology

For Dad

The most amazing father that ever walked the Earth

Acknowledgements

First and foremost, I'd like to express deepest appreciation to my advisor, Phil Townsend, for his guidance, help and advice throughout my graduate program. I thank him for cultivating a very diverse and fun lab, and exposing me to subjects more diverse than what would have been possible in a typical program. Thanks Phil, for showing me that there is always one more way to look at a problem, and to never miss the forest/trees for the satellite imagery. I have never met another person who can lay out big science in as simple words as him. Thanks also Phil, for helping me with my extremely convoluted English.

I would like to thank the members of my graduate committee, Eric Kruger, Steven Loheide, Mutlu Ozdogan, and Emily Stanley for all the help and patience with the numerous issues that came up during the course of this research. Thanks Eric, for being the inexhaustible source of knowledge for everything in tree physiology and forest ecology. Thanks Steve, for your expertise and inputs on everything hydrology and biogeochemistry. Thanks Mutlu, for your experience in remote sensing and for identifying blind spots in my reasoning. Thanks Emily, for your deep knowledge and experience of the hydrology of the region, and especially for your help with the chemistry. Thank you all, for being patient with me when I slipped dates or was generally sloppy. I deeply appreciate your time, expertise and advice throughout the course of this research, and look forward to great collaborations in the future.

I am indebted to the FERST lab for reasons too many to be listed. Shawn, for his help with concepts, some of which are still rocket surgery to me; Bernie, for showing me the ropes with species identification, often chewing through leaves and twigs in the process; Clayton; with managing seemingly intractable issues with consummate ease, and for being an all-round awesome human being in general; John for his amazing clear-headedness and uncanny ability to translate incomprehensible jargon into standard English; Huan for her indomitable spirit; Pete for his comprehensive knowledge of the region; lab mates Alex, Ryan, Ryan, Robi, and

numerous field techs and interns who valiantly march with us into the field and return with sore shoulders and bug bites, always resourceful and fun to be around.

Dad gifted me a yellow-orange paperback when I was nine. I remember reading and re-reading that little book until it frayed at the corners and eventually fell apart at the seams. The full import of the book dawned on me as I stood in a Russell lab conference room one fine day, staring at a picture of the department's first director. I hereby hold my dad responsible for consigning me to the life of an ecologist. Thanks Dad, Mom, Sis, for believing in me, for the encouragement, and for never insisting I do an MBA in financial management or software engineering instead of running around trees. Finally, my sincere apologies to my wife Preety. For making her suffer through my various degrees (I promise this is the last.) For making her move houses every three to five years and for never settling into a 'real' job. Thanks Preety, for being the most awesome cook ever. My sincere apologies to my kids, Akshara and Arihaan, for all the birthdays, school performances, PTO meetings and family outings missed or forgone. I promise I will make it up to you. I love you people and wouldn't be able to do this without your help, support and companionship.

I am indebted to my elementary school teachers, Ms. Sadanandan and Ms. Prabhakaran for inculcating a lifelong appreciation of the sciences in a six-year-old prodigious troublemaker. I realize how difficult that job is now that I am a parent myself. For never being annoyed with the messy "leaf collections". For taking in and assiduously caring for any injured or abandoned bird, cat, squirrel or dog that I would bring to their doorsteps. I sincerely apologize for the snake though. Thanks to Anish, Anuroop, and Manveer, lifelong friends and bushwhacking comrades-in-arms.

Last but not the least, thanks to the Administrative staff at Russell labs, and the UW International Student Services office. You guys are the best in the world.

Table of contents

General introduction

High nitrogen (N) and phosphorus (P) concentrations in streams can contribute to eutrophication and acidification of receiving waters, the loss of biological diversity and estuarine productivity, and present a public health concern (Vitousek et al. 1997). Stream water quality in mixed-use watersheds is a function of contributions from agricultural runoff as well as the interacting biotic and abiotic factors that control ecosystem-level nutrient cycling (Griffith et al. 2002, Meador and Goldstein 2003, Buck et al. 2004, Srivastava et al. 2007). Although nutrient concentrations in predominantly forested watersheds are generally small in comparison to agricultural or human land use dominated watersheds (Johnson et al. 1997, Lowrance et al. 1997), nitrate concentrations from forested watersheds can increase significantly in response to disturbance (Eshleman 2000, Eshleman et al. 2009). For effective management of receiving waters, accurate, repeatable and spatially explicit estimates of nutrient loading are required. Satellite and airborne remote sensing techniques allow synoptic long-term coverage of large regions, and in combination with climate data, can be leveraged to better predict the effects of land cover composition and disturbance events on nutrient export from watersheds.

Models based on land-use/land-cover (LULC) classifications derived from medium-to-coarse spatial scale multispectral (MX) satellite imagery have often been employed to predict variations in water quality across large regions. These models rely on LULC classifications, and, combined with other environmental data, have been shown to be effective in predicting water quality at varying spatial and temporal scales (Osborne and Wiley 1988, Allan et al. 1997, Krysanova et al. 1998, Basnyat et al. 2000, Meador and

Goldstein 2003, Maillard and Pinheiro Santos 2008). However, LULC maps are static generalizations of the land surface and do not capture the full spatial and temporal heterogeneity of land surface dynamics. Continuous measurements of land surface dynamics are needed to better characterize nutrient dynamics across large scales.

The drawbacks of limited spectral resolution of MX sensors can be overcome with imaging spectroscopy (or hyperspectral (HX) remote sensing). Recent research has shown that spectroscopic methods can be used to characterize key plant functional traits such as foliar nitrogen content (Townsend et al. 2003, Majeke et al. 2008, Martin et al. 2008), specific leaf area (SLA), foliar lignin and cellulose (Majeke et al. 2008, Kokaly et al. 2009) and δN^{15} concentrations (Kleinebecker et al. 2009, Elmore and Craine 2011). Recently, it has been shown that foliar nitrogen and lignin/cellulose concentrations characterize leaf lifespan (Wright et al. 2005, Shipley et al. 2006, Santiago 2007), influence soil C:N ratios (Ollinger et al. 2002) and in combination with disturbance events (Eshleman 2000, McNeil et al. 2007), may be strong controllers of nutrient cycling in forested landscapes (Aber et al. 1991, Fortunel et al. 2009, de Bello et al. 2010).

However, both multi-spectral and hyperspectral remote sensing techniques fail to accurately track ecosystem processes at a time scale fine enough to characterize the temporal dynamics of the land surface and related changes in nutrient cycling rates. Data on changes in the land surface spaced close enough in time can be leveraged to track changes in land surface characteristics on a continuous basis. This can be achieved from hypertemporal (TX) satellite imagery that provides near-daily coverage of the earth

surface, but at the loss of high spectral and spatial resolution of MX and HX sensors respectively.

Research overview

The principal aim of my dissertation is to characterize factors influencing nutrient export from forested landscapes using a combination of satellite remotes sensing and imaging spectroscopy. Specifically, the objective of **Chapter 1** (Singh et al. 2013) is to develop ecologically meaningful, landscape-scale indicators of water quality using remote sensing data and regional water quality data (sourced from Robertson et al. 2006, Stanley and Maxted 2008 for this study) for the state of Wisconsin. The approach is intended to generate an algorithm for inputting MODIS-derived products to predict water quality across years, with the ability to predict future (or past) years when data become available. The models formulated in this chapter intend to produce generalizable techniques to facilitate prediction of stream water nutrient concentrations based on MODIS data from a previous year. In other words, this raises the possibility for predicting summer baseflow nutrient concentrations approximately 8 months in advance.

Whereas the objective of Chapter 1 is to utilize the synoptic coverage of MODIS data for predicting summer baseflow water quality approximately one year in advance, in **Chapter 2**, I leverage the high temporal resolution of MODIS data to develop algorithms for predicting water quality measures on a near continuous time basis. Data for this part of the research are sourced from the Chesapeake Bay Watershed. The Chesapeake Bay has been the subject of intensive research on the effects of human land use on eutrophication, resulting in extensive efforts to reduce nutrient inputs (e.g. Fisher et al. 1992, Boynton et al. 1995, Paerl et al. 1998, Boesch et al. 2001, Anderson et al. 2002, Kemp et al. 2005, Phillips 2007, USEPA 2008). A central component to the suite of solutions proposed to

address water quality in the Bay includes establishment and apportioning total maximum daily loads (TMDLs) per land use among states. Although forested regions represent a significant portion of the Chesapeake Bay watershed (~54%), the Chesapeake Bay Phase 5.3 Community Watershed Model (USEPA 2010) prescribes a constant forest total nitrogen load that increases linearly with increases in atmospheric nitrogen deposition. It may therefore be that spatially *and* temporally continuous characterization of nutrient export from forested areas could result in more effective targeting of management actions such as setting of TMDLs by season and location. To this end, I develop predictive models using functional linear concurrent models to relate time series of nutrient loads in stream water with time series of satellite-derived (MODIS) measures of ecosystem variability and disturbance in conjunction with climate data. Functional models developed for this research allow integration of temporal variation in environmental factors such as climate and disturbance and biological factors such as vegetation phenology and provide insights into both the timing and magnitude of potential drivers of changes in water quality for forested areas in the Chesapeake Bay watershed.

Hypertemporal satellite imagery such as MODIS enables tracking land surface dynamics in near real time. In contrast, imaging spectroscopy has great potential for mapping vegetation traits that cannot be retrieved from broadband data such as MODIS. In **Chapter 3**, my goal is the development and application of generalizable algorithms to repeatedly and accurately map ecosystem properties such as foliar traits across space and time using spectroscopic imagery obtained from the AVIRIS sensor (NASA's Airborne Visible/Infrared Imaging Spectrometer; Vane et al. 1993, Green et al. 1998). In this study,

I develop spectroscopic calibrations for the determination of leaf chemical composition (nitrogen, carbon, and fiber constituents) and morphology (leaf mass per area, LMA) of temperate and boreal tree species using imaging spectroscopy. I also demonstrate techniques to explicitly propagate uncertainties from the leaf to the plot to the image scale. These data can be used to relate foliar traits with ecosystem processes such as biochemical effects of invasive species on forest canopies (Glenn et al. 2005, Asner et al. 2008, He et al. 2011), characterizing photosynthetic down-regulation (Gamon et al. 1990, Gamon et al. 1992, Gamon et al. 1997), measurement of the inductance of plant defense to perturbations (Couture et al. 2013) and assessment of landscape-scale streamwater nutrient export.

Using spatial predictions of foliar biochemistry obtained from Chapter 3, **Chapter 4** utilizes a structural equation modeling approach to assess the relative influences of foliar biochemistry, watershed physiography and human land use patterns on water quality in watersheds across the Upper Midwestern United States. Specifically, I explore the influence of four broad groups of variables on streamwater quality. These are: 1) nutrient retention due to foliar biochemistry, 2) nutrient retention due to watershed physiography, 3) an index of human activity (landscape composition dominated with urban and agricultural land use), and 4) indicators of watershed-scale nutrient 'leakiness'. I hypothesize that: A) higher foliar recalcitrance will have a direct positive effect on nutrient retention in watersheds and indirectly with overall water quality (i.e. lesser nutrient export), and will be negatively correlated with indicators of watershed leakiness and indicators of human activity; B) indicators of watershed leakiness and high human activity will have negative direct influences on water quality (i.e. high nutrient export), as

moderated indirectly by retention in watersheds and foliar recalcitrance. The overarching objective of this research is the identification of ecological associations in addition to landscape-scale physiographic and climatologic variables needed to characterize the range of drivers of water quality. Such an approach may help focus development and restoration policies towards building more resilient landscapes. This study also demonstrates that recent advances in satellite and airborne imaging technologies may enhance our ability to understand landscape-level processes associated with water quality, and through the use of remote sensing we can develop more standardized and accessible data sets for use by a broader audience of managers and stakeholders.

Literature cited

Aber, J. D., J. M. Melillo, K. J. Nadelhoffer, J. Pastor, and R. D. Boone. 1991. Factors Controlling Nitrogen Cycling and Nitrogen Saturation in Northern Temperate Forest Ecosystems. Ecological Applications **1**:303-315.

Allan, J. D., D. L. Erickson, and J. Fay. 1997. The influence of catchment land use on stream integrity across multiple spatial scales. Freshwater Biology **37**:149-161.

Anderson, D. M., P. M. Glibert, and J. M. Burkholder. 2002. Harmful algal blooms and eutrophication: Nutrient sources, composition, and consequences. Estuaries **25**:704-726.

Asner, G. P., M. O. Jones, R. E. Martin, D. E. Knapp, and R. F. Hughes. 2008. Remote sensing of native and invasive species in Hawaiian forests. Remote Sensing of Environment **112**:1912-1926.

Basnyat, P., L. D. Teeter, B. G. Lockaby, and K. M. Flynn. 2000. The use of remote sensing and GIS in watershed level analyses of non-point source pollution problems. Forest Ecology and Management **128**:65-73.

Boesch, D. F., R. B. Brinsfield, and R. E. Magnien. 2001. Chesapeake Bay eutrophication: Scientific understanding, ecosystem restoration, and challenges for agriculture. Journal of Environmental Quality **30**:303-320.

Boynton, W. R., J. H. Garber, R. Summers, and W. M. Kemp. 1995. Inputs, transformations, and transport of nitrogen and phosphorus in Chesapeake Bay and selected tributaries. Estuaries **18**:285-314.

Buck, O., D. K. Niyogi, and C. R. Townsend. 2004. Scale-dependence of land use effects on water quality of streams in agricultural catchments. Environmental Pollution **130**:287-299.

Couture, J. J., S. P. Serbin, and P. A. Townsend. 2013. Spectroscopic sensitivity of real-time, rapidly induced phytochemical change in response to damage. New Phytologist **198**:311-319.

de Bello, F., S. Lavorel, S. Diaz, R. Harrington, J. H. C. Cornelissen, R. D. Bardgett, M. P. Berg, P. Cipriotti, C. K. Feld, D. Hering, P. M. da Silva, S. G. Potts, L. Sandin, J. P. Sousa, J. Storkey, D. A. Wardle, and P. A. Harrison. 2010. Towards an assessment of multiple ecosystem processes and services via functional traits. Biodiversity and Conservation **19**:2873-2893.

Elmore, A. J., and J. M. Craine. 2011. Spectroscopic Analysis of Canopy Nitrogen and Nitrogen Isotopes in Managed Pastures and Hay Land. Ieee Transactions on Geoscience and Remote Sensing **49**:2491-2498.

Eshleman, K. N. 2000. A linear model of the effects of disturbance on dissolved nitrogen leakage from forested watersheds. Water Resources Research **36**:3325-3335.

Eshleman, K. N., B. E. McNeil, and P. A. Townsend. 2009. Validation of a remote sensing based index of forest disturbance using streamwater nitrogen data. Ecological Indicators **9**:476-484.

Fisher, T. R., E. R. Peele, J. W. Ammerman, and L. W. Harding. 1992. Nutrient limitation of phytoplankton in Chesapeake Bay. Marine Ecology Progress Series **82**:51-63.

Fortunel, C., E. Garnier, R. Joffre, E. Kazakou, H. Quested, K. Grigulis, S. Lavorel, P. Ansquer, H. Castro, P. Cruz, J. Dolezal, O. Eriksson, H. Freitas, C. Golodets, C. Jouany, J. Kigel, M. Kleyer, V. Lehsten, J. Leps, T. Meier, R. Pakeman, M. Papadimitriou, V. P. Papanastasis, F. Quetier, M. Robson, M. Sternberg, J. P. Theau, A. Thebault, and M. Zarovali. 2009. Leaf traits capture the effects of land use changes and climate on litter decomposability of grasslands across Europe. Ecology **90**:598-611.

Gamon, J. A., C. B. Field, W. Bilger, O. Bjorkman, A. L. Fredeen, and J. Penuelas. 1990. Remote-sensing of the xanthophyll cycle and chlorophyll fluorescence in sunflower leaves and canopies. Oecologia **85**:1-7.

Gamon, J. A., J. Penuelas, and C. B. Field. 1992. A narrow-waveband spectral index that tracks diurnal changes in photosynthetic efficiency. Remote Sensing of Environment **41**:35-44.

Gamon, J. A., L. Serrano, and J. S. Surfus. 1997. The photochemical reflectance index: an optical indicator of photosynthetic radiation use efficiency across species, functional types, and nutrient levels. Oecologia **112**:492-501.

Glenn, N. F., J. T. Mundt, K. T. Weber, T. S. Prather, L. W. Lass, and J. Pettingill. 2005. Hyperspectral data processing for repeat detection of small infestations of leafy spurge. Remote Sensing of Environment **95**:399-412.

Green, R. O., M. L. Eastwood, C. M. Sarture, T. G. Chrien, M. Aronsson, B. J. Chippendale, J. A. Faust, B. E. Pavri, C. J. Chovit, M. S. Solis, M. R. Olah, and O.

Williams. 1998. Imaging spectroscopy and the Airborne Visible Infrared Imaging Spectrometer (AVIRIS). Remote Sensing of Environment **65**:227-248.

Griffith, J. A., E. A. Martinko, J. L. Whistler, and K. P. Price. 2002. Interrelationships among landscapes, NDVI, and stream water quality in the US central plains. Ecological Applications **12**:1702-1718.

He, K. S., D. Rocchini, M. Neteler, and H. Nagendra. 2011. Benefits of hyperspectral remote sensing for tracking plant invasions. Diversity and Distributions **17**:381-392.

Johnson, L. B., C. Richards, G. E. Host, and J. W. Arthur. 1997. Landscape influences on water chemistry in Midwestern stream ecosystems. Freshwater Biology **37**:193-+.

Kemp, W. M., W. R. Boynton, J. E. Adolf, D. F. Boesch, W. C. Boicourt, G. Brush, J. C. Cornwell, T. R. Fisher, P. M. Glibert, J. D. Hagy, L. W. Harding, E. D. Houde, D. G. Kimmel, W. D. Miller, R. I. E. Newell, M. R. Roman, E. M. Smith, and J. C. Stevenson. 2005. Eutrophication of Chesapeake Bay: historical trends and ecological interactions. Marine Ecology Progress Series **303**:1-29.

Kleinebecker, T., S. R. Schmidt, C. Fritz, A. J. P. Smolders, and N. Holzel. 2009. Prediction of delta 13C and delta 15N in plant tissues with near-infrared reflectance spectroscopy. New Phytologist **184**:732-739.

Kokaly, R. F., G. P. Asner, S. V. Ollinger, M. E. Martin, and C. A. Wessman. 2009. Characterizing canopy biochemistry from imaging spectroscopy and its application to ecosystem studies. Remote Sensing of Environment **113**:S78-S91.

Krysanova, V., D. I. Muller-Wohlfeil, and A. Becker. 1998. Development and test of a spatially distributed hydrological water quality model for mesoscale watersheds. Ecological Modelling **106**:261-289.

Lowrance, R., L. S. Altier, J. D. Newbold, R. R. Schnabel, P. M. Groffman, J. M. Denver, D. L. Correll, J. W. Gilliam, J. L. Robinson, R. B. Brinsfield, K. W. Staver, W. Lucas, and A. H. Todd. 1997. Water quality functions of Riparian forest buffers in Chesapeake Bay watersheds. Environmental Management **21**:687-712.

Maillard, P., and N. A. Pinheiro Santos. 2008. A spatial-statistical approach for modeling the effect of non-point source pollution on different water quality parameters in the Velhas river watershed Brazil. Journal of Environmental Management **86**:158-170.

Majeke, B., J. A. N. van Aardt, and M. A. Cho. 2008. Imaging spectroscopy of foliar biochemistry in forestry environments. Southern Forests **70**:275-285.

Martin, M. E., L. C. Plourde, S. V. Ollinger, M. L. Smith, and B. E. McNeil. 2008. A generalizable method for remote sensing of canopy nitrogen across a wide range of forest ecosystems. Remote Sensing of Environment **112**:3511-3519.

McNeil, B. E., K. M. de Beurs, K. N. Eshleman, J. R. Foster, and P. A. Townsend. 2007. Maintenance of ecosystem nitrogen limitation by ephemeral forest disturbance: An assessment using MODIS, Hyperion, and Landsat ETM. Geophysical Research Letters **34**:-.

Meador, M. R., and R. M. Goldstein. 2003. Assessing water quality at large geographic scales: Relations among land use, water physicochemistry, riparian condition, and fish community structure. Environmental Management **31**:504-517.

Ollinger, S. V., M. L. Smith, M. E. Martin, R. A. Hallett, C. L. Goodale, and J. D. Aber. 2002. Regional variation in foliar chemistry and N cycling among forests of diverse history and composition. Ecology **83**:339-355.

Osborne, L. L., and M. J. Wiley. 1988. Empirical Relationships between Land-Use Cover and Stream Water-Quality in an Agricultural Watershed. Journal of Environmental Management **26**:9-27.

Paerl, H. W., J. L. Pinckney, J. M. Fear, and B. L. Peierls. 1998. Ecosystem responses to internal and watershed organic matter loading: consequences for hypoxia in the eutrophying Neuse river estuary, North Carolina, USA. Marine Ecology Progress Series **166**:17-25.

Phillips, S. W., editor. 2007. Synthesis of U.S. Geological Survey science for the Chesapeake Bay ecosystem and implications for environmental management. U.S. Geological Survey.

Robertson, D. M., D. J. Graczyk, P. J. Garrison, L. Wang, G. Laliberte, and R. Bannerman. 2006. Nutrient concentrations and their relations to biotic integrity of wadeable streams in Wisconsin. Page 156 United Sates Geological Survey Professional Paper 1722. USGS Wisconsin Water Science Center, Middleton, WI.

Santiago, L. S. 2007. Extending the leaf economics spectrum to decomposition: Evidence from a tropical forest. Ecology **88**:1126-1131.

Shipley, B., M. J. Lechowicz, I. Wright, and P. B. Reich. 2006. Fundamental trade-offs generating the worldwide leaf economics spectrum. Ecology **87**:535-541.

Singh, A., A. R. Jakubowski, I. Chidister, and P. A. Townsend. 2013. A MODIS approach to predicting stream water quality in Wisconsin. Remote Sensing of Environment **128**:74-86.

Srivastava, P., K. W. Migliaccio, and J. Simunek. 2007. Landscape models for simulating water quality at point, field, and watershed scales. Transactions of the Asabe **50**:1683-1693.

Stanley, E. H., and J. T. Maxted. 2008. Changes in the dissolved nitrogen pool across land cover gradients in Wisconsin streams. Ecological Applications **18**:1579-1590.

Townsend, P. A., J. R. Foster, R. A. Chastain, and W. S. Currie. 2003. Application of imaging spectroscopy to mapping canopy nitrogen in the forests of the central Appalachian Mountains using Hyperion and AVIRIS. Ieee Transactions on Geoscience and Remote Sensing **41**:1347-1354.

USEPA. 2008. Chesapeake Bay health and restoration assessment—A report to the citizens of the Bay region. U.S. Environmental Protection Agency.

USEPA. 2010. Chesapeake Bay Phase 5.3 Community Watershed Model. U.S. Environmental Protection Agency, Chesapeake Bay Program Office, Annapolis MD.

Vane, G., R. O. Green, T. G. Chrien, H. T. Enmark, E. G. Hansen, and W. M. Porter. 1993. The Airborne Visible Infrared Imaging Spectrometer (AVIRIS). Remote Sensing of Environment **44**:127-143.

Vitousek, P. M., J. D. Aber, R. W. Howarth, G. E. Likens, P. A. Matson, D. W. Schindler, W. H. Schlesinger, and G. D. Tilman. 1997. Human alteration of the global nitrogen cycle: Sources and consequences. Ecological Applications **7**:737-750.

Wright, I. J., P. B. Reich, J. H. C. Cornelissen, D. S. Falster, E. Garnier, K. Hikosaka, B. B. Lamont, W. Lee, J. Oleksyn, N. Osada, H. Poorter, R. Villar, D. I. Warton, and M. Westoby. 2005. Assessing the generality of global leaf trait relationships. New Phytologist **166**:485-496.

Chapter 1: A MODIS approach to predicting stream water quality in Wisconsin[1]

Abstract

Efforts to predict water quality often rely heavily on static landuse/land-cover (LULC) classifications derived from remote sensing imagery. However, LULC classifications are infrequently updated, and the development of regular (annual) land cover maps that accurately capture intra- and inter-annual change may be expensive in terms of data and labor costs. In addition, existing land cover products may not include classes relevant to the assessment of water quality. Conversely, data from the Moderate Resolution Imaging Spectroradiometer (MODIS) instruments are freely available, preprocessed, frequently updated, and available in a range of useful data products. Our goal was to predict water quality for streams in Wisconsin, USA using a simple model constructed from MODIS products. We used streamwater nitrate and dissolved phosphorus data from 2001 to 2004 from two previous studies (Robertson et al. 2006, Stanley and Maxted 2008) to evaluate the potential for using MODIS directly in an empirical model to predict water quality, thereby circumventing the classification process or reliance on dated land cover maps. Using predictors derived exclusively from MODIS data products; we successfully predicted 80% of the variation in measured nitrate concentrations and 51% of the variation in dissolved phosphorus concentrations. Predictions of water quality were developed on both a per-pixel and a watershed basis.

---

[1] Reprinted from: Singh, A., Jakubowski, A. R. ; Chidister, I.; and P. A. Townsend (2013) A MODIS approach to predicting stream water quality in Wisconsin. *Remote Sensing of Environment* **128**:74-86

Introduction

High nitrogen (N) and phosphorus (P) concentrations in streams contribute to eutrophication and acidification of receiving waters, the loss of biological diversity, and present a public health concern (Vitousek et al. 1997). In temperate landscapes with mixed land cover, a particular concern is high N contributions in the form of nitrate (NO_3^-) derived from agricultural runoff and other sources. The ability to predict nitrate-N (NO_3-N) levels of streams easily and accurately is needed to understand the consequences of increased nitrogen loading and to improve management. Nitrate concentrations of rivers are correlated with human population densities in watersheds (Peierls et al. 1991), point sources due to human sewage and wastewater inputs (Cole et al. 1993), and nonpoint sources due to runoff from agricultural and urban lands (Carpenter et al. 1998). With increasing human disturbance, total N fluxes rise due to increases of nitrate loading (Aber et al. 1989, Howarth et al. 1996).

Agricultural fertilization is the primary nonpoint source of nitrate, but disturbance to forests can also increase NO_3-N export (Eshleman et al. 2009). The classic watershed-nutrient cycle studies at Hubbard Brook show that the complete removal of vegetation from a watershed leads to large increases in the stream concentrations of many ions, including nitrate, as well as increases in the amount of particulate matter leaving the streams of a watershed (Likens et al. 1970). More recent studies of water quality in Wisconsin found strong correlations between human land use and wetland cover in a watershed and nitrate concentrations (Robertson et al. 2006, Stanley and Maxted 2008). While NO_3-N concentrations in predominantly forested watersheds are generally small in

comparison to agricultural watersheds (Johnson et al. 1997, Lowrance et al. 1997), nitrate concentrations can increase significantly in response to disturbance (Eshleman 2000, Eshleman et al. 2009). Like nitrate, streamwater phosphorus originates from a variety of sources, but in general is derived from nonpoint sources associated with agricultural and urban land use, and point sources associated with urbanization. Phosphorus is best predicted by urban and industrial activity in most cases (Chang 2008, Coskun et al. 2008) and in some cases agriculture (Pieterse et al. 2003, Zampella et al. 2007).

Traditional indicators of the effects of water quality on ecosystems generally employ metrics of the physical, biological or chemical dimensions of aquatic communities including vegetation (Karr and Schlosser 1978, Dennison et al. 1993), fossil records of algae (Hall et al. 1999), fish communities (Karr 1981), or channel morphology (Schlosser and Karr 1981). More recently, land-use/land-cover (LULC) classifications have been correlated with previously used indicators and used to predict water quality on broader scales. These predictive models rely on LULC classifications derived from satellite imagery, combined with other environmental data to extend predictions over varying spatial and temporal scales (Osborne and Wiley 1988, Allan et al. 1997, Krysanova et al. 1998, Basnyat et al. 2000, Meador and Goldstein 2003, Maillard and Pinheiro Santos 2008).

Two approaches are most widely used to incorporate LULC data into predictive models of water quality: (1) land cover maps classified from remote sensing imagery from a single time-step to characterize non-point inputs from the land, and (2) change-detection metrics to identify land-cover changes that are thought to affect water quality. The

majority of research using single image LULC techniques indicated a positive relation between agriculture and urban land cover and NO_3-N concentrations in an area (Johnson et al. 1997, Jordan et al. 1997, Buck et al. 2004, Robertson et al. 2006, Stanley and Maxted 2008). In areas with high forest cover (and low agriculture and urban land cover), models using land-cover data to predict water quality are not very accurate (Herlihy et al. 1998), although studies have shown that accurate models of NO_3-N export from forested systems are possible (Eshleman 2000). More complex models have used a coefficient of nitrogen or phosphorus export based on each land-cover class to improve predictive ability (Mattikalli and Richards 1996, Johnes and Heathwaite 1997), as has the use of spatial regression techniques that incorporate the spatial autocorrelation of water-quality data (Chang 2008). Many studies also found watershed structural parameters such as total area (Bhat et al. 2006) and shape complexity (Hwang et al. 2007) to be useful predictors of stream water quality.

Change detection techniques have shown that conversion of forested land or grasslands to agriculture or urban land cover, increases NO_3-N loading (Schilling and Spooner 2006). Conversely, the conversions of row-crop cover to perennial grasslands or prairie reduces NO_3-N loadings (Kaushal et al. 2006, Schilling and Spooner 2006). While the LULC approach to modeling water quality is valuable and remains widely used, other analyses attempt to derive more direct indicators of water quality from remotely sensed data. Such metrics have even been found to have higher correlations with water quality than land cover classifications (Griffith 2002). A suite of these studies focus on remote sensing of actual water bodies rather than the surrounding watershed (Yang et al. 1999,

Chen et al. 2007, Giardino et al. 2007). Other approaches target individual species (Underwood et al. 2006) and vegetation groups (Li et al. 2005, Phillips et al. 2005). More applicable to our study are a set of approaches that synthesize ecologically meaningful indices and classifications from remotely sensed data such as forest disturbance (Townsend et al. 2004, McNeil et al. 2007, Eshleman et al. 2009), sub-catchment arrangement of land cover (Lopez et al. 2008), normalized difference vegetation index (Jones et al. 1996, Whistler 1996, Griffith et al. 2002, Ma et al. 2008, Oki and Yasuoka 2008), vegetation phenological communities (Reed et al. 1994, Griffith 2002), and cover by natural and hydric vegetation communities (Phillips et al. 2005). All these approaches were performed through methods of raster map data extraction and analysis (Patil et al. 2004).

The vast majority of the papers apply regression to identify relationships between water quality metrics and remotely sensed variables: either simple bivariate regression (Griffith 2002, McNeil et al. 2007, Stanley and Maxted 2008, Eshleman et al. 2009), multiple regression (Osborne and Wiley 1988, Allan et al. 1997, Meador and Goldstein 2003, Townsend et al. 2004, Robertson et al. 2006, Maillard and Pinheiro Santos 2008), or partial least squares regression (Lopez et al. 2008). While it has been demonstrated that using certain regression models with remote sensed data to predict water quality may violate their underlying assumptions (i.e. no errors in measurement and attenuated variance in the prediction of the predicted variable: Curran and Hay 1986, Cohen et al. 2003), regression remains the most widely used method of analysis.

Regardless of the analytical approach, the key difference among these studies is the mode by which remotely sensed data are incorporated into the models. Many of the LULC

studies rely on supervised classification of aerial photography, satellite imagery, or other products to arrive at a land-cover map with static classifications (e.g. Stanley and Maxted 2008). Some LULC studies increase the richness of the input data by measuring LULC at different scales (Allan et al. 1997, Basnyat et al. 2000, Maillard and Pinheiro Santos 2008) or including GIS-derived landscape metrics (Lopez et al. 2008). While the data are often treated as continuous via percent cover of a certain land-use type within a watershed or contributing zone, other methods employing image-derived vegetative or disturbance indices (Griffith et al. 2002, McNeil et al. 2007, Oki and Yasuoka 2008, Eshleman et al. 2009) capture spatially distributed, continuous variables that can yield better explanatory power (Griffith et al. 2002). Another related body of literature addresses building and implementing spatially distributed models in a GIS environment to model nutrient and pollutant movement through watersheds such as SPARROW modeling (Alexander et al. 2008, Robertson et al. 2009). While these models often employ data derived from remotely sensed imagery (such as land cover classification) as inputs, process-based models of water quality are beyond the scope of this study.

Our objective is to develop an ecologically meaningful, landscape-scale indicator of water quality using remote sensing data and recently collected water quality data (Robertson et al. 2006, Stanley and Maxted 2008) for the state of Wisconsin, USA. The approach is intended to generate an algorithm for inputting MODIS-derived products to predict water quality across years, with the ability to predict future (or past) years when data become available. Our intent is to increase the efficiency of water-quality evaluation by deriving relationships from widely available Moderate Resolution Imaging

Spectroradiometer (MODIS) data products, thereby circumventing the reliance on static land-cover classifications. Use of MODIS data should increase the repeatability of our procedures both for Wisconsin and elsewhere.

Materials and methods

Study Area

The study area encompasses four ecoregions within the state of Wisconsin (Fig. 1A). The northern third of the state comprises the Northern Lakes and Forests and is dominated by a mixed-hardwood forest that has regenerated since being clear-cut in the early 20th century. This area was historically mixed-hardwoods and was glaciated approximately 10,000 years ago. The north-central portion of the state is classified as the North Central Hardwood Forest and is dominated by a mixture of agriculture and forest cover in an area that was glaciated approximately 10,000 years ago. The Southeastern Wisconsin Till Plains is dominated by agriculture with several urban areas (Fig 1B). This area was glaciated and was historically oak savanna grading into deciduous forest. The southwestern third of the state, known as the Driftless Area, was not glaciated during the most recent ice age. The terrain is a mixture of hills and valleys created by the erosion of dolomite and limestone parent material and is comprised of a mixture of agriculture and hardwood forest. Historically, the area was a mosaic of oak savanna and tall grass prairie.

Field methods

Water-quality data

We compiled a large stream water chemistry data set from two recent investigations (Robertson et al. 2006, Stanley and Maxted 2008). Robertson et al. (2006) sampled 240 wadeable streams during summer months between 2001-2003. They analyzed samples for total unfiltered N (TN), nitrite plus nitrate ($NO_2 + NO_3$-N), and dissolved phosphorous (DP). Samples were filtered in the field through 0.45-µm membrane filters. Chemical analyses of all water samples from this dataset were conducted by the Wisconsin State Laboratory of Hygiene in accordance with standard analytical procedures described in the "Manual of Analytical Methods, Inorganic Chemistry Unit" (WSLH 1993). The basins for each sampling point were manually digitized using USGS 1:24,000 topographic quadrangle maps (Fig. 2A). Stanley and Maxted (2008) sampled summertime base flow in 84 wadeable streams during July and August of 2004. Nitrite-N was analyzed using the sulfanilamide/dihydrochloride method (APHA 1998). $NO_2 + NO_3$-N were analyzed on a Technicon segmented flow autoanalyzer (Tarrytown, New York, USA), and NO_2-N was subtracted from $NO_2 + NO_3$-N to express results as NO_3-N alone. Total dissolved nitrogen (TDN) was measured using the autoanalyzer following persulfate digestion (APHA 1998). The basins for each sampling point in this study were delineated using a 30-m digital elevation model in ArcGIS 9.1 (Fig. 2B). Measurements of dissolved nitrate (nitrate-N or NO_3-N) and dissolved phosphorus (DP) are directly comparable between the Stanley and Maxted (2008) and Robertson et al. (2006) studies. Both NO_3-N and DP were heavily right-skewed and were log-transformed prior to all statistical analyses.

Satellite data analysis

MODIS imagery

The MODIS sensor operates aboard the NASA Aqua and Terra satellites. For this study, we used data products from MODIS-Terra. MODIS data are freely available through the U.S. Geological Survey (USGS) Land Processes Distributed Active Archive Center (LP-DAAC). We used the following MODIS Version 4 products for our analyses: 500m 8-day composite surface reflectance (MOD09A1), 1000m yearly land cover (MOD12Q1), 250m 16-day composite vegetation indices (MOD13Q1), 1000m 8-day fraction of photosynthetically active radiation and leaf area index composites (MOD15A2) and 1000m 8-day composite gross primary productivity (MOD17A2).

Data pre-processing

All data were reprojected to the Wisconsin Transverse Mercator projection (NAD 1980) and were clipped to the spatial extent of Wisconsin. Unified mask layers of water, cloud-shadow and snow were extracted from the Quality-Assurance (QA) layers included with each MODIS data set. Measurements corresponding to spring, summer, and fall dates were collected from the least cloud-contaminated image for each year within an 8- or 16-day window corresponding to the temporal compositing of each MODIS product. For each year of data, images were selected around day 137 (May 17) for spring, and within an eight-day range for summer (day 177, June 26) and fall (day 273, September 30).

We extracted average values of the MODIS data by watershed for the year previous to the year of the water sample. Recent research has indicated that previous-year land

management or disturbance events may have strong influences on the water quality in the present year (Eshleman et al. 1998, Lewis and Likens 2007). This is also especially pertinent to our case because satellite data of the current year may have been obtained after the date of the stream sample. Importantly, models based on previous-year satellite data could facilitate predicting water quality one year in advance. Because the period over which all of the water-quality samples were taken covered four years, the remotely sensing variables in our data set include values from four years of imagery. All MODIS data were analyzed using ENVI v. 4.7 (ITT Visual Information Solutions Inc., Boulder CO, USA).

Vegetation indices

All variables and acronyms used to describe the vegetative cover are listed in Table 1. MODIS bi-directional and atmospherically corrected surface reflectance in the blue, red, and infrared bands are combined to provide two standard vegetation indices: Normalized Difference Vegetation Index (NDVI) and Enhanced Vegetation Index (EVI), both of which characterize vegetation vigor based on absorption of red and reflection of infrared radiation in healthy vegetation. Previous research in other Midwestern states has found nitrogen concentrations in stream systems to be highly correlated with spring NDVI (Griffith et al. 2002). Following this, we expected mean spring NDVI and EVI values to have a strong negative correlation with nitrogen species concentrations, indicating presence of natural vegetation prior to emergence of crops. In addition, we used the coefficients derived by Lobser and Cohen (2007) to generate Tasseled Cap indices for MOD09A1 data. The Tasseled Cap indices (soil brightness, vegetation greenness and surface/vegetation wetness) are widely used in forest and agricultural studies to characterize vegetation

seasonal dynamics and disturbance (for e.g.: Skakun et al. 2003, Healey et al. 2005, Jin and Sader 2005). We hypothesized that the watershed-mean of the greenness index would correspond to vegetation vigor and would correlate negatively with stream water NO_3-N concentration, while the brightness index was expected to exhibit a positive relationship with stream NO_3-N concentration, since greater amounts of bare ground correspond to both direct and leaching-related nitrogen losses from watersheds. The wetness index corresponds generally to the amount of water contained in foliage (Cohen 1991) and is an indicator of vegetation health and was therefore hypothesized to correlate negatively with stream NO_3-N concentration. We also derived disturbance indices for forested areas for all selected images following Healey et al. (2005). A number of studies have linked forest disturbance to nitrogen export from watersheds (for e.g. Townsend et al. 2004, McNeil et al. 2007, Eshleman et al. 2009).

Gross Primary Productivity

MODIS gross primary productivity (GPP) is derived from daily estimates of absorbed photosynthetically active radiation (APAR) and a light-use efficiency parameter that is a function of vegetation type (Turner et al. 2003, LP-DAAC 2008). Our expectation was that in combination, spring, summer, and fall imagery GPP would capture differences among annual crops, perennial grasslands (e.g., pastures), and forests that are biologically meaningful with respect to nutrient uptake. In particular, annual crops would have low or no GPP for dates before crops are planted, while summer imagery would distinguish forest from other vegetation, because forest GPP is generally higher than that of annual crops and perennial grassland vegetation (Turner et al. 2006). Note that we provide the

interpretations of the MODIS variables here; the variables themselves are used without prejudice and were expected to capture the salient patterns without significant processing or other interpretation from their original products.

Spectral-mixture analysis

Spectral-mixture analysis (SMA) is used to quantify the relative proportion of specific land-surface components (end-members) in each pixel. SMA differs from land-cover classification in that it provides a quantitative estimate of the fractional proportion of surface types within a pixel rather than a singular classification for that pixel. Our target endmembers were green vegetation (GV), bare soil, urban, and non-photosynthetic vegetation (NPV) and shade. We hypothesized that basins with high fractional proportions of bare soil in the spring would have high stream nitrogen concentrations. Endmembers were selected using a combination of field data collected using a FieldSpec3 spectroradiometer (ASD Colorado, USA) and an averaged spectral signature of alfisols and mollisols (the primary soil orders in the study area, Hole 1976), derived from the USGS spectral library (Clark et al. 2007). The shade end-member was included to account for solar illumination effects. The SMA was performed using ENVI 4.7 (ITT 2010). The shade fraction was removed from the images by apportioning the shade fraction to the remaining end-members and rescaling to sum to one. We followed methods suggested by Brandt and Townsend (2006) that used results of a change detection of SMA proportions to identify degraded watersheds in southern Bolivia.

Vegetation phenology

We used vegetation phenology to characterize the temporal dynamics of vegetation within the watersheds. Phenology maps offer the opportunity to depict variations associated with nutrient dynamics without employing static land-cover classifications. For instance, a low seasonal maximum NDVI coupled with a large annual range in NDVI indicates a predominantly deciduous cover type corresponding to larger variations in nutrient fluxes compared to predominantly evergreen vegetation. Similarly, higher rates of increase and decline in NDVI during a year correspond to fast growing vegetation, such as crops. This captures the sharp transition of vegetation from the dormant stage (or bare ground) to full leaf-out, and could indicate nutrient uptake and resultant lower nutrient export. Correspondingly, a high rate of decline indicates either harvest or foliar abscission, possibly capturing the return of non-retranslocated nutrients back to the upper soil stratum and a resultant flush of nutrients out of the watershed via late-season rainfall events. Further, a longer growing season could correspond to higher biomass accumulation and therefore lower nutrient export to streams. The benefit to using phenology data is that it is directly based on reflectance data and avoids the necessity to characterize land-cover maps on a yearly basis.

To develop phenological curves for all of the vegetation types across Wisconsin, we extracted NDVI data from the MOD13Q1 (250m. 16-day composite) vegetation indices product. Vegetation phenology was modeled as a double-logistic function of NDVI and day-of-year using the nlinfit function in Matlab R2010a (Mathworks Inc. Natick MA, USA):

$$NDVI = N_{low} + N_{diff} \cdot \left[\left(\frac{1}{1 + exp\left(r_i \cdot (S_{st} - t)\right)}\right) + \left(\frac{1}{1 + exp\left(r_d \cdot (S_{en} - t)\right)}\right) - 1\right] \quad \text{(Eq. 1)}$$

Where:

N_{low} = Annual NDVI minimum (lower asymptote)

N_{diff} = Annual NDVI range (difference in lower and upper asymptote)

r_i = Maximum rate of increase in NDVI

S_{st} = First inflection point (start-of-season date)

r_d = Maximum rate of decline in NDVI

S_{en} = Second inflection point (end-of-season date)

t = Julian date from January the 1st of each year

Each parameter was calculated for all image pixels. We also calculated and stored model fit information (R^2) for each pixel. All pixels where the R^2 value was lower than 0.5 were masked and later interpolated from neighboring pixels using an inverse distance weighted interpolator.

Statistical analysis

Multivariate regression techniques have been extensively used in water-quality modeling (e.g. Osborne and Wiley 1988, Allan et al. 1997, Meador and Goldstein 2003, Townsend et al. 2004, Robertson et al. 2006, Maillard and Pinheiro Santos 2008). However, when data are highly correlated (such as between related vegetation indices), the assumptions of

traditional least-squares approach are violated leading to singular solutions or otherwise biased parameter estimates and/or confidence intervals. Inherent limitations of traditional approaches in handling multi-collinear and noisy data can be overcome by applying techniques based on multivariate statistical projection such as principal-component regression (PCR) and projection to latent-structure (PLS) regression. These techniques handle highly correlated noise-corrupted data sets by explicitly assuming the dependency between variables and estimating the underlying (or latent) structures that are essentially linear combination of the original variables.

We developed a new PLS method, the iterative variable exclusion PLS algorithm (hereafter xPLS) in Matlab v. R2010a (Mathworks Inc., Natick MA, USA) executed on a Condor distributed computing cluster (Epema et al. 1996) to model stream NO_3-N concentrations as functions of MODIS imagery. Our intent was to find the most parsimonious model that would explain the largest amount of variation in the dependent variables. PLS methods differ from stepwise and AIC/BIC approaches in that they use cross-validation to reduce the importance (or even eliminate) intra- and inter-correlated variables. xPLS extends this by making the algorithm iterative to simply reduce the number of input images required to map stream concentrations. PLS methods have achieved widest use in spectroscopy and chemometrics (Martens and Dardenne 1998, Wold et al. 2001), and are especially beneficial in that they allow the development of predictive models from datasets that are relatively oversampled with predictor variables compared to dependent variables. The structure of cross-validation during PLS model development largely precludes achieving model significance based on spurious

relationships or overfitting, regardless of the number of independent variables employed in the model (Martens and Dardenne 1998). PLS is therefore well suited to large image data sets with limited numbers of observations, and is becoming a more widespread approach in ecology (Carrascal et al. 2009). Full details on our xPLS algorithm are provided in Appendix A.

Validation

Once the best candidate models had been chosen from the xPLS algorithm, we used a two-fold validation scheme to test the robustness of each model. First, a 20-fold cross-validation scheme was used to evaluate the overall model fit. This stage produced cross-validated model coefficients to compare the relative importance of each variable in predicting stream water nutrient concentrations (using standardized model coefficients) and to produce spatially-explicit predictions of potential nutrient concentration for the entire state (using raw model coefficients). Second, the data were split by source and models were calibrated using data from one source (e.g. from Stanley and Maxted 2008) to predict nutrient concentrations in the other model (e.g. to Robertson et al. 2006) and vice-versa. This stage helped us identify 1) the robustness of the model fits when using disparate data sources, and 2) identify those factors that cause deviations in predicted concentration from observed values when using data sourced from different surveys. The cross-validation procedures were implemented in SAS v. 9.3 (SAS Institute Inc. Cary NC, USA).

Mapping

Raw variable coefficients, obtained from the 20-fold cross-validated models, were used to map estimates of stream water nutrient concentrations across the study area. Because the models were calibrated from multiple years using continuous data and for watersheds of different sizes, the models are essentially year- and scale-independent. Model coefficients can be used to predict water quality for any year for which appropriate MODIS data are available or for watersheds where data are collected at different scales (such as stream orders). This way, models can be progressively refined and cross-validated across both spatial and temporal scales as new data become available. Cross-validation can be conducted by either leaving a collection of watersheds out across years or by leaving a year out while using all watersheds. Further, models developed here can also be applied to predict stream water concentrations for watersheds in which water-quality data are not available.

Results

In the two datasets, concentrations of NO_3-N varied from 0.005 to 20.55 mg/L with a mean of 2.10 (± 0.161) mg/L. Dissolved phosphorus ranged from 0.004 to 1.46 mg/L with a mean of 0.08 (± 0.006) mg/L (Table 2). Data for total nitrogen were not available for the Stanley et al (2008) dataset and data for total dissolved nitrogen and dissolved inorganic nitrogen were not available for the Robertson et al (2006) dataset.

Model performance: NO_3-N

The most parsimonious model identified by the xPLS algorithm explained 80% of the variation in stream NO_3-N concentration (Fig. 3A) using 16 variables (of a total of 42 variables, Fig. 4) projected to 15 latent vectors. The 20-fold cross-validated root mean squared error of prediction (CV-RMSEP) for the model was 1.04 mg/L. Recall that PLS provides a synthesis of the independent variables, and resultant predictive equation (which is just one coefficient per variable) has already accounted for inter-correlation among independent variables. Spring measurements for vegetation fraction, soil fraction, EVI and fraction of non-photosynthetic vegetation had the strongest loadings on streamwater NO_3-N. Whereas spring soil fraction and spring EVI correlated positively with stream water NO_3-N concentration, spring green vegetation fraction and spring NPV were negatively correlated with stream water NO_3-N concentration (Fig. 4). Variables representing bare or disturbed landscapes (spring tasseled-cap brightness, fall soil fraction and summer disturbance index) had strong positive correlations with stream water NO_3-N concentration. In contrast, variables representing vegetation vigor and growth (spring gross primary productivity, spring wetness index and spring fraction of photosynthetically active radiation) weighted negatively on stream water NO_3-N concentration (Fig. 4).

Model performance: Dissolved phosphorus

The most parsimonious model for DP identified by the xPLS algorithm explained 51% of the variation in DP (Fig. 5A). The 20-fold cross-validated root mean squared error of prediction for the model was 1.05 mg/L. In the case of DP, the xPLS results are only marginally better than could be achieved using percent cropland (Robertson et al. 2006).

The model contained 12 variables (of a total of 42 variables, Fig. 6) expressed in 11 latent vectors. Fall EVI, green vegetation fraction in summer (positively correlated) and fall and summer NDVI (negatively correlated) had the strongest weighting in the PLS model to predict DP (Fig. 6). Summer soil fraction and spring forest disturbance also exhibited strong positive weighting in the model (Fig. 6). The phenological variable rate of initial growth was negatively correlated with stream water DP concentration, while phenological rate of decline was positively correlated with stream water DP concentration. Overall, variables representing exposed soil (spring and summer soil fractions), disturbance (tasseled cap disturbance index) and rapid decline in vegetation greenness (phenologic rate of decline) were positively correlated with stream water DP concentration. In contrast, variables representing vegetation vigor and growth (phenologic rate of growth, fall and summer NDVI) were negatively correlated with stream water DP concentration (Fig. 6).

Spatial predictions

Maps of stream nutrient concentration show that watersheds in southwestern Wisconsin bordering Minnesota and Iowa are hot spots for increased nitrate-N (Fig. 7) and dissolved phosphorus (Fig. 8) concentrations. Nitrate concentrations were highest in south and south-central Wisconsin in 2002 and DP concentrations were highest in 2003 and 2004 in regions around south-central Wisconsin and in coastal regions of Lake Michigan. Predominantly agricultural regions had consistently highest nitrate-N and DP concentrations. Stream water DP concentration increased in predominantly agricultural and urban watersheds over the study period. Although stream water NO_3-N was highest in 2002, a general temporal trend was not evident.

The maps (Figs. 7 and 8) show distinct differences from year to year in predicted stream water nutrient concentrations. Post-hoc tests revealed that temporal variation in nutrient concentrations were attributable in part to variations in weather. For example, the highest NO_3-N concentrations in 2002 were explained by a combination of an unusually warm spring (in terms of higher accumulated degree growing days in 2002) coupled with lower than average rainfall in southwestern Wisconsin (Fig. 9). Overall, cumulative rainfall and growing degree days (GDDs) accounted for 42% of the variation in the watershed predictions for NO_3-N. Higher precipitation was associated with lower NO_3-N concentrations and higher GDDs were associated with elevated NO_3-N concentrations (both $P < 0.0001$). However, weather variables did not explain as much variation in predicted stream water DP concentration (14%). In contrast to NO_3-N, both rainfall and GDD were positively associated with DP concentrations but the effect of cumulative rainfall was relatively weak ($P = 0.02$).

Discussion

Our aim was to develop models using free MODIS data to predict nutrient concentrations in streams throughout Wisconsin. Our empirical strategy was intended to produce a generalized technique that would facilitate prediction of stream water nutrient concentrations based on data from a previous year, meaning that the potential would exist to predict summer baseflow nutrient concentrations approximately 8 months in advance. The models predicted NO_3-N concentrations fairly accurately (80% of variation explained, CV-RMSEP: 1.04 mg/L, Fig. 3A) and were able to improve upon the regression-based

models presented by Robertson et al. (72% for total N; Robertson et al. 2006) using three variables (total forest, precipitation and row-cropped agriculture) and Stanley and Maxted (71% for N03-N; Stanley and Maxted 2008) using two variables (proportion of land under agricultural and urban land use).

Models developed for DP were less successful (51% variation explained, CV-RMSEP: 1.05 mg/L, Fig. 5) than the models presented by Robertson et al. (56% for total total P; Robertson et al. 2006). However, our models were based exclusively on satellite imagery, whereas Robertson et al. (2006) included a host of important point-source variables such as wastewater discharge locations and non-point variables including proportion of agricultural or urban land use that exert strong controls on DP concentrations. Most notably, our data are dynamic and can be modified based on availability. Inclusion of dynamic point-source data may improve DP predictions, but unlike satellite imagery may not be available for all locations.

The most important variables for predicting NO_3-N concentrations included the spring gross primary productivity (GPP), tasseled-cap wetness index, fraction of absorbed photosynthetically active radiation (FPAR), and NDVI. All these variables either measure or can be considered surrogate measures of vegetation cover or vegetation vigor, and may indicate either nitrogen storage in foliar biomass or nitrogen uptake by growing plants. Conversely, the variables correlated positively with NO_3-N concentrations included mean soil fraction (SOI), the MODIS forest disturbance index (DST) and tasseled-cap brightness (BGT). All of these variables are indicators of either foliar loss (e.g., disturbance index) or of the amount of soil exposed (soil fraction and the brightness index) and may indicate

denudation of groundcover after harvesting, foliar loss due to insect or logging related disturbances or land-management practices that result in the release or runoff of nitrogen to the soil and surface water.

The most important variables for predicting DP concentrations included NDVI in fall and summer, and the phenologic rate of growth. Although model fit for DP was lower than for NO_3-N, the overall sign for these variables matched expectations. These are measures of vegetation growth (rate of increase of greenness in vegetation) and the accumulation of foliar biomass by plants (NDVI), and may indicate either phosphorus storage in foliar biomass or uptake by growing plants. Conversely, the variables correlated positively with DP concentrations included soil fraction, EVI, the MODIS disturbance index and phenologic rate of greenness decline. Similar to the inferences for NO_3-N, these variables are indicators of either foliar loss or of the amount of soil exposed, therefore providing surrogate measures for the loss of phosphorus to the soil.

The cross-validation results show that watershed NO_3-N (Figs. 3B, 3C) and DP (Figs. 5B, 5C) concentrations in streams draining predominantly forested watersheds are systematically overestimated as agricultural land-cover increases. This suggests the potential divergence between the two functional types to retain nutrients (for e.g. see Correll et al. 1999, Fenn and Poth 1999, Poor and McDonnell 2007) and highlights the importance of uniform sampling across a variety of ecosystems when collecting data representative of a region. Although the variables did not include the effects of fertilizer use explicitly, we believe that variables such as NDVI, EVI and phenologic rate of growth (usually higher for agricultural landscapes) capture some of the variation expressed as the

response of vegetation to external nutrient inputs (for e.g., Stone et al. 1996, Basnyat et al. 2005, Inman et al. 2007). Use of additional remote sensing variables derived from stream buffers could increase DP prediction efficiency (Hwang et al. 2007, Chang 2008, Diebel et al. 2009).

Predicting year-to-year fluctuations

Remote sensing data from MODIS facilitated prediction of interannual stream water NO_3-N concentrations, and to some extent, DP, in Wisconsin. In turn, this allowed statewide mapping of NO_3-N and DP concentrations on both a per-pixel and watershed basis. Our best statistical models improved upon those of Stanley and Maxted (2008) and Robertson et al. (2006), who both used the Wisconsin Initiative for Statewide Cooperation on Landscape Analysis and Data (WISCLAND, Reese et al. 2002) land-cover database. The WISCLAND land cover data were developed using dual-date 30-m resolution Landsat Thematic Mapper imagery primarily from 1992. The use of such a static land-cover database yielded accurate models, indicating few major land-cover changes relevant to water quality during the long period between the map (circa 1992) and water quality sampling (early 2000's). However, the data are limited by the difference in timing of data sets. Use of yearly land-cover data or remote sensing products permits predictions of year-to-year fluctuations in stream nutrient concentrations. This could facilitate timely management responses if necessary. Our predictive models can be applied to any watersheds or watershed delineations for which the MODIS data exist. The approach can be updated/validated as new data become available, and can be extended to adjoining states if appropriate data for model development or testing are available. Note that our approach

does not directly take into consideration year-to-year differences in weather and streamflow that may affect annual loads of N or P; however, these data do incorporate changes that occur on the landscape as a result of the changes in weather. These data also provide an important baseline estimate of differences in stream water concentrations that could be used to better parameterize models of nutrient loads.

Although Robertson et al. (2006) and Stanley and Maxted (2008) used a smaller number of predictor variables (3 and 2 respectively), our approach synthesizes temporally rich MODIS imagery to characterize full landscape dynamics on an annual basis, rather than using a static classification. Although this results in a larger number of independent variables used, it also facilitates incorporation of dynamic landscape attributes that can only be derived from multiple image data sets. To this end, we implemented the xPLS algorithm to rigorously assess significance for the large xPLS models.

Because the data can be readily summarized from the pixel-based maps to the watershed basis, our approach is scalable and flexible. Nevertheless, our approach is based on imagery, so we primarily capture drivers of water quality associated with nonpoint sources. As such, independent water-quality data sets could be compared to our predictions, with the residuals used to identify watersheds where point sources may be problematic. Both pixel-wise and watershed-scale data summaries may have drawbacks. Whereas watershed-scale predictions may smooth-out variations important to designing mitigation interventions, per-pixel results may run the risk of contamination by random errors inherent in satellite imagery.

Management implications

An annually derived, spatially explicit model to predict water quality offers great promise for informing the management of stream water quality at the watershed scale. Not only does the model provide a tool to identify watersheds having need for mitigation activities, the pixel-wise data may also be useful for identifying watersheds in which small-scale, landowner specific management is worthwhile. For example, in a watershed identified as having high stream water nitrogen, a project designed to reduce sediment and nutrient runoff from a single landowner's property through the installation of buffers or a reduction in fertilizer use will likely have little impact because of larger scale processes occurring in the surrounding basin. In watersheds identified as having poor water quality, large-scale efforts that work with all of the landowners in the basin may be necessary to reduce the nitrogen concentrations. Conversely, efforts with individual landowners (i.e., small numbers pixels) exhibiting high NO_3-N concentrations may be worthwhile in areas having otherwise low predicted nitrogen levels.

Our predictions are also useful for locating areas in which rare aquatic species may be most at risk, if they are sensitive to competition with N-limited species or to the acidification associated with high N concentrations (e.g. Bobbink et al. 1998, Latham 2003, Kleijn et al. 2008). The model results can also be used to identify basins in which the reintroduction of previously extirpated sensitive species are possible or to target streams where exotic species are most prone to invade. In particular, we have found that our models accurately predict the distribution of species that are favored in high N or

disturbed conditions like *Phalaris arundinacea* (reed canarygrass) and *Lythrum salicaria* (purple loosestrife) (Rachich and Reader 1999, Jakubowski et al. 2010).

Future work

We were able to predict NO_3-N concentrations accurately on a watershed scale but were less successful with predicting DP. A number of modifications to our model could increase its accuracy. Aggregation of watersheds into small, medium, and large watersheds by area instead of lumping them together for analysis could increase the predictive power of our model by allowing the variable selection routine to employ different sets of variables that may be more sensitive to water quality at different scales. In addition, the derivation of remotely sensed variables for buffers around streams instead of or in addition to the whole watershed could increase model accuracy by characterizing near-channel processes that are important to water quality (Peterjohn and Correll 1984). Adding slope or other topographic variables to the model could improve our predictions of NO_3-N concentration, and possibly DPs (Diebel et al. 2009), as interactions between slope and land-surface properties can be important to runoff and hence stream water nutrient concentrations.

This effort would be greatly improved by the availability of regular and more frequent water-quality collections at each sampling location, both for model development and testing. Specifically, time series of streamwater nutrient concentrations in the same basins over many years would facilitate better characterization of annual nutrient fluxes and variations that may be associated with year-to-year differences in weather. For example, Mitchell et al. (1996) have shown the influence of weather patterns on watershed-scale nutrient export, a factor that we did not account for in the current model.

Although there are compelling arguments in the literature that summer baseflow measurements are a good indicator of annual N fluxes (Townsend et al. 2004, Stanley and Maxted 2008, Eshleman et al. 2009), a greater temporal sampling density will allow a more detailed analysis of the mechanisms revealed by the analysis of the MODIS data. Although continuous water-quality samples do exist (e.g., by USGS and state agencies), these watersheds tend to be large and largely urban or agricultural. For our method to be effective, water quality should be sampled across a range of watershed orders, with an emphasis on sampling across a range of land-cover distributions. Finally, the linkage of this remote sensing approach to mechanistic models of stream nutrient export has the potential to enhance both approaches to evaluating and predicting nutrient concentrations. In particular, our approach captures the effects of variations in land cover on water quality, such as disturbance of forests, that are not currently captured by existing models (e.g. HSPF: Donigian et al. 1983, SPARROW: Smith et al. 1997).

Evaluating the predictive ability of the model beyond the spatial extent of the state of Wisconsin may be worthwhile. Because our model includes parameters easily attainable from freely available satellite data, the model could be expanded to predict stream water quality for much of the Midwest and perhaps beyond. The availability of MODIS parameters calculated annually provides the opportunity to identify and predict inter-annual fluctuations of stream nitrogen concentrations with changing land cover conditions.

Literature cited

Aber, J. D., K. J. Nadelhoffer, P. Steudler, and J. M. Melillo. 1989. Nitrogen Saturation in Northern Forest Ecosystems. Bioscience **39**:378-386.

Alexander, R. B., R. A. Smith, G. E. Schwarz, E. W. Boyer, J. V. Nolan, and J. W. Brakebill. 2008. Differences in phosphorus and nitrogen delivery to the gulf of Mexico from the Mississippi river basin. Environmental Science & Technology **42**:822-830.

Allan, J. D., D. L. Erickson, and J. Fay. 1997. The influence of catchment land use on stream integrity across multiple spatial scales. Freshwater Biology **37**:149-161.

APHA. 1998. Standard methods for the examination of water and wastewater: Twentieth edition. Washington DC, USA.

Basnyat, P., B. G. McConkey, F. Selles, and L. B. Meinert. 2005. Effectiveness of using vegetation index to delineate zones of different soil and crop grain production characteristics. Canadian Journal of Soil Science **85**:319-328.

Basnyat, P., L. D. Teeter, B. G. Lockaby, and K. M. Flynn. 2000. The use of remote sensing and GIS in watershed level analyses of non-point source pollution problems. Forest Ecology and Management **128**:65-73.

Bhat, S., J. M. Jacobs, K. Hatfield, and J. Prenger. 2006. Relationships between stream water chemistry and military land use in forested watersheds in Fort Benning, Georgia. Ecological Indicators **6**:458-466.

Bobbink, R., M. Hornung, and J. G. M. Roelofs. 1998. The effects of air-borne nitrogen pollutants on species diversity in natural and semi-natural European vegetation. Journal of Ecology **86**:717-738.

Brandt, J. S., and P. A. Townsend. 2006. Land use - land cover conversion, regeneration and degradation in the high elevation Bolivian Andes. Landscape Ecology **21**:607-623.

Buck, O., D. K. Niyogi, and C. R. Townsend. 2004. Scale-dependence of land use effects on water quality of streams in agricultural catchments. Environmental Pollution **130**:287-299.

Carpenter, S. R., N. F. Caraco, D. L. Correll, R. W. Howarth, A. N. Sharpley, and V. H. Smith. 1998. Nonpoint pollution of surface waters with phosphorus and nitrogen. Ecological Applications **8**:559-568.

Carrascal, L. M., I. Galvan, and O. Gordo. 2009. Partial least squares regression as an alternative to current regression methods used in ecology. Oikos **118**:681-690.

Chander, G., C. Q. Huang, L. M. Yang, C. Homer, and C. Larson. 2009. Developing Consistent Landsat Data Sets for Large Area Applications: The MRLC 2001 Protocol. Ieee Geoscience and Remote Sensing Letters **6**:777-781.

Chang, H. 2008. Spatial analysis of water quality trends in the Han River basin, South Korea. Water Research **42**:3285-3304.

Chen, Z. Q., C. M. Hu, and F. Muller-Karger. 2007. Monitoring turbidity in Tampa Bay using MODIS/Aqua 250-m imagery. Remote Sensing of Environment **109**:207-220.

Clark, R. N., G. A. Swayze, R. A. Wise, K. E. Livo, T. M. Hoefen, R. F. Kokaly, and S. J. Sutley. 2007. USGS Digital Spectral Library splib06a. Denver, CO.

Cohen, W. B. 1991. Response of Vegetation Indexes to Changes in 3 Measures of Leaf Water-Stress. Photogrammetric Engineering and Remote Sensing **57**:195-202.

Cohen, W. B., T. K. Maiersperger, S. T. Gower, and D. P. Turner. 2003. An improved strategy for regression of biophysical variables and Landsat ETM+ data. Remote Sensing of Environment **84**:561-571.

Cole, J. J., B. L. Peierls, N. F. Caraco, and M. L. Pace. 1993. Nitrogen loading of rivers as a human-driven process. Springer-Verlag Inc., New York.

Correll, D. L., T. E. Jordan, and D. E. Weller. 1999. Transport of nitrogen and phosphorus from Rhode River watersheds during storm events. Water Resources Research **35**:2513-2521.

Coskun, H. G., A. Tanik, U. Alganci, and H. K. Cigizoglu. 2008. Determination of environmental quality of a drinking water reservoir by remote sensing, GIS and regression analysis. Water Air and Soil Pollution **194**:275-285.

Curran, P. J., and A. M. Hay. 1986. The Importance of Measurement Error for Certain Procedures in Remote-Sensing at Optical Wavelengths. Photogrammetric Engineering and Remote Sensing **52**:229-241.

Dennison, W. C., R. J. Orth, K. A. Moore, J. C. Stevenson, V. Carter, S. Kollar, P. W. Bergstrom, and R. A. Batiuk. 1993. Assessing Water-Quality with Submersed Aquatic Vegetation. Bioscience **43**:86-94.

Diebel, M., J. Maxted, D. Robertson, S. Han, and M. Vander Zanden. 2009. Landscape Planning for Agricultural Nonpoint Source Pollution Reduction III: Assessing Phosphorus and Sediment Reduction Potential. Environmental Management **43**:69-83.

Donigian, A. S., J. C. Imhoff, and B. R. Bicknell, editors. 1983. Predicting water quality resulting from agricultural nonpoint source pollution via simulation-HSPF. Iowa State University Press, Ames, Iowa.

Epema, D. H. J., M. Livny, R. vanDantzig, X. Evers, and J. Pruyne. 1996. A worldwide flock of Condors: Load sharing among workstation clusters. Future Generation Computer Systems **12**:53-65.

Eshleman, K. N. 2000. A linear model of the effects of disturbance on dissolved nitrogen leakage from forested watersheds. Water Resources Research **36**:3325-3335.

Eshleman, K. N., B. E. McNeil, and P. A. Townsend. 2009. Validation of a remote sensing based index of forest disturbance using streamwater nitrogen data. Ecological Indicators **9**:476-484.

Eshleman, K. N., R. P. Morgan, J. R. Webb, F. A. Deviney, and J. N. Galloway. 1998. Temporal patterns of nitrogen leakage from mid-Appalachian forested watersheds: Role of insect defoliation. Water Resources Research **34**:2005-2016.

Fenn, M. E., and M. A. Poth. 1999. Temporal and spatial trends in streamwater nitrate concentrations in the San Bernardino Mountains, southern California. Journal of Environmental Quality **28**:822-836.

Giardino, C., V. E. Brando, A. G. Dekker, N. Strombeck, and G. Candiani. 2007. Assessment of water quality in Lake Garda (Italy) using Hyperion. Remote Sensing of Environment **109**:183-195.

Griffith, J. A. 2002. Geographic techniques and recent applications of remote sensing to landscape-water quality studies. Water Air and Soil Pollution **138**:181-197.

Griffith, J. A., E. A. Martinko, J. L. Whistler, and K. P. Price. 2002. Interrelationships among landscapes, NDVI, and stream water quality in the US central plains. Ecological Applications **12**:1702-1718.

Hall, R. I., P. R. Leavitt, R. Quinlan, A. S. Dixit, and J. P. Smol. 1999. Effects of agriculture, urbanization, and climate on water quality in the northern Great Plains. Limnology and Oceanography **44**:739-756.

Healey, S. P., W. B. Cohen, Z. Q. Yang, and O. N. Krankina. 2005. Comparison of Tasseled Cap-based Landsat data structures for use in forest disturbance detection. Remote Sensing of Environment **97**:301-310.

Herlihy, A. T., J. L. Stoddard, and C. B. Johnson. 1998. The relationship between stream chemistry and watershed land cover data in the mid-Atlantic region, US. Water Air and Soil Pollution **105**:377-386.

Hole, F. D. 1976. Soils of Wisconsin. University of Wisconsin, Madison, Madison, WI.

Howarth, R. W., G. Billen, D. Swaney, A. Townsend, N. Jaworski, K. Lajtha, J. A. Downing, R. Elmgren, N. Caraco, T. Jordan, F. Berendse, J. Freney, V. Kudeyarov, P. Murdoch, and Z. L. Zhu. 1996. Regional nitrogen budgets and riverine N&P fluxes for the drainages to the North Atlantic Ocean: Natural and human influences. Biogeochemistry **35**:75-139.

Hwang, S. J., S. W. Lee, J. Y. Son, G. A. Park, and S. J. Kim. 2007. Moderating effects of the geometry of reservoirs on the relation between urban land use and water quality. Landscape and Urban Planning **82**:175-183.

Inman, D., R. Khosla, R. M. Reich, and D. G. Westfall. 2007. Active remote sensing and grain yield in irrigated maize. Precision Agriculture **8**:241-252.

ITT. 2010. ENVI.*in* I. V. I. S. Inc., editor., Boulder, CO.

Jakubowski, A. R., M. D. Casler, and R. D. Jackson. 2010. Landscape Context Predicts Reed Canarygrass Invasion: Implications for Management. Wetlands **30**:685-692.

Jin, S. M., and S. A. Sader. 2005. Comparison of time series tasseled cap wetness and the normalized difference moisture index in detecting forest disturbances. Remote Sensing of Environment **94**:364-372.

Johnes, P. J., and A. L. Heathwaite. 1997. Modelling the impact of land use change on water quality in agricultural catchments. Hydrological Processes **11**:269-286.

Johnson, L. B., C. Richards, G. E. Host, and J. W. Arthur. 1997. Landscape influences on water chemistry in Midwestern stream ecosystems. Freshwater Biology **37**:193-208.

Jones, K. B., J. Walker, K. Riiters, J. Wickham, and C. Nicoll. 1996. Indicators of Landscape Integrity. Pages 155-168 *in* J. Walker and D. Reuter, editors. Indicators of Catchment Health. CSIRO, Melbourne, Australia.

Jordan, T. E., D. L. Correll, and D. E. Weller. 1997. Relating nutrient discharges from watersheds to land use and streamflow variability. Water Resources Research **33**:2579-2590.

Karr, J. R. 1981. Assessment of Biotic Integrity Using Fish Communities. Fisheries **6**:21-27.

Karr, J. R., and I. J. Schlosser. 1978. Water-Resources and Land-Water Interface. Science **201**:229-234.

Kaushal, S. S., W. M. Lewis, and J. H. McCutchan. 2006. Land use change and nitrogen enrichment of a Rocky Mountain watershed. Ecological Applications **16**:299-312.

Kleijn, D., R. M. Bekker, R. Bobbink, M. C. C. De Graaf, and J. G. M. Roelofs. 2008. In search for key biogeochemical factors affecting plant species persistence in heathland and acidic grasslands: a comparison of common and rare species. Journal of Applied Ecology **45**:680-687.

Krysanova, V., D. I. Muller-Wohlfeil, and A. Becker. 1998. Development and test of a spatially distributed hydrological water quality model for mesoscale watersheds. Ecological Modelling **106**:261-289.

Latham, R. E. 2003. Shrubland longevity and rare plant species in the northeastern United States. Forest Ecology and Management **185**:21-39.

Lewis, G. P., and G. E. Likens. 2007. Changes in stream chemistry associated with insect defoliation in a Pennsylvania hemlock-hardwoods forest. Forest Ecology and Management **238**:199-211.

Li, L., S. L. Ustin, and M. Lay. 2005. Application of multiple endmember spectral mixture analysis (MESMA) to AVIRIS imagery for coastal salt marsh mapping: a case study in China Camp, CA, USA. International Journal of Remote Sensing **26**:5193-5207.

Likens, G. E., F. H. Bormann, N. M. Johnson, D. W. Fisher, and R. S. Pierce. 1970. Effects of Forest Cutting and Herbicide Treatment on Nutrient Budgets in Hubbard Brook Watershed-Ecosystem. Ecological Monographs **40**:23-&.

Lobser, S. E., and W. B. Cohen. 2007. MODIS tasselled cap: land cover characteristics expressed through transformed MODIS data. International Journal of Remote Sensing **28**:5079-5101.

Lopez, R. D., M. S. Nash, D. T. Heggem, and D. W. Ebert. 2008. Watershed vulnerability predictions for the Ozarks using landscape models. Journal of Environmental Quality **37**:1769-1780.

Lowrance, R., L. S. Altier, J. D. Newbold, R. R. Schnabel, P. M. Groffman, J. M. Denver, D. L. Correll, J. W. Gilliam, J. L. Robinson, R. B. Brinsfield, K. W. Staver, W. Lucas, and A. H. Todd. 1997. Water quality functions of riparian forest buffers in Chesapeake Bay watersheds. Environmental Management **21**:687-712.

LP-DAAC. 2008. Gross Primary Productivity 8-day L4 Global 1km.*in* U. S. G. Survey, editor. Land Processes Distributed Active Archive Center.

Ma, R. H., H. T. Duan, X. H. Gu, and S. X. Zhang. 2008. Detecting aquatic vegetation changes in Taihu Lake, China using multi-temporal satellite imagery. Sensors **8**:3988-4005.

Maillard, P., and N. A. Pinheiro Santos. 2008. A spatial-statistical approach for modeling the effect of non-point source pollution on different water quality parameters in the Velhas river watershed Brazil. Journal of Environmental Management **86**:158-170.

Martens, H. A., and P. Dardenne. 1998. Validation and verification of regression in small data sets. Chemometrics and Intelligent Laboratory Systems **44**:99-121.

Mattikalli, N. M., and K. S. Richards. 1996. Estimation of surface water quality changes in response to land use change: Application of the export coefficient model using remote sensing and geographical information system. Journal of Environmental Management **48**:263-282.

McNeil, B. E., K. M. de Beurs, K. N. Eshleman, J. R. Foster, and P. A. Townsend. 2007. Maintenance of ecosystem nitrogen limitation by ephemeral forest disturbance: An assessment using MODIS, Hyperion, and Landsat ETM. Geophysical Research Letters **34**:-.

Meador, M. R., and R. M. Goldstein. 2003. Assessing water quality at large geographic scales: Relations among land use, water physicochemistry, riparian condition, and fish community structure. Environmental Management **31**:504-517.

Mitchell, M. J., C. T. Driscoll, J. S. Kahl, G. E. Likens, P. S. Murdoch, and L. H. Pardo. 1996. Climatic control of nitrate loss from forested watersheds in the northeast United States. Environmental Science & Technology **30**:2609-2612.

Oki, K., and Y. Yasuoka. 2008. Mapping the potential annual total nitrogen load in the river basins of Japan with remotely sensed imagery. Remote Sensing of Environment **112**:3091-3098.

Omernik, J. M., S. S. Chapman, R. A. Lillie, and R. T. Dumke. 2000. Ecoregions of Wisconsin.

Osborne, L. L., and M. J. Wiley. 1988. Empirical Relationships between Land-Use Cover and Stream Water-Quality in an Agricultural Watershed. Journal of Environmental Management **26**:9-27.

Patil, G. P., J. Balbus, G. Biging, J. Jaja, W. L. Myers, and C. Taillie. 2004. Multiscale advanced raster map analysis system: Definition, design and development. Environmental and Ecological Statistics **11**:113-138.

Peierls, B. L., N. F. Caraco, M. L. Pace, and J. J. Cole. 1991. Human Influence on River Nitrogen. Nature **350**:386-387.

Peterjohn, W. T., and D. L. Correll. 1984. Nutrient Dynamics in an Agricultural Watershed - Observations on the Role of a Riparian Forest. Ecology **65**:1466-1475.

Phillips, R. L., O. Beeri, and E. S. DeKeyser. 2005. Remote wetland assessment for Missouri Coteau prairie glacial basins. Wetlands **25**:335-349.

Pieterse, N. M., W. Bleuten, and S. E. Jorgensen. 2003. Contribution of point sources and diffuse sources to nitrogen and phosphorus loads in lowland river tributaries. Journal of Hydrology **271**:213-225.

Poor, C. J., and J. J. McDonnell. 2007. The effects of land use on stream nitrate dynamics. Journal of Hydrology **332**:54-68.

Rachich, J., and R. J. Reader. 1999. An experimental study of wetland invasibility by purple loosestrife (Lythrum salicaria). Canadian Journal of Botany-Revue Canadienne De Botanique **77**:1499-1503.

Reed, B. C., J. F. Brown, D. Vanderzee, T. R. Loveland, J. W. Merchant, and D. O. Ohlen. 1994. Measuring Phenological Variability from Satellite Imagery. Journal of Vegetation Science **5**:703-714.

Reese, H. M., T. M. Lillesand, D. E. Nagel, J. S. Stewart, R. A. Goldmann, T. E. Simmons, J. W. Chipman, and P. A. Tessar. 2002. Statewide land cover derived from multiseasonal Landsat TM data - A retrospective of the WISCLAND project. Remote Sensing of Environment **82**:224-237.

Robertson, D. M., D. J. Graczyk, P. J. Garrison, L. Wang, G. Laliberte, and R. Bannerman. 2006. Nutrient concentrations and their relations to biotic integrity of wadeable streams in Wisconsin. Page 156 United Sates Geological Survey Professional Paper 1722. USGS Wisconsin Water Science Center, Middleton, WI.

Robertson, D. M., G. E. Schwarz, D. A. Saad, and R. B. Alexander. 2009. Incorporating uncertainty into the ranking of SPARROW model nutrient yields from Mississippi/Atchafalaya river basin watersheds. Journal of the American Water Resources Association **45**:534-549.

Schilling, K. E., and J. Spooner. 2006. Effects of watershed-scale land use change on stream nitrate concentrations. Journal of Environmental Quality **35**:2132-2145.

Schlosser, I. J., and J. R. Karr. 1981. Riparian Vegetation and Channel Morphology Impact on Spatial Patterns of Water-Quality in Agricultural Watersheds. Environmental Management **5**:233-243.

Serbin, S. P., and C. J. Kucharik. 2009. Spatiotemporal Mapping of Temperature and Precipitation for the Development of a Multidecadal Climatic Dataset for Wisconsin. Journal of Applied Meteorology and Climatology **48**:742-757.

Skakun, R. S., M. A. Wulder, and S. E. Franklin. 2003. Sensitivity of the thematic mapper enhanced wetness difference index to detect mountain pine beetle red-attack damage. Remote Sensing of Environment **86**:433-443.

Smith, R. A., G. E. Schwarz, and R. B. Alexander. 1997. Regional interpretation of water-quality monitoring data. Water Resources Research **33**:2781-2798.

Stanley, E. H., and J. T. Maxted. 2008. Changes in the dissolved nitrogen pool across land cover gradients in Wisconsin streams. Ecological Applications **18**:1579-1590.

Stone, M. L., J. B. Solie, W. R. Raun, R. W. Whitney, S. L. Taylor, and J. D. Ringer. 1996. Use of spectral radiance for correcting in-season fertilizer nitrogen deficiencies in winter wheat. Transactions of the Asae **39**:1623-1631.

Townsend, P. A., K. N. Eshleman, and C. Welcker. 2004. Remote sensing of gypsy moth defoliation to assess variations in stream nitrogen concentrations. Ecological Applications **14**:504-516.

Turner, D. P., W. D. Ritts, W. B. Cohen, S. T. Gower, S. W. Running, M. S. Zhao, M. H. Costa, A. A. Kirschbaum, J. M. Ham, S. R. Saleska, and D. E. Ahl. 2006. Evaluation of MODIS NPP and GPP products across multiple biomes. Remote Sensing of Environment **102**:282-292.

Turner, D. P., W. D. Ritts, W. B. Cohen, S. T. Gower, M. S. Zhao, S. W. Running, S. C. Wofsy, S. Urbanski, A. L. Dunn, and J. W. Munger. 2003. Scaling Gross Primary Production (GPP) over boreal and deciduous forest landscapes in support of MODIS GPP product validation. Remote Sensing of Environment **88**:256-270.

Underwood, E. C., M. J. Mulitsch, J. A. Greenberg, M. L. Whiting, S. L. Ustin, and S. C. Kefauver. 2006. Mapping invasive aquatic vegetation in the Sacramento-San Joaquin Delta using hyperspectral imagery. Environmental Monitoring and Assessment **121**:47-64.

Vitousek, P. M., J. D. Aber, R. W. Howarth, G. E. Likens, P. A. Matson, D. W. Schindler, W. H. Schlesinger, and G. D. Tilman. 1997. Human alteration of the global nitrogen cycle: Sources and consequences. Ecological Applications **7**:737-750.

Whistler, J. L. 1996. A phenological approach to land cover characterization using Landsat MSS data for analysis of nonpoint source pollution. University of Kansas, Lawrence, KS.

Wold, S., M. Sjostrom, and L. Eriksson. 2001. PLS-regression: a basic tool of chemometrics. Chemometrics and Intelligent Laboratory Systems **58**:109-130.

WSLH. 1993. Manual of analytical methods, inorganic chemistry unit. Wisconsin State Laboratory of Hygiene, Environmental Sciences Section:[variously paged].

Yang, M. D., C. J. Merry, and R. M. Sykes. 1999. Integration of water quality modeling, remote sensing, and GIS. Journal of the American Water Resources Association **35**:253-263.

Zampella, R. A., N. A. Procopio, R. G. Lathrop, and C. L. Dow. 2007. Relationship of land-use/land-cover patterns and surface-water quality in the Mullica River basin. Journal of the American Water Resources Association **43**:594-604.

Tables

Table 1. List of acronyms.

MODIS Product	Code	Variable	Method
MOD09A1	WET	Wetness Index	Tasselled cap transformation
	BGT	Brightness Index	
	GRN	Greenness Index	
	DST	Disturbance Index	Healy et. al. 2005
	GVF	Green vegetation	Spectral unmixing
	NPV	Non-photosynthetic vegetation	
	SOI	Soil	
	URB	Urban	
MOD13A1	NDV	Normalized difference vegetation index	From product
	EVI	Enhanced vegetation index	
MOD13Q1	ROI	Rate of increase	Phenologic Curve fitting (eqn. 1)
	ROD	Rate of decrease	
	LGS	Length of growing season	
	SOS	Start of season	
	EOS	End of season	
MOD15A2	FPR	Fraction of photosynthetically active radiation	From product
	LAI	Leaf area index	
MOD17A2	GPP	Gross primary productivity	From product

Table 2: Mean (± 1 SE) and range values of concentration (in mg/l) for nitrate (NO_3-N) total nitrogen (TN), total dissolved nitrogen (TDN), dissolved inorganic nitrogen (DIN) and dissolved phosphorous (DP); stream concentrations are averaged across the entire state for Stanley and Maxted (2008; n = 76) and Robertson et al. (2006; n = 239).

	Stanley and Maxted (2008) n = 76		Robertson et al. (2006) n = 239	
Water quality variable	Mean	Range	Mean	Range
NO_3	2.12 (0.329)	0.005 - 12.615	2.09 (0.185)	0.005 - 20.550
TN	-	-	2.81 (0.185)	0.131 - 21.26
TDN	2.79 (0.360)	0.089 - 14.014	-	-
DIN	2.17 (0.331)	0.0182 - 12.703	-	-
DP	0.08 (0.009)	0.011 - 0.389	0.079 (0.007)	0.004 - 1.460

Figures

Figure 1: Level 4 ecoregions of Wisconsin (Omernik et al. 2000). B. Agricultural areas in Wisconsin (derived from NLCD 2001: Chander et al. 2009).

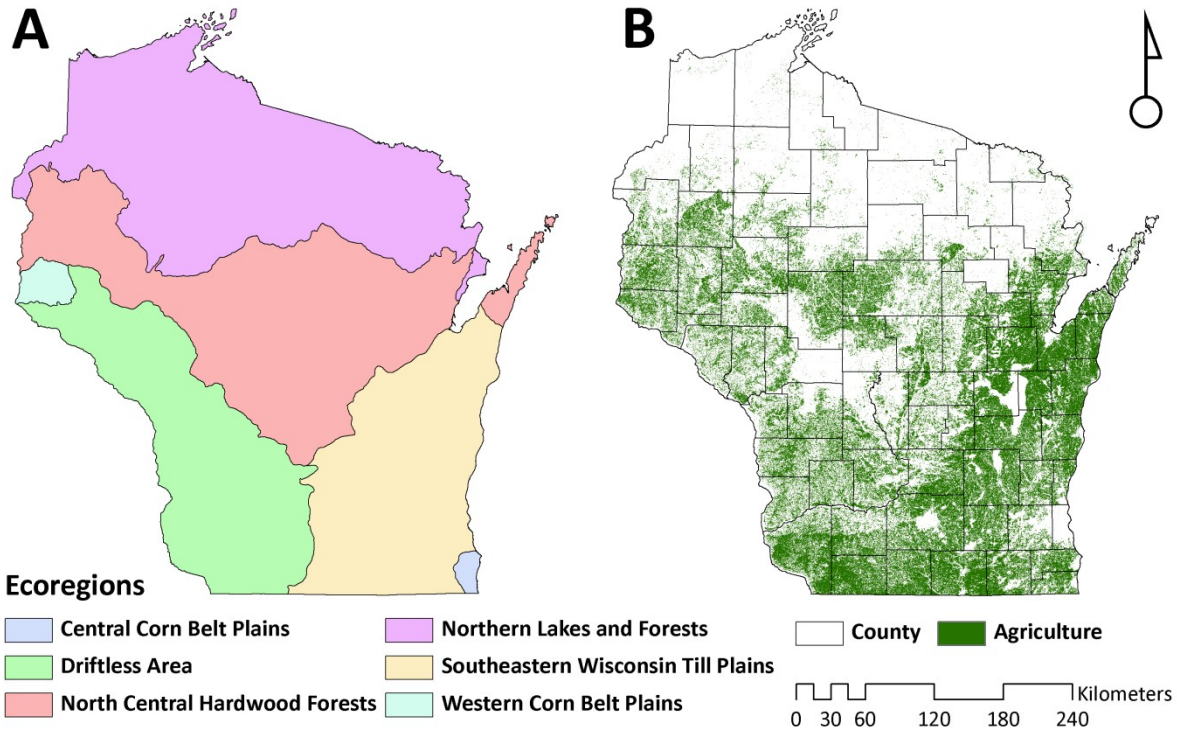

Figure 2: Watersheds sampled by Robertson et al. (2006) in 2001-2003. B. Watersheds sampled by Stanley et al. (2008) in 2004. We excluded nested watersheds, and masked all water bodies and areas outside the bounds of Wisconsin.

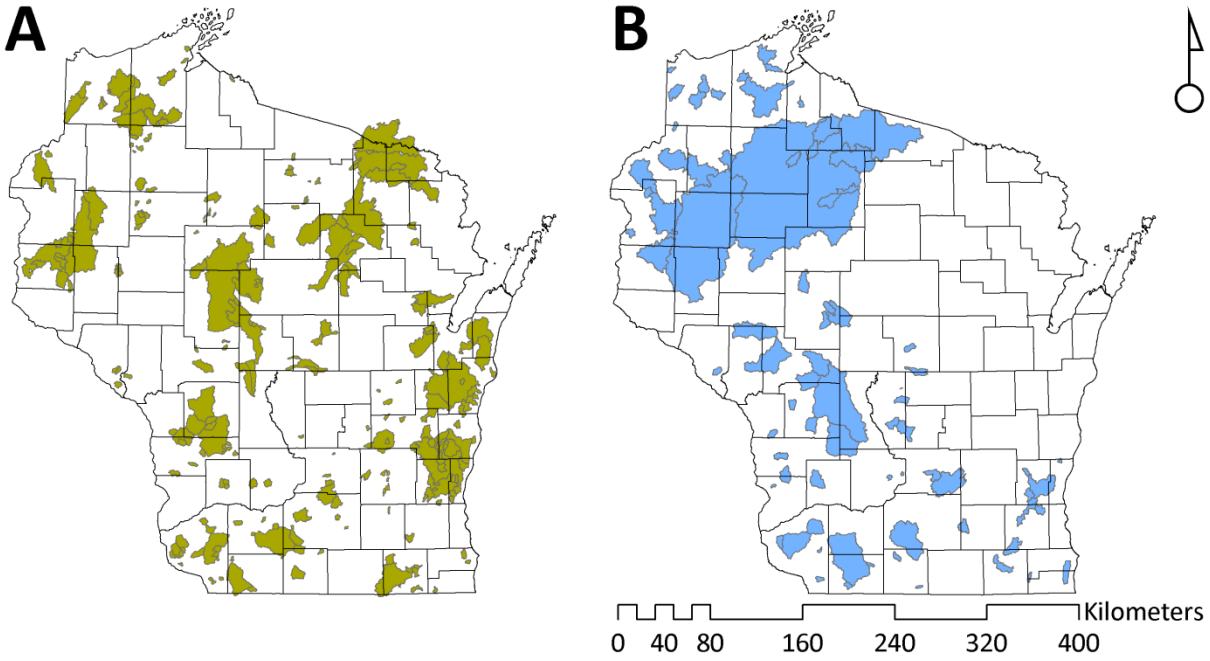

Figure 3: Predicted NO_3-N concentration from the PLS model vs. observed concentration using all data. B. Cross-validation of the PLS model calibrated with Robertson et al. (2006) data to predict data from Stanley and Maxted (2008), and C) vice-versa. Color of points indicates amount of forest cover in each watershed and follows the percentage shown in the color ramp to the right. Red dashed line indicates the 1:1 line. Black dashed line indicates model fit. Deviation from the 1:1 line illustrates model bias.

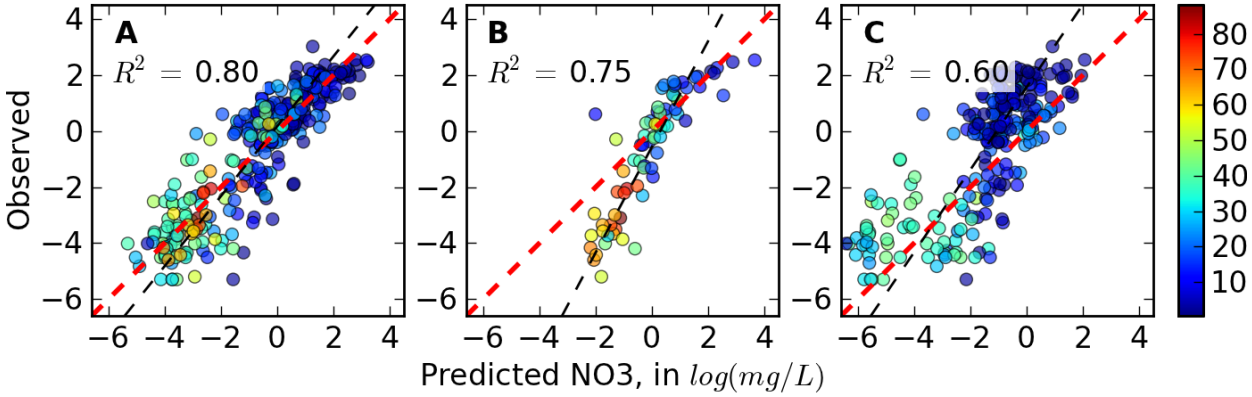

Figure 4: Standardized coefficients of variables selected by the xPLS algorithm for predicting ln(NO_3-N). Absolute values of standardized coefficients (blue bars) are presented to facilitate comparison. Hatched bars indicate partial correlations of each variable with observed ln (NO_3-N). Asterisks indicate significance levels for the correlation (*** $P < 0.0001$, ** $P < 0.05$, * $P < 0.01$). Variable names are provided in Table 1.

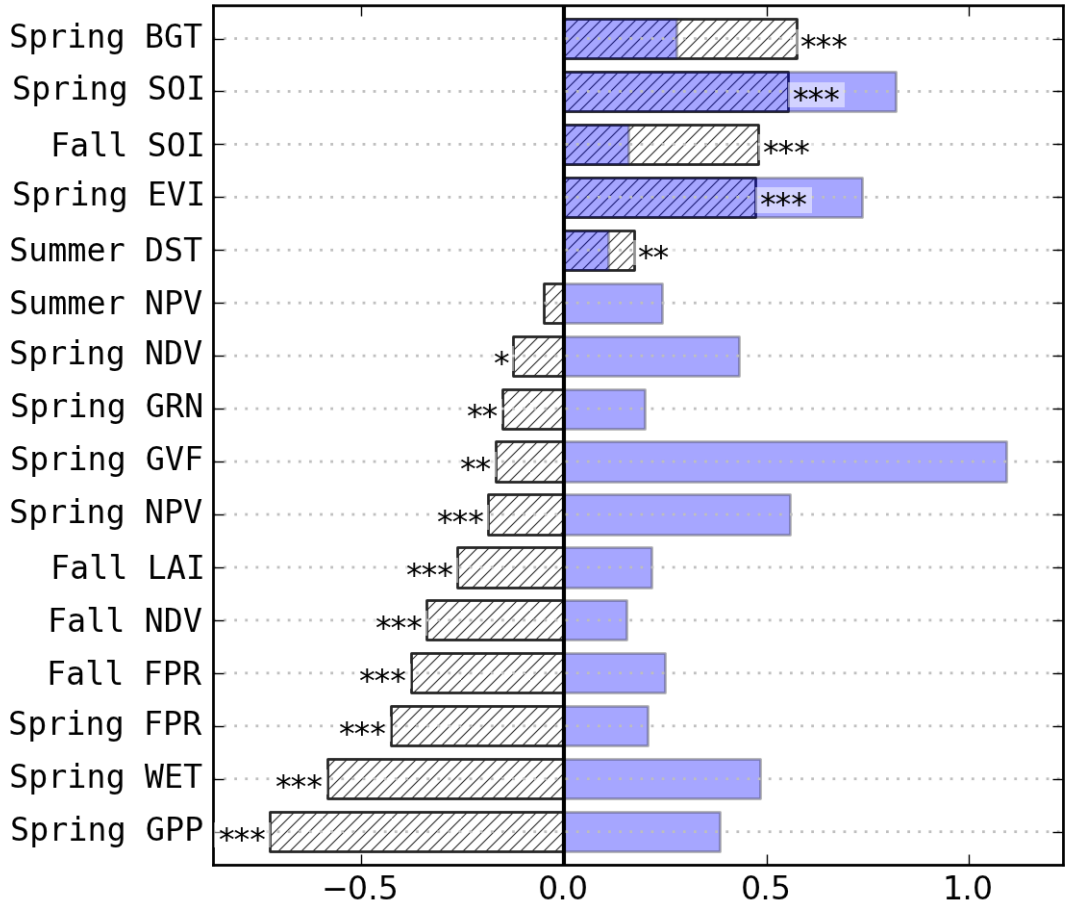

Figure 5: Plots of predicted dissolved phosphorus (DP) concentration vs. observed measurements. Details follow those of Figure 3.

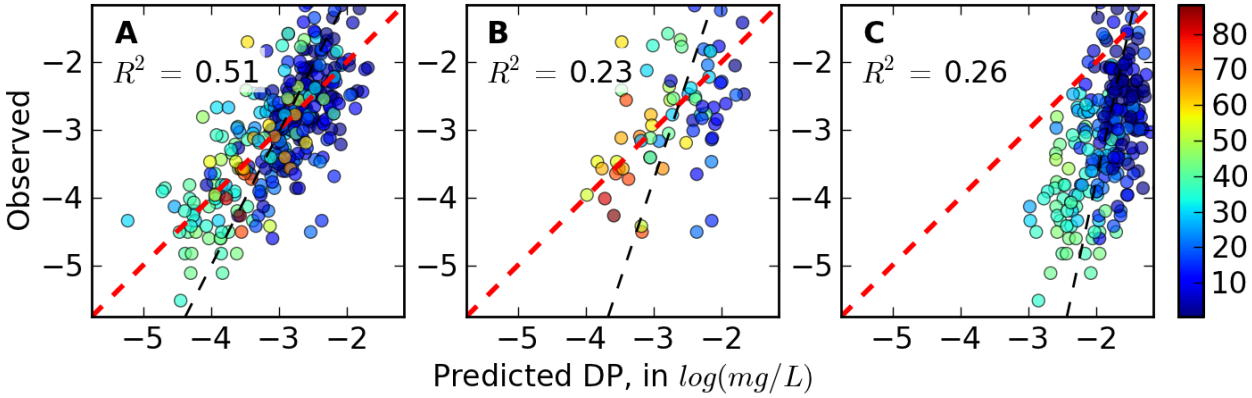

Figure 6: Absolute values of standardized coefficients of variables selected by the xPLS algorithm for predicting natural log(DP) and partial correlations of those variables with log(DP). Details follow those of Fig. 4. Variable names are provided in Table 1.

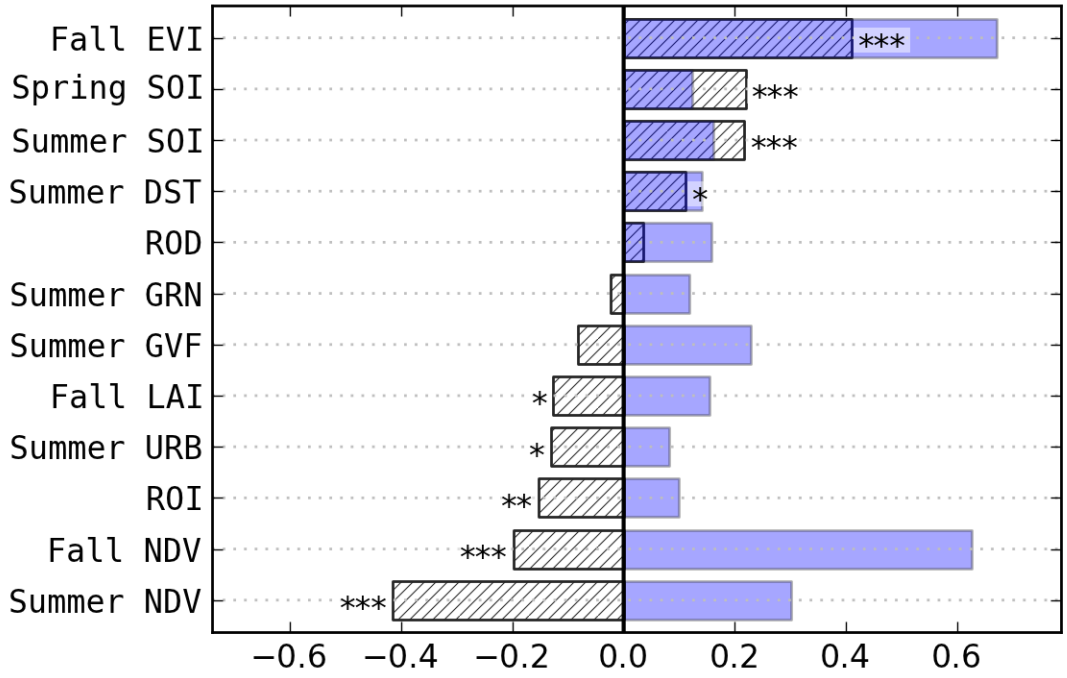

Figure 7: Maps of predicted NO_3-N concentrations across the four years of the study using coefficients derived from the PLS model. The left panel shows pixel-wise predictions, the right panel shows data averaged across Wisconsin DNR watersheds (sourced from: http://dnr.wi.gov/maps/gis/metadata.html). Note log-scale of color bar, color bar units in mg/L.

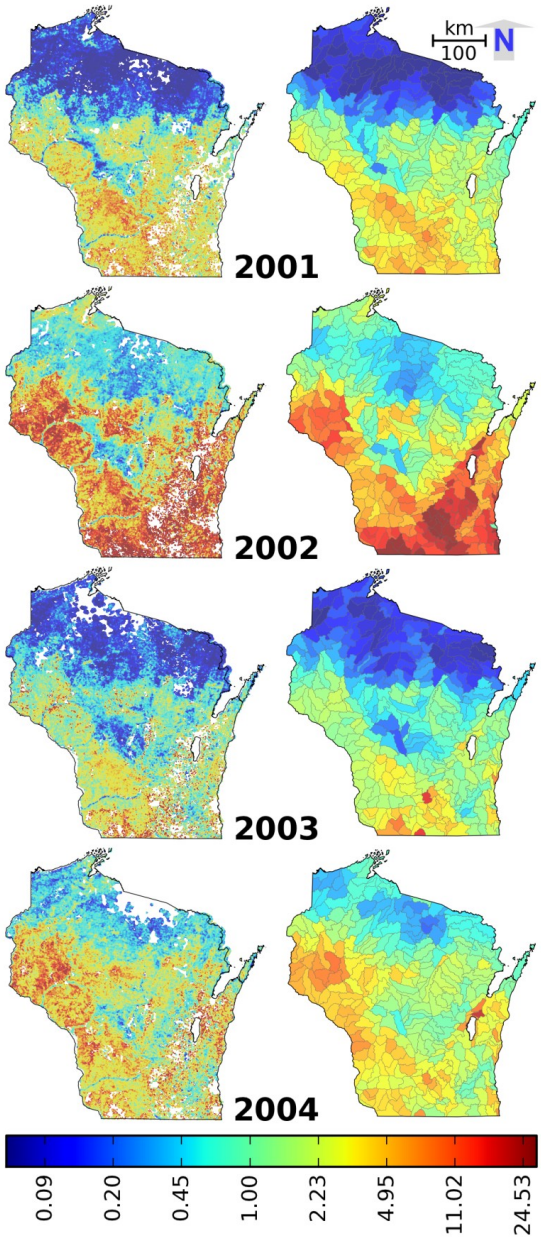

Figure 8: Maps of predicted DP concentrations across the four years of the study using coefficients derived from PLS model. The left panel shows pixel-wise predictions, the right panel shows data averaged across Wisconsin DNR watersheds. Note log-scale of color bar, color bar units in mg/L.

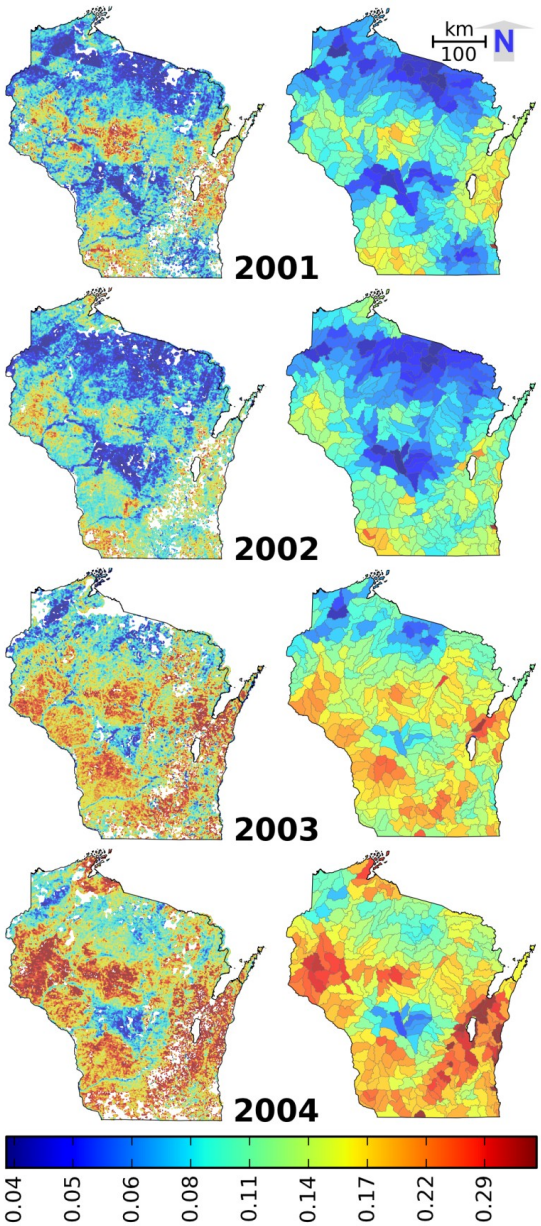

Figure 9: Maps of cumulative growing degree days (left panel, base temperature = 0°C, ceiling temperature = 30°C) and cumulative daily rainfall (in mm.) measured from the 1st of October the previous year to the 1st of June of the current year (data source: Serbin and Kucharik 2009).

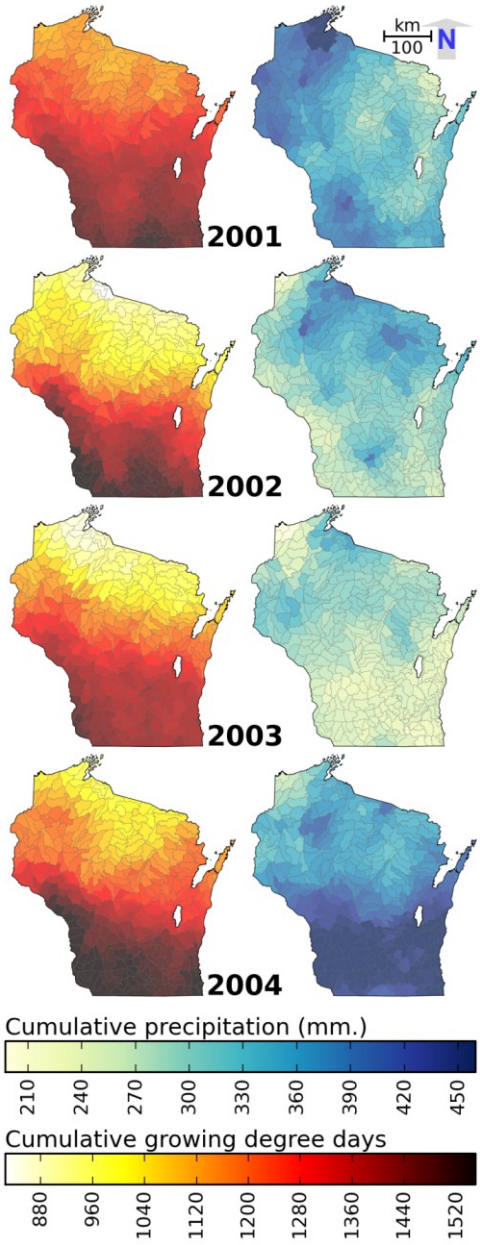

Supplementary materials

Appendix A

Details of the 'iterative exclusion' projection to latent structures regression (xPLS) algorithm

Background

The chief value of projection to latent structures (PLS) regression over traditional multiple linear regression models is that it works well with over-sampled predictor data sets, i.e. when the number of independent variables approaches or even exceeds the number of observations (Geladi and Kowalski 1986; Wold et al. 1984; Wold et al. 2001). PLS handles highly correlated noise-corrupted data sets by explicitly assuming the dependency between variables and estimating the underlying (or latent) structures that are essentially linear combination of the original variables. PLS is preferred to traditional regression for multi-collinear data sets because it takes advantage of correlations within the large number of predictors without the issues associated with data reduction approaches, for example difficulties in interpretation of synthetic PCA variables or the potential for modeling spurious relationships using stepwise regression (Grossman et al. 1996). Original variables are retained and their importance is evaluated by a review of their standardized prediction coefficients.

In particular, PLS regression replaces the set of predictors by a smaller number of latent variables. As the derivation of the factors is based on principal components

transformations, the factors are orthogonal by design, and are linear combinations of the original predictors. While similar to principal component regression, where the factors are determined by the predictors only, PLS identifies factors taking into consideration each factor's individual usefulness in predicting the dependent variables by maximizing its covariance with the dependent variable while simultaneously maintaining the constraint of being orthogonal to the previously determined factors (Frank and Friedman 1993; Geladi and Kowalski 1986; Wold et al. 1984; Wold et al. 2001).

Our intent was to find the most parsimonious PLS model that would explain the largest amount of variation in the dependent variables while using a minimal number of orthogonal components. Typically, the root mean square (RMS) error of a PLS model decreases as components are added, with each new component incrementally contributing to explaining the variation in the dependent set. Eventually, a point is reached where adding any more components introduces noise in the model and the RMS error starts to increase. If the number of components is greater than or equal to the rank of the sample factor space, PLS essentially becomes equivalent to multivariate linear regression. It is therefore important to balance the number of components that are used to fit the PLS model to avoid both under-specified and over-fitted models (Geladi and Kowalski 1986; Lindgren et al. 1994). In practice, some heuristic is applied to select the number of components that are used to fit the model.

To this end, we designed an iterative algorithm that would test the importance of each predictor at a time by excluding it from the set of predictors and evaluating the fit (in terms of overall leave-one-out cross-validated root mean squared [CV-RMS] error) of the

model using all predictors that remained in the model. If, on excluding the predictor, the overall model fit increased, the predictor was permanently excluded from the candidate model and a new search initiated. Specifically, at each step, one variable was excluded from the set of 'k' predictors and a standard PLS model was fit with the reduced set of predictors (k-1 predictors). The optimal number of latent components to use for fitting this PLS model was determined by sequentially fitting PLS models with an increasing number of components until the leave-one-out CV-RMS error of the reduced model started to increase. Once the optimal number of components was determined, the CV-RMS error of the reduced PLS model was retained in a vector.

As each predictor variable in the data set was sequentially excluded, the CV-RMS error vector was evaluated to determine the set of k-1 predictors having the lowest CV-RMS error. The dropped variable resulting in the smallest RMS error was excluded permanently from the set of predictors, and a new iteration was initiated with the remaining predictors. Iterations continued until all but one predictor remained in the model. At the end of all iterations, a candidate set of models equal to the number of predictors were generated. By design, each model contained progressively fewer predictors (i.e. from k variables to 1 variable). All candidate models were sorted by their respective CV-RMS errors and the model with the lowest CV-RMS error was identified as the best model. Importantly, as all variables were tested iteratively within each candidate set of predictors, and as a leave-one-out cross-validation scheme was used to assess the CV-RMS error, the procedure ensured that the model would arrive at the exact same set of models for any number of runs. The iterative variable exclusion PLS algorithm (hereafter xPLS)

was developed and implemented in Matlab v. R2010a (Mathworks Inc., Natick MA, USA) and executed on a Condor distributed computing cluster (Epema et al. 1996).

Literature cited

Epema, D.H.J., Livny, M., vanDantzig, R., Evers, X., & Pruyne, J. (1996). A worldwide flock of Condors: Load sharing among workstation clusters. *Future Generation Computer Systems, 12*, 53-65

Frank, I.E., & Friedman, J.H. (1993). A statistical view of some chemometrics regression tools. *Technometrics, 35*, 109-135

Geladi, P., & Kowalski, B.R. (1986). Partial least-squares regression - a tutorial. *Analytica Chimica Acta, 185*, 1-17

Grossman, Y.L., Ustin, S.L., Jacquemoud, S., Sanderson, E.W., Schmuck, G., & Verdebout, J. (1996). Critique of stepwise multiple linear regression for the extraction of leaf biochemistry information from leaf reflectance data. *Remote Sensing of Environment, 56*, 182-193

Lindgren, F., Geladi, P., Rannar, S., & Wold, S. (1994). Interactive variable selection (IVS) for PLS .1. Theory and algorithms. *Journal of Chemometrics, 8*, 349-363

Wold, S., Ruhe, A., Wold, H., & Dunn, W.J. (1984). The Collinearity Problem in Linear-Regression - the Partial Least-Squares (Pls) Approach to Generalized Inverses. *Siam Journal on Scientific and Statistical Computing, 5*, 735-743

Wold, S., Sjostrom, M., & Eriksson, L. (2001). PLS-regression: a basic tool of chemometrics. *Chemometrics and Intelligent Laboratory Systems, 58*, 109-130

Chapter 2: Continuous-time modeling of streamwater nutrient loading from forests in the Chesapeake Bay watershed using MODIS and meteorological data

Abstract

Despite concerted and extensive efforts by multiple state and federal agencies, streams in the Chesapeake Bay watershed continue to show poor indicators of water quality due to nitrogen and phosphorus loading from agricultural operations, urban and suburban runoff, wastewater, airborne contaminants and other sources. Although urban point sources and agricultural area sources are well characterized by existing models such as the BASINS-HSPF system used by watershed managers, characterization of nutrient loads from forests remain difficult to quantify. This study presents the application of a new modeling technique, functional linear concurrent modeling (FLCM), to predict monthly variation in nitrate-N loading for 2001-2008 from streams draining forested watersheds in the Chesapeake Bay basin, with the ultimate objective being to better estimate nutrient loading from forested areas using freely available, spatially explicit satellite, meteorological and other geospatial data. In our application, FLCMs use time series in both response and predictor variables to identify the relative importance in the magnitude and timing of hypothesized drivers of intra-annual variations in water quality. Models built using FLCMs explained 81% of the variation in monthly streamwater nitrate loads for nine mostly forested watersheds over eight years of monitoring data. Cross-validation (dropping one watershed or year and rerunning the model) accuracies ranged from 50-85% for dropped watersheds and 60-87% for dropped years. Variables derived from remote sensing proved

especially useful for predicting monthly nitrate-N loading from forests, with monthly MODIS NDVI being positively related to higher water quality in all but late summer months (and unrelated in summer months), a remote sensing disturbance index positively related to higher late summer loads of stream nitrate-N (and unimportant the rest of the year), and evergreen/deciduous proportions important during non-growing season months. While our model confirms that mean nitrate-N loads from forests assumed by BASINS-HSPF are well-founded (HSPF: 2.76 kg/ha/yr, our model median: 2.75 kg/ha/yr), our model suggests that inter-annual loads from forests can vary from 2.31 kg/ha/yr to 4.43 kg/ha/yr. Spatial predictions obtained from the FLCMs may be instrumental in targeting management efforts and for better representing forests in process-based models such as BASINS-HSPF.

Introduction

The Chesapeake Bay has been the subject of intensive research on the effects of human land use on eutrophication, resulting in extensive efforts to reduce nutrient inputs (e.g. Fisher et al. 1992, Boynton et al. 1995, Paerl et al. 1998, Boesch et al. 2001, Anderson et al. 2002, Kemp et al. 2005, Phillips 2007, USEPA 2008). However, monitoring data continue to show poor indicators of water quality related to low populations of many species of fish and shellfish (USEPA 2013). Although the Bay waters did not meet 79% of water quality goals set by the EPA in 2009 (CBPO 2009), there have been improvements since then, with approximately 7.12 M kg less nitrogen delivered to the Bay in 2011 than 2009 (CBPO 2012), amounting to a 24.5 M kg decline from the 1990-2008 average load. Phosphorus loads have declined 0.4 M kg (2009-2011: CBPO 2012) and additional significant gains have been made in restoring wetlands (15.27 km^2 in 2010-2011), opening fish migration pathways (238 km in 2011) and planting forest buffers (386 km added in 2011). Despite these advances, goals to improve dissolved oxygen levels and water clarity and restore bottom habitat have yet to be achieved, and issues with nutrient management remain central concerns for agencies. In particular, there is great interest in closing uncertainties in nutrient budgets from non-point sources (Townsend et al. 2004, Yanai et al. 2012).

Point sources of nitrogen, phosphorus, and sediment to the Bay include municipal wastewater facilities, industrial discharge facilities, combined sewer outflows (CSOs), sanitary sewer outflows (SSOs), National pollutant discharge elimination system (NPDES) permitted stormwater (municipal separate storm sewer systems and construction and

industrial sites), and concentrated animal feeding operations (CAFOs). Nonpoint sources include agricultural lands (animal feeding operations, croplands, hay and pastures), atmospheric deposition, forest disturbance and nonregulated stormwater runoff (USEPA 2010b). A central component to the suite of solutions proposed to address water quality in the Bay includes establishment and apportioning of total maximum daily loads (TMDLs) per land use among states. The TMDL, the largest ever developed by EPA, encompass the 165,759 km^2 watershed, identifies the necessary pollution reductions from major sources of nitrogen, phosphorus and sediment across the District of Columbia and large sections of Delaware, Maryland, New York, Pennsylvania, Virginia and West Virginia, and sets pollution limits necessary to meet water quality standards in the Bay and its tidal rivers (USEPA 2010c). A TMDL refers to the maximum amount of a pollutant that a body of water can receive and still meet state water quality standards designed to ensure waterways meet a national primary goal of being swimmable and fishable (USEPA 2010c). TMDLs are typically determined using modeling approaches calibrated to water quality monitoring data. The modeling approaches, in turn, are conditioned on present and future land use patterns (USEPA 2010a).

Forested regions represent a significant portion of the Chesapeake Bay watershed (~54%). According to estimates by the Chesapeake Bay Program Office (CBPO), forested land contributes the lowest loading rate per unit area of all the land uses (Koroncai et al. 2003). Studies have also indicated that a significant portion of the loads do not originate in the forests but from atmospheric deposition of nitrogen (Langland et al. 1995, Aber and Driscoll 1997, Goodale et al. 2002, Pan et al. 2004). The Chesapeake Bay Phase 5.3

Community Watershed Model (USEPA 2010a) assumes only atmospheric deposition as an input load for forests, woodlots, and wooded land use. The model prescribes a median forest total nitrogen load to be 3.47 kg/ha/yr (un-harvested: 1.82 kg/ha, harvested: 11.56 kg/ha, and assumed to correspond with an average atmospheric deposition of about 23.52 kg/ha/yr), which increases linearly with increases in atmospheric deposition. The loads from forested components of watersheds are estimated through model calibration based on a small number of monitoring stations in forested areas (USEPA 2010d). Although reasonable under moderate levels of nitrogen loading from forests, it has been suggested that nitrogen saturation occurs in forests at high levels of deposition, and the rate of export can increase at a rate higher than the rate of deposition increase (Aber et al. 1989, Aber et al. 1993, Hunsaker et al. 1993, Goodale et al. 2002) or during disturbance events such as defoliation by insects (Eshleman 2000, Eshleman et al. 2000, Goodale et al. 2000, Aber et al. 2002, Townsend et al. 2004, McNeil et al. 2007, Eshleman et al. 2009). Similarly, the long-term experiment in the Hubbard-Brook Experimental Forest (HBEF; Bormann and Likens 1979) has demonstrated that while nitrogen is generally retained in forest ecosystems, nitrogen losses several orders of magnitude can occur during extensive disturbances. The HBEF work also demonstrated that there are reproducible seasonal patterns in nutrient effluence, with lower export during the growing season and highest export during the dormant season.

Non-point processes can have a disproportionate impact on water quality indicators for watersheds of all sizes (Grayson et al. 1997, Howarth 1998, Basnyat et al. 2000, Maillard and Pinheiro Santos 2008). As such, spatial data have been employed

increasingly as inputs for building and calibrating both empirical and mechanistic water - quality models. At the simplest, land-use/land-cover (LULC) classifications have often been employed to predict water quality on broader scales (for e.g. Mattikalli and Richards 1996, Johnes and Heathwaite 1997, Bhat et al. 2006) and a majority of studies have indicated positive correlations between agriculture and urban land cover and NO_3-N concentrations in receiving waters (Johnson et al. 1997, Jordan et al. 1997, Buck et al. 2004, Robertson et al. 2006, Stanley and Maxted 2008). In areas with high forest cover, however, models using land cover data to predict water quality are not very accurate (Herlihy et al. 1998). Methodologically, when using remotely sensed variables in addition to LULC data, most empirical models employ regression techniques to identify relationships between water quality metrics and remotely sensed variables: either simple bivariate regression (Griffith 2002, McNeil et al. 2007, Stanley and Maxted 2008, Eshleman et al. 2009), multiple regression (Osborne and Wiley 1988, Allan et al. 1997, Meador and Goldstein 2003, Townsend et al. 2004, Robertson et al. 2006, Maillard and Pinheiro Santos 2008), or partial least squares regression (Lopez et al. 2008, Singh et al. 2013). Although these techniques have been successful to varying degrees, and many allow building predictive models that are spatially-explicit, most such models are fixed in time (i.e. predictions are often made for summer baseflow conditions or annual averages).

Spatially and temporally continuous predictions of water quality could result in more effective targeting of management actions such as setting of TMDLs by season *and* location. Classical statistics techniques such as linear, multiple or PLS regressions are not conducive for such applications due to the inherent temporal autocorrelation in the data.

Although techniques such as ARMA (Harding and Perry 1997) offer an alternative, the size-effect of the temporal trajectories of the variables (i.e. rate and timing of vegetation green-up, climatic variations and timing of disturbance events) cannot be explicitly modeled. In contrast, the widely used SPARROW nonlinear optimization model (Brakebill and Preston 2003) has been successfully applied in an empirical context for many studies in the Chesapeake Bay (for e.g.: Roberts et al. 2009, Brakebill et al. 2010, Roberts and Prince 2010), but to date only one study has generalized it to explain inter-annual variations in nutrient loading using Bayesian means (Wellen et al. 2012).

Our objective is to develop ecologically meaningful, landscape-scale and *near-continuous* time empirical models for predicting nitrate loads from forested regions of the Chesapeake Bay Watershed using remote sensing, meteorological and GIS data. Specifically, the approach is intended to generate an algorithm for inputting MODIS-derived and gridded climate data products to estimate monthly nitrogen loads from the forested portions of watersheds across years. To this end, we use a newly developed technique, functional regression, to relate time series of nutrient loads in stream water with time series of satellite-derived measures of ecosystem variability and disturbance, GIS descriptors of watershed physiography, and climate data to generate predictive models. Overall, we: 1) investigate what factors influence streamwater nutrient loading in predominantly forested watersheds, 2) build nutrient loading models independent of direct water quality measures, 3) integrate temporal variation in environmental factors such as climate and disturbance and biological factors such as vegetation phenology, 4) provide

insights into when a variable matters (in addition to how much) and, 5) build nutrient loading models are generalizable across space and time.

Material and methods

Study area

The current land use in the Chesapeake Bay watershed (Fig 1) is about 54 percent forest or wooded, 26 percent agriculture and pasture, and 8 percent developed land. Nearly 17.7 million people live in the basin, and the population is estimated to increase to about 20 million by 2030 (USEPA 2010b). Runoff and groundwater from the Chesapeake watershed flow into an estuary with a surface area of 11,655 km^2 (~4,500 square miles). The largest estuary in the U.S., the Chesapeake has been the subject of considerable conservation efforts due to its exceptional biological productivity and cultural importance.

Our objective is the development of a general model to predict nutrient loading from forested areas of the watershed. To calibrate such a model, we require loading data from primarily forested watersheds, in which the contribution from agricultural nonpoint sources are minimal. Our study therefore focuses on watersheds that are largely forested (>80%) and for which water quality data are available for the MODIS record (2001-onwards). We employ data from nine predominantly forested watersheds ranging in area from 8 km^2 to 2,536 km^2 and in forested proportions ranging from 87.5% to 93.9%: Blacklick Run, Cedar creek, Jackson River, Pine Creek, Cowpasture River, Sinnemahoning Creek, Kettle Creek, Upper Big Run, Deep Run (Fig 2). Table 1 shows the location, area and relative distribution of forest land cover in each watershed.

Water quality data

The nine gaged watersheds have extensive daily discharge and periodic (monthly or higher frequency) nutrient concentration data that are suitable for analysis of long-term nitrate-N load and concentration trends. The six larger watersheds have been continuously gaged by U.S. Geological Survey, and water samples have been periodically collected at the outlet of these watersheds by state water quality agencies and analyzed for nitrate-N in accredited water quality laboratories. The three smaller watersheds have been monitored for more than ten years by the authors following comparable methods. Water samples were analyzed for nitrate-N concentration using a flow injection or segmented flow instrument in which the nitrate ion reacts with sulfanilamide and N-(1-naphthyl) ethylenediamine following cadmium reduction; nitrite-N concentrations were subtracted to obtain nitrate-N values. We computed continuous daily nitrate-N loads from the streamflow and nitrate-N time series for each station using (LOADEST: Runkel et al. 2004) following Eshleman et al. (in press). Daily loads were aggregated and normalized by watershed area to generate monthly nitrate-N yields (kg/ha). We log-transformed nitrate-N loads before all analysis to conform to assumptions on normality.

Satellite data

MODIS data from the NASA Terra satellite platform was obtained through the online Data Pool at the NASA Land Processes Distributed Active Archive Center (LP DAAC), USGS/Earth Resources Observation and Science (EROS) Center, Sioux Falls, South Dakota (https://lpdaac.usgs.gov/data_access). We used MODIS Version 5 product

MOD09A1 (500m 8-day composite surface reflectance) for our analyses. Data from four MODIS tiles (h11-h12, v04-v05) were reprojected to a common reference system and datum (UTM18N, NAD83) mosaicked, clipped to the study area, and masked by quality control flags. Basic vegetation indices – NDVI [(NIR-RED)/(NIR+RED)] and NDII [(SWIR1-NIR)/(SWIR1+NIR)] were estimated for each satellite image. In addition, we generated Tasseled Cap indices using coefficients following Lobser and Cohen (2007). Tasseled Cap indices (soil brightness, vegetation greenness and surface/vegetation wetness) have previously been utilized for characterizing vegetation seasonal dynamics for forest disturbance and agricultural studies (for e.g.: Skakun et al. 2003, Healey et al. 2005, Jin and Sader 2005). The Tasseled Cap indices were used in the disturbance index (following Healey et al. 2005), formulations of which have also been used to link forest disturbance to nitrogen export from watersheds (for e.g. Townsend et al. 2004, McNeil et al. 2007, Eshleman et al. 2009). We hypothesized that increasing vegetation greenness in the spring months would correspond to lower nitrate loads in the corresponding time period, while greater brightness and disturbance indices would correlate positively with nitrate loads since greater amounts of exposed soil and disturbance would lead to a greater nutrient flushing potential, especially when coupled with concurrent precipitation. All remote sensing measures were averaged by month and by watershed for analysis.

Meteorological data

Monthly gridded precipitation data were sourced from the PRISM climate database (http://www.prism.oregonstate.edu/) and aggregated to the watershed level similar to the MODIS data. We also included total atmospheric nitrate deposition data (monthly,

gridded) from the National Atmospheric Deposition Program (NADP, http://nadp.sws.uiuc.edu/) to account for direct nitrate inputs to watersheds.

Watershed characteristics

We included simple and widely used parameters to describe the physiography and landcover of each watershed. The variables considered were: Stream length, stream density and deciduous forest landcover. Stream length and density were obtained by clipping streamwater networks obtained from the NHDplus dataset (NHDPlus 2010) to watershed polygons followed by spatial measurements in a GIS. Deciduous land cover proportion was obtained from the National Land Cover Database (NLCD 2006: Fry et al. 2011). We hypothesized that 1) longer stream lengths ameliorate nitrate loads in watershed outlets by increasing residence time and resulting in higher in-stream processing and uptake of nutrients, 2) higher stream densities represent faster-draining watersheds and have an amplifying effect on nitrate loads, and 3) greater deciduous land cover characterizes the residual variation of nitrate loading between coniferous and deciduous-dominated watersheds.

Statistical methods

Functional data analysis

Our modeling strategy was designed to provide 1) temporally dynamic predictions, 2) predictions down-scalable to periods shorter than the observation time frame, and 3) information on when a predictor had a significant effect on the response (NO_3-N loads) as well as, in the classical regression sense, how much. Classical regression approaches can provide information on how much a variable is important (in terms of coefficient effect

sizes), but dynamic predictions generally have required data-intensive process-based models (e.g. HSPF: Bicknell et al. 1996). Recent developments in functional data analysis (FDA; Ramsay 1997, Ramsay and Silverman 2002) have somewhat narrowed this gap for a number of applications, including remote sensing (Zhang et al. 2011). However, applications of FDA techniques in ecology remain relatively rare. In brief, FDA techniques are predicated on approximating time-varying predictors using continuously derivable functions that are then regressed on similarly approximated time-varying (functional) or scalar responses. Ordinary least squares (OLS) regression models are formulated such that:

$$y_i = \alpha + \sum \beta_j x_i + \in_i, \quad (1)$$

Where: α = model intercept, β = model coefficients, y = responses, x = predictors, and $\in$ = model error term. In contrast, a functional model with a scalar response (with the β having an explicit dependency on t) has the basic form:

$$y_i = \alpha + \sum \beta_j x_i(t_j) + \in_i. \quad (2)$$

Letting t_j be increasingly dense, a functional linear model becomes conceptually similar to a multivariate OLS model with the sums replaced by integrals:

$$y_i = \alpha + \int \beta(t)\, x_i(t_j) + \in_i, \quad (3)$$

Where t is represented as a continuum, and $x_i(t_i)$ and $\beta(t)$ represented as smooth functions using a variety of basis function expansions (Fourier, cubic, polynomial, etc.). When the response also varies in the corresponding time period as the predictors, the formulation is termed a functional linear *concurrent* model (FLCM) with responses, predictors and model coefficients all approximated using sets of (possibly different) basis expansions:

$$y_i(t) = \alpha + \int \beta(t)\, x_i(t_j) + \in_i. \quad (4)$$

The flexibility of functional data objects to be approximated using a variety of basis function expansions makes it convenient to model smoothly varying periodic (e.g. Fourier), non-periodic (e.g. bicubic spline, polynomial), or episodic (e.g. wavelet) time series. While the formulation and estimation of functional linear models differ significantly from OLS models, the results are interpreted in much the same manner, but also provide richer information due to the effect of timing being explicitly captured in the models. That is, beta coefficients obtained from OLS regression provide information on whether the particular predictor(s) explains a significant amount of variation in the response; functional coefficients also show when in the time series that predictor is significant. Functional models therefore allow building dynamic models, but it is important to emphasize that they are statistical-empirical constructs that, while valid across the domain of the inputs, may not provide reliable predictions during exceptional events. Full details of the mathematical formulation of functional data analysis are provided in the seminal work by Ramsay and Silverman (2002). We used the package fda (Ramsay et al. 2013) in R (R 2008) for all analyses.

We modeled the water quality information from each year*watershed combination as a single observation. Modeled observations comprised one year of data (12-data points), with a total of 90 observations (9 watersheds * 10 years) derived from 1080 (90 * 12 months) data points of original load estimates. We used Fourier basis expansions for approximating the monthly variation in nitrate loads and for all time-varying predictor variables (NDVI, precipitation, disturbance) because: 1) bicubic spline approximations

produced over/under shoots estimates at the ends of time series, and 2) most of these variables were essentially periodic and could be considered stationary for the purpose of one (annual) observation. To avoid overfitting smoothed observations when approximating functions for time-varying responses and predictors, the amount of smoothing applied for each profile was determined by conducting a grid search of number of basis functions ranging from three to eleven (in steps of twos) and values of the roughness penalty ranging from 0.1 – 5.0 (in steps of 0.1) and selecting the combination that provided the lowest generalized cross-validation error (following Ramsay et al. 2007). Other temporally static explanatory variables (e.g. stream length, stream density, deciduous land cover) were entered in the models as scalars.

Missing data were estimated by fitting cubic splines to the entire time series of each watershed and replacing missing observations with fitted values. We preferred cubic splines for data filling because Fourier series approximations obscured annual-scale trends when data from all years were used. During initial tests, generalized cross-validation statistics showed agreement between predicted and randomly dropped observations, although cubic splines caused artifacts (under- and over- shooting the range of data) at the end of time series. We consequently dropped the first (2000) and last (2009) years of available data from the analyses. The study consequently uses data only from the 2001-2008 periods (eight years).

Lag effects

FDA regression techniques allow the predictions of continuously varying responses on similarly structured functions or scalar predictors, with the model responses assumed to be

concurrent. In other words, an effect scales to a response at the same observation time (e.g. precipitation at time *t* affects flushing at time *t*). This assumption might hold true for many applications, but nutrient flushing effects may be significantly lagged per the timing and extent of ecosystem perturbations in watersheds. Lag effects in nutrient flushing have long been recognized (Bormann and Likens 1979), especially by Eshleman et al. (1998) in a study conducted in watersheds within our study region. To investigate and adjust for lag effects in our data, we conducted cross-correlation analyses of all predictors lagged up to two years with observed NO_3-N loads at watershed outlets. We identified peaks in the cross-correlation coefficients, and then pre-lagged the corresponding variables before including them as predictors in the final models.

Validation

Statistical analyses using continuous-time long-term records pose considerable constraints on validation due to the inherently small sample size of such records. Instead of using a classical leave-observation-out validation strategy that risks pseudo-replication (the watershed being in the training sample set), we followed a conservative cross-validation strategy wherein 1) a watershed's entire record was dropped from the training dataset and predicted using the rest to test how the model performed on a randomly sampled watershed and 2) all watersheds were iteratively dropped from a given year and the model built with the training dataset comprising all other years to predict how well the model performed on a randomly sampled year.

Results

Functional approximations of nitrate-N loads across all watersheds and years closely matched observed patterns of variation ($R^2 = 0.91$, Fig 3). Nitrate-N loads at watershed outlets generally followed annual cyclic patterns that peaked in the spring months (February-May) and were the lowest in the fall (August-October, Fig 3). Cross-correlation analysis of nitrate loads against predictor variables suggested different but expected lag periods (Fig 4). Nitrate-N loads did not lag precipitation, but were lagged in NDVI by approximately a month ($r_{1\ month} = -0.54$), nitrate-N loads lagged the disturbance index by a 13 months ($r_{13\ months} = 0.14$). We lagged the disturbance index by one year ($r_{1\ year} = 0.09$), since lagging data by 13 months would incur the loss of one entire year of data across all watersheds; also, studies in similar landscapes have found empirical evidence of nitrate loads lagging disturbance by a year (Eshleman et al. 1998, Eshleman 2000, Eshleman et al. 2000).

Beta coefficients obtained from fitted FLCMs revealed that precipitation was highly and positively related with nitrate loads throughout the year, with the effect of precipitation peaking in the fall (Fig 5). The pattern of influence of NDVI was markedly seasonal, with nitrate-N loads declining with increasing NDVI in the green-up and brown-down phases of vegetation phenology and not significant elsewhere. In contrast, nitrate-N loads were highly positively correlated in the mid-growing season with one-year-lagged disturbance index (higher disturbance during the previous summer corresponded to higher nitrate-N load). Stream density had a similar response profile as disturbance (positively related during the growing season), stream length had the opposite effect, indicating

watersheds with greater lengths of streams retaining larger amounts of nitrate throughout year except during the growing season when the effect was not significant. As expected, N-deposition had a generally amplifying effect on nitrate loads throughout the year, but this effect was the most apparent during the green-up and brown-down shoulder seasons. A larger proportion of deciduous forest cover dampened overall nitrate-N loads, but the effect was not significant in the mid-growing season.

Overall, the model agreed well with observed data (Fig 6, Table 2). Across all years and watersheds, the model explained around 81% of the variation in data (74% with the raw data, i.e. non-Fourier smoothed nitrate-N data.) Per-watershed predictions were consistently high ($R^2 = 0.74 – 0.90$) except for Jackson River ($R^2 = 0.65$, RMSE = 0.294). The model performed well across all years ($R^2 = 0.73 – 0.90$), with the worst performance in 2004 ($R^2 = 0.68$). Month-by-month predictions had the lowest fits ($R^2 = 0.63 – 0.75$), likely as a consequence of using a constant lag for all watersheds. Cross-validation statistics confirmed the Jackson River watershed (CV $R^2 = 0.59$, CVRMSE = 0.376), the Pine Creek watershed (CV $R^2 = 0.50$, CVRMSE = 0.601) and the year 2004 (CV $R^2 = 0.60$, CVRMSE = 0.377) as persistent outliers. When aggregated across all watersheds, the model predicted ~95% of all variation in the data (89% using unsmoothed data) indicating the effectiveness of the model in capturing large-scale seasonal changes in nitrate loads (Fig 7, 8A). Aggregated across watersheds and years, the model tracks inter-annual variations in nitrate-N loads as they related to precipitation and vegetation phenology. Moreover, our results capture observed declining trends in nitrate-N loading into the Bay from 2004 onwards (Eshleman et al. in press, Fig 8B).

Discussion

The intent of this study was to develop ecologically meaningful, landscape-scale and nearly continuous-time indicators of nutrient loads from forests using remote sensing data for the Chesapeake Bay watershed. To this end, we developed predictive models using functional linear concurrent models to relate time series of nutrient loads in stream water with time series of satellite-derived measures of ecosystem variability and disturbance, as well as climate data. For broader application, the proposed models needed to both use data independent of direct water quality measures, and integrate temporal variation in environmental factors such as climate, disturbance, and vegetation phenology in addition to classically used parameters of watershed physiography and land cover. Our models matched observations well, and provided insights into when as well as how much each hypothesized predictor was important. We expect that similar accuracies could be obtained using other empirical techniques, but the FLCM approach provided unique insights into the temporal pattern of relationships between the putative environmental drivers and nitrate-N loads at watershed outlets. For example, significant and large coefficients for precipitation confirm the role of precipitation in flushing nutrients from watersheds, with the maximum flushing occurring in the end-of-season phenological phase of vegetation, when uptake by vegetation is lowest and contributions due to senescence is highest.

The interaction of the seasonality of precipitation effects and vegetation phenology is likely related to the general pattern of nutrient attenuation in streams, in which watersheds with longer stream lengths retain more nutrients, but only during the vegetation

uptake period and in the fall when in-stream heterotrophic uptake of N is prevalent (McDowell and Fisher 1976, Goodale et al. 2009). Similarly, the correspondence between the timing of influence of disturbance and stream density may indicate precipitation-facilitated nutrient flushing from disturbed ecosystems (Goodale et al. 2000, Aber et al. 2002, Eshleman et al. 2009) in comparatively more dissected landscapes. Patterns of nitrogen deposition followed expected reinforcing effects on stream water nitrate export (Fenn and Poth 1999, Aber et al. 2002, Eshleman et al. 2009). Increasing deciduous cover corresponded to lower nitrate-N loading into streamwater both in the spring and fall (Fig 5). Increased uptake of nutrients during green-up is a widely recognized phenomenon (Koyama et al. 2008, Ueda et al. 2009, El Zein et al. 2011), explaining the importance of deciduous forest cover in the spring. The relative importance of deciduous compared to evergreen forests in the fall is likely due to faster decomposability of fall foliage from broadleaved deciduous trees and therefore greater immediate in-stream heterotrophic uptake (McDowell and Fisher 1976, Goodale et al. 2009).

Overall model fits and cross-validations indicate that our model was robust to variations in forest dynamics and environmental conditions. However, predictions of nitrate-N loads in some years and watersheds were persistently under- or over- predicted, most notably the year 2004. 2004 followed a record wet year (2003) that had followed a record dry year (2001). Kaushal et al (2008) studied approximately 1000 streams in Maryland around the same time period and found that watershed-scale nitrate retention declined drastically in 2003. We believe that the patterns we observed in our data are the continuation of this phenomenon. Watershed-wise, nitrate-N loads from the Pine Creek

and Jackson River watersheds were under-predicted when cross-validated against other watersheds. Given that variations in nitrate-N loads from these watersheds were largely similar to those from other watersheds, we suspect this is an interaction of the larger size and relatively higher non-forest landcover of these watersheds (mean 2107 km^2, 14.71% non-forest) compared to the rest (mean 435 km^2, 11.02% non-forest). On average, these differences translate to an over six-fold difference in non-forest land area that contributes to nitrate-N loads at the watershed outlet. As our model is applicable to (and only applied to) forested pixels in a watershed, the contribution of non-forest pixels is likely under-represented in predicted loads and thus negatively biases the predictions. This illustrates the difficulty in accurately characterizing nutrient loads from forests, i.e., the lack of suitably large, entirely forested watersheds for model calibration/validation.

Aggregated across months and watersheds, predicted nitrate-N loads followed a pattern of decline (Fig 8) that has been observed in streamwater data post-2004 (CBPO 2012) and in general in the past decade (Eshleman et al. in press). While model uncertainty may be highest at the monthly scale, the fact that the modeled trends in loads match observations provides confidence that our methodology is robust to decadal-scale variations in water quality, while also matching the larger patterns in intra-annual variations. The results of our work provide insights that may benefit other empirical approaches, such as the SWALLOW model of Wellen et al. (2012), and may provide an alternate strategy to parameterization of forests in process-based models.

Finally, the effect of N-deposition was not a major predictor in the model (in comparison to say, precipitation (Fig 5), even though annually aggregated trends in

predicted nitrate loads correlated highly with trends in N deposition ($r = 0.863$, $P = 0.005$). N deposition was included in the model as a monthly-static but yearly-varying variable, and likely captured the effect of declining N deposition (Burns 2011) in influencing the water quality of streams across the Chesapeake Bay Watershed.

Conclusion

Overall, this study reaffirms that climate and landscape variables have a strong influence on nutrient loading to streams from the forested component of watersheds. We also provide new insights into when these variables exert the greatest influence in addition to their relative influence. Information on the timing of the importance of a variable should help in targeting management efforts in both space and time. Such models may also be of use to management agencies for scenario generation under varying land management policies. Though the inherent limitations of empirical models constrain them to operate within the range of observed data, temporally-varying predictions may be instrumental in better calibrating mechanistic models such as BASINS-HSPF (Bicknell et al. 1996), which currently assumes constant loads from forested ecosystems. While mean annual predictions from our model matched those assumed by HSPF well (HSPF: 2.76 kg/ha/yr, our model median: 2.75 kg/ha/yr), our model suggests annual nitrate-N loads can vary from 2.31 kg/ha/yr to 4.43 kg/ha/yr. The study also shows that FLCMs coupled with readily available satellite, meteorological and climate data may be viable for making continuous-time models for many other natural resource management applications or for mixed land uses. Our modeling approach used MODIS data as a major input, data from sensors with similar

measurements strategies such as the VIIRS aboard the Suomi-NPP mission could ensure long-term continuity.

Literature cited

Aber, J. D., and C. T. Driscoll. 1997. Effects of land use, climate variation, and N deposition on N cycling and C storage in northern hardwood forests. Global Biogeochemical Cycles **11**:639-648.

Aber, J. D., A. Magill, R. Boone, J. M. Melillo, P. Steudler, and R. Bowden. 1993. Plant and soil responses to chronic nitrogen additions at the Harvard Forest, Massachusetts. Ecological Applications **3**:156-166.

Aber, J. D., K. J. Nadelhoffer, P. Steudler, and J. M. Melillo. 1989. Nitrogen Saturation in Northern Forest Ecosystems. Bioscience **39**:378-386.

Aber, J. D., S. V. Ollinger, C. T. Driscoll, G. E. Likens, R. T. Holmes, R. J. Freuder, and C. L. Goodale. 2002. Inorganic nitrogen losses from a forested ecosystem in response to physical, chemical, biotic, and climatic perturbations. Ecosystems **5**:648-658.

Allan, J. D., D. L. Erickson, and J. Fay. 1997. The influence of catchment land use on stream integrity across multiple spatial scales. Freshwater Biology **37**:149-161.

Anderson, D. M., P. M. Glibert, and J. M. Burkholder. 2002. Harmful algal blooms and eutrophication: Nutrient sources, composition, and consequences. Estuaries **25**:704-726.

Basnyat, P., L. D. Teeter, B. G. Lockaby, and K. M. Flynn. 2000. The use of remote sensing and GIS in watershed level analyses of non-point source pollution problems. Forest Ecology and Management **128**:65-73.

Bhat, S., J. M. Jacobs, K. Hatfield, and J. Prenger. 2006. Relationships between stream water chemistry and military land use in forested watersheds in Fort Benning, Georgia. Ecological Indicators **6**:458-466.

Bicknell, B. R., J. C. Imhoff, J. L. Kittle, Jr., and A. S. J. Donigian. 1996. Hydrological simulation program—FORTRAN user's manual for release 11. U.S. Environmental Protection Agency.

Boesch, D. F., R. B. Brinsfield, and R. E. Magnien. 2001. Chesapeake Bay eutrophication: Scientific understanding, ecosystem restoration, and challenges for agriculture. Journal of Environmental Quality **30**:303-320.

Bormann, D. B., and G. E. Likens. 1979. Pattern and process in a forested ecosystem. Springer-Verlag, New York.

Boynton, W. R., J. H. Garber, R. Summers, and W. M. Kemp. 1995. Inputs, transformations, and transport of nitrogen and phosphorus in Chesapeake Bay and selected tributaries. Estuaries **18**:285-314.

Brakebill, J. W., S. W. Ator, and G. E. Schwarz. 2010. Sources of Suspended-Sediment Flux in Streams of the Chesapeake Bay Watershed: A Regional Application of the SPARROW Model1. Journal of the American Water Resources Association **46**:757-776.

Brakebill, J. W., and S. D. Preston. 2003. A hydrologic network supporting spatially referenced regression modeling in the Chesapeake Bay watershed. Environmental Monitoring and Assessment **81**:73-84.

Buck, O., D. K. Niyogi, and C. R. Townsend. 2004. Scale-dependence of land use effects on water quality of streams in agricultural catchments. Environmental Pollution **130**:287-299.

Burns, D. A. 2011. NAPAP: National Acid Precipitation Assessment: Program report to congress 2011: An integrated assessment. US Geological Survey.

CBPO. 2009. Bay Barometer: Spotlight on health and restoration in the Chesapeake Bay and its watershed. US ENvironmental protection agency, Annapolis, MD.

CBPO. 2012. Bay Barometer: Spotlight on health and restoration in the Chesapeake Bay and its watershed. US ENvironmental protection agency, Annapolis, MD.

El Zein, R., N. Breda, D. Gerant, B. Zeller, and P. Maillard. 2011. Nitrogen sources for current-year shoot growth in 50-year-old sessile oak trees: an in situ N-15 labeling approach. Tree Physiology **31**:1390-1400.

Eshleman, K. N. 2000. A linear model of the effects of disturbance on dissolved nitrogen leakage from forested watersheds. Water Resources Research **36**:3325-3335.

Eshleman, K. N., R. H. Gardner, S. W. Seagle, N. M. Castro, D. A. Fiscus, J. R. Webb, J. N. Galloway, F. A. Deviney, and A. T. Herlihy. 2000. Effects of disturbance on nitrogen export from forested lands of the Chesapeake Bay watershed. Environmental Monitoring and Assessment **63**:187-197.

Eshleman, K. N., B. E. McNeil, and P. A. Townsend. 2009. Validation of a remote sensing based index of forest disturbance using streamwater nitrogen data. Ecological Indicators **9**:476-484.

Eshleman, K. N., R. P. Morgan, J. R. Webb, F. A. Deviney, and J. N. Galloway. 1998. Temporal patterns of nitrogen leakage from mid-Appalachian forested watersheds: Role of insect defoliation. Water Resources Research **34**:2005-2016.

Eshleman, K. N., R. A. Sabo, and K. M. Kline. in press. Surface water quality is improving due to declining atmospheric N deposition. Environmental Science & Technology.

Fenn, M. E., and M. A. Poth. 1999. Temporal and spatial trends in streamwater nitrate concentrations in the San Bernardino Mountains, southern California. Journal of Environmental Quality **28**:822-836.

Fisher, T. R., E. R. Peele, J. W. Ammerman, and L. W. Harding. 1992. Nutrient limitation of phytoplankton in Chesapeake Bay. Marine Ecology Progress Series **82**:51-63.

Fry, J., G. Xian, S. Jin, J. Dewitz, C. Homer, L. Yang, C. Barnes, N. Herold, and J. Wickham. 2011. Completion of the 2006 National Land Cover Database for the Conterminous United States. PE&RS **77**:858-864.

Goodale, C. L., J. D. Aber, and W. H. McDowell. 2000. The long-term effects of disturbance on organic and inorganic nitrogen export in the White Mountains, New Hampshire. Ecosystems **3**:433-450.

Goodale, C. L., K. Lajtha, K. J. Nadelhoffer, E. W. Boyer, and N. A. Jaworski. 2002. Forest nitrogen sinks in large eastern US watersheds: estimates from forest inventory and an ecosystem model. Biogeochemistry **57**:239-266.

Goodale, C. L., S. A. Thomas, G. Fredriksen, E. M. Elliott, K. M. Flinn, T. J. Butler, and M. T. Walter. 2009. Unusual seasonal patterns and inferred processes of nitrogen retention in forested headwaters of the Upper Susquehanna River. Biogeochemistry **93**:197-218.

Grayson, R. B., C. J. Gippel, B. L. Finlayson, and B. T. Hart. 1997. Catchment-wide impacts on water quality: the use of 'snapshot' sampling during stable flow. Journal of Hydrology **199**:121-134.

Griffith, J. A. 2002. Geographic techniques and recent applications of remote sensing to landscape-water quality studies. Water Air and Soil Pollution **138**:181-197.

Harding, L. W., and E. S. Perry. 1997. Long-term increase of phytoplankton biomass in Chesapeake Bay, 1950-1994. Marine Ecology Progress Series **157**:39-52.

Healey, S. P., W. B. Cohen, Z. Q. Yang, and O. N. Krankina. 2005. Comparison of Tasseled Cap-based Landsat data structures for use in forest disturbance detection. Remote Sensing of Environment **97**:301-310.

Herlihy, A. T., J. L. Stoddard, and C. B. Johnson. 1998. The relationship between stream chemistry and watershed land cover data in the mid-Atlantic region, US. Water Air and Soil Pollution **105**:377-386.

Howarth, R. W. 1998. An assessment of human influences on fluxes of nitrogen from the terrestrial landscape to the estuaries and continental shelves of the North Atlantic Ocean. Nutrient Cycling in Agroecosystems **52**:213-223.

Hunsaker, C., R. Graham, R. S. Turner, P. L. Ringold, G. R. Holdren, and T. C. Strickland. 1993. A National Critical Loads Framework for Atmospheric Deposition Effects Assessments: II. Defining Assessment End Points, Indicators, and Functional Subregions. Environmental Management **17**:335-341.

Jin, S. M., and S. A. Sader. 2005. Comparison of time series tasseled cap wetness and the normalized difference moisture index in detecting forest disturbances. Remote Sensing of Environment **94**:364-372.

Johnes, P. J., and A. L. Heathwaite. 1997. Modelling the impact of land use change on water quality in agricultural catchments. Hydrological Processes **11**:269-286.

Johnson, L. B., C. Richards, G. E. Host, and J. W. Arthur. 1997. Landscape influences on water chemistry in Midwestern stream ecosystems. Freshwater Biology **37**:193-+.

Jordan, T. E., D. L. Correll, and D. E. Weller. 1997. Relating nutrient discharges from watersheds to land use and streamflow variability. Water Resources Research **33**:2579-2590.

Kaushal, S. S., P. M. Groffman, L. E. Band, C. A. Shields, R. P. Morgan, M. A. Palmer, K. T. Belt, C. M. Swan, S. E. G. Findlay, and G. T. Fisher. 2008. Interaction between

urbanization and climate variability amplifies watershed nitrate export in Maryland. Environmental Science & Technology **42**:5872-5878.

Kemp, W. M., W. R. Boynton, J. E. Adolf, D. F. Boesch, W. C. Boicourt, G. Brush, J. C. Cornwell, T. R. Fisher, P. M. Glibert, J. D. Hagy, L. W. Harding, E. D. Houde, D. G. Kimmel, W. D. Miller, R. I. E. Newell, M. R. Roman, E. M. Smith, and J. C. Stevenson. 2005. Eutrophication of Chesapeake Bay: historical trends and ecological interactions. Marine Ecology Progress Series **303**:1-29.

Koroncai, R., L. Linker, J. Sweeney, and R. A. Batiuk. 2003. Setting and allocating the Chesapeake Bay basin nutrient and sediment loads: the collaborative process, technical tools and innovative approaches. US Environmental Protection Agency, Chesapeake Bay Program Office, Annapolis, Maryland.

Koyama, L., N. Tokuchi, K. Fukushima, M. Terai, and Y. Yamamoto. 2008. Seasonal changes in nitrate use by three woody species: the importance of the leaf-expansion period. Trees-Structure and Function **22**:851-859.

Langland, M. J., P. L. Lietman, and S. Hoffman. 1995. Synthesis of nutrient and sediment data for watersheds within the Chesapeake Bay drainage basin. US Geological Survey, Annapolis, Maryland.

Lobser, S. E., and W. B. Cohen. 2007. MODIS tasselled cap: land cover characteristics expressed through transformed MODIS data. International Journal of Remote Sensing **28**:5079-5101.

Lopez, R. D., M. S. Nash, D. T. Heggem, and D. W. Ebert. 2008. Watershed vulnerability predictions for the Ozarks using landscape models. Journal of Environmental Quality **37**:1769-1780.

Maillard, P., and N. A. Pinheiro Santos. 2008. A spatial-statistical approach for modeling the effect of non-point source pollution on different water quality parameters in the Velhas river watershed Brazil. Journal of Environmental Management **86**:158-170.

Mattikalli, N. M., and K. S. Richards. 1996. Estimation of surface water quality changes in response to land use change: Application of the export coefficient model using remote sensing and geographical information system. Journal of Environmental Management **48**:263-282.

McDowell, W. H., and S. G. Fisher. 1976. Autumnal processing of dissolved organic-matter in a small woodland stream ecosystem. Ecology **57**:561-569.

McNeil, B. E., K. M. de Beurs, K. N. Eshleman, J. R. Foster, and P. A. Townsend. 2007. Maintenance of ecosystem nitrogen limitation by ephemeral forest disturbance: An assessment using MODIS, Hyperion, and Landsat ETM. Geophysical Research Letters **34**:-.

Meador, M. R., and R. M. Goldstein. 2003. Assessing water quality at large geographic scales: Relations among land use, water physicochemistry, riparian condition, and fish community structure. Environmental Management **31**:504-517.

NHDPlus. 2010. Horizon Systems, NHDPlus documentation, version1, available online at http://www.horizon-systems.com/nhdplus/documentation.php.

Osborne, L. L., and M. J. Wiley. 1988. Empirical Relationships between Land-Use Cover and Stream Water-Quality in an Agricultural Watershed. Journal of Environmental Management **26**:9-27.

Paerl, H. W., J. L. Pinckney, J. M. Fear, and B. L. Peierls. 1998. Ecosystem responses to internal and watershed organic matter loading: consequences for hypoxia in the eutrophying Neuse river estuary, North Carolina, USA. Marine Ecology Progress Series **166**:17-25.

Pan, Y., J. Hom, R. Birdsey, and K. McCullough. 2004. Impacts of rising nitrogen deposition on N exports from forests to surface waters in the Chesapeake Bay watershed. Environmental Management **33**:S120-S131.

Phillips, S. W., editor. 2007. Synthesis of U.S. Geological Survey science for the Chesapeake Bay ecosystem and implications for environmental management. U.S. Geological Survey.

R. 2008. R: A language and environment for statistical computing. R Foundation for Statistical Computing.*in* R. D. C. Team, editor., Vienna, Austria.

Ramsay, J. O. 1997. Functional data analysis. Wiley, New York.

Ramsay, J. O., G. Hooker, J. Cao, and D. Campbell. 2007. Parameter estimation for differential equations: A generalized smoothing approach. Journal of the Royal Statistical Society, Series B **69**:741-796.

Ramsay, J. O., and B. W. Silverman. 2002. Applied Functional Data Analysis: Methods and case studies. Springer-Verlag., New York.

Ramsay, J. O., H. Wickham, S. Graves, and G. Hooker. 2013. FDA: functional data analysis.

Roberts, A. D., and S. D. Prince. 2010. Effects of urban and non-urban land cover on nitrogen and phosphorus runoff to Chesapeake Bay. Ecological Indicators **10**:459-474.

Roberts, A. D., S. D. Prince, C. A. Jantz, and S. J. Goetz. 2009. Effects of projected future urban land cover on nitrogen and phosphorus runoff to Chesapeake Bay. Ecological Engineering **35**:1758-1772.

Robertson, D. M., D. J. Graczyk, P. J. Garrison, L. Wang, G. Laliberte, and R. Bannerman. 2006. Nutrient Concentrations and their relations to biotic integrity of wadeable streams in Wisconsin.

Runkel, R. L., C. G. Crawford, and T. A. Cohn. 2004. Load Estimator (LOADEST): A FORTRAN Program for Estimating Constituent Loads in Streams and Rivers. Page 69 U.S. Geological Survey Techniques and Methods Book 4, Chapter A5. US Geological Survey.

Singh, A., A. R. Jakubowski, I. Chidister, and P. A. Townsend. 2013. A MODIS approach to predicting stream water quality in Wisconsin. Remote Sensing of Environment **128**:74-86.

Skakun, R. S., M. A. Wulder, and S. E. Franklin. 2003. Sensitivity of the thematic mapper enhanced wetness difference index to detect mountain pine beetle red-attack damage. Remote Sensing of Environment **86**:433-443.

Stanley, E. H., and J. T. Maxted. 2008. Changes in the dissolved nitrogen pool across land cover gradients in Wisconsin streams. Ecological Applications **18**:1579-1590.

Townsend, P. A., K. N. Eshleman, and C. Welcker. 2004. Remote sensing of gypsy moth defoliation to assess variations in stream nitrogen concentrations. Ecological Applications **14**:504-516.

Ueda, M. U., E. Mizumachi, and N. Tokuchi. 2009. Allocation of nitrogen within the crown during leaf expansion in Quercus serrata saplings. Tree Physiology **29**:913-919.

USEPA. 2008. Chesapeake Bay health and restoration assessment—A report to the citizens of the Bay region. U.S. Environmental Protection Agency.

USEPA. 2010a. Chesapeake Bay Phase 5.3 Community Watershed Model. U.S. Environmental Protection Agency, Chesapeake Bay Program Office, Annapolis MD.

USEPA. 2010b. Chesapeake Bay total maximum daily load for nitrogen, phosphorus and sediment : Indroduction, description, Chesapeake Bay water quality standards. United States Environment Protection Agency, Philadelphia, Pennsylvania.

USEPA. 2010c. Chesapeake Bay Total Maximum Daily Load for Nitrogen, Phosphorus and Sediment, executive summary., US Environmental Protection Agency, Annapolis, MD.

USEPA. 2010d. Chesapeake Bay total maximum daily load for nitrogen, phosphorus and sediment: Chesapeake Bay monitoring and modeling frameworks United States Environment Protection Agency, Philadelphia, Pennsylvania.

USEPA. 2013. A model program for onsite management in the Chesapeake Bay watershed. US Environment Protection Agency, Annapolis, MD.

Wellen, C., G. B. Arhonditsis, T. Labencki, and D. Boyd. 2012. A Bayesian methodological framework for accommodating interannual variability of nutrient loading with the SPARROW model. Water Resources Research **48**.

Yanai, R. D., C. R. Levine, M. B. Green, and J. L. Campbell. 2012. Quantifying Uncertainty in Forest Nutrient Budgets. Journal of Forestry **110**:448-456.

Tables

Table 1: Study watersheds sorted in order of increasing forest cover.

Name	Latitude	Longitude	% Forest	Area (km^2)
Pine Creek	41.273611	-77.324444	83.38	2536.75
Upper Big Run	39.596472	-79.176348	85.71	3.50
Jackson River	37.788611	-80.000833	87.19	1678.25
Cedar Creek	39.081111	-78.329722	87.45	292.75
Blacklick Run	39.609337	-79.082551	87.50	8.00
Cowpasture River	37.791667	-79.759722	87.93	1242.75
Sinnemahoning Creek	41.413333	-78.197222	89.34	813.75
Kettle Creek	41.319444	-77.874167	91.03	668.75
Deep Run	39.653586	-78.452090	93.90	20.50

Table 2: FLCM Model fit statistics stratified by watershed, year and month. Results are presented as coefficients of determination, model root mean square error, relative bias and sample size. Results are shown for models compared with Fourier-smoothed data (that the model was built with) and unsmoothed (raw) data.

		Smoothed data			Unsmoothed data		
Watershed		R^2	RMSE	Bias	R^2	RMSE	Bias
N = 96	Upper Big Run	0.81	0.332	0.086	0.75	0.376	0.086
	Blacklick Run	0.81	0.324	0.049	0.72	0.417	0.049
	Cedar Creek	0.74	0.269	0.083	0.66	0.293	0.083
	Cowpasture River	0.78	0.324	-0.166	0.68	0.383	-0.166
	Deep Run	0.84	0.513	-0.075	0.72	0.660	-0.075
	Sinnemahoning Creek	0.89	0.228	-0.101	0.82	0.293	-0.101
	Jackson River	0.65	0.294	0.046	0.56	0.351	0.046
	Kettle Creek	0.89	0.225	0.009	0.83	0.288	0.009
	Pine Creek	0.90	0.282	0.069	0.84	0.338	0.069
Year							
N = 108	2001	0.73	0.413	0.036	0.69	0.453	0.036
	2002	0.83	0.318	-0.074	0.78	0.373	-0.074
	2003	0.73	0.240	0.055	0.52	0.369	0.055
	2004	0.68	0.319	0.115	0.56	0.392	0.115
	2005	0.90	0.240	0.107	0.83	0.308	0.107
	2006	0.78	0.320	-0.015	0.68	0.408	-0.015
	2007	0.87	0.312	-0.141	0.77	0.417	-0.141
	2008	0.83	0.363	-0.083	0.79	0.408	-0.083
Month							
N = 72	January	0.71	0.278	0.000	0.62	0.341	0.016
	February	0.71	0.272	0.000	0.57	0.367	-0.123
	March	0.65	0.267	0.000	0.65	0.335	0.071
	April	0.62	0.257	0.000	0.45	0.283	0.036
	May	0.67	0.240	0.000	0.60	0.295	-0.040
	June	0.71	0.238	0.000	0.61	0.355	0.003
	July	0.67	0.325	0.000	0.45	0.444	-0.020
	August	0.63	0.422	0.000	0.52	0.501	0.013
	September	0.64	0.431	0.000	0.64	0.512	0.074
	October	0.72	0.381	0.000	0.65	0.422	-0.106
	November	0.75	0.344	0.000	0.76	0.380	0.001
	December	0.72	0.311	0.000	0.55	0.405	0.074
Overall							
N = 864		**0.81**	**0.320**	**0.000**	**0.74**	**0.393**	**0.000**

Table 3: FLCM Model validation statistics stratified by watershed and year, validations were conducted using a leave-watershed-out and leave-year-out strategy in which data from an entire year (or watershed) were withheld and predicted using the rest of the data used as a model training dataset. All models were built with Fourier-smoothed data; predictions on unsmoothed data are also presented.

	Training						Validation					
	Smoothed			Unsmoothed			Smoothed			Unsmoothed		
Watershed	R^2	RMSE	Bias	R^2	RMSE	Bias	R^2	RMSE	Bias	R^2	RMSE	Bias
Upper Big Run	0.83	0.309	0.000	0.76	0.387	0.000	0.80	0.659	-0.399	0.75	0.678	-0.399
Blacklick Run	0.81	0.313	0.000	0.74	0.384	0.000	0.68	0.434	-0.101	0.60	0.505	-0.101
Cedar Creek	0.83	0.323	0.000	0.75	0.401	0.000	0.69	0.369	-0.133	0.63	0.383	-0.133
Cowpasture River	0.82	0.313	0.000	0.75	0.389	0.000	0.72	0.441	0.263	0.63	0.486	0.263
Deep Run	0.84	0.271	0.000	0.77	0.332	0.000	0.73	0.747	0.214	0.63	0.853	0.214
Sinnemahoning Creek	0.81	0.327	0.000	0.73	0.401	0.000	0.85	0.309	0.180	0.79	0.352	0.180
Jackson River	0.82	0.321	0.000	0.75	0.396	0.000	0.59	0.376	-0.163	0.51	0.421	-0.163
Kettle Creek	0.80	0.329	0.000	0.73	0.403	0.000	0.86	0.256	-0.019	0.81	0.301	-0.019
Pine Creek	0.82	0.313	0.000	0.75	0.390	0.000	0.50	0.601	-0.262	0.48	0.628	-0.262
Year												
2001	0.83	0.301	0.000	0.75	0.381	0.000	0.68	0.456	-0.057	0.64	0.491	-0.057
2002	0.81	0.318	0.000	0.74	0.394	0.000	0.79	0.358	0.095	0.74	0.411	0.095
2003	0.81	0.328	0.000	0.74	0.394	0.000	0.62	0.301	-0.088	0.52	0.381	-0.088
2004	0.82	0.317	0.000	0.75	0.391	0.000	0.60	0.377	-0.141	0.43	0.468	-0.141
2005	0.81	0.328	0.000	0.74	0.402	0.000	0.87	0.294	-0.168	0.82	0.346	-0.168
2006	0.82	0.320	0.000	0.75	0.390	0.000	0.70	0.368	0.017	0.64	0.437	0.017
2007	0.81	0.318	0.000	0.74	0.386	0.000	0.80	0.412	0.195	0.75	0.456	0.195
2008	0.81	0.310	0.000	0.73	0.388	0.000	0.78	0.430	0.134	0.75	0.463	0.134

Figures

Figure 1: Land cover of the Chesapeake Bay watershed (NLCD 2006).

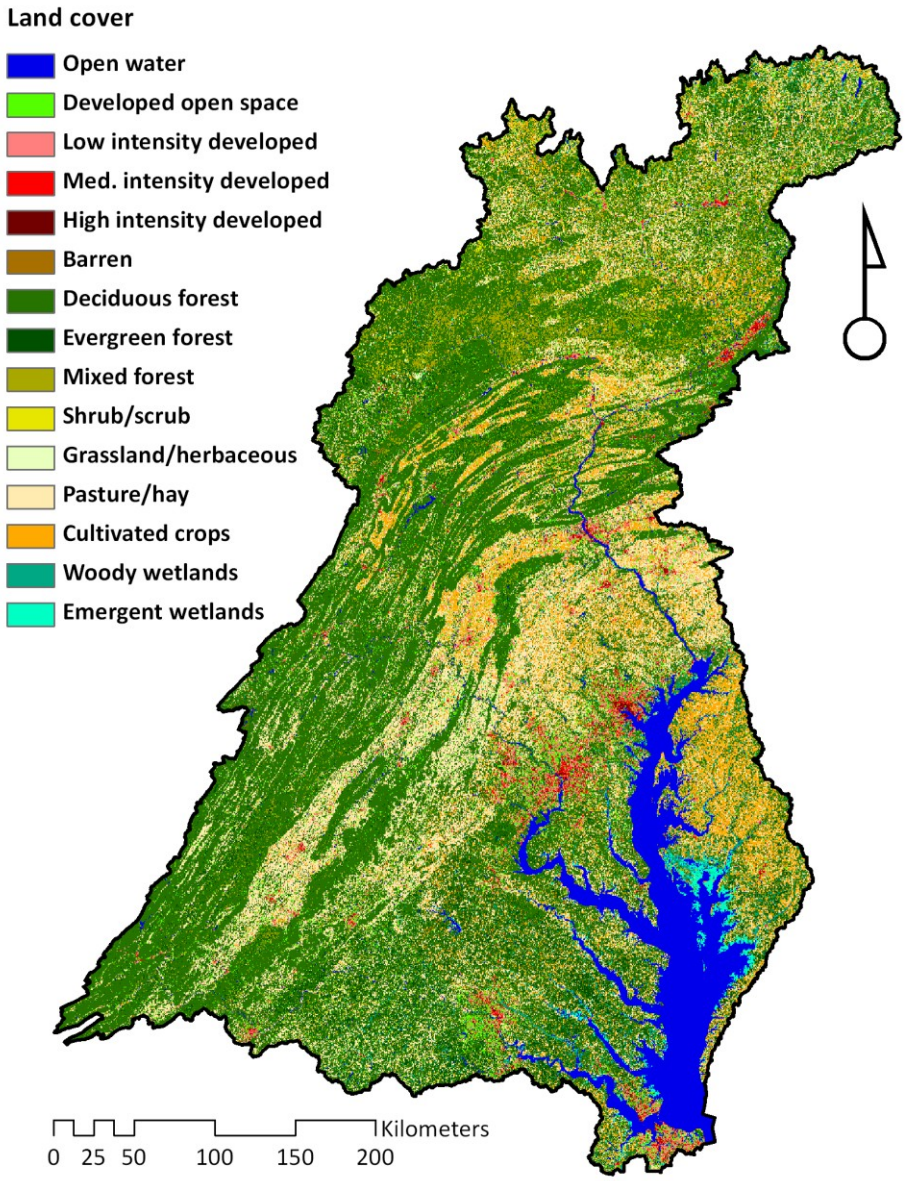

Figure 2: Location of sampled watersheds.

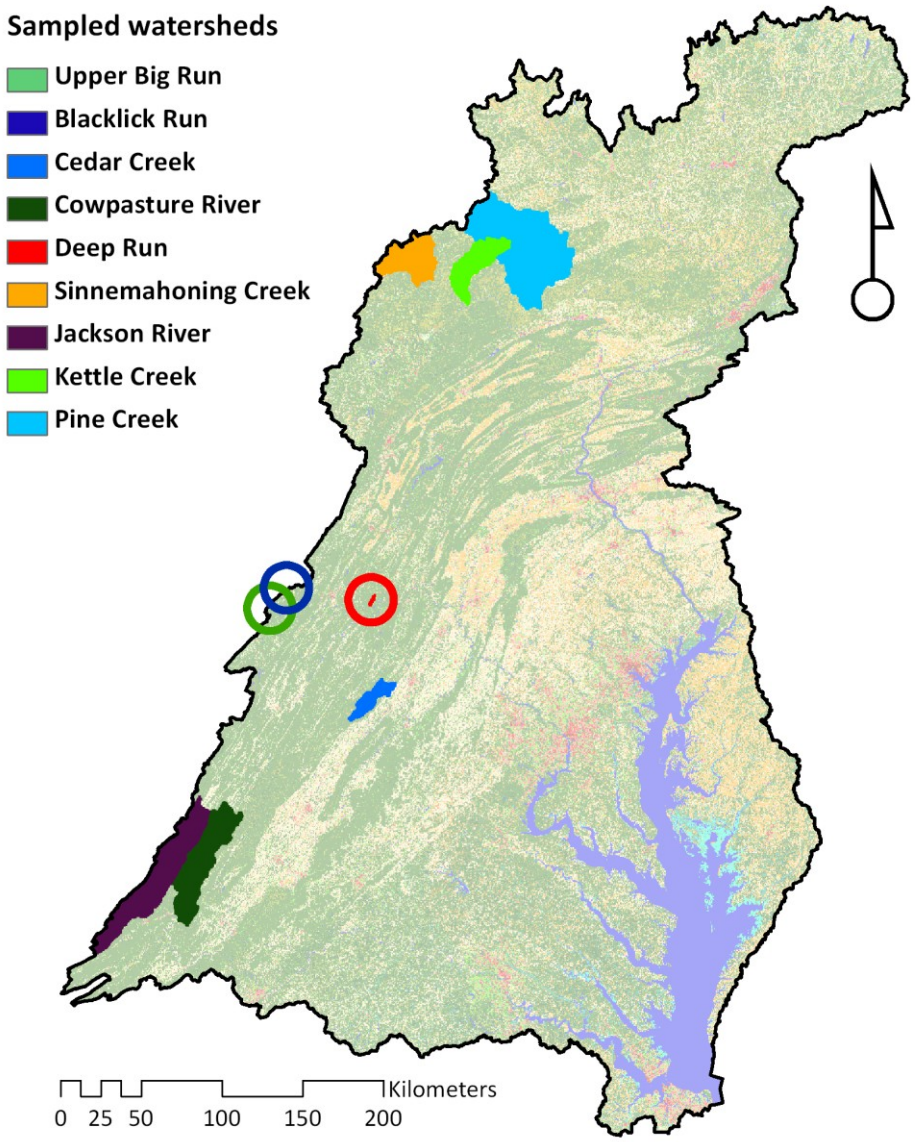

Figure 3: Comparison of (A) raw and (B) Fourier-basis smoothed profiles of log-transformed NO_3-N loads in study watersheds. (C) Illustrates match between raw and smoothed data. Line colors indicate year (2001-2008) and symbols indicate watersheds. The FLCM model utilizes Fourier-smoothed data (B) for all analyses.

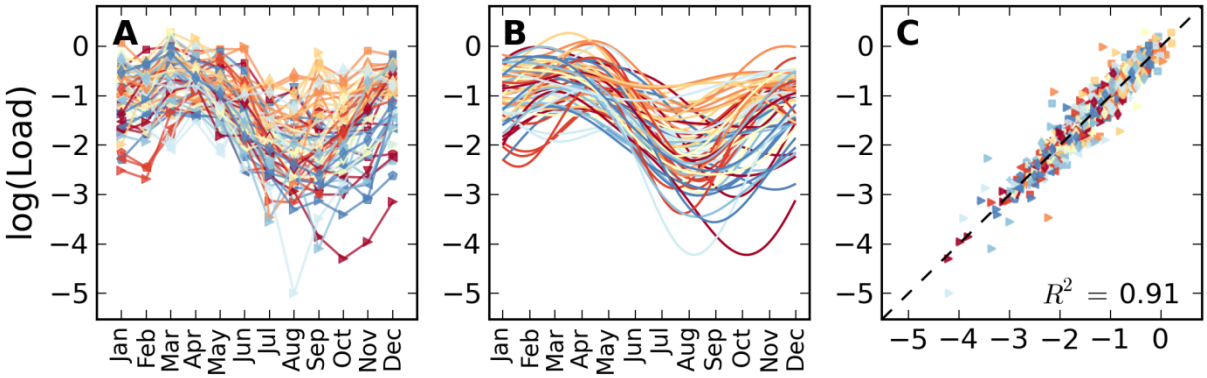

Figure 4: Cross-correlation plots of predictor variables with log (NO_3-N) loads. Cross-correlations were conducted to determine if NO_3-N loads had lagged responses to predictor variables. Cross-correlation coefficients averaged across watersheds (with standard deviation bars) are plotted (blue circles) for lag values ranging from zero to 17 months. Shaded regions indicate the period when the cross-correlation had the largest absolute value.

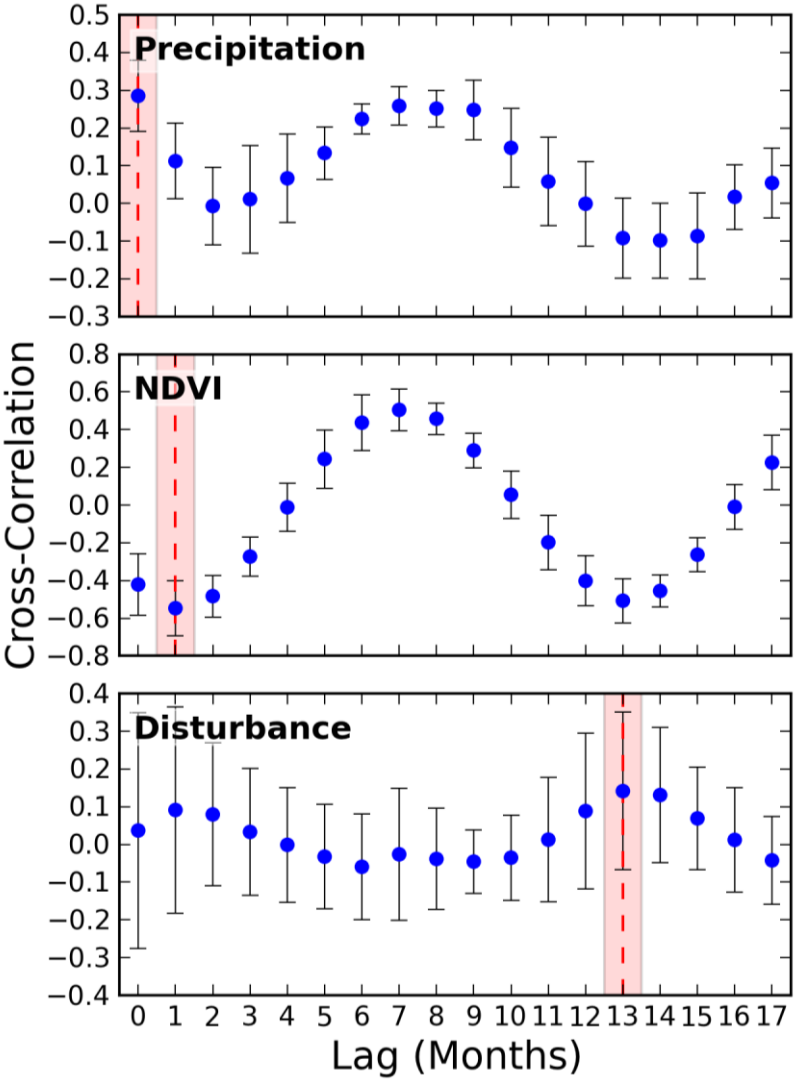

Figure 5: Beta coefficients obtained by fitting the functional linear concurrent linear model (FLCM) to Fourier-smoothed log nitrate-N load data. Shaded regions indicate the time periods where the 95% confidence intervals did not contain zero (i.e. the parameter was significant at α=95% level).

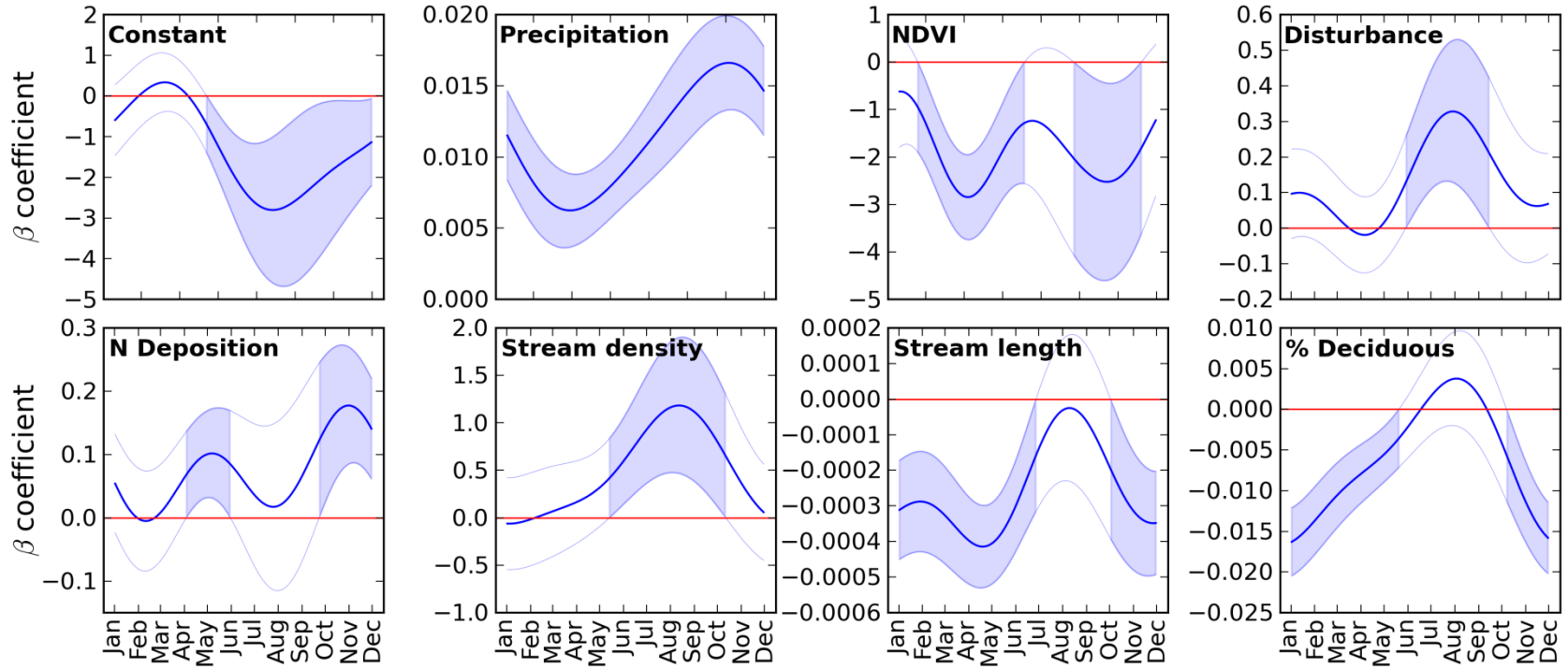

Figure 6: Model fits obtained from the functional linear concurrent model, with the model coefficient of determination (R^2) and associated root mean square error (RMSE). A) Fit between the Fourier smoothed data and unsmoothed data. B) Fit between Fourier smoothed data and model predictions. C) Fit between unsmoothed data and model predictions. Colors indicate different years (2001-2008) and symbols indicate different watersheds.

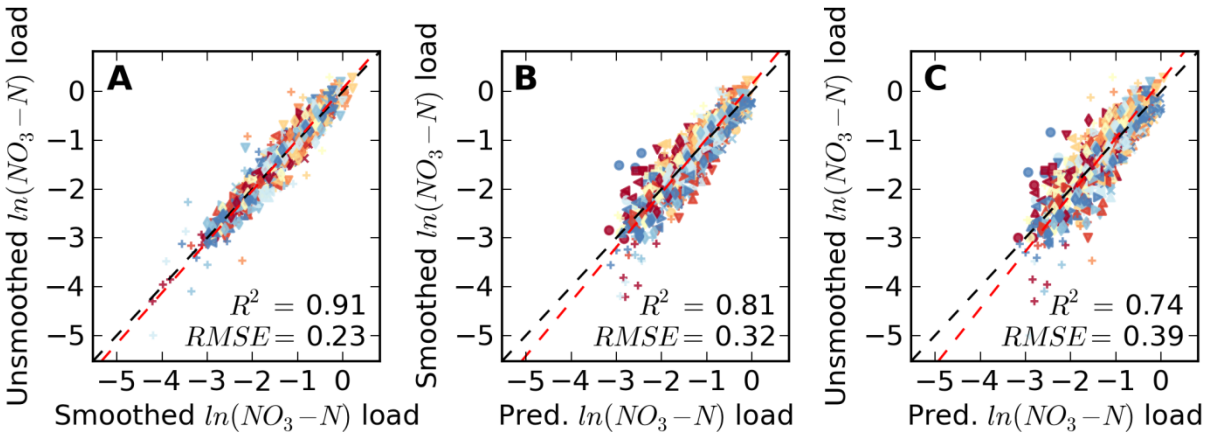

Figure 7: Model fits obtained from the functional linear concurrent model aggregated across watersheds, with coefficient of determination (R^2) and associated root mean square error (RMSE). Error bars show standard deviation in nitrate-N load by watershed. A) Fit between the Fourier-smoothed ln(NO_3-N) data and model predictions. B) Fit between unsmoothed data and model predictions. Note that models were built using Fourier smoothed data. Colors indicate different years (2001-2008).

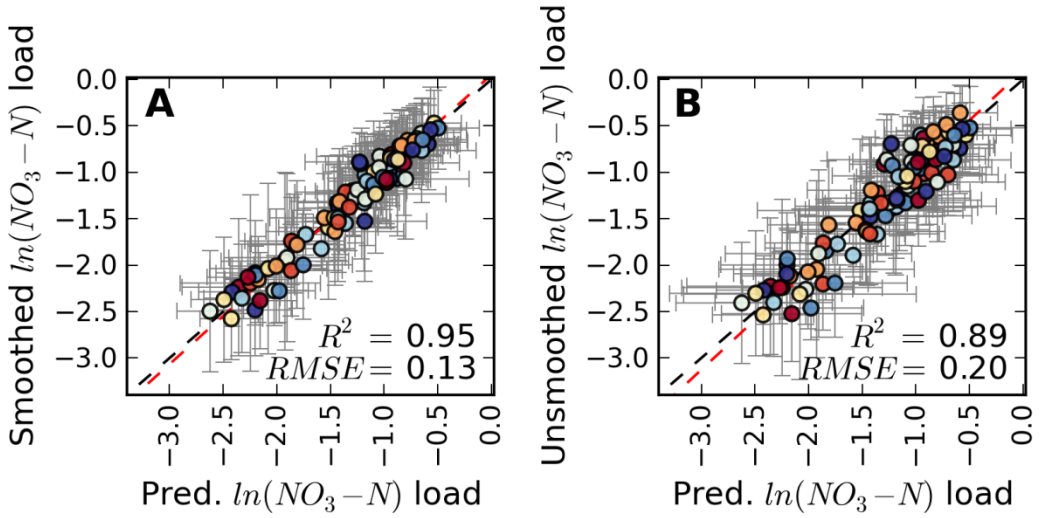

Figure 8: Model fits obtained from the functional linear concurrent model aggregated across watersheds through time. A) Monthly unsmoothed ln(NO_3-N) (red circles) and model predictions (green circles). B) Unsmoothed data and model predictions aggregated by year. Dotted lines denote trends in ln(NO_3-N) loads from 2004 onwards observed in raw data (red) and model predictions (green). Note that individual points in both subplots are offset from year centerlines for clarity.

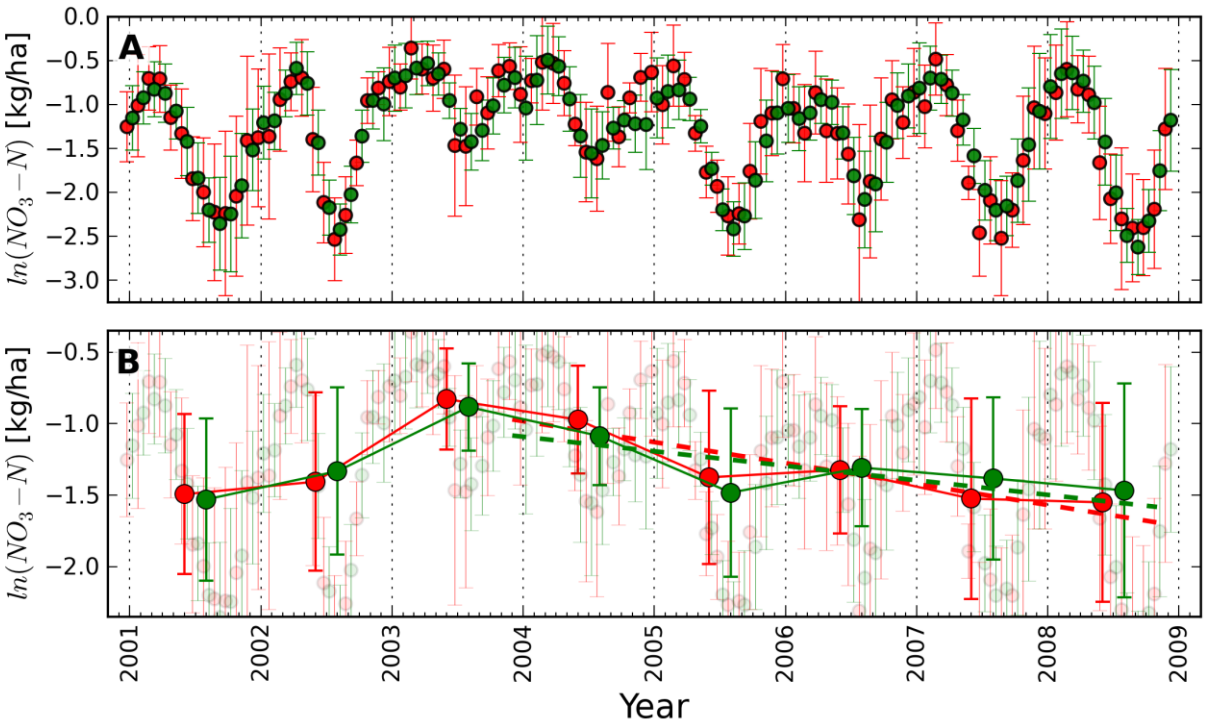

Figure 9: Spatial predictions obtained by applying the FLCM model on forest pixels (left panels) of the entire Chesapeake Bay watershed, and aggregated to HUC11 watersheds (right panels). Note log scale of color ramp. Predictions for the first four months of 2004 are shown. Pixel-scale predictions would be needed to be aggregated by total drainage-area weighted forest cover per stream outlets for streamwater assessments.

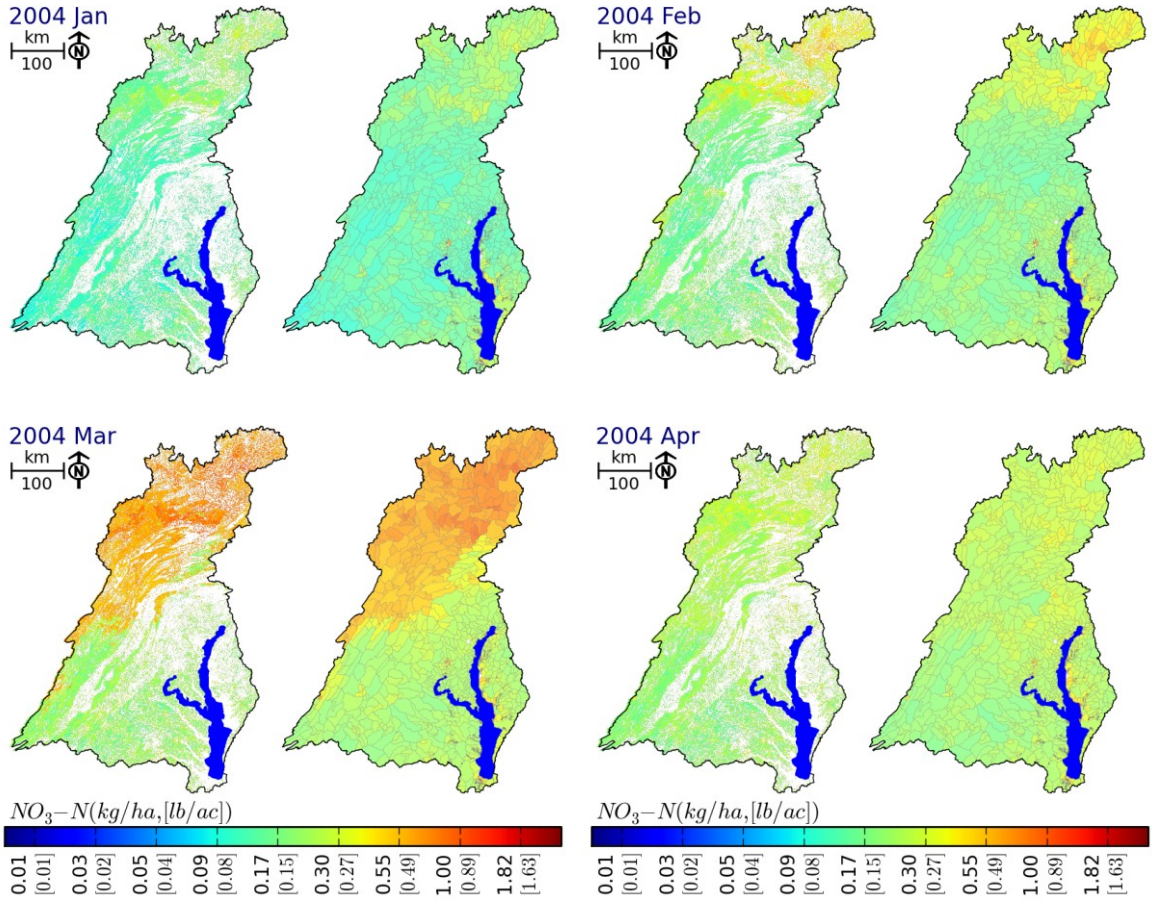

Chapter 3: Retrieval of canopy foliar chemical and morphological traits and their uncertainty from imaging spectroscopy

Abstract

A major goal of remote sensing is the development of generalizable algorithms to repeatedly and accurately map ecosystem properties across space and time. Imaging spectroscopy in particular has great potential for mapping vegetation traits that cannot be retrieved from broadband data, but has traditionally been limited by location-specific approaches. Here we illustrate a general approach for the estimation of key foliar chemical and morphological traits and the propagation of errors from the leaf to the image scale using partial least squares regression (PLSR) applied to data from 164 field plots within 51 AVIRIS images acquired between 2008-2011. We use a series of 500 randomized 50/50 subsets of the original data to generate spatially explicit maps of six traits (leaf mass per area (LMA), and percent nitrogen, carbon, fiber, lignin and cellulose) as well as pixel-wise uncertainty in their mapped estimates. Both LMA and %N PLSR models had a R^2 greater than 0.85. Root mean square errors (RMSEs) for both variables were less than 9% of the range of data. Fiber and lignin were predicted with $R^2 > 0.70$ and carbon and cellulose greater than 0.5. Although R^2 of %C and cellulose were lower than LMA and %N, the range in variability of these constituents (especially %C) was lower than %N or LMA, and their RMSE values were beneath 12%. The resulting maps of nutritional and morphological properties together with their overall uncertainties represent a first-of-its-kind data approach for examining the spatio-temporal patterns of forest functioning and

nutrient cycling. Specifically, these results offer an alternative to categorical maps of functional or physiognomic types by providing spatially continuous maps of the traits that define those functional types. A key contribution of this work is the ability to assign retrieval uncertainties by pixel, enabling more efficient assimilation of these data products into ecosystem models to help constrain carbon and nutrient cycling projections.

Introduction

Terrestrial ecosystems play an important role in the global carbon by sequestering 3-5 Pg of carbon (C) per year from the atmosphere via photosynthesis (Schimel 1995, Cramer et al. 2001, 2007, Le Quere et al. 2009). Characterization of the factors that influence the magnitude of terrestrial C uptake is required to develop a process-based understanding of ecosystem dynamics and accurately model vegetation response to environmental change. In particular, the chemical, structural and morphological properties of the foliage in vegetation canopies correlate strongly with plant function, including ecosystem-wide nutrient cycling rates (Scott and Binkley 1997, Craine et al. 2002, Santiago et al. 2004, Meier and Bowman 2008) and photosynthetic capacity (Reich et al. 1997, Reich et al. 1999, Shipley et al. 2005, Kergoat et al. 2008). Thus, research and modeling efforts to estimate the dynamics of global carbon stocks make use of the covariance between plant traits and patterns of biogeochemical cycling to determine ecosystem productivity (Enquist et al. 2007).

Recent research has shown that global patterns of nutrient cycling and primary productivity in forested ecosystems are driven in large part by a small suite of foliar structural and biochemical traits representing a tradeoff between leaf construction costs and photosynthesis (Reich et al. 1992, Shipley and Lechowicz 2000, Wright et al. 2004, Shipley et al. 2005, Shipley et al. 2006). Specifically, coordination between foliar nitrogen content and specific leaf area (SLA, or its reciprocal, leaf mass per area LMA) maximizes C-fixation (Shipley et al. 2005) and forms a fundamental axis describing tradeoffs between leaf lifespan and plant growth (Reich et al. 1991, Wright et al. 2004, Shipley et al. 2006).

Foliar nitrogen levels determine stomatal regulation in relation to the marginal cost of water loss relative to carbon gain as a tradeoff between allocation to structural tissues versus liquid phase processes (Shipley and Lechowicz 2000, Shipley et al. 2006). Whereas lower SLA results in lower foliage photosynthetic potential per unit dry mass (Niinemets 2001) it leads to greater leaf structural strength and consequently longer leaf life spans (Wright and Westoby 2002, Wright et al. 2005a, Violle et al. 2009). These patterns have been found to be consistent between broadleaf, needleleaf and herbaceous species (Reich et al. 1991, Reich et al. 1992, Grime 2006) and have been found to operate independent of growth form or phylogeny (Shipley et al. 2006). Foliar nitrogen also scales with the content of RuBisCo, the key protein in plants responsible for the carboxylation of RuBP in the initial steps of CO_2 fixation (Long 1991, Collatz et al. 1992, Ainsworth and Rogers 2007), and therefore modulates key photosynthesis parameters such as the maximum rate of carboxylation (V_{cmax}) and electron transport (J_{max}) (Long 1991, Ripullone et al. 2003).

Not surprisingly, these plant traits also co-vary strongly with decomposition and nitrogen mineralization rates across ecosystems (Chapin 2003, Kazakou et al. 2006, Quested et al. 2007, Santiago 2007). Decomposition is a critical source of plant nutrients and drives the largest flux of terrestrial C to the atmosphere (Meier and Bowman 2008). When controlled for climate, decomposition rates are positively correlated with nitrogen content of litter, SLA and leaf water content (Bonan 1993, Schadler et al. 2003). Litter decomposability is generally negatively correlated with leaf dry matter content (Garnier et al. 2004, Kazakou et al. 2006, Quested et al. 2007, Fortunel et al. 2009, Kazakou et al. 2009), foliar lignin concentrations (Robinson and Jolidon 2005, Hobbie et al. 2007,

Johnson et al. 2007, Carrera and Bertiller 2010) and positively with foliar nitrogen concentrations (Hattenschwiler et al. 2005, Kazakou et al. 2006, Fortunel et al. 2009). Lignin-to-nitrogen ratios have shown to be strong indicators of litter quality and consistent predictors of litter decomposability across a number of biomes (Melillo et al. 1982, Aerts 1997, Knorr et al. 2005, Hobbie et al. 2006, Quested et al. 2007, Fortunel et al. 2009) and together with cellulose concentration are considered rate regulating factors in late stages of forest litter decomposition (McClaugherty and Berg 1987, Berg 2000, Johnson et al. 2007). As such, synoptic, repeatable and consistent retrievals of key foliar traits such as foliar nitrogen, SLA (or LMA) and foliar lignin and cellulose may be invaluable for characterizing determinants of ecosystem function across large regions (Chapin et al. 1996, Diaz et al. 2004, Ustin and Gamon 2010), and may provide valuable inputs for modeling nutrient fluxes and vegetation range shifts under changing land-use and climate scenarios (Wright et al. 2004, Townsend et al. 2008).

Imaging spectrometers measure radiation reflected off the earth's surface in narrow, contiguous wavebands (typically ≤10-15 nm) over a large portion of the incident solar spectrum (e.g., 350-2500 nm for NASA's Airborne Visible/Infrared Imaging Spectrometer, AVIRIS, Vane et al. 1993, Green et al. 1998). It has long been demonstrated that spectroscopy is sensitive to foliar chemistry, and indeed this is the basis for standard spectroscopic approaches in a range of disciplines to estimate chemistry on dried samples (Kokaly 2001, Richardson and Reeves 2005, Petisco et al. 2006) or to non-destructively estimate chemistry or photosynthetic properties of fresh leaves (Curran et al. 1992, Sims and Gamon 2002, Blackburn 2007, Menesatti et al. 2010). The ability to do this is a

consequence of well-known biochemical absorption features (Curran 1989, Curran et al. 1992, Fourty et al. 1996, Curran et al. 2001) at different wavelengths of light related to electron transitions and bending and stretching of chemical bonds (Curran 1989, Fourty et al. 1996).

The ability to retrieve chemistry from remotely sensed imagery is more complicated, although it is clear that chemical features related to leaf chlorophyll (Curran et al. 1992, Yoder and Pettigrewcrosby 1995, Curran et al. 2001) and water content are clearly expressed in both narrowband and broadband imagery (Gates et al. 1965, Tucker 1980, Asner and Vitousek 2005, Sanchez-Azofeifa et al. 2009, Ustin et al. 2012). The effects of canopy structure on reflectance do confound the identification of absorption features in foliage (Knyazikhin et al. 2013), but these occur primarily in the near infrared wavelengths where leaf scattering is highest and there are not features commonly associated with biochemical retrieval. Further, there is evidence that features identifiable at the leaf-level can be enhanced at the canopy level (Baret et al. 1994). Ultimately, the coordination of traits at both the leaf and canopy level facilitates using spectral information to map traits of interest, even if the physical basis for strong correlations have not been fully characterized (Townsend et al. 2003, Ollinger 2011, Ollinger et al. 2013).

A considerable and growing body of literature has demonstrated very strong sensitivity of imaging spectroscopy data to foliar traits relevant to photosynthesis (Wessman et al. 1989, Matson et al. 1994, Curran et al. 1997, Martin and Aber 1997, Coops et al. 2003, Smith et al. 2003, Townsend et al. 2003, Asner and Martin 2008, Martin et al. 2008, McNeil et al. 2008, Kokaly et al. 2009). One of the key findings of the research to date is

that spectra in the shortwave infrared (especially 1400-1850 nm and 2000-2400 nm) are critical to retrieval of parameters related to photosynthesis on account of strong absorption features related to nitrogen bonds in proteins that are expressed in those regions (Fourty et al. 1996). Supplementary Table S1 summarizes recent literature on the direct use of canopy spectra obtained from spectroscopic imagery to map foliar biochemical and morphological traits of forest canopies.

Additional studies have shown that radiative transfer models (Asner 1998, Asner et al. 2008, Asner and Martin 2008, 2009, Asner et al. 2011a) can be used in conjunction with imaging spectroscopy to map foliar traits effectively. To our knowledge, however, apart from Martin et al. (2008), studies that incorporate information from multiple scenes across multiple locations are rare. Site-specific studies include Coops et al. (2003) and Townsend et al. (2003), who employed only a single or small number of images from a single study area, and Ollinger et al. (2002a), who used a large number of images of one study area acquired on a single date. Martin and Aber (1997) demonstrated for a small data set that a regression-based calibration could be built for two study sites, Harvard Forest (Massachusetts) and Blackhawk Island (Wisconsin), although predictions from one site to the other were not successful.

Our goal is the development and application of generalizable algorithms to repeatedly and accurately map ecosystem properties such as foliar traits across space and time (Townsend et al. 2003, Ustin et al. 2004, Majeke et al. 2008, Ustin and Gamon 2010). Remote sensing research at the leaf and canopy scales has demonstrated the capacity to characterize the biochemical status of forest canopies from stand to landscape scales using

air- and space-borne imaging spectrometers (Ustin et al. 2004, Carlson et al. 2007, Asner et al. 2011a). In this study, we report a set of spectroscopic calibrations for the determination of leaf chemical composition (nitrogen, carbon, and fiber constituents) and morphology (leaf mass per area, LMA) of temperate and boreal tree species using imaging spectroscopy. We demonstrate techniques to explicitly propagate uncertainties from the leaf to the plot to the image scale. The resulting maps of nutritional and morphological properties together with their overall uncertainties represent a first-of-its-kind data product for examining the spatio-temporal patterns of forest functioning and nutrient cycling. These data can be used to relate foliar traits with ecosystem processes such as streamwater nutrient export and insect herbivory. In addition, the ability to assign a retrieval uncertainty enables more efficient assimilation of these data products into ecosystem models to help constrain carbon and nutrient cycling projections.

Materials and methods

Study sites

We established 164 sample sites in diverse forest types across seven major ecoregions (Omernik 1987, Omernik et al. 2000, McMahon et al. 2001) spanning the upper Midwest (n=106) and Eastern U.S. (n = 58, Figure 1, see list of dominant species in Supplementary Table S2 and all plots and their locations in Supplementary Table S3). 54 plots were located in The Northern Lakes and Forests ecoregion, characterized by nutrient-poor glacial soils, undulating till plains, morainal hills, broad lacustrine basins, and extensive sandy outwash plains dominated by coniferous and northern hardwood forests. This region

is mostly dominated by *Acer saccharum* and *Betula alleghaniensis*, interspersed with *Pinus resinosa* and *Populus tremuloides* stands. *Pinus banksiana* is the dominant species in the Pine Barrens, co-dominant with *Quercus macrocarpa*. Bogs and wetlands in the region are generally dominated by *Larix laricina*, *Picea mariana* and in some locations *Thuja occidentalis*. Large stands of old-growth *Tsuga canadensis* can be found in the Porcupine mountains and have been sites of intensive research of stand dynamics and forest regeneration (Frelich and Lorimer 1991, Dahir and Lorimer 1996) and biogeochemical cycling (Mladenoff 1987). Much of this region is dominated by highly-productive second-growth hardwood forests that were largely clearcut between 1850-1930 (Rhemtulla et al. 2009). The high productivity of this ecosystem has been intensively studied for carbon stock assessments and energy flux studies (Davis et al. 2003, Cook et al. 2004, Desai et al. 2008) and is also the location of the Chequamegon Ecosystem Atmosphere Study (ChEAS) studying the impacts of disturbance and environmental influences on forest carbon and energy fluxes within northern temperate forests (Burrows et al. 2003, Ahl et al. 2004, Cook et al. 2004, Schulte et al. 2005).

Ten plots were located on Blackhawk Island in the North Central Hardwood Forests ecoregion. The island is dominated with large stands of *A. saccharum* and *Quercus rubra* interspersed with stands of *Pinus strobus* with *Ostrya virginiana* in the understory. Blackhawk Island has hosted intensive studies on nutrient cycling (Pastor et al. 1982, 1984) and was the location of some of the first uses of imaging spectroscopy (Wessman et al. 1988) as well as the use of AVIRIS imagery to map foliar nutrients for incorporation into biogeochemical models (Martin and Aber 1997). Eleven plots were located in the

Wisconsin's Driftless Area, consisting of deeply dissected, loess-capped, bedrock dominated plateaus. The diverse forests and woodlots in this region are characterized by *A. saccharum* dominated stands with *Q. rubra* co-dominant, and large stands of *P. strobus* and *P. resinosa* co-dominant with *Acer rubrum* and *Carya ovata*. The Southeastern Wisconsin Till Plains to the south contained another 31 plots, the majority of which (29) were located within intact urban forests of the Madison metropolitan area and are characteristic of the North Central Hardwoods region. These plots fall in the transition zone between the hardwood forests and oak savannas to the west and the tallgrass prairies of the Central Corn Belt Plains to the south. Ecosystems in this region have been studied extensively for the effects of anthropogenic disturbance (Bresee et al. 2004, Grossmann and Mladenoff 2008) and the effects of land cover on regional water quality (Meador and Goldstein 2003, Lathrop 2007, Diebel et al. 2008, Singh et al. 2013).

In the eastern U.S., 22 plots were located in the Adirondacks Park in the North Appalachian and Atlantic Maritime Highlaneds ecoregion. These plots were dominated by *Fagus grandifolia* and *A. saccharum* associations, with *B. alleghaniensis* and *P. resinosa* co-dominants and considerable understory of *A. rubrum* and *Abies balsamifera*. This ecoregion is characterized by hills and mountains, mostly forested land cover, nutrient-poor soils, and numerous high-gradient streams and glacial lakes. Lakes and streams in this region have been impacted by acidification due to atmospheric deposition originating in industrialized areas upwind from the ecoregion to the west and this area has been the subject of numerous studies of N deposition on forests (Aber et al. 1997, McNeil et al. 2007b, Crowley et al. 2012).

Finally, 36 plots were located in the Ridge and Valley and Central Appalachians Ecoregions to the south of the Adirondacks. The Central Appalachian sites were located in cool, wet mountainous areas of the Appalachian Plateau, while the Ridge and Valley plots occur in comparatively warmer, drier ridgelines in the rain shadow of the Appalachians (Chastain et al. 2006). Present-day forests are dominated by a variety of oak associations including *Q. alba, Q. prinoides*, *Q. rubra*, and *Q. velutina*, as well as *A. saccharum*, *A. rubrum, Pinus strobus, T. canedensis*, with *Carya glabra and Fraxinus americana* as the sub-dominant species. Forests in this larger region have been affected by post-industrial acid deposition and subsequent recovery. A large number of studies have been conducted on the effects of acidic deposition on N saturation of these forests (Aber et al. 1989, Aber et al. 1998, Aber et al. 2003), and consequently the effects of N deposition on soil and foliar C:N ratios (McNeil et al. 2007b, Bedison and Johnson 2009, Davis et al. 2009, Piatek et al. 2009), ecosystem productivity and growth (May et al. 2005, Davis et al. 2008, Bedison and McNeil 2009) and nitrogen leakage from disturbance events (Eshleman et al. 1998, Eshleman 2000, Townsend et al. 2004, McNeil et al. 2007a, Eshleman et al. 2009, Townsend et al. 2012).

Field methods

All field plots were sampled in July or August in 2008-2011, within ±2 weeks of AVIRIS image acquisition. We assumed that canopy chemistry would remain relatively stable during this midsummer sampling window (Matson et al. 1994, Scogings et al. 2004, Migita et al. 2007). Twenty plots were sampled in multiple years in locations where repeat

acquisitions of AVIRIS imagery occurred. Our field effort focused on characterizing forest canopy foliar properties and well as forest composition, both based on basal area by species (Townsend et al. 2003) and by leaf area following the method of Smith et al. (2002). At each plot we collected leaves via shotgun, line launcher or pole pruner for all canopy species. Leaves were sampled from the top, middle and bottom of the canopy, stored fully hydrated in a cooler and measured in a field laboratory within six hours of sampling. We measured green-leaf spectra using an ASD FieldSpec3 or FieldSpec2 350-2500 nm spectroradiometer (PANalytical Inc. Boulder, CO). Reflectance and transmittance were measured using both a contact probe and an integrating sphere. We measured hydrated leaf mass, standardized by leaf area. Samples were air dried, then stored for return to the lab, where we measured dry leaf mass, dry spectra and chemical concentrations following after oven drying samples at 70°C for 72 hours. All leaf traits were determined chemometrically from leaf spectra, following methods outlined in Serbin et al. (in review). The use of chemometric retrievals facilitated estimation of leaf traits for a much larger sample of foliage from our plots that would have been possible if we had relied on chemical analyses, which is very time consuming and expensive compared to spectroscopy. In addition, the use of spectroscopy to retrieve leaf traits also allowed us to compute uncertainty for each sample used in our analyses, based on the uncertainty estimates reported by Serbin et al. (in review). Table 1 provides a summary of measurements taken over the course of the project.

Leaf to Canopy Scaling

A variety of methods exist to scale leaf level estimates of foliar traits to the canopy, all of which are based on the relative abundance of species at a plot. We tested both a relative LAI-by-species (Macarthur and Horn 1969, Aber 1979, Smith and Martin 2001) and a relative basal area-by-species approach (Townsend et al. 2003), and found that canopy-level estimates of functional traits correlated with $r > 0.9$ between the two methods. Here we employ scaling by relative basal area, in which we assume that contribution by any one tree to canopy level trait signal is proportional to tree size. We prefer this method over scaling by relative LAI because methods based on rapid sampling of LAI by species following MacArthur and Horn (1969) are strongly biased towards prominent understory species, which was problematic in areas with extensive sugar maple subcanopies. In addition, Townsend et al. (2003) found that scaling by basal area correlated as well with total leaf biomass as scaling by LAI. Leaf traits (and associated uncertainties) were obtained from Serbin et al. (in review), and canopy-average traits were calculated as the sum of the products of the trait measurement times relative basal area of each species recorded on the 60x60 m plot. The scaling was conducted using multiple replicates (1000) drawn from the distributions of leaf-level estimates and uncertainties from Serbin (in review) to generate plot-level trait estimates and uncertainty.

Image Processing

AVIRIS data were provided by the Jet Propulsion Laboratory as orthorectified, calibrated radiance images (Vane et al. 1993, Green et al. 1998). Our study employed a total of 145

AVIRIS images (Fig 1), for which 51 were used for model development and testing, and the remainder were used for mapping and analysis. All images were processed using a common processing stream to ensure comparability among measurements. We performed post-hoc georectification as needed to align images with other geospatial data, such as digital orthophoto quads. We atmospherically corrected images using ATREM (TAFKAA: Gao et al. 2000, Montes and Gao 2004). Images were topographically corrected using the modified sun-canopy-sensor topographic method (Soenen et al. 2005) and BRDF corrected using a quadratic function of the volumetric scattering term of the Ross-Thick BRDF model (Roujean et al. 1992, Lucht et al. 2000). Pixel sizes for the AVIRIS imagery ranged from 12-18 m, depending on flight altitude, with registration errors < 0.5 pixels.

Statistical analysis

The general approach to the estimation of canopy traits (including chemistry) from imaging spectroscopy (IS) is illustrated in Fig. 2. We build upon the approach taken by Martin et al. (2008), in which they used data from 8 study sites and 137 field plots to develop a general, cross-scene predictive equation for foliar nitrogen. We extend their effort by additionally deriving maps of carbon, leaf mass per area (LMA), fiber, lignin and cellulose, as well as mapping uncertainties in all traits of interest. We employed the Partial Least-Squares Regression (PLSR, also called "projection to latent structures") modeling approach (Wold et al. 1984, Geladi and Kowalski 1986, Wolter et al. 2008) to predict canopy traits from imaging spectroscopy, as used by Smith et al. (2003), Coops et al. (2003), Townsend et al. (2003), McNeil et al. (2008), and Martin et al. (2008). In practice,

PLSR involves the derivation of wavelength-by-wavelength calibration factors based on the iterative transformation of latent vectors correlated with the dependent variable of interest. PLSR techniques achieve computational efficiency by maximizing the covariance of independent variables with the dependent variable while simultaneously maintaining the constraint of being orthogonal to the previously determined factors (Wold et al. 1984, Geladi and Kowalski 1986, Frank and Friedman 1993, Wold et al. 2001). The chief value of PLSR over traditional multiple linear regression models is that it is designed to work well with highly multi-collinear and over-sampled predictor data sets, i.e. when the number of independent variables approaches or even exceeds the number of observations (Wold et al. 1984, Geladi and Kowalski 1986, Wold et al. 2001). PLSR avoids difficulties in interpretation of synthetic PCA variables or the potential for modeling spurious relationships using stepwise regression (Grossman et al. 1996).

Scaling

Spectra from field plot locations were extracted from AVIRIS imagery and averaged for 3x3 pixels, ensuring one AVIRIS spectra per plot assumed to represent the entire 60x60 m plot. We postulate that averaging of multiple pixels is desirable because a) in practice a field plot of a closed-canopy stand can rarely be identified to a specific pixel and b) averaging of pixels provides a measure of uncertainty and heterogeneity of spectral response in the ensuing statistical model. For some plots, multiple AVIRIS scenes were available in the same year and season raising the possibility of pseudo-replication. To address this, we randomly split our plots into 50/50 calibration-validation sets ensuring that

only one spectrum for each per plot was used to generate trait-predictive PLSR models. We repeated this process 500 times, each time randomly sampling from the uncertainty distributions of the plot-level trait estimates to propagate uncertainties to the image scale. Ultimately, our full methodology allows the propagation of uncertainty from the leaf-level (derived from contact spectroscopy) to the plot level (through leaf-to-plot scaling) and finally to the image scale. PLSR coefficients obtained from each of the 500 permutations were applied to generate 500 predictions of the trait per pixel, from which we estimated pixel-wise means and standard deviations to report uncertainty.

Results

Geographic variation in foliar traits

The ranges of plot-level trait estimates stratified by leaf morphology are presented in Table 1. Plot level foliar traits aggregated by species are provided in Supplemental Table S2, and by plot in Supplemental Table S3. There was a nearly two-fold difference in M_{area} between needleleaf and broadleaf species ($T = 21.75$, $P < 0.0001$), and mass-based nitrogen content of broadleaf species was around 1.5 times that of needleleaf species ($T = 17.88$, $P < 0.0001$). There was less variation in differences in carbon content, fiber, lignin and cellulose between needle-leaf and broadleaf species, but all differences were significant ($P < 0.0001$). Correlation analyses revealed a strong negative relationship between leaf nitrogen and M_{area} ($r = -0.804$, $P < 0.0001$) as well as significant negative relationships with other leaf structural compounds (Table 2, Fig. 3), in agreement with the broader concept of the leaf economic spectrum (Wright et al. 2004, Wright et al. 2005a, Wright et

al. 2005b). Leaf nitrogen content decreased with latitude, while M_{area} increased, a reflection of an increasing dominance of needleleaf species in the north. We also found a significant positive correlation between foliar nitrogen and patterns of nitrogen deposition across our sites ($r = 0.394$, $P < 0.0001$). To further explore this relationship, we fit a mixed-effects model to predict foliar nitrogen concentrations while controlling for latitude with Gaussian random effects specified for species. The model explained 88.7% in the variation in foliar nitrogen, of which 59% was attributed to differences between species alone. The effect elevated foliar nitrogen concentrations corresponding to N deposition gradient were apparent ($P < 0.0001$) even after taking into consideration latitudinal gradients and inherent differences between species. This finding corroborates evidence of foliar N enrichment that has been reported from many studies in Northeastern forests (McNeil et al. 2007b, Davis et al. 2009, McNeil et al. 2012).

Canopy spectra

Canopy spectra were highly variable (Fig. 4) with nearly complete separation (±1 standard deviation) between spectra of all broadleaf and all needle-leaf plots in the NIR (700-1400nm) and the 1400-1900 nm SWIR1 regions. Spectra of the two physiognomic types overlapped some in the visible (400-700nm) and SWIR2 (1900-2400 nm) wavelengths. The most spectral variability (in terms of the coefficient of variation) was observed in the visible regions of the spectrum (> 23-50%) and was generally constant across the rest of the spectrum (~22%). Plots dominated by needle-leaf species had around 10% less spectral variability than broadleaf species.

PLSR model results

The results of the PLS predictions for forest traits are shown in Table 3 and graphed in Figs. 5 - 10. Note that error bars are shown in both directions: error on the Y-axis is due to uncertainty of trait values from the scaling from leaf level spectra to plot level traits (Serbin et al. in review), while uncertainty on the X-axis is due to uncertainty from the image-based PLSR model. To our knowledge, this is the first time that such a comprehensive analysis of uncertainty has been provided, including both uncertainties in the training data and in the mapped estimates. In Figs 5-10, we graph standardized coefficients (upper right), which facilitate comparison among bands and traits due to scale differences in reflectance between different wavelength regions (i.e. higher reflectance and greater variability in the NIR equate to smaller coefficients, but not necessarily less important coefficients). We also show the Variable Importance of Projection (VIP) statistic (lower right panels, see Wold 1994), which indicates the value of each predictor (waveband) in fitting the PLS model for both predictors and responses based on its absolute coefficient size and its partial-R^2 in the overall PLS model. For practical application, the raw PLS coefficients are what are used for mapping, but are not as useful for model assessment and interpretation. Supplemental Table S4 lists the PLS coefficients and their uncertainties for the traits reported in this paper. These are the values that users should apply to make maps from novel imagery that have been processed in a method comparable to this study. Further, we also show wavelength regions that correspond to known absorption features (from Curran 1989, Fourty et al. 1996, Curran et al. 2001).

Both LMA and %N had model fits with R^2 greater than 0.85, which are comparable to the results reported by Martin et al. (2008, Supplementary table S1). Root mean square errors (RMSEs) for both variables were less than 9% of the range of data (Tables 3, 5). Fiber (ADF) and lignin (ADL) were predicted with $R^2 > 0.70$ and carbon and cellulose greater than 0.5. Although R^2 of fiber and lignin were lower than LMA and %N, their RMSE values were within 10% of the range of data. The comparatively lower R^2 values for %C and cellulose are related to the low amount of natural variability in these constituents.

Mapping

We used the PLSR coefficients (Supplementary Table S4) to generate spatially explicit maps of our traits and the results of the permutations to map uncertainty in our estimates (Figs 11, 12). Because of the large number of images used in this study, we show results from a subset of the scenes. Maps of trait combinations provide an alternate to land cover maps for characterizing vegetation gradients. For example, we can synthesize foliar trait maps into functional type maps by constructing false color composites of key foliar traits such as nitrogen, lignin and leaf mass per area (Fig. 13) to illustrate continuous gradients of canopy biochemical and morphological traits that are likely also related to species associations. However, the maps of traits are interpretable as patterns of plant investment in foliar nutrients vs. structural compounds across environmental gradients on the landscape. Mapping individual traits across regions (Fig. 14, 15) reveals significant variability in relative abundance of dominant traits that could not otherwise be captured by

landcover classifications alone (right panels on Fig. 13). Maps of functional *traits* from a single hyperspectral image can reveal differences in species associations across gradients that are otherwise only apparent in multi-date imagery (Fig. 16), and moreover can help identify disturbance events through changes in estimated functional traits and associated increases in mapped uncertainty (Fig. 17).

Discussion

We confirm the capacity of imaging spectroscopy to accurately and repeatedly map foliar traits important to photosynthetic metabolism and foliar nutrient cycling. Our method for the estimation of canopy chemistry involved the integration of three types of data representing different scales of observation, thus allowing the propagation of uncertainty from the leaf-level dependent variables to the plot/canopy level, and finally to maps created from image spectra. Imaging spectroscopy has been used in numerous studies to map foliar traits (Wessman et al. 1989, Curran et al. 1997, Serrano et al. 2002, Townsend et al. 2003, Asner et al. 2008, Huber et al. 2008, Martin et al. 2008), ours is the first study to demonstrate the capacity to map multiple functional traits from such data across a diversity of sites and years and to explicitly account for the propagation of measurement and modeling uncertainty through to the end product.

We used our calibration coefficients to 1) investigate physiological basis for the PLSR results and 2) assess which wavelength regions were important in modeling the trait of interest and if these were generalizable across other studies. Reviewing the literature, leaf-level, fresh-leaf standardized coefficients were available for M_{area} (from Serbin et al.

in review), while the only published image-level (raw) coefficients were available from Martin et al. (2008). The standardized leaf-level coefficients for M_{area} generated from an ASD spectroradiometer by Serbin et al. (in review) agreed almost completely with AVIRIS results (Fig. 5 top right). Importantly, although standardized coefficients matched almost the entire spectrum, there was a reversal of sign in coefficients across the red-edge (500-700nm). Leaf-level NIR reflectance in this range results from scattering at the interface between cell walls and intercellular air spaces, while canopy (i.e., image) reflectance is strongly dominated by canopy structure and leaf morphology (needle vs. broad leaf) (Jacquemoud et al. 2009). In leaves, NIR reflectance generally increases with leaf thickness (Ehleringer and Mooney 1978, Lin and Ehleringer 1983, DeLucia et al. 1996, Slaton et al. 2001), but canopy reflectance in the NIR reverses between thin broadleaved forests to clumped needleleaf canopies in which thick leaves have higher NIR reflectance compared to broadleaves but lower canopy reflectance due to the effects of needle clumping and shading. The fact that direction of coefficients switch between leaf and canopy-level models of LMA provides confidence that imaging spectroscopy captures sufficient information about the canopy and constituent foliage for purposes of mapping (Ollinger et al. 2013, Townsend et al. 2013) than has been suggested (Knyazikhin et al. 2013).

To further assess the wider applicability of our models, we compared coefficients obtained from our analysis of %N with those published by Martin et al. (2008), the only other study we found for which comparable coefficients have been published. Patterns of loadings of standardized coefficients of our models predicting foliar N content also showed

general agreement with the Martin et al. models (2008) (Fig. 6). Discrepancies in locations of dips and spikes in coefficients result primarily from our use of a standardized dataset (i.e., centered and scaled) compared to raw coefficients from Martin et al. (2008). Martin et al.'s (2008) study, while limited to 11 images (5 AVIRIS, 6 Hyperion), covered a wide variety of ecosystems across the world and was a pioneering effort demonstrating the capacity to build general models to map foliar traits across large regions. Studies using larger numbers of images, such as Smith et al. (2002) and Ollinger et al. (2002), have also been successful, but limited to a single study region.

We included a large number of forest types and species in our analyses (Suppl Tables S2 and S3), but by no means were our field samples comprehensive. However, we assume that our database covers the breadth of forest functional variability within the region, and therefore missing species or types are bracketed by the range of our data. In this regard, spatial patterns of uncertainties are likely indicative of gaps in our database for different forest optical types (sensu Ustin and Gamon 2010) rather than due to weaknesses in model performance. The largest uncertainties were observed in locations where 1) the vegetation was not represented in our database of foliar traits due to our focus on forests (i.e., grasses, forbs, crops, wetlands); 2) there were strong terrain effects in the imagery; or 3) along forest edges and disturbed areas. In particular, the uncertainty mapping helped identify areas that had been recently disturbed (Fig. 17). Clearcuts showed a consistent pattern of higher lignin and M_{area} and lower foliar nitrogen content compared to adjacent undisturbed areas, and consistently high uncertainties due to optical properties of disturbances being outside the range of optical properties for the intact forests sampled for this study. Future

analysis of vegetation traits in disturbed areas using imaging spectroscopy may provide the opportunity to better understand changes in ecosystem dynamics brought about by human or natural perturbations.

Composite maps of functional traits (e.g., Fig. 13) revealed a greater amount of variability in forest canopies than was apparent in individual maps (Figs.11 and 12) or landcover classifications. For example, in the Central Appalachian sites, co-dominant conifers in ridges and valleys were revealed by the higher lignin content and M_{area} of conifers (Figure 13, panel 2). Comparisons between maps of individual traits (Fig. 14, 15) revealed gradients in functional traits that follow the inverse relationship between investments in leaf structural mass in contrast to leaf nutrients (Wright and Westoby 2002, Reich et al. 2003, Wright et al. 2004). Regions showing higher foliar nitrogen concentrations were associated with lower values of M_{area} and vice versa. While this is widely known from multiple species inhabiting diverse ecosystems (Reich et al. 1998, Reich et al. 1999, Wright et al. 2001, Sanchez-Azofeifa et al. 2009, Asner et al. 2011b), imaging spectroscopy allowed these associations to be mapped explicitly and across multiple ecoregions.

Maps of foliar traits obtained from this study can be leveraged to drive ecosystem process models requiring parameterization of foliar nitrogen content and leaf mass per area, which are coordinated in leaves to maximize carbon fixation (Shipley et al. 2005) in patterns independent of species-level physiognomy (Reich et al. 1991, Reich et al. 1992, Grime 2006). This offers the potential to estimate carboxylation capacity of forests, e.g. following Kattge et al. (2009) who proposed a general model to estimate this parameter

based on M_{area} and %N. Similarly, Green et al. (2003) showed that canopy light use efficiency can be retrieved from canopy foliar content, M_{area} and the fraction of absorbed photosynthetically active radiation (fPAR), all of which can be retrieved from imaging spectroscopy. This offers the potential to develop datasets needed to drive spatially explicit ecosystem process models at large scales from proposed forthcoming satellites (e.g. HyspIRI, EnMAP: Stuffler et al. 2007, Middleton et al. 2013).

Imaging spectroscopy offers the opportunity for applications ranging from assessment of biochemical effects of invasive species (Glenn et al. 2005, Asner et al. 2008, He et al. 2011), to characterizing photosynthetic down-regulation (Gamon et al. 1990, Gamon et al. 1992, Gamon et al. 1997) and measurement of the inductance of plant defense to perturbations (Couture et al. 2013). By directly measuring the chemical and physiological consequences of disturbances and other environmental drivers on vegetation, spaceborne imaging spectroscopy should provide the ability to directly quantify the consequences of environmental change rather than inferring it from landcover maps or vegetation indices. This will provide agencies the tools to measure impacts of invasions or help better guide management activities.

Conclusion

Ultimately the trait mapping from imaging spectroscopy will allow us to address questions such as: How do forest functional types (FFTs, or, more generally, plant functional types, PFTs) mediate ecosystem response to environmental change? For a given perturbation (e.g. atmospheric N deposition, insect defoliation), spatial variability in ecosystem response

(e.g. forest productivity, nitrogen retention) can be characterized via spectroscopy to measure the key suite of leaf-based functional traits that may change with perturbations. Using data from a wide range of forest ecosystems, we rigorously tested the capacity of hyperspectral imagery to map forest functional trait. Our ultimate objective was to provide a much-needed generalized framework for making regional scale predictions from imaging spectroscopy of the delivery of key ecosystem services from complex forest environments that are increasingly subjected to multiple agents of global environmental change.

These results allow us to use maps of functional traits to map the fundamental axes of variability in plant physiology (Reich et al. 1991, Reich et al. 1992, Reich et al. 1999, Craine et al. 2002, Wright et al. 2005a, Wright et al. 2005b, Sanchez-Azofeifa et al. 2009). These traits synthetically define a spectrum ranging from "fast" (high nutrients and low lignin, thin, low LMA leaves) to "slow" patterns of forest nutrient cycling. An important next step is the integration of data collected from across the globe (Asner and Martin 2009, Asner et al. 2012) to further determine the extent of the generality of these methods, and to integrate data across sensor types and measurement or analytical strategies to fully evaluate the generality of the relationships and then refine and standardize approaches across investigations as needed. Along with Martin et al. (2008) and efforts underway by Asner and colleagues, this research represents one step toward the development of global approaches to mapping plant functional properties from imaging spectroscopy. This ongoing research will provide a solid foundation for the development of "trait" products from the proposed HyspIRI mission and NEON's Aerial Observatory Platform (Kampe et al. 2010, Middleton et al. 2013, Sims et al. 2013).

Literature cited

Aber, J., W. McDowell, K. Nadelhoffer, A. Magill, G. Berntson, M. Kamakea, S. McNulty, W. Currie, L. Rustad, and I. Fernandez. 1998. Nitrogen saturation in temperate forest ecosystems - Hypotheses revisited. Bioscience **48**:921-934.

Aber, J. D. 1979. Method for estimating foliage-height profiles in broad-leaved forests. Journal of Ecology **67**:35-40.

Aber, J. D., C. L. Goodale, S. V. Ollinger, M. L. Smith, A. H. Magill, M. E. Martin, R. A. Hallett, and J. L. Stoddard. 2003. Is nitrogen deposition altering the nitrogen status of northeastern forests? Bioscience **53**:375-389.

Aber, J. D., K. J. Nadelhoffer, P. Steudler, and J. M. Melillo. 1989. Nitrogen Saturation in Northern Forest Ecosystems. Bioscience **39**:378-386.

Aber, J. D., S. V. Ollinger, and C. T. Driscoll. 1997. Modeling nitrogen saturation in forest ecosystems in response to land use and atmospheric deposition. Ecological Modelling **101**:61-78.

Aerts, R. 1997. Climate, leaf litter chemistry and leaf litter decomposition in terrestrial ecosystems: A triangular relationship. Oikos **79**:439-449.

Ahl, D. E., S. T. Gower, D. S. Mackay, S. N. Burrows, J. M. Norman, and G. R. Diak. 2004. Heterogeneity of light use efficiency in a northern Wisconsin forest: implications for modeling net primary production with remote sensing. Remote Sensing of Environment **93**:168-178.

Ainsworth, E. A., and A. Rogers. 2007. The response of photosynthesis and stomatal conductance to rising CO2 : mechanisms and environmental interactions. Plant Cell and Environment **30**:258-270.

Asner, G. P. 1998. Biophysical and biochemical sources of variability in canopy reflectance. Remote Sensing of Environment **64**:234-253.

Asner, G. P., M. O. Jones, R. E. Martin, D. E. Knapp, and R. F. Hughes. 2008. Remote sensing of native and invasive species in Hawaiian forests. Remote Sensing of Environment **112**:1912-1926.

Asner, G. P., D. E. Knapp, J. Boardman, R. O. Green, T. Kennedy-Bowdoin, M. Eastwood, R. E. Martin, C. Anderson, and C. B. Field. 2012. Carnegie Airborne Observatory-2: Increasing science data dimensionality via high-fidelity multi-sensor fusion. Remote Sensing of Environment **124**:454-465.

Asner, G. P., and R. E. Martin. 2008. Spectral and chemical analysis of tropical forests: Scaling from leaf to canopy levels. Remote Sensing of Environment **112**:3958-3970.

Asner, G. P., and R. E. Martin. 2009. Airborne spectranomics: mapping canopy chemical and taxonomic diversity in tropical forests. Frontiers in Ecology and the Environment **7**:269-276.

Asner, G. P., R. E. Martin, D. E. Knapp, R. Tupayachi, C. Anderson, L. Carranza, P. Martinez, M. Houcheime, F. Sinca, and P. Weiss. 2011a. Spectroscopy of canopy chemicals in humid tropical forests. Remote Sensing of Environment **115**:3587-3598.

Asner, G. P., R. E. Martin, R. Tupayachi, R. Emerson, P. Martinez, F. Sinca, G. V. N. Powell, S. J. Wright, and A. E. Lugo. 2011b. Taxonomy and remote sensing of leaf mass per area (LMA) in humid tropical forests. Ecological Applications **21**:85-98.

Asner, G. P., and P. M. Vitousek. 2005. Remote analysis of biological invasion and biogeochemical change. Proceedings of the National Academy of Sciences of the United States of America **102**:4383-4386.

Baret, F., V. C. Vanderbilt, M. D. Steven, and S. Jacquemoud. 1994. Use of spectral analogy to evaluate canopy reflectance sensitivity to leaf optical-properties. Remote Sensing of Environment **48**:253-260.

Bedison, J. E., and A. H. Johnson. 2009. Controls on the Spatial Patterns of Carbon and Nitrogen in Adirondack Forest Soils along a Gradient of Nitrogen Deposition. Soil Science Society of America Journal **73**:2105-2117.

Bedison, J. E., and B. E. McNeil. 2009. Is the growth of temperate forest trees enhanced along an ambient nitrogen deposition gradient? Ecology **90**:1736-1742.

Berg, B. 2000. Litter decomposition and organic matter turnover in northern forest soils. Forest Ecology and Management **133**:13-22.

Blackburn, G. A. 2007. Hyperspectral remote sensing of plant pigments. Journal of Experimental Botany **58**:855-867.

Bonan, G. B. 1993. Physiological controls of the carbon balance of boreal forest ecosystems. Canadian Journal of Forest Research-Revue Canadienne De Recherche Forestiere **23**:1453-1471.

Bresee, M. K., J. Le Moine, S. Mather, K. D. Brosofske, J. Q. Chen, T. R. Crow, and J. Rademacher. 2004. Disturbance and landscape dynamics in the Chequamegon National Forest Wisconsin, USA, from 1972 to 2001. Landscape Ecology **19**:291-309.

Burrows, S. N., S. T. Gower, J. M. Norman, G. Diak, D. S. Mackay, D. E. Ahl, and M. K. Clayton. 2003. Spatial variability of aboveground net primary production for a forested landscape in northern Wisconsin. Canadian Journal of Forest Research-Revue Canadienne De Recherche Forestiere **33**:2007-2018.

Canadell, J. G., C. Le Quere, M. R. Raupach, C. B. Field, E. T. Buitenhuis, P. Ciais, T. J. Conway, N. P. Gillett, R. A. Houghton, and G. Marland. 2007. Contributions to accelerating atmospheric CO(2) growth from economic activity, carbon intensity, and efficiency of natural sinks. Proceedings of the National Academy of Sciences of the United States of America **104**:18866-18870.

Carlson, K. M., G. P. Asner, R. F. Hughes, R. Ostertag, and R. E. Martin. 2007. Hyperspectral remote sensing of canopy biodiversity in Hawaiian lowland rainforests. Ecosystems **10**:536-549.

Carrera, A. L., and M. B. Bertiller. 2010. Relationships among plant litter, fine roots, and soil organic C and N across an aridity gradient in northern Patagonia, Argentina. Ecoscience **17**:276-286.

Chapin, F. S. 2003. Effects of plant traits on ecosystem and regional processes: a conceptual framework for predicting the consequences of global change. Annals of Botany **91**:455-463.

Chapin, F. S., M. S. BretHarte, S. E. Hobbie, and H. L. Zhong. 1996. Plant functional types as predictors of transient responses of arctic vegetation to global change. Journal of Vegetation Science **7**:347-358.

Chastain, R. A., W. S. Currie, and P. A. Townsend. 2006. Carbon sequestration and nutrient cycling implications of the evergreen understory layer in Appalachian forests. Forest Ecology and Management **231**:63-77.

Collatz, G. J., M. Ribas-Carbo, and J. A. Berry. 1992. Coupled photosynthesis-stomatal conductance model for leaves of C4 plants. Australian Journal of Plant Physiology **19**:519-538.

Cook, B. D., K. J. Davis, W. G. Wang, A. Desai, B. W. Berger, R. M. Teclaw, J. G. Martin, P. V. Bolstad, P. S. Bakwin, C. X. Yi, and W. Heilman. 2004. Carbon exchange and venting anomalies in an upland deciduous forest in northern Wisconsin, USA. Agricultural and Forest Meteorology **126**:271-295.

Coops, N. C., M. L. Smith, M. E. Martin, and S. V. Ollinger. 2003. Prediction of eucalypt foliage nitrogen content from satellite-derived hyperspectral data. Ieee Transactions on Geoscience and Remote Sensing **41**:1338-1346.

Couture, J. J., S. P. Serbin, and P. A. Townsend. 2013. Spectroscopic sensitivity of real-time, rapidly induced phytochemical change in response to damage. New Phytologist **198**:311-319.

Craine, J. M., D. Tilman, D. Wedin, P. Reich, M. Tjoelker, and J. Knops. 2002. Functional traits, productivity and effects on nitrogen cycling of 33 grassland species. Functional Ecology **16**:563-574.

Cramer, W., A. Bondeau, F. I. Woodward, I. C. Prentice, R. A. Betts, V. Brovkin, P. M. Cox, V. Fisher, J. A. Foley, A. D. Friend, C. Kucharik, M. R. Lomas, N. Ramankutty, S. Sitch, B. Smith, A. White, and C. Young-Molling. 2001. Global response of terrestrial ecosystem structure and function to CO2 and climate change: results from six dynamic global vegetation models. Global Change Biology **7**:357-373.

Crowley, K. F., B. E. McNeil, G. M. Lovett, C. D. Canham, C. T. Driscoll, L. E. Rustad, E. Denny, R. A. Hallett, M. A. Arthur, J. L. Boggs, C. L. Goodale, J. S. Kahl, S. G. McNulty, S. V. Ollinger, L. H. Pardo, P. G. Schaberg, J. L. Stoddard, M. P. Weand, and K. C. Weathers. 2012. Do nutrient limitation patterns shift from nitrogen toward phosphorus with increasing nitrogen deposition across the northeastern United States? Ecosystems **15**:940-957.

Curran, P. J. 1989. Remote-sensing of foliar chemistry. Remote Sensing of Environment **30**:271-278.

Curran, P. J., J. L. Dungan, B. A. Macler, S. E. Plummer, and D. L. Peterson. 1992. Reflectance spectroscopy of fresh whole leaves for the estimation of chemical concentration. Remote Sensing of Environment **39**:153-166.

Curran, P. J., J. L. Dungan, and D. L. Peterson. 2001. Estimating the foliar biochemical concentration of leaves with reflectance spectrometry testing the Kokaly and Clark methodologies. Remote Sensing of Environment **76**:349-359.

Curran, P. J., J. A. Kupiec, and G. M. Smith. 1997. Remote sensing the biochemical composition of a slash pine canopy. Ieee Transactions on Geoscience and Remote Sensing **35**:415-420.

Dahir, S. E., and C. G. Lorimer. 1996. Variation in canopy gap formation among developmental stages of northern hardwood stands. Canadian Journal of Forest Research-Revue Canadienne De Recherche Forestiere **26**:1875-1892.

Davis, K. J., P. S. Bakwin, C. X. Yi, B. W. Berger, C. L. Zhao, R. M. Teclaw, and J. G. Isebrands. 2003. The annual cycles of CO2 and H2O exchange over a northern mixed forest as observed from a very tall tower. Global Change Biology **9**:1278-1293.

Davis, S. C., K. E. Dragan, C. R. Buyarski, and R. B. Thomas. 2009. High foliar and soil nitrogen concentrations in central Appalachian forests. Ecosystems **12**:46-56.

Davis, S. C., A. E. Hessl, and R. B. Thomas. 2008. A modified nitrogen budget for temperate deciduous forests in an advanced stage of nitrogen saturation. Global Biogeochemical Cycles **22**.

DeLucia, E. H., K. Nelson, T. C. Vogelmann, and W. K. Smith. 1996. Contribution of intercellular reflectance to photosynthesis in shade leaves. Plant Cell and Environment **19**:159-170.

Desai, A. R., A. Noormets, P. V. Bolstad, J. Q. Chen, B. D. Cook, K. J. Davis, E. S. Euskirchen, C. M. Gough, J. G. Martin, D. M. Ricciuto, H. P. Schmid, J. W. Tang, and W. G. Wang. 2008. Influence of vegetation and seasonal forcing on carbon dioxide fluxes across the Upper Midwest, USA: Implications for regional scaling. Agricultural and Forest Meteorology **148**:288-308.

Diaz, S., J. G. Hodgson, K. Thompson, M. Cabido, J. H. C. Cornelissen, A. Jalili, G. Montserrat-Marti, J. P. Grime, F. Zarrinkamar, Y. Asri, S. R. Band, S. Basconcelo, P. Castro-Diez, G. Funes, B. Hamzehee, M. Khoshnevi, N. Perez-Harguindeguy, M. C. Perez-Rontome, F. A. Shirvany, F. Vendramini, S. Yazdani, R. Abbas-Azimi, A. Bogaard, S. Boustani, M. Charles, M. Dehghan, L. de Torres-Espuny, V. Falczuk, J. Guerrero-Campo, A. Hynd, G. Jones, E. Kowsary, F. Kazemi-Saeed, M. Maestro-Martinez, A. Romo-Diez, S. Shaw, B. Siavash, P. Villar-Salvador, and M. R. Zak. 2004. The plant traits that drive ecosystems: Evidence from three continents. Journal of Vegetation Science **15**:295-304.

Diebel, M. W., J. T. Maxted, P. J. Nowak, and M. J. Vander Zanden. 2008. Landscape Planning for Agricultural Nonpoint Source Pollution Reduction I: A Geographical Allocation Framework. Environmental Management **42**:789-802.

Ehleringer, J. R., and H. A. Mooney. 1978. Leaf hairs - effects on physiological-activity and adaptive value to a desert shrub. Oecologia **37**:183-200.

Enquist, B. J., A. J. Kerkhoff, T. E. Huxman, and E. P. Economo. 2007. Adaptive differences in plant physiology and ecosystem paradoxes: insights from metabolic scaling theory. Global Change Biology **13**:591-609.

Eshleman, K. N. 2000. A linear model of the effects of disturbance on dissolved nitrogen leakage from forested watersheds. Water Resources Research **36**:3325-3335.

Eshleman, K. N., B. E. McNeil, and P. A. Townsend. 2009. Validation of a remote sensing based index of forest disturbance using streamwater nitrogen data. Ecological Indicators **9**:476-484.

Eshleman, K. N., R. P. Morgan, J. R. Webb, F. A. Deviney, and J. N. Galloway. 1998. Temporal patterns of nitrogen leakage from mid-Appalachian forested watersheds: Role of insect defoliation. Water Resources Research **34**:2005-2016.

Fortunel, C., E. Garnier, R. Joffre, E. Kazakou, H. Quested, K. Grigulis, S. Lavorel, P. Ansquer, H. Castro, P. Cruz, J. Dolezal, O. Eriksson, H. Freitas, C. Golodets, C. Jouany, J. Kigel, M. Kleyer, V. Lehsten, J. Leps, T. Meier, R. Pakeman, M. Papadimitriou, V. P. Papanastasis, F. Quetier, M. Robson, M. Sternberg, J. P. Theau, A. Thebault, and M. Zarovali. 2009. Leaf traits capture the effects of land use changes and climate on litter decomposability of grasslands across Europe. Ecology **90**:598-611.

Fourty, T., F. Baret, S. Jacquemoud, G. Schmuck, and J. Verdebout. 1996. Leaf optical properties with explicit description of its biochemical composition: Direct and inverse problems. Remote Sensing of Environment **56**:104-117.

Frank, I. E., and J. H. Friedman. 1993. A statistical view of some chemometrics regression tools. Technometrics **35**:109-135.

Frelich, L. E., and C. G. Lorimer. 1991. Natural disturbance regimes in hemlock hardwood forests of the upper Great-Lakes region. Ecological Monographs **61**:145-164.

Gamon, J. A., C. B. Field, W. Bilger, O. Bjorkman, A. L. Fredeen, and J. Penuelas. 1990. Remote-sensing of the xanthophyll cycle and chlorophyll fluorescence in sunflower leaves and canopies. Oecologia **85**:1-7.

Gamon, J. A., J. Penuelas, and C. B. Field. 1992. A narrow-waveband spectral index that tracks diurnal changes in photosynthetic efficiency. Remote Sensing of Environment **41**:35-44.

Gamon, J. A., L. Serrano, and J. S. Surfus. 1997. The photochemical reflectance index: an optical indicator of photosynthetic radiation use efficiency across species, functional types, and nutrient levels. Oecologia **112**:492-501.

Gao, B. C., M. J. Montes, Z. Ahmad, and C. O. Davis. 2000. Atmospheric correction algorithm for hyperspectral remote sensing of ocean color from space. Applied Optics **39**:887-896.

Garnier, E., J. Cortez, G. Billes, M. L. Navas, C. Roumet, M. Debussche, G. Laurent, A. Blanchard, D. Aubry, A. Bellmann, C. Neill, and J. P. Toussaint. 2004. Plant functional markers capture ecosystem properties during secondary succession. Ecology **85**:2630-2637.

Gates, D. M., H. J. Keegan, J. C. Schleter, and V. R. Weidner. 1965. Spectral properties of plants. Applied Optics **4**:11-&.

Geladi, P., and B. R. Kowalski. 1986. Partial least-squares regression - a tutorial. Analytica Chimica Acta **185**:1-17.

Glenn, N. F., J. T. Mundt, K. T. Weber, T. S. Prather, L. W. Lass, and J. Pettingill. 2005. Hyperspectral data processing for repeat detection of small infestations of leafy spurge. Remote Sensing of Environment **95**:399-412.

Green, D. S., J. E. Erickson, and E. L. Kruger. 2003. Foliar morphology and canopy nitrogen as predictors of light-use efficiency in terrestrial vegetation. Agricultural and Forest Meteorology **115**:163-171.

Green, R. O., M. L. Eastwood, C. M. Sarture, T. G. Chrien, M. Aronsson, B. J. Chippendale, J. A. Faust, B. E. Pavri, C. J. Chovit, M. S. Solis, M. R. Olah, and O. Williams. 1998. Imaging spectroscopy and the Airborne Visible Infrared Imaging Spectrometer (AVIRIS). Remote Sensing of Environment **65**:227-248.

Grime, J. P. 2006. Trait convergence and trait divergence in herbaceous plant communities: Mechanisms and consequences. Journal of Vegetation Science **17**:255-260.

Grossman, Y. L., S. L. Ustin, S. Jacquemoud, E. W. Sanderson, G. Schmuck, and J. Verdebout. 1996. Critique of stepwise multiple linear regression for the extraction of leaf biochemistry information from leaf reflectance data. Remote Sensing of Environment **56**:182-193.

Grossmann, E. B., and D. J. Mladenoff. 2008. Farms, fires, and forestry: Disturbance legacies in the soils of the Northwest Wisconsin (USA) Sand Plain. Forest Ecology and Management **256**:827-836.

Hattenschwiler, S., A. V. Tiunov, and S. Scheu. 2005. Biodiversity and litter decomposition interrestrial ecosystems. Pages 191-218 Annual Review of Ecology Evolution and Systematics.

He, K. S., D. Rocchini, M. Neteler, and H. Nagendra. 2011. Benefits of hyperspectral remote sensing for tracking plant invasions. Diversity and Distributions **17**:381-392.

Hilker, T., L. Lepine, N. C. Coops, R. S. Jassal, T. A. Black, M. A. Wulder, S. Ollinger, O. Tsui, and M. Day. 2012. Assessing the impact of N-fertilization on biochemical composition and biomass of a Douglas-fir canopy-A remote sensing approach. Agricultural and Forest Meteorology **153**:124-133.

Hobbie, S. E., M. Ogdahl, J. Chorover, O. A. Chadwick, J. Oleksyn, R. Zytkowiak, and P. B. Reich. 2007. Tree species effects on soil organic matter dynamics: The role of soil cation composition. Ecosystems **10**:999-1018.

Hobbie, S. E., P. B. Reich, J. Oleksyn, M. Ogdahl, R. Zytkowiak, C. Hale, and P. Karolewski. 2006. Tree species effects on decomposition and forest floor dynamics in a common garden. Ecology **87**:2288-2297.

Huber, S., M. Kneubuhler, A. Psomas, K. Itten, and N. E. Zimmermann. 2008. Estimating foliar biochemistry from hyperspectral data in mixed forest canopy. Forest Ecology and Management **256**:491-501.

Jacquemoud, S., W. Verhoef, F. Baret, C. Bacour, P. J. Zarco-Tejada, G. P. Asner, C. Francois, and S. L. Ustin. 2009. PROSPECT plus SAIL models: A review of use for vegetation characterization. Remote Sensing of Environment **113**:S56-S66.

Johnson, J. M. F., N. W. Barbour, and S. L. Weyers. 2007. Chemical composition of crop biomass impacts its decomposition. Soil Science Society of America Journal **71**:155-162.

Johnson, L. F., C. A. Hlavka, and D. L. Peterson. 1994. Multivariate-analysis of aviris data for canopy biochemical estimation along the oregon transect. Remote Sensing of Environment **47**:216-230.

Kampe, T. U., B. R. Johnson, M. Kuester, and M. Keller. 2010. NEON: the first continental-scale ecological observatory with airborne remote sensing of vegetation canopy biochemistry and structure. Journal of Applied Remote Sensing **4**.

Kattge, J., W. Knorr, T. Raddatz, and C. Wirth. 2009. Quantifying photosynthetic capacity and its relationship to leaf nitrogen content for global-scale terrestrial biosphere models. Global Change Biology **15**:976-991.

Kazakou, E., D. Vile, B. Shipley, C. Gallet, and E. Garnier. 2006. Co-variations in litter decomposition, leaf traits and plant growth in species from a Mediterranean old-field succession. Functional Ecology **20**:21-30.

Kazakou, E., C. Violle, C. Roumet, C. Pintor, O. Gimenez, and E. Garnier. 2009. Litter quality and decomposability of species from a Mediterranean succession depend on leaf traits but not on nitrogen supply. Annals of Botany **104**:1151-1161.

Kergoat, L., S. Lafont, A. Arneth, V. Le Dantec, and B. Saugier. 2008. Nitrogen controls plant canopy light-use efficiency in temperate and boreal ecosystems. Journal of Geophysical Research-Biogeosciences **113**.

Knorr, M., S. D. Frey, and P. S. Curtis. 2005. Nitrogen additions and litter decomposition: A meta-analysis. Ecology **86**:3252-3257.

Knyazikhin, Y., M. A. Schull, P. Stenberg, M. Mottus, M. Rautiainen, Y. Yang, A. Marshak, P. L. Carmona, R. K. Kaufmann, P. Lewis, M. I. Disney, V. Vanderbilt, A. B. Davis, F. Baret, S. Jacquemoud, A. Lyapustin, and R. B. Myneni. 2013. Hyperspectral remote sensing of foliar nitrogen content. Proceedings of the National Academy of Sciences of the United States of America **110**:E185-E192.

Kokaly, R. F. 2001. Investigating a physical basis for spectroscopic estimates of leaf nitrogen concentration. Remote Sensing of Environment **75**:153-161.

Kokaly, R. F., G. P. Asner, S. V. Ollinger, M. E. Martin, and C. A. Wessman. 2009. Characterizing canopy biochemistry from imaging spectroscopy and its application to ecosystem studies. Remote Sensing of Environment **113**:S78-S91.

Lathrop, R. C. 2007. Perspectives on the eutrophication of the Yahara lakes. Lake and Reservoir Management **23**:345-365.

Le Quere, C., M. R. Raupach, J. G. Canadell, G. Marland, L. Bopp, P. Ciais, T. J. Conway, S. C. Doney, R. A. Feely, P. Foster, P. Friedlingstein, K. Gurney, R. A. Houghton, J. I. House, C. Huntingford, P. E. Levy, M. R. Lomas, J. Majkut, N. Metzl, J. P. Ometto, G. P. Peters, I. C. Prentice, J. T. Randerson, S. W. Running, J. L. Sarmiento, U. Schuster, S. Sitch, T. Takahashi, N. Viovy, G. R. van der Werf, and F. I. Woodward. 2009. Trends in the sources and sinks of carbon dioxide. Nature Geoscience **2**:831-836.

Lin, Z. F., and J. Ehleringer. 1983. Epidermis effects on spectral properties of leaves of 4 herbaceous species. Physiologia Plantarum **59**:91-94.

Long, S. P. 1991. Modification of the response of photosynthetic productivity to rising temperature by atmospheric CO_2 concentrations - has its importance been underestimated. Plant Cell and Environment **14**:729-739.

Lucht, W., C. B. Schaaf, and A. H. Strahler. 2000. An algorithm for the retrieval of albedo from space using semiempirical BRDF models. Ieee Transactions on Geoscience and Remote Sensing **38**:977-998.

Macarthur, R. H., and H. S. Horn. 1969. Foliage profile by vertical measurements. Ecology (Washington D C) **50**:802-804.

Majeke, B., J. A. N. van Aardt, and M. A. Cho. 2008. Imaging spectroscopy of foliar biochemistry in forestry environments. Southern Forests **70**:275-285.

Martin, M. E., and J. D. Aber. 1997. High spectral resolution remote sensing of forest canopy lignin, nitrogen, and ecosystem processes. Ecological Applications **7**:431-443.

Martin, M. E., L. C. Plourde, S. V. Ollinger, M. L. Smith, and B. E. McNeil. 2008. A generalizable method for remote sensing of canopy nitrogen across a wide range of forest ecosystems. Remote Sensing of Environment **112**:3511-3519.

Matson, P., L. Johnson, C. Billow, J. Miller, and R. L. Pu. 1994. Seasonal patterns and remote spectral estimation of canopy chemistry across the Oregon transect. Ecological Applications **4**:280-298.

May, J. D., S. B. Burdette, F. S. Gilliam, and M. B. Adams. 2005. Interspecific divergence in foliar nutrient dynamics and stem growth in a temperate forest in response to chronic nitrogen inputs. Canadian Journal of Forest Research-Revue Canadienne De Recherche Forestiere **35**:1023-1030.

McClaugherty, C., and B. Berg. 1987. Cellulose, lignin and nitrogen concentrations as rate regulating factors in late stages of forest litter decomposition. Pedobiologia **30**:101-112.

McMahon, G., S. M. Gregonis, S. W. Waltman, J. M. Omernik, T. D. Thorson, J. A. Freeouf, A. H. Rorick, and J. E. Keys. 2001. Developing a spatial framework of common ecological regions for the conterminous United States. Environmental Management **28**:293-316.

McNeil, B. E., K. M. de Beurs, K. N. Eshleman, J. R. Foster, and P. A. Townsend. 2007a. Maintenance of ecosystem nitrogen limitation by ephemeral forest disturbance: An assessment using MODIS, Hyperion, and Landsat ETM. Geophysical Research Letters **34**:-.

McNeil, B. E., J. M. Read, and C. T. Driscoll. 2007b. Foliar nitrogen responses to elevated atmospheric nitrogen deposition in nine temperate forest canopy species. Environmental Science & Technology **41**:5191-5197.

McNeil, B. E., J. M. Read, and C. T. Driscoll. 2012. Foliar Nitrogen Responses to the Environmental Gradient Matrix of the Adirondack Park, New York. Annals of the Association of American Geographers **102**:1-16.

McNeil, B. E., J. M. Read, T. J. Sullivan, T. C. McDonnell, I. J. Fernandez, and C. T. Driscoll. 2008. The spatial pattern of nitrogen cycling in the Adirondack Park, New York. Ecological Applications **18**:438-452.

Meador, M. R., and R. M. Goldstein. 2003. Assessing water quality at large geographic scales: Relations among land use, water physicochemistry, riparian condition, and fish community structure. Environmental Management **31**:504-517.

Meier, C. L., and W. D. Bowman. 2008. Links between plant litter chemistry, species diversity, and below-ground ecosystem function. Proceedings of the National Academy of Sciences of the United States of America **105**:19780-19785.

Melillo, J. M., J. D. Aber, and J. F. Muratore. 1982. Nitrogen and lignin control of hardwood leaf litter decomposition dynamics. Ecology **63**:621-626.

Menesatti, P., F. Antonucci, F. Pallottino, G. Roccuzzo, M. Allegra, F. Stagno, and F. Intrigliolo. 2010. Estimation of plant nutritional status by Vis-NIR spectrophotometric analysis on orange leaves Citrus sinensis (L) Osbeck cv Tarocco. Biosystems Engineering **105**:448-454.

Middleton, E. M., S. G. Ungar, D. J. Mandl, L. Ong, S. W. Frye, P. E. Campbell, D. R. Landis, J. P. Young, and N. H. Pollack. 2013. The Earth Observing One (EO-1) Satellite Mission: Over a Decade in Space. Ieee Journal of Selected Topics in Applied Earth Observations and Remote Sensing **6**:243-256.

Migita, C., Y. Chiba, and T. Tange. 2007. Seasonal and spatial variations in leaf nitrogen content and resorption in a Quercus serrata canopy. Tree Physiology **27**:63-70.

Mitchell, J. J., N. F. Glenn, T. T. Sankey, D. R. Derryberry, and M. J. Germino. 2012. Remote sensing of sagebrush canopy nitrogen. Remote Sensing of Environment **124**:217-223.

Mladenoff, D. J. 1987. Dynamics of nitrogen mineralization and nitrification in hemlock and hardwood treefall gaps. Ecology **68**:1171-1180.

Montes, M. J., and B.-C. Gao. 2004. NRL Atmospheric Correction Algorithms for Oceans: TAFKAA Users' Guide.

Niinemets, U. 2001. Global-scale climatic controls of leaf dry mass per area, density, and thickness in trees and shrubs. Ecology **82**:453-469.

Ollinger, S. V. 2011. Sources of variability in canopy reflectance and the convergent properties of plants. New Phytologist **189**:375-394.

Ollinger, S. V., P. B. Reich, S. Frolking, L. C. Lepine, D. Y. Hollinger, and A. D. Richardson. 2013. Nitrogen cycling, forest canopy reflectance, and emergent properties of ecosystems. Proceedings of the National Academy of Sciences of the United States of America **110**:E2437-E2437.

Ollinger, S. V., and M. L. Smith. 2005. Net primary production and canopy nitrogen in a temperate forest landscape: An analysis using imaging spectroscopy, modeling and field data. Ecosystems **8**:760-778.

Ollinger, S. V., M. L. Smith, M. E. Martin, R. A. Hallett, C. L. Goodale, and J. D. Aber. 2002. Regional variation in foliar chemistry and N cycling among forests of diverse history and composition. Ecology **83**:339-355.

Omernik, J. M. 1987. Ecoregions of the conterminous United States: Map (scale 1:7,500,000). Annals of the Association of American Geographers **77**:118-125.

Omernik, J. M., S. S. Chapman, R. A. Lillie, and R. T. Dumke. 2000. Ecoregions of Wisconsin.

Pastor, J., J. D. Aber, C. A. McClaugherty, and J. M. Melillo. 1982. Geology, soils and vegetation of Blackhawk Island, Wisconsin. American Midland Naturalist **108**:266-277.

Pastor, J., J. D. Aber, C. A. McClaugherty, and J. M. Melillo. 1984. Above-ground production and N and P cycling along a nitrogen mineralization gradient on Blackhawk Island, Wisconsin. Ecology **65**:256-268.

Petisco, C., B. Garcia-Criado, S. Mediavilla, B. R. V. de Aldana, I. Zabalgogeazcoa, and A. Garcia-Ciudad. 2006. Near-infrared reflectance spectroscopy as a fast and non-destructive tool to predict foliar organic constituents of several woody species. Analytical and Bioanalytical Chemistry **386**:1823-1833.

Piatek, K. B., P. Munasinghe, W. T. Peterjohn, M. B. Adams, and J. R. Cumming. 2009. Oak contribution to litter nutrient dynamics in an Appalachian forest receiving elevated nitrogen and dolomite. Canadian Journal of Forest Research-Revue Canadienne De Recherche Forestiere **39**:936-944.

Quested, H., O. Eriksson, C. Fortunel, and E. Garnier. 2007. Plant traits relate to whole-community litter quality and decomposition following land use change. Functional Ecology **21**:1016-1026.

Reich, P. B., D. S. Ellsworth, and M. B. Walters. 1998. Leaf structure (specific leaf area) modulates photosynthesis-nitrogen relations: evidence from within and across species and functional groups. Functional Ecology **12**:948-958.

Reich, P. B., D. S. Ellsworth, M. B. Walters, J. M. Vose, C. Gresham, J. C. Volin, and W. D. Bowman. 1999. Generality of leaf trait relationships: A test across six biomes. Ecology **80**:1955-1969.

Reich, P. B., C. Uhl, M. B. Walters, and D. S. Ellsworth. 1991. Leaf life-span as a determinant of leaf structure and function among 23 Amazonian tree species. Oecologia **86**:16-24.

Reich, P. B., M. B. Walters, and D. S. Ellsworth. 1992. Leaf life-span in relation to leaf, plant, and stand characteristics among diverse ecosystems Ecological Monographs **62**:365-392.

Reich, P. B., M. B. Walters, and D. S. Ellsworth. 1997. From tropics to tundra: Global convergence in plant functioning. Proceedings of the National Academy of Sciences of the United States of America **94**:13730-13734.

Reich, P. B., I. J. Wright, J. Cavender-Bares, J. M. Craine, J. Oleksyn, M. Westoby, and M. B. Walters. 2003. The evolution of plant functional variation: Traits, spectra, and strategies. International Journal of Plant Sciences **164**:S143-S164.

Rhemtulla, J. M., D. J. Mladenoff, and M. K. Clayton. 2009. Historical forest baselines reveal potential for continued carbon sequestration. Proceedings of the National Academy of Sciences of the United States of America **106**:6082-6087.

Richardson, A. D., and J. B. Reeves. 2005. Quantitative reflectance spectroscopy as an alternative to traditional wet lab analysis of foliar chemistry: near-infrared and mid-infrared calibrations compared. Canadian Journal of Forest Research-Revue Canadienne De Recherche Forestiere **35**:1122-1130.

Ripullone, F., G. Grassi, M. Lauteri, and M. Borghetti. 2003. Photosynthesis-nitrogen relationships: interpretation of different patterns between Pseudotsuga menziesii and Populus x euroamericana in a mini-stand experiment. Tree Physiology **23**:137-144.

Robinson, C. T., and C. Jolidon. 2005. Leaf breakdown and the ecosystem functioning of alpine streams. Journal of the North American Benthological Society **24**:495-507.

Roujean, J. L., M. Leroy, and P. Y. Deschamps. 1992. A bidirectional reflectance model of the earth's surface for the correction of remote sensing data Journal of Geophysical Research **97**:20455-20468.

Sanchez-Azofeifa, G. A., K. Castro, S. J. Wright, J. Gamon, M. Kalacska, B. Rivard, S. A. Schnitzer, and J. L. Feng. 2009. Differences in leaf traits, leaf internal structure, and spectral reflectance between two communities of lianas and trees: Implications for remote sensing in tropical environments. Remote Sensing of Environment **113**:2076-2088.

Santiago, L. S. 2007. Extending the leaf economics spectrum to decomposition: Evidence from a tropical forest. Ecology **88**:1126-1131.

Santiago, L. S., K. Kitajima, S. J. Wright, and S. S. Mulkey. 2004. Coordinated changes in photosynthesis, water relations and leaf nutritional traits of canopy trees along a precipitation gradient in lowland tropical forest. Oecologia **139**:495-502.

Schadler, M., G. Jung, H. Auge, and R. Brandl. 2003. Palatability, decomposition and insect herbivory: patterns in a successional old-field plant community. Oikos **103**:121-132.

Schimel, D. S. 1995. Terrestrial ecosystems and the carbon-cycle. Global Change Biology **1**:77-91.

Schlerf, M., C. Atzberger, J. Hill, H. Buddenbaum, W. Werner, and G. Schuler. 2010. Retrieval of chlorophyll and nitrogen in Norway spruce (*Picea abies* L. Karst.) using imaging spectroscopy. International Journal of Applied Earth Observation and Geoinformation **12**:17-26.

Schulte, L. A., D. J. Mladenoff, S. N. Burrows, T. A. Sickley, and E. V. Nordheim. 2005. Spatial controls of Pre-Euro-American wind and fire disturbance in Northern Wisconsin (USA) forest landscapes. Ecosystems **8**:73-94.

Scogings, P. F., L. E. Dziba, and I. J. Gordon. 2004. Leaf chemistry of woody plants in relation to season, canopy retention and goat browsing in a semiarid subtropical savanna. Austral Ecology **29**:278-286.

Scott, N. A., and D. Binkley. 1997. Foliage litter quality and annual net N mineralization: Comparison across North American forest sites. Oecologia **111**:151-159.

Serrano, L., J. Penuelas, and S. L. Ustin. 2002. Remote sensing of nitrogen and lignin in Mediterranean vegetation from AVIRIS data: Decomposing biochemical from structural signals. Remote Sensing of Environment **81**:355-364.

Shipley, B., and M. J. Lechowicz. 2000. The functional co-ordination of leaf morphology, nitrogen concentration, and gas exchange in 40 wetland species. Ecoscience **7**:183-194.

Shipley, B., M. J. Lechowicz, I. Wright, and P. B. Reich. 2006. Fundamental trade-offs generating the worldwide leaf economics spectrum. Ecology **87**:535-541.

Shipley, B., D. Vile, E. Garnier, I. J. Wright, and H. Poorter. 2005. Functional linkages between leaf traits and net photosynthetic rate: reconciling empirical and mechanistic models. Functional Ecology **19**:602-615.

Sims, D. A., and J. A. Gamon. 2002. Relationships between leaf pigment content and spectral reflectance across a wide range of species, leaf structures and developmental stages. Remote Sensing of Environment **81**:337-354.

Sims, N. C., D. Culvenor, G. Newnham, N. C. Coops, and P. Hopmans. 2013. Towards the Operational Use of Satellite Hyperspectral Image Data for Mapping Nutrient Status and Fertilizer Requirements in Australian Plantation Forests. Ieee Journal of Selected Topics in Applied Earth Observations and Remote Sensing **6**:320-328.

Singh, A., A. R. Jakubowski, I. Chidister, and P. A. Townsend. 2013. A MODIS approach to predicting stream water quality in Wisconsin. Remote Sensing of Environment **128**:74-86.

Slaton, M. R., E. R. Hunt, and W. K. Smith. 2001. Estimating near-infrared leaf reflectance from leaf structural characteristics. American Journal of Botany **88**:278-284.

Smith, M. L., and M. E. Martin. 2001. A plot-based method for rapid estimation of forest canopy chemistry. Canadian Journal of Forest Research-Revue Canadienne De Recherche Forestiere **31**:549-555.

Smith, M. L., M. E. Martin, L. Plourde, and S. V. Ollinger. 2003. Analysis of hyperspectral data for estimation of temperate forest canopy nitrogen concentration: Comparison between an airborne (AVIRIS) and a spaceborne (Hyperion) sensor. Ieee Transactions on Geoscience and Remote Sensing **41**:1332-1337.

Smith, M. L., S. V. Ollinger, M. E. Martin, J. D. Aber, R. A. Hallett, and C. L. Goodale. 2002. Direct estimation of aboveground forest productivity through hyperspectral remote sensing of canopy nitrogen. Ecological Applications **12**:1286-1302.

Soenen, S. A., D. R. Peddle, and C. A. Coburn. 2005. SCS+C: A modified sun-canopy-sensor topographic correction in forested terrain. Ieee Transactions on Geoscience and Remote Sensing **43**:2148-2159.

Stuffler, T., C. Kaufmann, S. Hofer, K. P. Forster, G. Schreier, A. Mueller, A. Eckardt, H. Bach, B. Penne, U. Benz, and R. Haydn. 2007. The EnMAP hyperspectral imager-An advanced optical payload for future applications in Earth observation programmes. Acta Astronautica **61**:115-120.

Townsend, A. R., G. P. Asner, and C. C. Cleveland. 2008. The biogeochemical heterogeneity of tropical forests. Trends in Ecology & Evolution **23**:424-431.

Townsend, P. A., K. N. Eshleman, and C. Welcker. 2004. Remote sensing of gypsy moth defoliation to assess variations in stream nitrogen concentrations. Ecological Applications **14**:504-516.

Townsend, P. A., J. R. Foster, R. A. Chastain, and W. S. Currie. 2003. Application of imaging spectroscopy to mapping canopy nitrogen in the forests of the central

Appalachian Mountains using Hyperion and AVIRIS. Ieee Transactions on Geoscience and Remote Sensing **41**:1347-1354.

Townsend, P. A., S. P. Serbin, E. L. Kruger, and J. A. Gamon. 2013. Disentangling the contribution of biological and physical properties of leaves and canopies in imaging spectroscopy data. Proceedings of the National Academy of Sciences of the United States of America **110**:E1074-E1074.

Townsend, P. A., A. Singh, J. R. Foster, N. J. Rehberg, C. C. Kingdon, K. N. Eshleman, and S. W. Seagle. 2012. A general Landsat model to predict canopy defoliation in broadleaf deciduous forests. Remote Sensing of Environment **119**:255-265.

Tucker, C. J. 1980. Remote-sensing of leaf water-content in the near-infrared. Remote Sensing of Environment **10**:23-32.

Ustin, S. L., and J. A. Gamon. 2010. Remote sensing of plant functional types. New Phytologist **186**:795-816.

Ustin, S. L., D. Riano, and E. R. Hunt. 2012. Estimating canopy water content from spectroscopy. Israel Journal of Plant Sciences **60**:9-23.

Ustin, S. L., D. A. Roberts, J. A. Gamon, G. P. Asner, and R. O. Green. 2004. Using imaging spectroscopy to study ecosystem processes and properties. Bioscience **54**:523-534.

Vane, G., R. O. Green, T. G. Chrien, H. T. Enmark, E. G. Hansen, and W. M. Porter. 1993. The Airborne Visible Infrared Imaging Spectrometer (AVIRIS). Remote Sensing of Environment **44**:127-143.

Violle, C., E. Garnier, J. Lecoeur, C. Roumet, C. Podeur, A. Blanchard, and M. L. Navas. 2009. Competition, traits and resource depletion in plant communities. Oecologia **160**:747-755.

Wessman, C. A., J. D. Aber, and D. L. Peterson. 1989. An evaluation of imaging spectrometry for estimating forest canopy chemistry. International Journal of Remote Sensing **10**:1293-1316.

Wold, S. 1994. PLS for Multivariate Linear Modeling. Page 359 *in* H. Waterbeemd, H. Timmerman, R. Mannhold, and P. Kroqsgaard-Larsen, editors. QSAR: Chemometric Methods in Molecular Design. Methods and Principles in Medicinal Chemistry. Wiley.

Wold, S., A. Ruhe, H. Wold, and W. J. Dunn. 1984. The Collinearity Problem in Linear-Regression - the Partial Least-Squares (Pls) Approach to Generalized Inverses. Siam Journal on Scientific and Statistical Computing **5**:735-743.

Wold, S., M. Sjostrom, and L. Eriksson. 2001. PLS-regression: a basic tool of chemometrics. Chemometrics and Intelligent Laboratory Systems **58**:109-130.

Wolter, P. T., P. A. Townsend, B. R. Sturtevant, and C. C. Kingdon. 2008. Remote sensing of the distribution and abundance of host species for spruce budworm in Northern Minnesota and Ontario. Remote Sensing of Environment **112**:3971-3982.

Wright, I. J., P. B. Reich, J. H. C. Cornelissen, D. S. Falster, E. Garnier, K. Hikosaka, B. B. Lamont, W. Lee, J. Oleksyn, N. Osada, H. Poorter, R. Villar, D. I. Warton, and M. Westoby. 2005a. Assessing the generality of global leaf trait relationships. New Phytologist **166**:485-496.

Wright, I. J., P. B. Reich, J. H. C. Cornelissen, D. S. Falster, P. K. Groom, K. Hikosaka, W. Lee, C. H. Lusk, U. Niinemets, J. Oleksyn, N. Osada, H. Poorter, D. I. Warton, and M. Westoby. 2005b. Modulation of leaf economic traits and trait relationships by climate. Global Ecology and Biogeography **14**:411-421.

Wright, I. J., P. B. Reich, and M. Westoby. 2001. Strategy shifts in leaf physiology, structure and nutrient content between species of high- and low-rainfall and high- and low-nutrient habitats. Functional Ecology **15**:423-434.

Wright, I. J., P. B. Reich, M. Westoby, D. D. Ackerly, Z. Baruch, F. Bongers, J. Cavender-Bares, T. Chapin, J. H. C. Cornelissen, M. Diemer, J. Flexas, E. Garnier, P. K. Groom, J. Gulias, K. Hikosaka, B. B. Lamont, T. Lee, W. Lee, C. Lusk, J. J. Midgley, M. L. Navas, U. Niinemets, J. Oleksyn, N. Osada, H. Poorter, P. Poot, L. Prior, V. I. Pyankov, C. Roumet, S. C. Thomas, M. G. Tjoelker, E. J. Veneklaas, and R. Villar. 2004. The worldwide leaf economics spectrum. Nature **428**:821-827.

Wright, I. J., and M. Westoby. 2002. Leaves at low versus high rainfall: coordination of structure, lifespan and physiology. New Phytologist **155**:403-416.

Yoder, B. J., and R. E. Pettigrewcrosby. 1995. Predicting nitrogen and chlorophyll content and concentrations from reflectance spectra (400-2500 nm) at leaf and canopy scales. Remote Sensing of Environment **53**:199-211.

Youngentob, K. N., L. J. Renzullo, A. A. Held, X. P. Jia, D. B. Lindenmayer, and W. J. Foley. 2012. Using imaging spectroscopy to estimate integrated measures of foliage nutritional quality. Methods in Ecology and Evolution **3**:416-426.

Tables

Table 1 Summary statistics for canopy-level nutritional and morphological traits examined in this study. Means, standard deviations and ranges of leaf traits are presented aggregated across 164 plots sampled from 2008-2011.

	Overall		Needleleaf		Broadleaf	
Trait	Mean (SD)	Range	Mean (SD)	Range	Mean (SD)	Range
$M_{area}(g/m_2)$	101.55 (43.61)	46.50 - 255.92	156.77 (30.91)	98.77 - 255.92	77.18 (19.45)	46.50 - 203.72
N%	2.25 (0.55)	0.94 - 3.34	1.6 (0.33)	0.94 - 2.35	2.53 (0.36)	1.66 - 3.34
C%	49.57 (1.00)	46.23 - 53.51	50.47 (0.62)	48.98 - 53.51	49.18 (0.87)	46.23 - 51.74
ADF%	36.81 (6.74)	20.82 - 53.71	44.27 (5.10)	35.1 - 53.71	33.51 (4.31)	20.82 - 45.54
ADL%	21.21 (4.47)	11.04 - 36.17	25.69 (3.03)	20.42 - 36.17	19.23 (3.46)	11.04 - 28.78
Cellulose%	16.39 (2.44)	9.57 - 22.58	18.53 (2.27)	12.37 - 22.58	15.44 (1.84)	9.57 - 20.21

Table 2 Pearson product moment correlation coefficients between plot-level traits, mean annual precipitation (MAP), mean annual temperature (MAT), latitude and NADP total annual NO_3 deposition (http://nadp.sws.uiuc.edu/).

	M_{area}	N%	C%	ADF%	ADL%	Cellulose%	MAP	MAT	Lat.
N%	-0.804***								
C%	0.601***	-0.554***							
ADF%	0.751***	-0.655***	0.584***						
ADL%	0.680***	-0.514***	0.619***	0.926***					
Cellulose%	0.586***	-0.520***	0.398***	0.869***	0.757***				
MAP	-0.227***	-0.064	0.132	0.033	0.003	-0.077			
MAT	-0.322***	0.424***	-0.152*	-0.247***	-0.162*	-0.291***	0.083		
Lat.	0.371***	-0.343***	0.080	0.204***	0.138	0.295***	-0.482***	-0.899***	
N Dep.	-0.209***	0.394***	-0.202***	-0.146	-0.123	-0.155*	0.047	0.226***	-0.221***

$P < 0.0001$***; $P < 0.01$**; $P < 0.05$*

Table 3 Summary of PLSR models built using AVIRIS spectra and foliar traits scaled to the plot level. Means of coefficients of determination (R^2) and associated root mean squared error (RMSE) statistics of 500 randomized models are presented along with associated uncertainty estimates (S.D. in parenthesis). Model-averaged fits indicate the accuracies obtained at the image level after averaging predictions from 500 models.

				Calibration		Validation		Model-averaged	
Property	N	Train %	*h*	R^2	RMSE	R^2	RMSE	R^2	RMSE
M_{area} (g/m^2)	223	25.89	10	0.92 (0.160)	12.11 (1.117)	0.81 (0.024)	18.15 (1.189)	0.87	15.006
N_{mass} (%)	224	26.91	10	0.91 (0.017)	0.17 (0.150)	0.81 (0.024)	0.24 (0.015)	0.87	0.205
C_{mass} (%)	216	25.84	8	0.61 (0.059)	0.56 (0.052)	0.44 (0.070)	0.65 (0.047)	0.58	0.571
ADF (%)	221	27.08	10	0.81 (0.034)	3.00 (0.269)	0.59 (0.053)	4.18 (0.274)	0.74	3.419
ADL (%)	222	26.00	10	0.81 (0.039)	1.94 (0.201)	0.58 (0.052)	2.87 (0.183)	0.73	2.297
Cellulose (%)	223	25.96	9	0.67 (0.057)	1.42 (0.123)	0.34 (0.059)	1.93 (0.094)	0.54	1.621

Train%: Fraction of data used for model calibration; *h*: Number of PLSR components used to build PLSR models.

Figures

Figure 1: Locations of field sampling plots (164) overlaid on AVIRIS acquisitions (143) from 2008-2011. Boxes indicate locations of sites graphed in subsequent figures; A: Porcupine Mountains SF, MI; B: Ottawa NF, MI; C Flambeau River SF, WI; D: Devil's Lake State Park, WI; E: Fernow Experimental Forest, WV; F: Green River SF, MD.

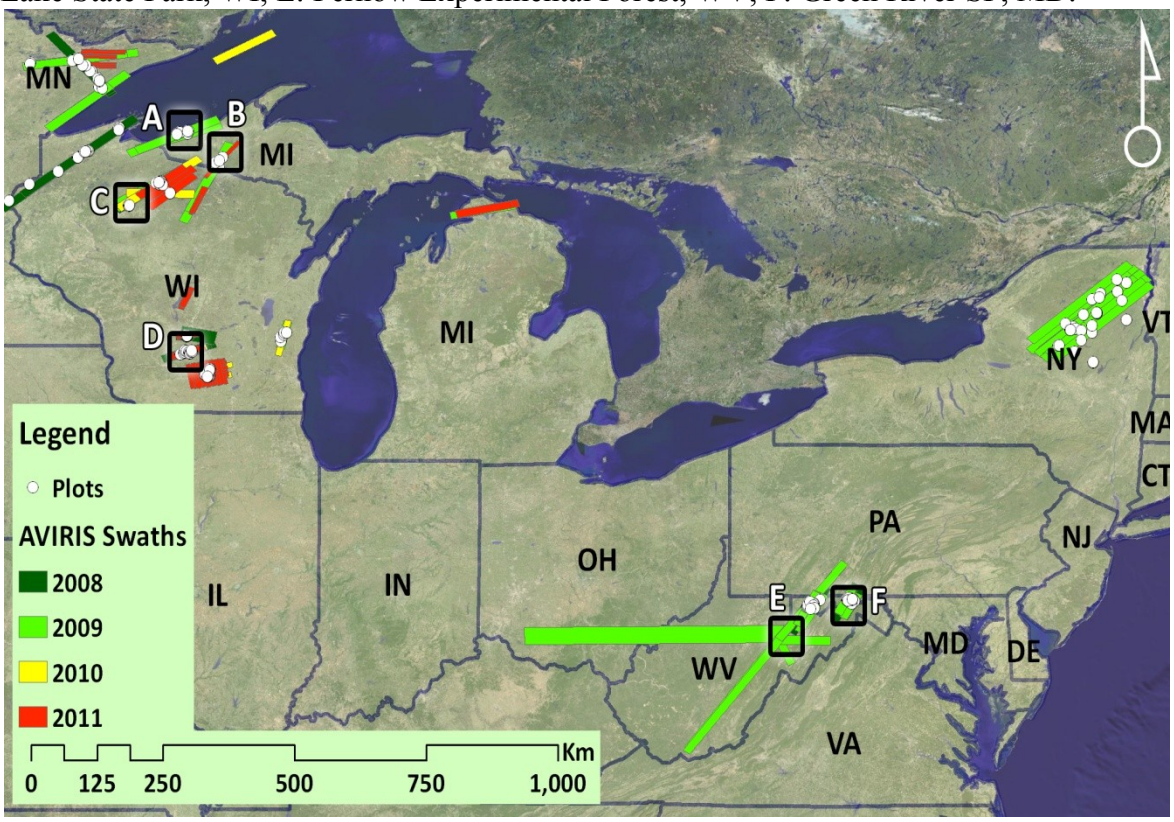

Figure 2: Scaling leaf-level functional traits to the canopy using AVIRIS imagery.

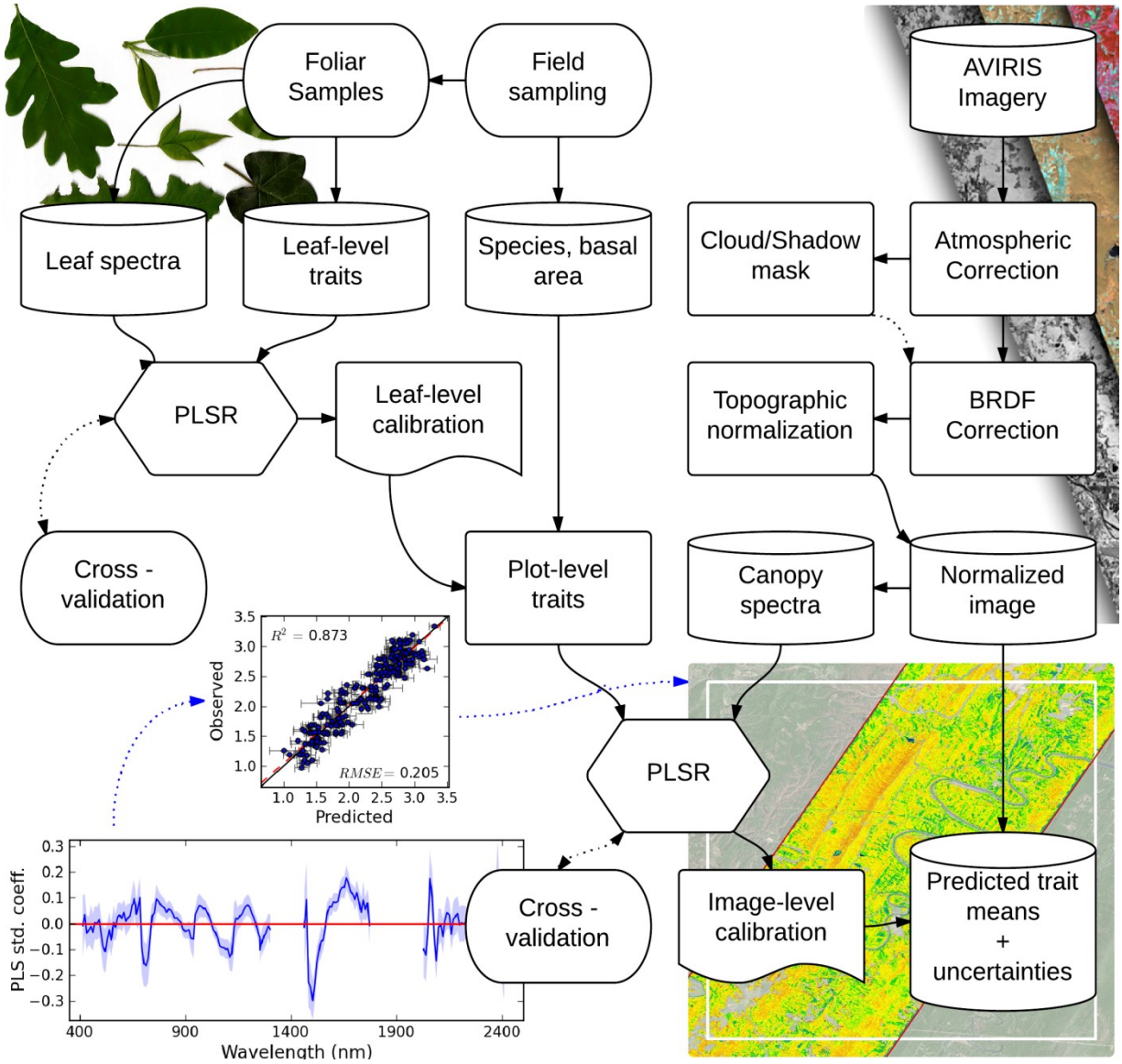

Figure 3: Figure illustrating covariance between foliar biochemical and morphological traits measured in this study. *X*-axis: leaf mass per area (M_{area}, g/m^2), *y*-axis: Acid Dissolvable Lignin (ADL%); *z*-axis: leaf nitrogen content on a mass basis (N%).

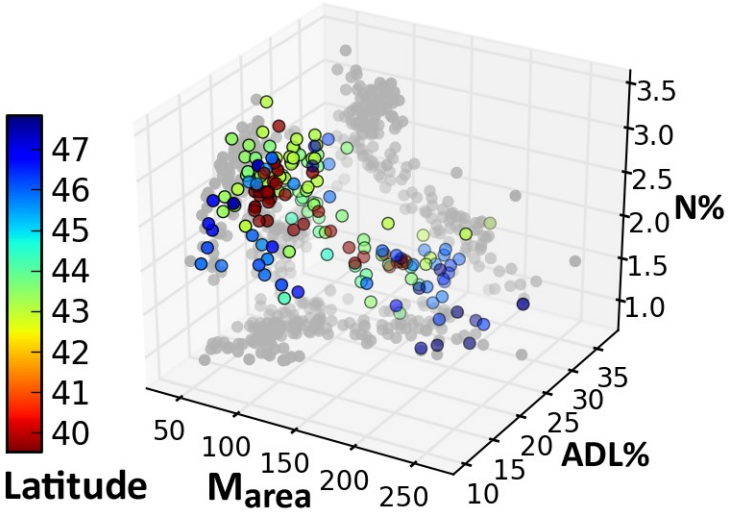

Figure 4: Means (with standard deviation bands) of AVIRIS spectra obtained from 51 images and 164 plots stratified by dominant leaf habit (deciduous, needleleaf).

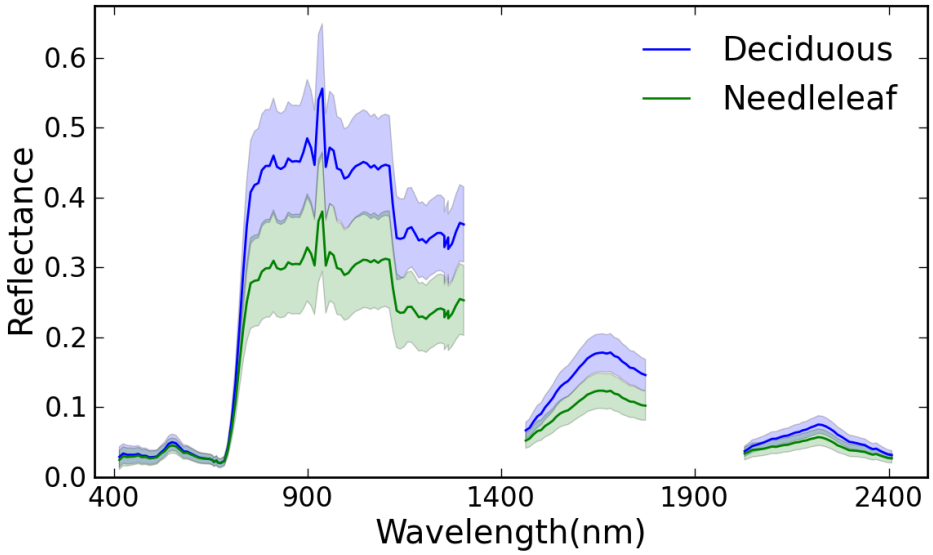

Figure 5: Results of PLSR models using AVIRIS-derived spectra fitted to leaf mass per area (M_{area}) scaled from leaves to the canopy. Top left: Profile of the PRESS (predicted residual sum of squares) statistic (with ±1 S.D. bars) obtained by fitting 500 randomized models, each using an increasing number of PLS components (*h*, on the *x*-axis). The final model was fit using the components that minimized the PRESS statistic. Top right: Standardized PLSR coefficients of the final model indicating the magnitude and direction of influence of each wavelength (with ±1 S.D. bands.) Note that raw coefficients are applied to image spectra to derive spatial predictions. Bottom right: Profile of the Variable Importance of Prediction (VIP) statistic with ±1 S.D. bands. The VIP describes the relative importance of each wavelength in predicting the quantity of interest, and is considered significant if > 0.8. Bottom left: Model performance evaluated by averaging 500 randomized models built with a 50/50 calibration/validation split. Horizontal bars indicate uncertainty in predictions; vertical bars indicate uncertainty in plot-level estimates propagated from leaf-level measurements. The purple line in the top right plot indicates PLSR coefficients obtained for leaf-level estimates of M_{area}. Vertical green bars are absorption features at wavelengths known from previous studies.

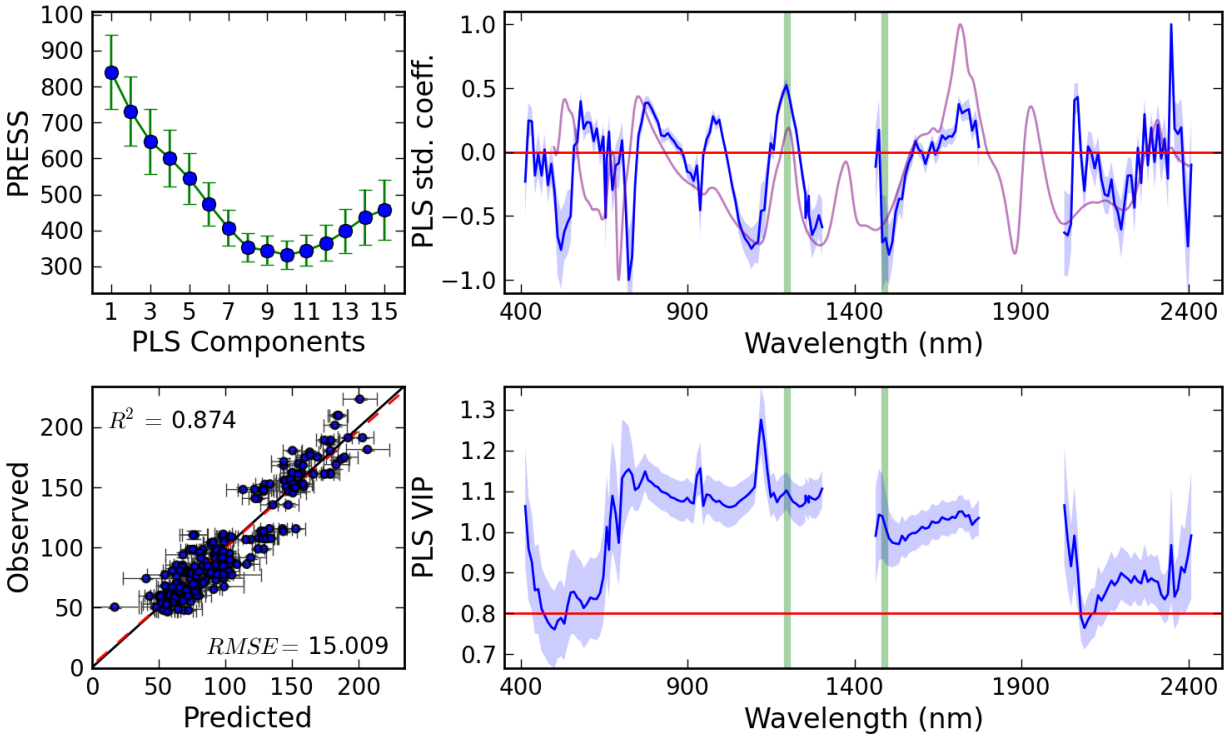

Figure 6: Results of PLSR models using AVIRIS-derived spectra fitted to leaf nitrogen content (mass-based %N) scaled from leaves to the canopy. See Figure 5 for description. The purple line in the top right plot indicates raw PLSR coefficients from Martin et al (2008).

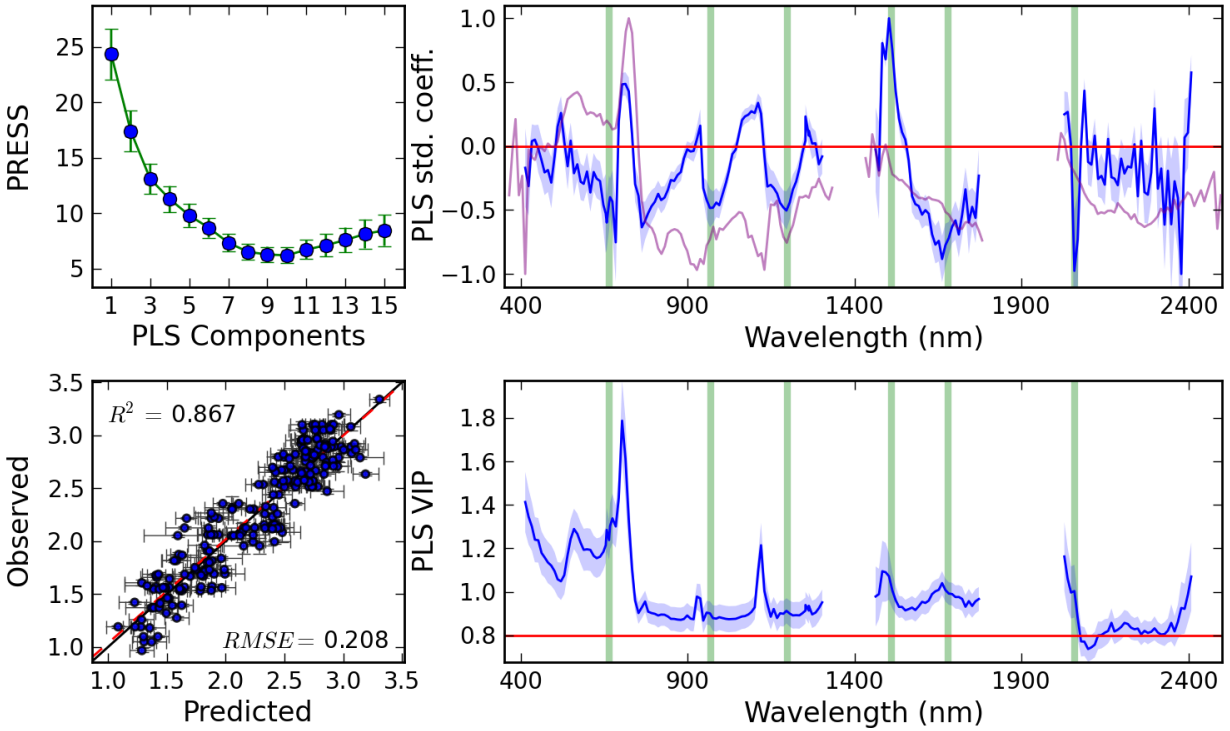

Figure 7: Results of PLSR models using AVIRIS-derived spectra fitted to leaf carbon content (mass-based %C) scaled from leaves to the canopy. See Figure 5 for description.

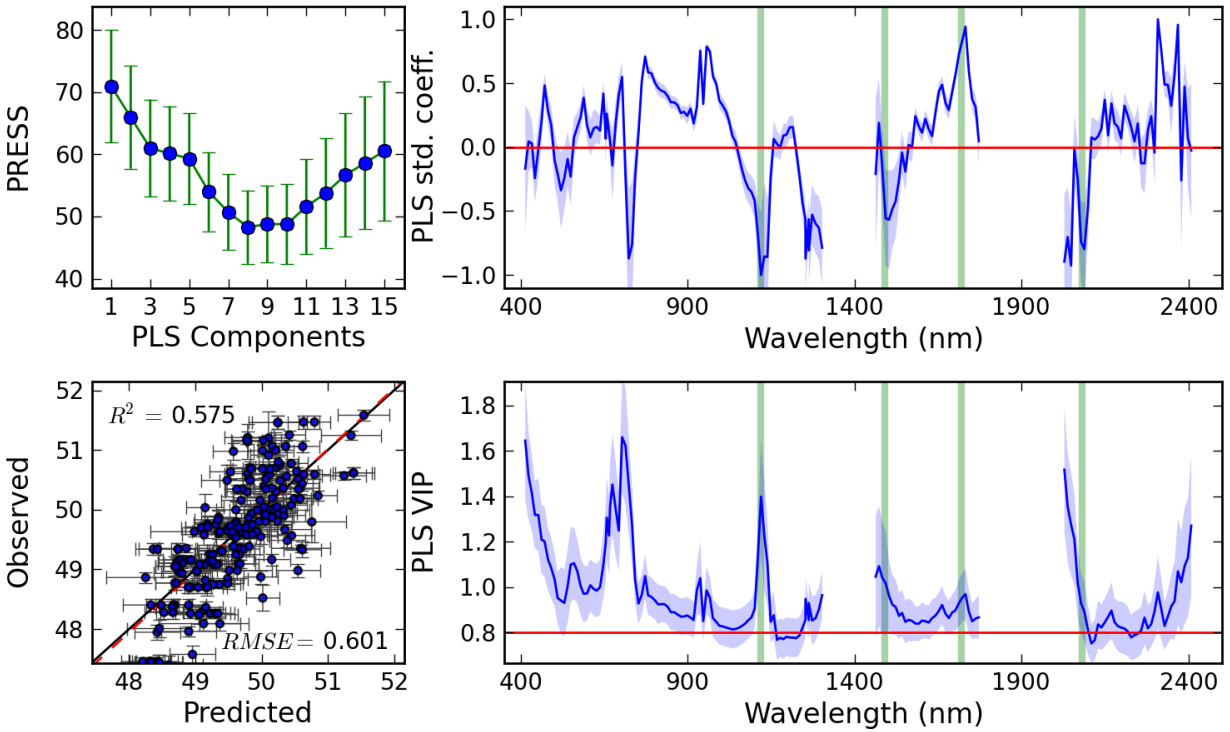

Figure 8: Results of PLSR models using AVIRIS-derived spectra fitted to leaf fiber content (acid detergent fiber %ADL) scaled from leaves to the canopy. See Figure 5 for description.

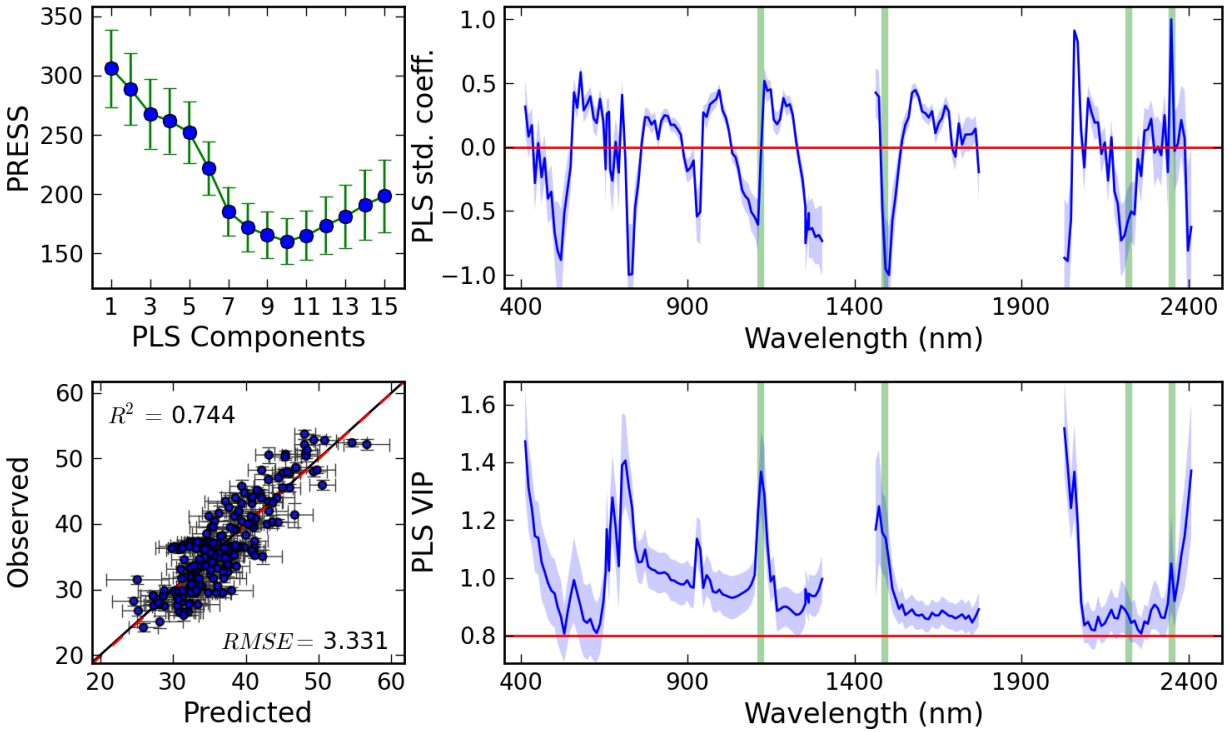

Figure 9: Results of PLSR models using AVIRIS-derived spectra fitted to leaf lignin content (acid detergent lignin %ADL) scaled from leaves to the canopy. See Figure 5 for description.

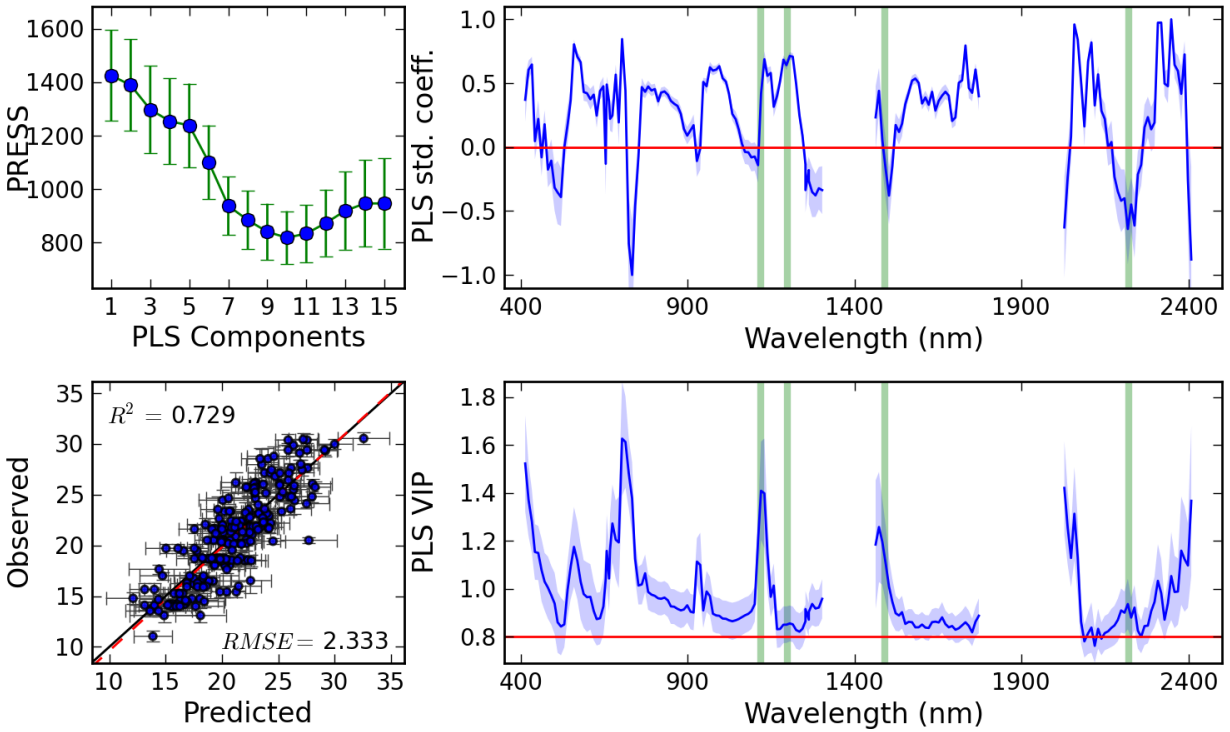

Figure 10: Results of PLSR models using AVIRIS-derived spectra fitted to leaf cellulose content (% Cellulose) scaled from leaves to the canopy. See Figure 5 for description.

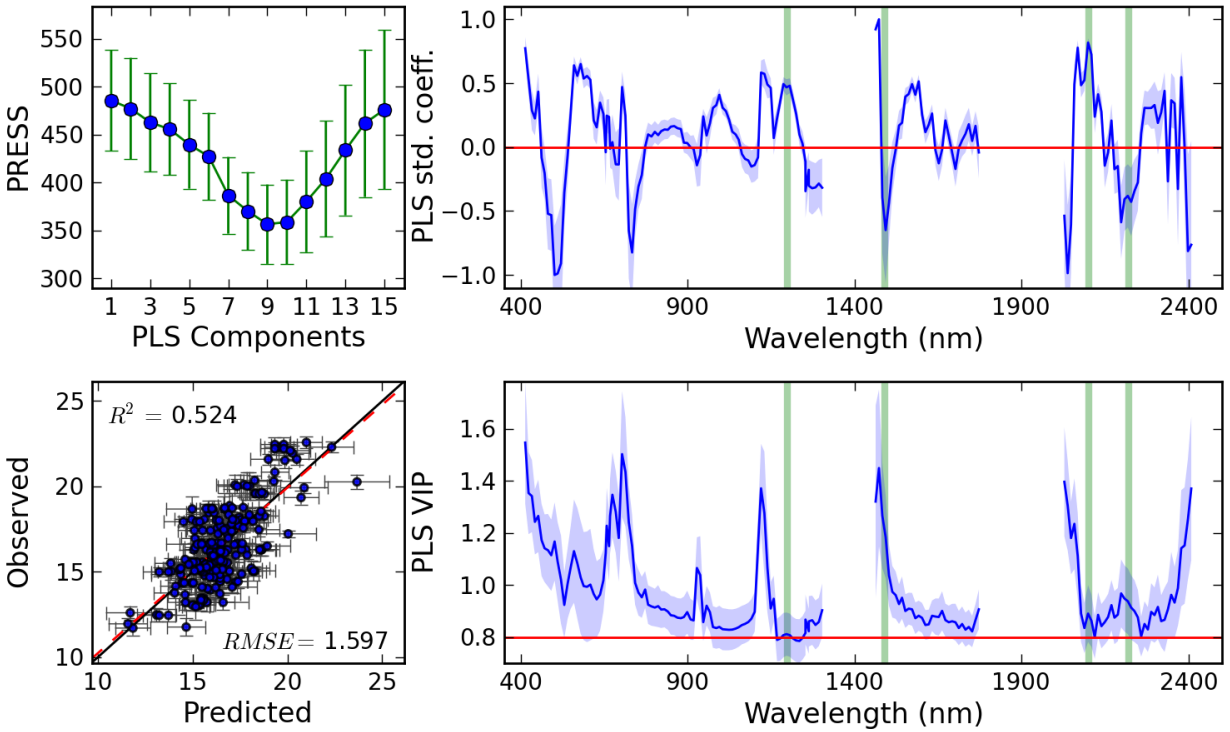

Figure 11: Spatial predictions of M_{area}, %N, and %C (left panels; and uncertainties, right panels) obtained by applying coefficients obtained from 500 randomized PLSR models to AVIRIS imagery acquired over the Green Ridge State forest MD (box F, Fig. 1). Each model was built with a 50/50 calibration/validation split. Left panels are pixel-wise means of 500 model predictions; right panels are standard deviations. See Table 3 for model statistics; Table S2 in supplementary materials for model coefficients.

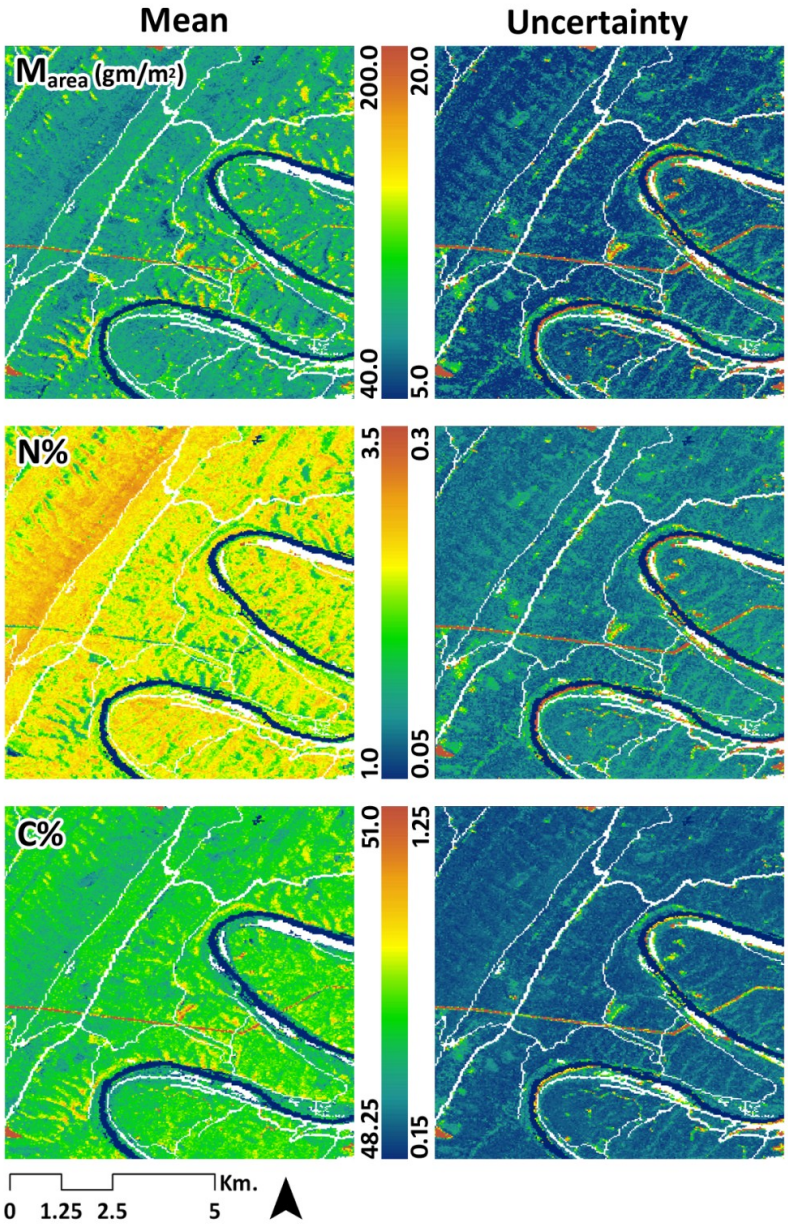

Figure 12: Spatial predictions of %ADF, %ADL and %Cellulose (left panels; and uncertainties, right panels) obtained by applying coefficients obtained from 500 randomized PLSR models to AVIRIS imagery acquired over the Green Ridge State forest MD (box F, Fig. 1). Each model was built with a 50/50 calibration/validation split. Left panels are pixel-wise means of 500 model predictions; right panels are 1.0 standard deviations. See Table 3 for model statistics; Table S2 in supplementary materials for model coefficients.

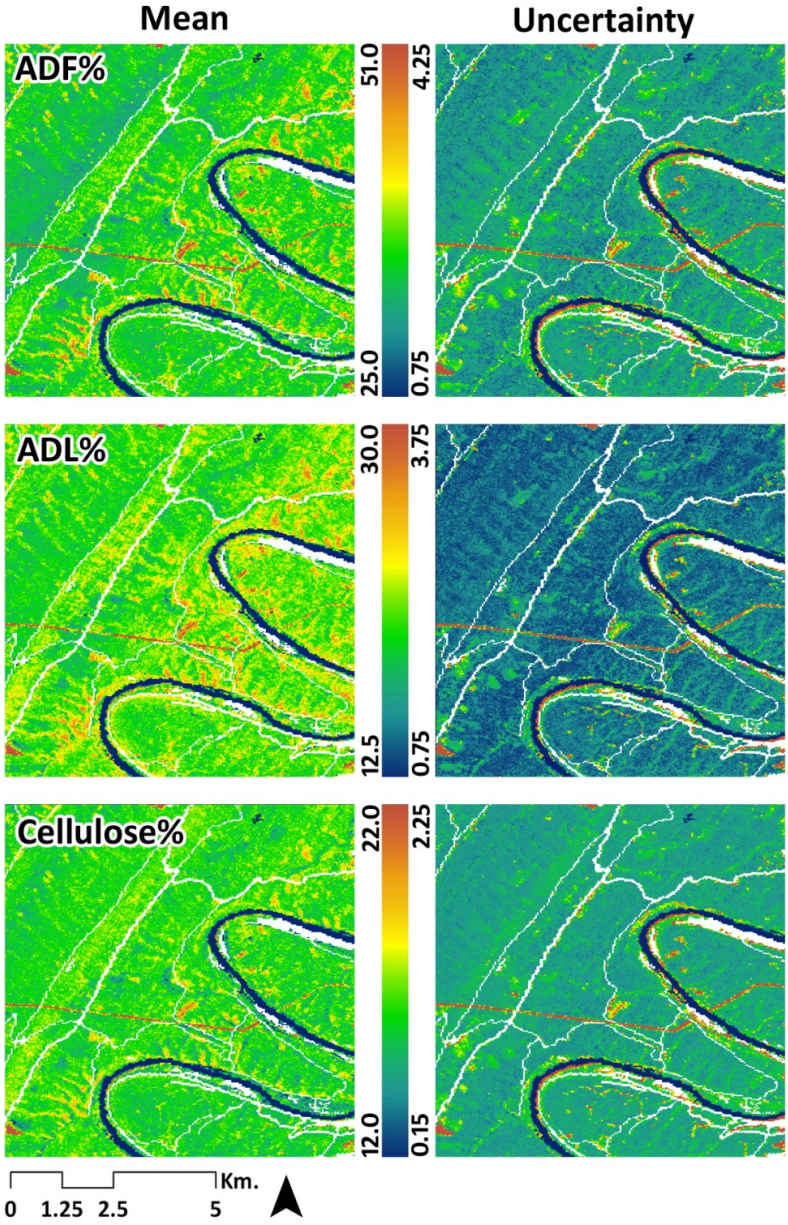

Figure 13: False color composites of foliar traits (left panels; R/G/B = ADL/Nitrogen/M_{area}) compared with NLCD 2006 landcover maps (right panels). Foliar trait association maps provide richer information on foliar traits across forest ecotones than discrete classes. Subplot locations are A: Porcupine Mountains SF; B: Ottawa National Forest, MI; and F: Green Ridge SF, MD (boxes in Fig. 1, Landcover classification legend is Figure S5 in supplementary materials)

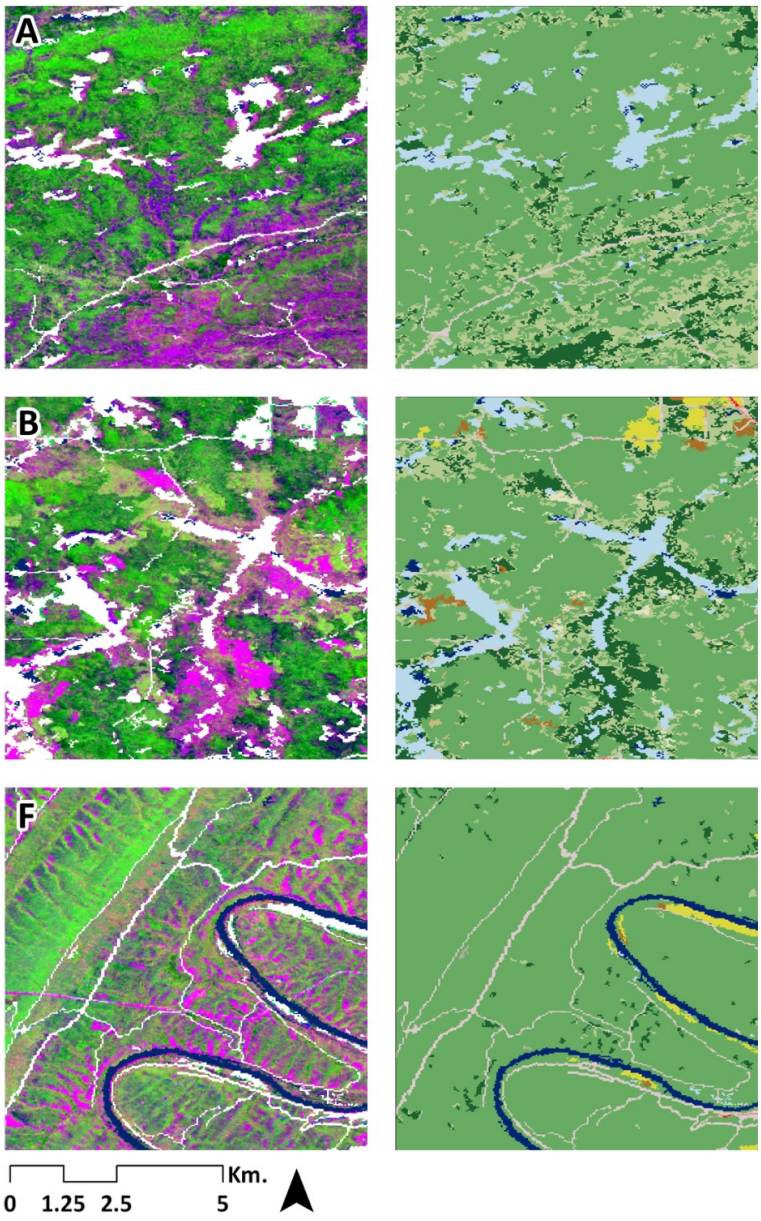

Figure 14: Spatial variation in predicted foliar nitrogen content (%N) in forested regions sampled across the Midwestern and Northeastern United States. Letters denote boxes in Fig. 1.

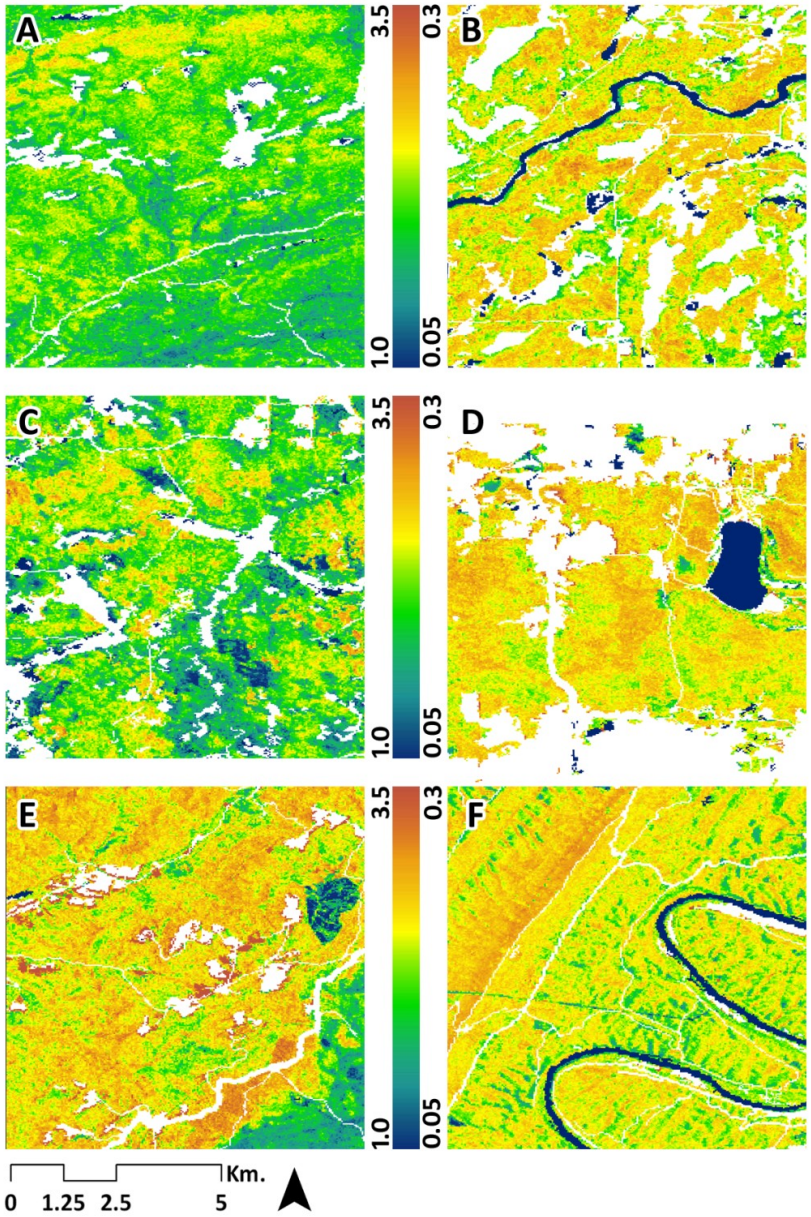

Figure 15: Spatial variation in predicted leaf mass per area (M_{area} g/m^2) in forested regions sampled across the Midwestern and Northeastern United States. Letters denote boxes in Fig. 1.

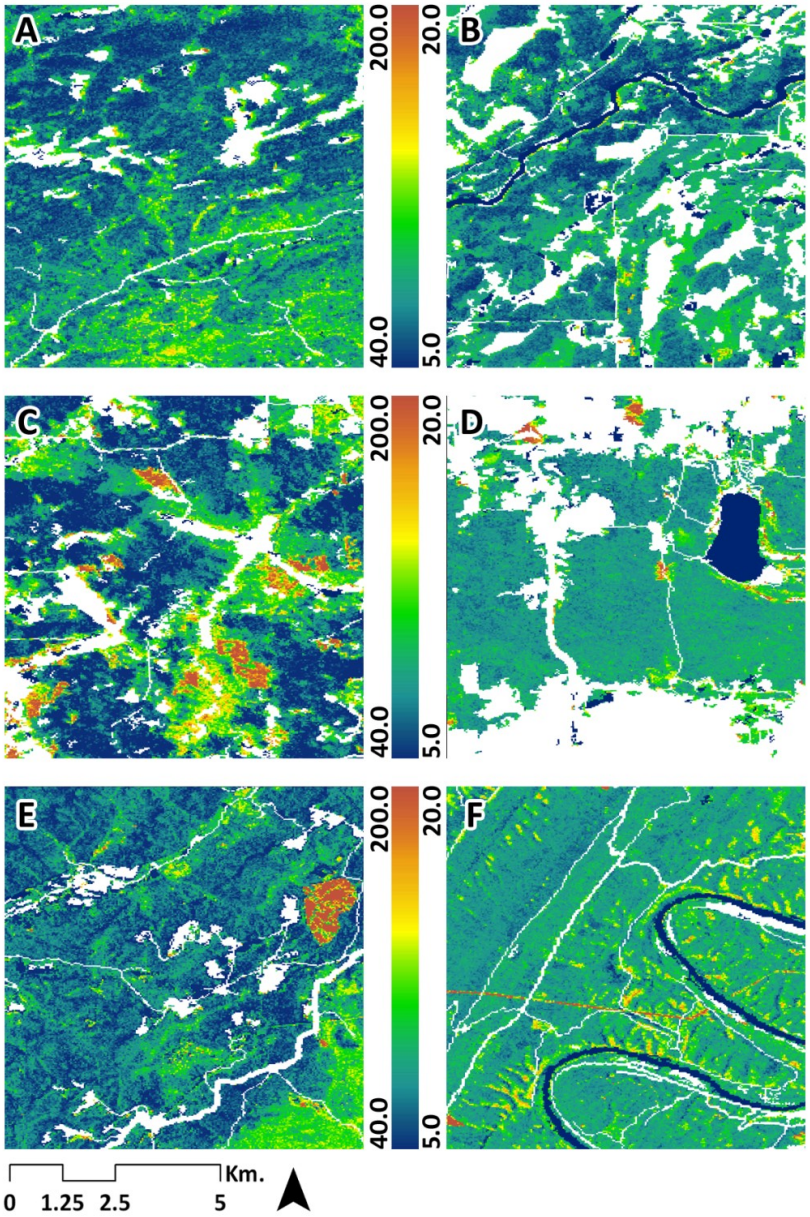

Figure 16: Foliar trait association maps (subplot A: false color composite R/G/B = ADL/Nitrogen/M_{area}) provide richer detail than NLCD 2006 landcover classifications (subplot B), or from fall aerial imagery (subplot C; 11/08/2010 GoogleEarth™). While leaf-off aerial imagery (subplot D; 4/14/2005 GoogleEarth™) clearly identifies needleleaf forest stands (also see high lignin+M_{area} [magenta] areas in subplot B), color enhancement of fall aerial imagery (subplot C) shows phenological differences (subplot E) between dominant deciduous species (*Quercus rubrum, Acer saccharum*) corresponding to spatial patterns of foliar traits in subplot A. Subplot F indicates high confidence in mapping traits (%N shown) across deciduous forest landcover. High prediction uncertainties are only observed in edges or non-forest areas.

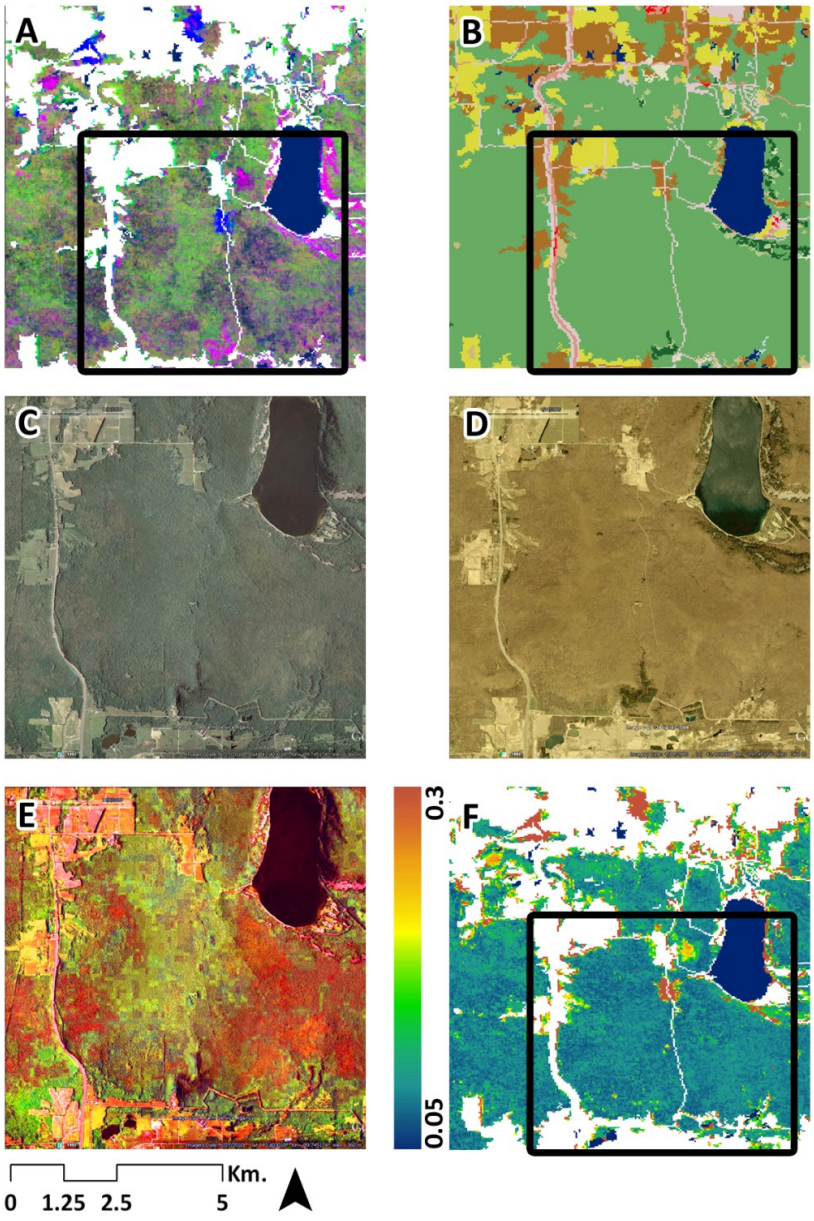

Figure 17: Recently disturbed regions show up as sharp boundaries in trait association maps (subplot A: false color composite R/G/B = ADL/Nitrogen/M_{area}, compare with subplot B: landcover from NLCD 2006). Changes in foliar nutrient content (%N subplot C) and elevated uncertainties (subplot D) capture logging activities (pre-cut subplot E: 8/24/2007, post-logging subplot F 10/19/2009, images from GoogleEarth™) near the Fernow Experimental Forest, WV.

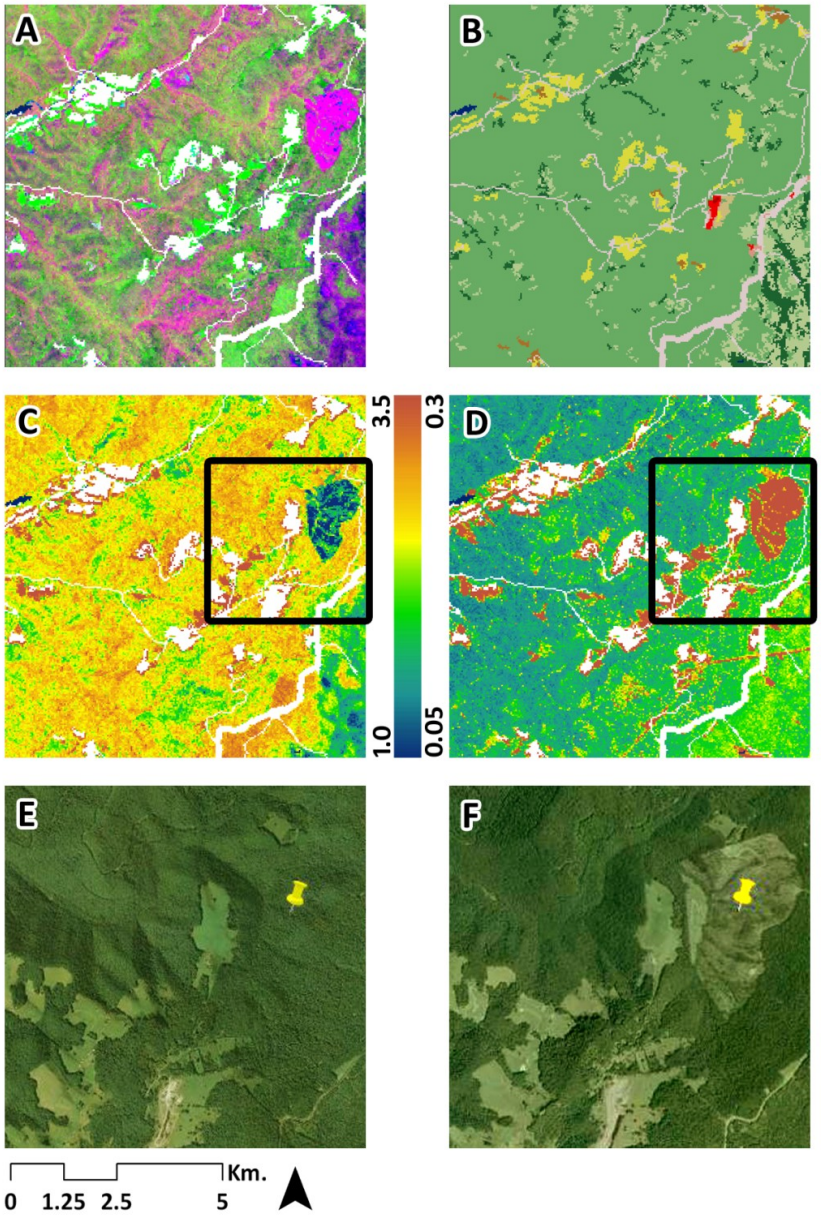

Supplementary material

S1: Review of recent literature on the application of imaging spectroscopy to map foliar chemistry. Note that we do not include studies that employ inversion of radiative transfer models to map canopy chemical properties to conform to this study.

Trait	Vegetation type	Location	Sensor	Plots	Images	Method	R2Cal	RMSECal	R2Val	RMSEVal	Source
C	Mixed needleleaf-broadleaf	Switzerland	HyMap	28	4	B&B	0.31	1.21 (RMSE)			Huber et al. (2008)
Lig	Oak, Pine	Wisconsin	AIS	20	1	MLR	0.85	1.9 (SE)			Wessman et al. (1989)
Lig	Juniper - Coastal rainforest	West-central Oregon	AVIRIS	17	4	MLR	0.93	277.80 (SEC)			Johnson et al. (1994)
Lig	N Hardwood and needleleaf	Harvard Forest, MA	AVIRIS	21	1	MLR	0.70	2.38 (SECV)	0.27	3.87 (SEP)	Martin and Aber (1997)
Lig	N Hardwood and needleleaf	Blackhawk Island, WI	AVIRIS	20	1	MLR	0.90	0.85 (SECV)	0.01	4.33 (SEP)	Martin and Aber (1997)
Lig:N	N Hardwood and needleleaf	White Mountain NF, NH	AVIRIS	81	56	PLSR	0.69	0.23 (SEC)		0.23 (SECV)	Ollinger et al. (2002)
Lignin	Juniper - Coastal rainforest	West-central Oregon	AVIRIS	9	1	MLR	0.75	17.90 (SEE)			Matson et al. (1994)
Lignin	Slash Pine	Gainesville, FL	AVIRIS	14	4	MLR	0.98				Curran et al. (1997)
Lignin	Chaparral	Santa Monica, CA	AVIRIS	23	1	MLR	0.81	5.39 (RMSE)			Serrano et al. (Serrano et al. 2002)
N	N Hardwood and needleleaf	Wisconsin	AIS	20	1	MLR	0.83	0.04 (SE)			Wessman et al. (1989)
N	Juniper - Coastal rainforest	West-central Oregon	AVIRIS	9	1	MLR	0.72	2.40 (SEE)			Matson et al. (1994)
N	Juniper - Coastal rainforest	West-central Oregon	AVIRIS	25	4	MLR	0.90	0.70 (SEC)			Johnson et al.(1994)
N	Slash Pine	Gainesville, FL	AVIRIS	14	4	MLR	0.98				Curran et al. (1997)
N	N Hardwood and needleleaf	Harvard Forest, MA	AVIRIS	21	1	MLR	0.87	0.23 (SECV)	0.83	0.27 (SEP)	Martin and Aber (1997)
N	N Hardwood and needleleaf	Blackhawk Island, WI	AVIRIS	20	1	MLR	0.85	0.15 (SECV)	0.75	1.32 (SEP)	Martin and Aber (1997)
N	Chaparral	Santa Monica, CA	AVIRIS	23	1	MLR	0.75	0.55 (RMSE)			Serrano et al. (2002)
N	N Hardwood and needleleaf	White Mountain NF, NH	AVIRIS	53	36	PLSR	0.82			0.23 (SECV)	Smith et al. (2002)
N	Eucalyptus spp.	Tumbarumba, Australia	Hyperion	14	1	PLSR	0.95	0.11 (SEC)	0.68	0.27 (SECV)	Coops et al. (2003)
N	Eucalyptus spp.	Tumbarumba, Australia	Hyperion	14	1	MLR	0.83	0.10 (SEC)			Coops et al. (2003)
N	N Hardwood and needleleaf	Bartlett Exp. Forest, NH	AVIRIS	49	1	PLSR	0.83	0.17 (SEC)	0.79	0.19 (RMSEP)	Smith et al. (2003)
N	N Hardwood and needleleaf	Bartlett Exp. Forest, NH	Hyperion	49	1	PLSR	0.82	0.17 (SEC)	0.60	0.25 (RMSEP)	Smith et al. (2003)
N	Deciduous Oak	Green Ridge SF, MD	Hyperion	20	1	PLSR	0.97				Townsend et al. (2003)

Trait	Vegetation type	Location	Sensor	Plots	Images	Method	R2Cal	RMSECal	R2Val	RMSEVal	Source
C	Mixed needleleaf-broadleaf	Switzerland	HyMap	28	4	B&B	0.31	1.21 (RMSE)			Huber et al. (2008)
N	Deciduous Oak	Green Ridge SF, MD	AVIRIS	17	1	PLSR	0.84				Townsend et al. (2003)
N	N Hardwood and needleleaf	Bartlett Exp. Forest, NH	AVIRIS	56	1	PLSR	0.83	0.17(SEC)	0.70	0.19(RMSEP)	Ollinger and Smith (2005)
N	N Hardwood and needleleaf	Bartlett Exp. Forest, NH	Hyperion	56	1	PLSR	0.82	0.17(SEC)	0.25	0.25(RMSEP)	Ollinger and Smith (2005)
N	N Hardwood and boreal	Adirondacks, NY	Hyperion	28	2	PLSR	0.93	0.28(%)			McNeil et al. (2008)
N	Mixed needleleaf-broadleaf	Switzerland	HyMap	28	4	B&B	0.53	0.38 (RMSE)			Huber et al. (2008)
N	Various	USA, Costa Rica, Australia	AVIRIS	42-75	5	PLSR	0.83	0.14 (SEC)		0.19 (SECV)	Martin et al. (2008)
N	Various	USA, Costa Rica, Australia	Hyperion	42-75	6	PLSR	0.82	0.22 (SEC)		0.25 (SECV)	Martin et al. (2008)
N	*Picea abies*	Gerolstein, Germany	HyMap	13	1	MLR	0.57	0.05 (RMSE)			Schlerf et al. (2010)
N	Needleleaf	Vancouver Island, Canada	AVIRIS	17	1	PLSR	0.77	0.21 (SECV)			Hilker et al. (2012)
N	Needleleaf, Eucalyptus spp.	Tumut, NSW, Australia	HyMap	80	5	PLSR	0.54	0.90 (SEC)		0.11 (SECV)	Youngentob et al. (2012)
N	Needleleaf, Eucalyptus spp.	Tumut, NSW, Australia	HyMap	80	5	MLR	0.60	0.10 (SEC)		0.10 (SECV)	Youngentob et al. (2012)
N	Needleleaf, Eucalyptus spp.	Tumut, NSW, Australia	HyMap	80	5	MLR	0.58	0.10 (SEC)		0.10 (SECV)	Youngentob et al. (2012)
N	Sagebrush	Eastern Idaho	HyMap	35	1	PLSR	0.95		0.56	0.25 (PRESS)	Mitchell et al. (2012)

S2: Estimates of foliar traits measured in this study stratified by dominant canopy species. Species sorted by leaf habit (needleleaf, deciduous), and by relative frequency (%) in the overall dataset. Estimates of mean traits are presented along with standard deviations.

			$M_{area}(g/m_2)$		N%		C%		ADF%		ADL%		Cellulose%	
			Mean	SD	Mean	SD	Mean	SD	Mean	SD	Mean	SD	Mean	SD
Sp. Code	Overall	Rel. Freq.	101.55	43.61	2.25	0.55	49.57	1.00	36.81	6.74	21.21	4.47	16.39	2.44
Needle leaf	Species		156.77	30.91	1.60	0.33	50.47	0.62	44.27	5.10	25.69	3.03	18.53	2.27
PIST	*Pinus strobus*	7.06	139.03	34.71	1.79	0.29	50.34	0.60	42.12	3.93	25.49	3.17	17.26	1.13
ABBA	*Abies balsamifera*	5.42	144.87	18.52	1.67	0.14	51.50	0.99	36.82	2.41	21.61	1.51	15.27	1.57
PIRE	*Pinus resinosa*	4.76	187.48	17.44	1.35	0.21	50.57	0.57	47.46	1.81	26.34	1.38	19.96	1.44
TSCA	*Tsuga candensis*	4.76	97.78	11.23	1.99	0.18	49.70	0.26	31.49	3.85	17.31	2.75	14.34	1.39
PIBA	*Pinus banksiana*	2.30	171.19	10.44	1.57	0.14	50.60	0.43	51.07	2.60	29.01	1.57	21.62	1.01
PIRU	*Picea rubens*	1.81	144.94	5.83	1.43	0.27	50.53	0.52	42.88	5.08	23.69	1.89	18.35	2.75
THOC	*Thuja occidentalis*	1.15	162.53	22.21	1.37	0.25	49.85	0.50	40.27	2.31	24.95	2.13	16.29	0.96
PIMA	*Pinus mariana*	0.99	209.18	6.99	0.97	0.06	50.72	0.07	46.12	3.62	24.61	1.95	21.17	1.00
LALA	*Larix laricina*	0.66	157.28	5.38	1.53	0.08	49.99	0.03	50.05	0.56	30.32	0.05	19.67	0.49
PISY	*Pinus sylvatica*	0.66	152.68	0.25	2.23	0.00	50.15	0.01	41.92	0.01	23.63	0.03	18.35	0.01
JUVI	*Juniperous nigra*	0.33	203.59	0.19	2.12	0.00	48.53	0.01	40.77	0.10	26.84	0.04	17.00	0.05
PIVI	*Pinus virginiana*	0.33	131.73	0.00	1.78	0.00	50.28	0.00	39.24	0.00	22.07	0.00	18.40	0.00
Broadleaf			77.18	19.45	2.53	0.36	49.18	0.87	33.51	4.31	19.23	3.46	15.44	1.84
ACSM	*Acer saccharum*	19.87	68.43	12.42	2.51	0.32	48.90	0.62	31.91	3.61	17.25	2.95	15.02	1.50
QURU	*Quercus rubra*	10.02	87.91	8.87	2.81	0.15	49.60	0.70	35.39	2.39	21.34	2.37	15.90	1.18
ACRU	*Acer rubrum*	9.52	69.11	8.10	2.39	0.17	49.74	0.42	32.61	4.48	18.70	2.62	14.55	1.52
QUAL	*Quercus alba*	7.39	80.26	10.72	2.78	0.20	49.47	0.49	32.64	1.99	18.55	1.25	15.61	0.52
POTR	*Populus tremuloides*	3.28	69.72	11.57	2.73	0.25	49.86	0.92	34.43	3.13	23.34	4.13	17.60	1.29
TIAM	*Tilia americana*	2.96	81.06	3.76	2.85	0.18	48.30	0.90	35.91	1.07	21.75	0.19	16.16	0.10
FAGR	*Fagus grandifolia*	2.63	75.53	10.06	2.15	0.11	49.82	0.24	43.22	1.88	24.81	1.05	18.49	0.96
QUPR	*Quercus*	2.46	85.77	15.56	2.41	0.35	49.75	0.45	36.27	1.74	21.58	1.53	16.01	0.44
NYSY	*Nyssa sylvatica*	1.81	77.13	0.89	2.44	0.07	49.75	0.00	32.29	0.28	18.21	0.28	14.29	0.28

			$M_{area}(g/m_2)$		N%		C%		ADF%		ADL%		Cellulose%	
			Mean	SD	Mean	SD	Mean	SD	Mean	SD	Mean	SD	Mean	SD
PODE	*Populus deltoides*	1.81	75.49	1.79	2.76	0.20	48.82	0.01	32.27	0.06	20.05	0.25	13.17	0.07
CAOV	*Carya ovata*	1.64	70.25	26.64	2.86	0.28	47.49	0.73	37.06	0.22	19.14	1.30	17.80	1.06
FRNI	*Fraxinus nigra*	1.15	76.25	3.86	2.94	0.03	47.55	0.26	29.94	4.35	17.58	1.26	12.57	2.53
LITU	*Liriodendron tulipifera*	1.15	79.62	14.20	2.57	0.04	48.71	0.34	34.28	0.59	20.43	0.42	14.50	0.23
FRPE	*Fraxinus pennsylvanica*	0.99	55.10	0.00	2.89	0.00	47.45	0.00	31.88	0.00	18.74	0.00	15.92	0.00
QUMA	*Quercus macrocarpa*	0.99	98.69	7.42	2.82	0.16	48.84	0.51	35.34	0.78	20.31	0.87	16.03	0.31
ROPS	*Robinia pseudoacacia*	0.82	58.42	5.60	3.26	0.14	47.93	0.60	35.30	0.77	22.51	0.08	16.89	0.06
CEOC	*Celtis occidentalis*	0.66	64.17	4.94	3.14	0.12	47.28	1.48	32.39	4.97	20.03	3.06	15.27	1.81
ACSN	*Aces saccharinum*	0.49	82.88	1.72	2.53	0.11	50.20	0.82	25.35	7.79	15.53	4.16	11.42	3.15
QUEL	*Quercus ellipsoidalis*	0.16	101.99		2.91		49.87		33.22		21.28		14.98	

S3: Estimates of foliar traits measured in this study stratified by plot and year sampled and sorted by plot name. Estimates of mean traits are presented along with standard deviations and locations of the plot. Dominant and co-dominant species are specified in columns SPP1 and SPP2, along with the proportion of relative basal area (RBA1, RBA2) represented on the plot. See methods section for complete description.

								M_{area} g/m^2		N%		C%		ADF%		ADL%		Cellulose%	
Plot	Year	SPP1	RBA1	SPP2	RBA1	Latitude	Longitude	mean	S.D.	mean	S.D.	mean	S.D.	mean	S.D.	mean	S.D.	mean	S.D.
Adirondacks, NY																			
AK01	2009	PIST	0.49	PIRE	0.35	-73.741362	44.452065	155.74	0.59	1.56	0.01	51.06	0.10	44.78	0.55	27.15	0.43	18.20	0.30
AK02	2009	ABBA	0.29	ACRU	0.27	-73.907469	44.503280	113.66	1.22	1.87	0.02	51.06	0.11	35.10	0.69	20.88	0.48	14.56	0.34
AK06	2009	THOC	0.70	ABBA	0.11	-73.899105	44.321100	161.94	1.61	1.37	0.03	50.20	0.18	43.17	0.86	27.29	0.61	17.39	0.49
AK08	2009	ACSM	0.49	FAGR	0.32	-73.897096	44.319901	74.34	3.60	2.08	0.15	49.97	0.28	39.90	1.86	22.61	1.01	17.27	1.35
AK11	2009	THOC	0.34	TSCA	0.26	-74.180802	44.292497	126.73	6.50	1.67	0.04	49.91	0.16	38.51	0.68	23.13	0.46	15.87	0.51
AK12	2009	TSCA	0.82	BEAL	0.11	-74.180898	44.291904	107.90	0.65	1.66	0.02	50.39	0.15	27.87	1.13	14.65	0.79	11.60	0.61
AK17	2009	PIRU	0.62	BEAL	0.13	-74.243694	43.995302	140.79	0.56	1.67	0.02	49.94	0.12	39.98	0.64	22.20	0.49	17.74	0.39
AK18	2009	PIRU	0.53	ACRU	0.19	-74.245096	43.994897	135.46	1.23	1.56	0.03	50.30	0.23	39.14	0.96	22.38	0.81	15.54	0.64
AK21	2009	FAGR	0.29	BEAL	0.22	-74.243003	43.994703	94.53	1.47	1.95	0.07	49.57	0.23	41.64	1.17	23.34	0.88	18.46	0.70
AK23	2009	ACSM	0.40	TIAM	0.24	-74.245694	44.003796	66.99	2.68	2.54	0.06	49.08	0.24	38.50	1.04	22.64	0.83	15.67	0.74
AK24	2009	FAGR	0.43	ACSM	0.25	-74.249202	44.004602	66.40	1.63	2.31	0.11	49.79	0.35	40.38	1.65	23.54	1.25	17.54	0.95
AK27	2009	FAGR	0.41	ACSM	0.32	-74.478111	43.975824	70.30	2.47	2.16	0.12	50.13	0.41	43.16	1.71	25.09	1.32	17.55	1.04
AK29	2009	FAGR	0.48	ACSM	0.33	-74.328406	43.697889	77.73	2.51	2.12	0.05	49.86	0.24	43.15	1.18	25.73	0.83	18.04	0.75
AK32	2009	FAGR	0.53	BEAL	0.26	-74.650395	43.794102	70.29	3.63	2.17	0.08	49.52	0.32	45.54	1.41	25.35	1.04	20.21	0.93
AK33	2009	PIRU	0.66	ABBA	0.24	-74.610198	43.765196	150.65	3.86	1.05	0.05	50.36	0.22	50.71	1.12	26.19	1.01	22.43	0.76
AK38	2009	ACSM	0.35	FAGR	0.27	-74.782603	43.837801	84.22	4.60	1.99	0.14	50.07	0.37	44.14	1.82	25.37	1.16	18.31	1.26
AK44	2009	FAGR	0.53	BEAL	0.20	-74.710666	43.743074	79.48	3.36	2.11	0.15	50.07	0.49	44.97	2.19	25.97	1.57	18.67	1.19
AK46	2009	ACRU	0.35	FAGR	0.35	-74.701949	43.737785	79.12	1.30	2.08	0.09	49.99	0.29	43.45	1.35	24.46	1.02	18.67	0.73
AK57	2009	PIRU	0.41	ABBA	0.34	-74.509520	43.735635	148.22	1.75	1.69	0.02	51.46	0.11	41.20	0.81	24.65	0.54	16.29	0.38
AK58	2009	PIRU	0.40	ABBA	0.33	-74.912299	43.509498	146.72	1.86	1.39	0.02	50.70	0.11	39.45	0.61	21.77	0.44	17.69	0.36
AK59	2009	FAGR	0.43	ACSM	0.35	-74.895198	43.504901	66.66	3.03	2.24	0.15	49.79	0.41	44.18	2.02	25.37	1.32	19.05	1.29

								M_{area} g/m^2		N%		C%		ADF%		ADL%		Cellulose%	
Plot	Year	SPP1	RBA1	SPP2	RBA1	Latitude	Longitude	mean	S.D.	mean	S.D.	mean	S.D.	mean	S.D.	mean	S.D.	mean	S.D.
AK60	2009	ABBA	0.93	BEPA	0.08	-74.510670	43.582058	168.91	3.77	1.61	0.03	53.51	0.33	41.38	1.85	24.43	1.29	12.37	0.95
Baraboo Hills, WI																			
BH02	2008	TSCA	0.55	QURU	0.23	-89.907107	43.372408	108.93	0.88	2.15	0.02	49.76	0.07	29.49	0.67	15.42	0.50	14.43	0.40
BH03	2008	ACSM	0.76	QUAL	0.11	-89.845353	43.391867	60.82	0.31	2.67	0.01	48.70	0.09	28.82	0.45	14.21	0.38	14.35	0.25
BH05	2008	ACSM	0.90	CACO	0.03	-89.823128	43.407996	60.19	0.38	2.51	0.01	48.40	0.11	29.74	0.55	14.00	0.44	15.56	0.29
BH06	2008	CAOV	0.57	QUAL	0.19	-89.829339	43.428794	47.79	0.62	3.10	0.01	46.87	0.13	37.24	0.68	18.04	0.38	18.70	0.25
BH07	2008	POTR	0.43	ACSM	0.23	-89.801137	43.419924	60.03	0.45	3.05	0.01	49.16	0.07	30.47	0.63	18.50	0.45	16.27	0.44
BH10	2008	ACRU	0.71	ACSM	0.12	-89.761912	43.405221	63.62	0.69	2.53	0.01	49.34	0.10	26.55	0.60	15.25	0.47	13.05	0.32
BH11	2008	PIST	0.73	PODE	0.18	-89.746493	43.387964	107.49	0.65	2.06	0.01	49.67	0.09	36.48	0.69	21.85	0.51	16.29	0.35
BH12	2008	QURU	0.49	QUAL	0.22	-89.740063	43.393539	80.20	0.62	2.79	0.01	49.09	0.07	33.10	0.42	18.69	0.37	15.43	0.31
BH14	2008	CAOV	0.25	QURU	0.25	-89.723483	43.415683	98.33	0.31	2.57	0.01	48.26	0.08	36.83	0.45	20.51	0.33	16.68	0.22
BH15	2008	PIST	0.54	QUAL	0.18	-89.697692	43.415336	98.77	0.48	2.35	0.01	49.61	0.10	35.87	0.66	21.68	0.44	15.03	0.27
BH16	2008	FRPE	0.36	ACRU	0.28	-89.708653	43.435205	55.10	0.32	2.89	0.01	47.45	0.08	31.88	0.41	18.74	0.36	15.92	0.23
Blackhawk Island, WI																			
BI01	2008	ACSM	0.61	QURU	0.21	-89.788470	43.651922	68.09	0.64	2.83	0.01	48.97	0.07	30.69	0.40	16.49	0.34	14.90	0.23
BI01	2010	ACSM	0.47	QURU	0.37	-89.788470	43.651922	82.52	2.06	2.94	0.02	50.03	0.23	36.73	0.85	21.65	0.68	15.01	0.49
BI02	2008	ACSM	0.38	QURU	0.23	-89.791557	43.652047	67.50	0.28	2.97	0.01	49.35	0.06	35.61	0.28	20.50	0.28	17.22	0.18
BI02	2010	ACSM	0.36	QURU	0.34	-89.791557	43.652047	87.52	1.93	2.75	0.02	50.48	0.22	38.27	0.84	22.93	0.69	14.62	0.51
BI03	2008	ACSM	0.54	QURU	0.26	-89.790020	43.650716	65.30	0.31	2.92	0.01	49.08	0.07	33.58	0.36	18.55	0.33	16.28	0.21
BI03	2010	QURU	0.44	ACSM	0.42	-89.790020	43.650716	90.97	2.37	2.79	0.03	51.14	0.29	38.20	1.14	24.00	0.90	13.94	0.66
BI04	2008	QURU	0.62	ACRU	0.14	-89.795528	43.651376	85.38	1.37	2.86	0.01	49.70	0.09	37.26	0.45	22.01	0.42	18.01	0.30
BI04	2010	QURU	0.70	ACRU	0.14	-89.795528	43.651376	96.39	3.35	2.71	0.05	51.20	0.44	42.51	1.89	27.97	1.57	14.78	1.04
BI05	2008	PIST	0.65	PIRE	0.30	-89.800067	43.649941	156.50	0.57	1.73	0.01	49.95	0.06	43.99	0.48	25.16	0.35	19.58	0.23
BI05	2010	PIST	0.60	PIRE	0.29	-89.800067	43.649941	141.16	4.58	1.76	0.03	50.37	0.18	43.97	0.54	24.94	0.66	18.62	0.64
BI06	2008	PIST	0.57	QURU	0.16	-89.796174	43.649093	115.58	0.38	2.21	0.01	49.80	0.06	39.97	0.38	23.15	0.31	17.97	0.20
BI06	2010	PIST	0.62	QURU	0.12	-89.796174	43.649093	129.40	6.53	1.94	0.03	50.28	0.23	41.75	0.67	24.10	0.77	17.48	0.64
BI07	2010	ACRU	0.40	QURU	0.39	-89.794458	43.652251	94.89	2.45	2.71	0.03	50.99	0.30	36.54	1.34	23.23	1.00	12.95	0.75

								M_{area} g/m^2		N%		C%		ADF%		ADL%		Cellulose%	
Plot	Year	SPP1	RBA1	SPP2	RBA1	Latitude	Longitude	mean	S.D.	mean	S.D.	mean	S.D.	mean	S.D.	mean	S.D.	mean	S.D.
BI08	2010	PIST	0.79	ACRU	0.08	-89.797097	43.652612	131.17	6.13	1.86	0.03	50.07	0.21	42.09	0.61	23.89	0.77	17.85	0.78
BI09	2010	QURU	0.36	ACSM	0.21	-89.789908	43.653120	88.59	1.52	2.87	0.03	49.58	0.17	33.85	0.65	20.23	0.53	14.15	0.45
BI10	2010	ACSM	0.30	QURU	0.30	-89.787067	43.651122	82.62	1.66	2.81	0.03	50.04	0.20	35.56	0.70	21.06	0.55	14.01	0.44
Madison, WI																			
DC02	2010	ACSN	0.92	PODE	0.06	-89.407675	43.056497	83.88	1.52	2.47	0.03	49.73	0.19	20.85	1.08	13.13	0.83	9.60	0.58
DC03	2010	ACSM	0.43	QUAL	0.24	-89.424058	43.046001	85.24	3.11	2.74	0.05	49.15	0.11	31.19	0.61	16.66	0.45	13.71	0.33
DC04	2010	PISY	0.68	PRSE	0.13	-89.428549	43.045415	152.68	4.71	2.23	0.02	50.15	0.12	41.92	0.97	23.63	0.63	18.35	0.77
DC05	2010	PIRE	0.64	PIST	0.16	-89.438258	43.038217	169.74	1.80	1.69	0.02	50.90	0.09	45.11	0.61	27.69	0.45	18.17	0.43
DC08	2010	TIAM	0.20	FRPE	0.13	-89.423047	43.056072	78.90	2.94	2.75	0.07	47.78	0.11	36.47	0.88	21.84	0.53	16.18	0.44
DC09	2010	QUMA	0.72	QURU	0.08	-89.444185	43.066524	105.06	4.33	2.67	0.02	49.28	0.09	35.94	0.75	21.04	0.54	16.04	0.47
DC10	2010	CEOC	0.38	ROPS	0.32	-89.441459	43.073068	64.17	0.42	3.14	0.03	47.28	0.14	32.39	0.99	20.03	0.77	15.27	0.63
DC12	2010	ACSM	0.51	QUAL	0.14	-89.486230	43.074808	76.04	2.28	2.73	0.03	49.25	0.12	31.89	0.72	17.76	0.56	14.69	0.44
DC13	2010	QUAL	0.59	QURU	0.18	-89.485336	43.074324	88.12	1.65	3.03	0.03	49.58	0.10	35.01	0.79	20.39	0.65	16.23	0.51
DC14	2010	PODE	0.56	ACNE	0.16	-89.399428	43.045429	74.45	1.72	2.87	0.04	48.82	0.15	32.30	0.95	20.20	0.70	13.21	0.53
DC15	2010	PIST	0.63	PRSE	0.17	-89.437541	43.037738	148.56	1.26	1.73	0.03	50.98	0.14	45.75	1.02	30.88	0.73	17.38	0.81
DC20	2010	JUVI	0.76	MOAL	0.13	-89.427635	43.085337	203.59	1.44	2.12	0.03	48.53	0.23	40.77	1.54	26.84	0.94	17.00	0.73
DC21	2010	ROPS	0.76	CEOC	0.05	-89.428922	43.086415	55.19	1.10	3.34	0.02	47.58	0.15	34.86	0.98	22.47	0.79	16.89	0.63
DC22	2010	QUAL	0.63	PRSE	0.09	-89.429492	43.085891	89.95	0.56	2.97	0.02	49.21	0.12	33.84	0.88	19.48	0.74	16.01	0.62
DC23	2010	QURU	0.73	PRSE	0.10	-89.430312	43.090128	97.79	0.79	2.99	0.03	49.76	0.13	34.92	0.79	22.46	0.70	16.32	0.64
DC24	2010	ACSM	0.59	TIAM	0.22	-89.441737	43.087796	66.15	3.34	2.72	0.08	47.41	0.17	27.68	0.84	15.36	0.85	12.61	0.42
DC30	2010	QUMA	0.28	QUAL	0.28	-89.429205	43.085390	92.32	3.34	2.96	0.03	48.40	0.08	34.75	0.49	19.57	0.40	16.03	0.27
DC31	2010	QURU	0.57	QUAL	0.15	-89.425258	43.087116	96.25	5.39	2.86	0.08	48.90	0.16	35.62	0.65	21.99	0.48	16.75	0.34
DC32	2010	ACSM	0.37	QURU	0.26	-89.427583	43.088191	78.65	4.67	2.87	0.08	48.51	0.15	29.31	0.53	16.64	0.57	13.87	0.27
DC40	2010	TIAM	0.26	QURU	0.21	-89.489059	43.071481	85.38	1.28	3.06	0.04	49.34	0.09	34.78	0.72	21.55	0.57	16.11	0.59
DC41	2010	QUEL	0.33	CAOV	0.33	-89.387479	43.155984	101.99	1.16	2.91	0.03	49.87	0.11	33.22	0.86	21.28	0.67	14.98	0.68
DC42	2010	PIST	0.79	PIRE	0.14	-89.442340	43.033988	182.33	1.54	1.73	0.04	52.24	0.18	52.09	1.28	36.17	0.97	18.87	0.97
DC43	2010	ACSN	0.75	PODE	0.15	-89.407122	43.056480	80.90	0.74	2.66	0.04	51.15	0.16	34.34	1.30	20.34	0.86	15.06	0.94

								M_{area} g/m^2		N%		C%		ADF%		ADL%		Cellulose%	
Plot	Year	SPP1	RBA1	SPP2	RBA1	Latitude	Longitude	mean	S.D.	mean	S.D.	mean	S.D.	mean	S.D.	mean	S.D.	mean	S.D.
DC44	2010	QURU	0.47	QUAL	0.21	-89.404621	43.140370	95.00	0.74	3.08	0.03	49.72	0.13	34.86	0.93	22.75	0.70	15.86	0.76
DC45	2010	QUAL	0.79	PRSE	0.10	-89.434529	43.058659	96.50	0.58	2.90	0.04	50.56	0.18	28.10	1.63	16.53	1.25	14.84	1.07
DC49	2010	PODE	0.66	ACNE	0.27	-89.398224	43.148241	77.55	0.92	2.53	0.03	48.83	0.20	32.20	1.16	19.77	0.85	13.09	0.61
DC50	2010	LITU	0.22	QURU	0.15	-89.482144	43.090062	100.38	2.26	2.62	0.03	48.77	0.09	34.59	0.54	20.40	0.39	14.73	0.30
DC51	2010	PIRE	0.77	ACNE	0.17	-89.403746	43.135843	173.96	7.11	1.71	0.04	50.45	0.16	44.89	0.67	26.00	0.67	18.31	0.46
DC52	2010	PIST	0.83	PIRE	0.09	-89.442442	43.033052	160.13	12.38	1.72	0.05	50.97	0.20	42.42	0.85	25.40	1.34	17.12	0.48
Green Ridge SF, MD																			
GR01	2009	QUPR	0.36	PIST	0.23	-78.425429	39.670754	96.63	8.28	2.22	0.10	49.78	0.40	38.09	1.11	22.86	0.79	16.56	0.65
GR02	2009	QUPR	0.29	QUAL	0.13	-78.423019	39.673141	79.30	6.71	2.46	0.09	49.72	0.37	34.81	1.15	20.63	0.88	15.40	0.61
GR03	2009	QUAL	0.40	NYSY	0.30	-78.411885	39.669979	69.27	5.86	2.61	0.10	49.07	0.37	30.69	1.42	17.52	1.05	14.87	0.56
GR04	2009	QUAL	0.39	ACRU	0.23	-78.404334	39.674758	66.91	5.77	2.50	0.09	49.37	0.33	33.00	1.45	18.72	1.12	15.59	0.58
GR05	2009	ACSM	0.36	QUAL	0.26	-78.525246	39.676829	70.59	5.26	2.55	0.09	49.65	0.28	33.38	1.20	18.77	0.89	15.34	0.50
GR06	2009	ACSM	0.41	QUPR	0.31	-78.519740	39.671724	70.73	8.29	2.42	0.13	49.62	0.46	34.53	1.27	19.83	0.88	15.37	0.78
GR07	2009	PIST	0.49	CAGL	0.20	-78.484306	39.688260	118.04	9.91	1.83	0.08	50.37	0.32	39.77	1.33	23.82	1.15	16.56	0.72
GR08	2008	PIST	0.81	ACRU	0.06	-78.466112	39.694965	147.51	1.02	1.56	0.02	50.99	0.10	44.12	0.99	27.46	0.71	16.66	0.54
GR08	2009	PIST	0.78	QURU	0.09	-78.466112	39.694965	131.21	12.03	1.62	0.05	50.61	0.29	44.33	1.38	27.45	1.23	17.38	0.85
GR09	2009	PIST	0.83	QUAL	0.04	-78.483460	39.692448	138.01	13.21	1.50	0.05	50.67	0.31	45.43	1.50	28.34	1.35	17.47	0.91
GR10	2009	QUAL	0.53	QURU	0.37	-78.496803	39.653256	79.85	7.31	2.64	0.13	50.00	0.46	31.20	2.39	17.33	2.02	15.30	0.71
GR11	2009	ACRU	0.30	QUAL	0.25	-78.414367	39.666293	69.45	5.57	2.43	0.07	49.48	0.30	31.19	1.05	17.48	0.91	14.74	0.52
GR12	2009	QUAL	0.18	QUPR	0.18	-78.511564	39.659868	64.25	5.45	2.51	0.10	49.04	0.40	34.07	1.18	19.24	0.93	15.83	0.56
GR14	2009	PIST	0.57	ACRU	0.14	-78.459268	39.666760	125.27	9.42	1.69	0.04	50.45	0.22	41.63	1.11	24.92	0.96	17.19	0.67
GR15	2009	PIVI	0.55	ACRU	0.18	-78.478366	39.637245	131.73	7.23	1.78	0.04	50.28	0.22	39.24	0.95	22.07	0.71	18.40	0.83
GR16	2009	QUAL	0.37	ACSM	0.22	-78.457438	39.668188	70.74	4.63	2.67	0.09	49.11	0.28	32.08	1.38	17.56	1.04	15.38	0.50
GR18	2009	ROPS	0.40	QUPR	0.27	-78.415504	39.672750	64.88	5.50	3.09	0.11	48.62	0.38	36.19	2.28	22.59	1.81	16.89	0.74
GR19	2009	QURU	0.24	ACSM	0.24	-78.386901	39.648153	74.01	5.61	2.53	0.08	49.32	0.26	33.67	1.51	18.89	1.26	15.38	0.47
GR21	2009	QUPR	0.33	ACSM	0.26	-78.430828	39.605952	69.53	7.26	2.57	0.10	49.28	0.40	35.05	1.23	20.58	0.94	15.41	0.63
IDS01	2008	QUPR	0.43	PIST	0.26	-78.425429	39.670754	104.50	0.31	1.99	0.02	50.34	0.07	38.14	0.59	23.36	0.50	16.14	0.33

								M_{area} g/m^2		N%		C%		ADF%		ADL%		Cellulose%	
Plot	Year	SPP1	RBA1	SPP2	RBA1	Latitude	Longitude	mean	S.D.	mean	S.D.	mean	S.D.	mean	S.D.	mean	S.D.	mean	S.D.
IDS05	2008	QUAL	0.59	QURU	0.35	-78.496803	39.653256	84.47	0.48	2.85	0.02	49.64	0.09	32.67	0.69	18.50	0.55	15.60	0.35
IDS10	2008	QUPR	0.43	QUVE	0.20	-78.423019	39.673141	72.98	1.25	2.82	0.04	49.39	0.18	34.82	1.03	20.14	0.79	16.20	0.44
IDS25	2008	LITU	0.58	TSCA	0.19	-79.183152	39.592356	70.80	0.53	2.51	0.03	47.96	0.08	32.97	0.92	19.53	0.66	14.07	0.43
IDS34	2008	QURU	0.55	ACRU	0.25	-78.971143	39.665071	96.00	0.91	2.70	0.03	50.52	0.09	36.34	0.73	22.07	0.60	15.26	0.40
IDS35	2008	TSCA	0.44	ACSM	0.19	-79.083811	39.611706	91.21	0.90	2.13	0.02	49.58	0.06	36.78	0.44	21.33	0.35	15.67	0.23
IDS36	2008	ACSM	0.26	QURU	0.17	-79.085443	39.611926	64.37	0.62	2.71	0.02	48.75	0.06	37.09	0.50	21.78	0.39	15.94	0.27
IDS40	2008	NYSY	0.31	QURU	0.25	-79.209825	39.557244	78.95	0.31	2.30	0.01	49.75	0.06	31.72	0.57	17.63	0.38	13.71	0.27
Kettle Moraine SF, WI																			
KM01	2009	ACSM	0.63	FRAM	0.08	-88.187772	43.572094	74.15	0.47	2.79	0.01	48.86	0.09	31.48	0.60	17.65	0.47	14.84	0.30
KM02	2009	FRNI	0.78	ULAM	0.16	-88.198752	43.632442	70.68	0.68	2.89	0.02	47.40	0.15	25.08	0.92	16.23	0.84	9.63	0.57
Minnesota Arrowhead, MN																			
MN01	2008	PIST	0.79	BEPA	0.15	-91.418322	47.651063	255.92	2.24	1.53	0.01	50.59	0.13	44.01	0.75	26.09	0.53	17.46	0.41
MN02	2008	PIBA	0.46	ABBA	0.32	-91.446190	47.655831	152.87	0.49	1.71	0.01	50.91	0.05	45.17	0.47	25.94	0.37	20.36	0.27
MN03	2008	PIRE	0.93	PIGL	0.05	-91.511545	47.740876	209.79	0.94	1.10	0.01	50.18	0.08	50.63	0.58	27.63	0.46	22.29	0.31
MN04	2008	PIMA	0.99	ALIN	0.01	-91.574093	47.740664	213.22	1.30	0.94	0.01	50.68	0.08	48.21	0.54	25.74	0.42	21.75	0.35
MN05	2008	POTR	0.78	BEPA	0.15	-91.294432	47.408030	79.96	0.62	2.78	0.02	50.63	0.12	34.14	1.12	25.63	0.79	17.81	0.73
MN06	2008	FRNI	0.73	ACSP	0.08	-91.232320	47.386867	76.65	0.82	2.95	0.02	47.95	0.12	27.47	0.66	16.78	0.60	11.27	0.39
MN07	2008	THOC	0.92	PIMA	0.05	-91.288505	47.497285	187.59	1.37	0.97	0.02	48.98	0.11	37.39	0.42	22.29	0.35	14.87	0.19
MN09	2008	ACSM	0.74	BEAL	0.12	-91.280609	47.502458	69.98	0.43	2.64	0.01	49.31	0.09	27.71	0.50	13.92	0.50	13.76	0.31
Chequamegon-Nicolet SF, WI																			
NC01	2008	POTR	0.28	ACSM	0.27	-90.782899	45.624196	57.96	0.43	2.63	0.01	49.10	0.09	36.11	0.54	21.60	0.40	17.42	0.31
NC02	2008	ACSM	0.38	TSCA	0.32	-90.793649	45.628044	77.18	0.32	2.05	0.01	49.63	0.08	31.67	0.50	17.00	0.38	15.14	0.26
NC03	2008	ACSM	0.48	FRAM	0.30	-90.781750	45.618091	53.99	0.70	2.57	0.02	48.36	0.10	36.56	0.57	19.46	0.45	18.07	0.29
NC04	2008	ACSM	0.62	FRAM	0.21	-90.775306	45.623890	59.56	0.38	2.56	0.01	48.28	0.11	36.28	0.56	19.70	0.45	17.93	0.29
NC05	2008	ACSM	0.60	ABBA	0.19	-90.260771	45.940320	90.06	2.49	1.85	0.04	48.91	0.14	29.03	0.62	14.88	0.53	13.72	0.32
NC06	2008	PIRE	0.93	ACRU	0.03	-90.231660	45.943170	183.57	13.22	1.32	0.09	50.15	0.82	48.28	1.64	26.97	1.14	19.76	1.15
NC07	2008	POTR	0.93	PIRE	0.05	-90.219529	45.975752	77.66	0.97	2.44	0.02	51.74	0.14	36.31	1.31	28.54	1.04	18.74	0.86

								M_{area} g/m^2		N%		C%		ADF%		ADL%		Cellulose%	
Plot	Year	SPP1	RBA1	SPP2	RBA1	Latitude	Longitude	mean	S.D.	mean	S.D.	mean	S.D.	mean	S.D.	mean	S.D.	mean	S.D.
NC08	2008	LALA	0.85	PIMA	0.15	-90.276255	45.948169	161.95	1.79	1.46	0.02	50.02	0.15	50.53	1.19	30.36	0.51	20.09	0.61
NC09	2008	FRNI	0.75	ABBA	0.11	-90.284027	45.971387	78.84	0.57	2.95	0.02	47.44	0.12	33.62	0.69	18.65	0.59	14.68	0.39
NC10	2008	LALA	0.94	ACRU	0.02	-90.225745	45.958328	152.62	1.99	1.60	0.02	49.97	0.17	49.56	1.13	30.28	0.55	19.24	0.62
NC11	2008	ACSM	0.91	TIAM	0.06	-90.229292	45.978107	73.77	1.48	2.19	0.01	49.20	0.14	29.70	0.78	16.10	0.54	13.40	0.32
NC12	2008	PIBA	0.97	PRUNUS	0.03	-90.250862	45.951767	171.36	1.53	1.62	0.02	50.43	0.10	52.91	0.76	29.90	0.61	22.33	0.38
NC13	2008	PIRE	0.89	ACRU	0.06	-90.234778	45.961482	175.16	1.82	1.46	0.01	51.03	0.09	46.63	0.60	25.96	0.50	18.91	0.35
NC14	2008	ABBA	0.67	POTR	0.10	-90.317748	45.965706	146.66	5.22	1.64	0.05	51.10	0.13	36.10	0.66	21.09	0.57	16.17	0.31
NC15	2010	ACSM	0.72	TIAM	0.22	-90.232638	45.980701	53.01	0.66	1.84	0.02	48.24	0.15	28.21	0.62	14.78	0.58	12.59	0.39
NC16	2010	PIBA	0.84	PIRE	0.08	-90.244013	45.958567	175.18	1.30	1.73	0.01	49.49	0.12	50.37	0.79	29.34	0.60	20.83	0.45
NC17	2010	ACSM	0.62	TIAM	0.25	-90.259094	45.944752	55.69	0.59	2.05	0.02	46.91	0.14	24.20	0.66	11.04	0.54	11.70	0.43
NC18	2010	PIST	0.84	ACSM	0.06	-90.264544	45.959311	160.75	0.99	1.64	0.02	49.87	0.17	40.32	1.01	26.43	0.71	15.21	0.46
NC19	2010	PIRE	0.85	ABBA	0.08	-90.199670	45.936436	173.41	1.64	1.19	0.02	49.33	0.13	48.60	0.75	27.44	0.56	19.64	0.40
NC20	2010	PIST	0.69	BEAL	0.17	-90.259820	45.979639	145.45	0.73	1.87	0.01	49.67	0.08	40.24	0.52	24.11	0.36	16.51	0.27
NC21	2010	POTR	0.70	ABBA	0.24	-90.267624	45.970568	94.31	3.36	2.27	0.03	49.90	0.15	35.03	1.07	25.28	0.88	16.59	0.63
NC22	2010	ACSM	0.61	FRAM	0.20	-90.080497	45.805295	93.91	2.02	2.06	0.05	48.01	0.14	26.75	0.73	14.68	0.56	11.95	0.34
NC23	2010	QURU	0.69	ACSM	0.21	-90.079725	45.802666	84.12	1.35	2.57	0.02	48.97	0.11	34.54	0.55	21.18	0.44	15.49	0.31
Ottawa NF, MI																			
OF01	2009	TSCA	0.64	BEAL	0.17	-89.241465	46.193519	86.05	0.68	1.96	0.01	49.91	0.09	27.70	0.73	14.74	0.55	13.20	0.44
OF02	2009	PIRE	0.99	ACRU	0.01	-89.181233	46.346780	191.27	0.61	1.19	0.01	50.62	0.10	47.96	0.66	24.80	0.55	21.59	0.33
OF03	2009	TSCA	0.69	BEAL	0.16	-89.350798	46.240058	106.61	0.65	1.82	0.02	50.05	0.10	26.05	0.81	14.47	0.59	11.76	0.50
OF04	2009	ACSM	0.99	THOC	0.01	-89.301404	46.267401	50.43	0.56	2.12	0.02	48.98	0.16	29.81	0.89	13.09	0.71	16.61	0.47
OF05	2009	POTR	0.76	ABBA	0.08	-89.238086	46.302286	76.05	1.59	2.71	0.06	50.49	0.26	39.54	1.48	28.78	0.97	20.02	0.82
Pine Barrens, WI																			
PB04	2008	PIST	0.58	PIRE	0.30	-90.955950	46.762841	161.07	1.04	1.32	0.01	50.68	0.07	43.29	0.38	23.34	0.29	18.55	0.23
PB05	2008	PIBA	0.85	QUMA	0.13	-91.661389	46.352443	179.27	0.96	1.55	0.01	50.77	0.07	52.75	0.58	29.42	0.47	22.58	0.34
PB06	2008	PIRE	0.96	QUMA	0.04	-91.654452	46.351951	223.32	0.84	1.18	0.01	51.58	0.09	48.23	0.53	26.08	0.46	19.92	0.31
PB07	2008	PIBA	0.73	AMEL	0.18	-91.467617	46.440214	149.69	1.62	1.75	0.10	50.75	0.36	45.93	0.75	25.74	0.58	19.35	0.41

								M_{area} g/m^2		N%		C%		ADF%		ADL%		Cellulose%	
Plot	Year	SPP1	RBA1	SPP2	RBA1	Latitude	Longitude	mean	S.D.	mean	S.D.	mean	S.D.	mean	S.D.	mean	S.D.	mean	S.D.
PB08	2008	PIBA	0.96	BENI	0.02	-91.490467	46.442723	169.50	0.85	1.27	0.02	50.44	0.11	52.84	0.79	30.46	0.62	21.94	0.43
PB09	2008	PIBA	1.00		0.00	-91.519893	46.432515	175.06	0.75	1.42	0.01	50.57	0.07	52.39	0.60	29.98	0.50	22.30	0.31
PB10	2008	PIBA	1.00		0.00	-91.547574	46.433085	174.58	0.81	1.39	0.01	51.25	0.08	51.26	0.81	29.11	0.66	21.53	0.46
PB13	2008	PIBA	1.00		0.00	-91.989182	46.136704	181.48	0.73	1.58	0.01	51.24	0.08	52.14	0.79	30.55	0.59	20.26	0.43
Porcupine Mountains SF, MI																			
PM01	2009	ACSM	0.79	FRNI	0.05	-89.776171	46.707030	52.92	0.58	2.30	0.01	48.09	0.12	27.53	0.60	13.53	0.50	15.21	0.28
PM02	2009	TSCA	0.51	ACSM	0.29	-89.915098	46.725868	91.51	1.35	2.12	0.01	49.25	0.08	29.84	0.55	15.98	0.44	14.10	0.30
PM03	2009	ACSM	0.78	BEAL	0.09	-89.760363	46.743030	46.50	1.18	2.33	0.02	48.70	0.14	28.00	0.73	14.13	0.61	15.43	0.35
PM04	2009	ACSM	0.69	QURU	0.22	-89.775531	46.743458	48.60	0.43	2.57	0.01	48.93	0.10	28.48	0.57	14.58	0.47	15.09	0.28
PM05	2009	TSCA	0.70	BEAL	0.14	-89.962111	46.697942	113.42	0.58	1.69	0.02	49.70	0.10	30.81	0.87	15.89	0.64	15.05	0.57
Sylvania NF, MI																			
SF01	2009	PIMA	0.95	ALIN	0.05	-91.674762	47.838453	201.11	0.76	1.05	0.01	50.80	0.09	41.94	0.57	22.36	0.49	20.01	0.41
SF02	2009	PIRE	0.89	ABBA	0.06	-91.744474	47.807787	201.63	0.83	1.26	0.01	50.24	0.08	47.04	0.50	25.89	0.43	20.30	0.27
SF03	2009	POTR	0.84	ABBA	0.11	-92.458612	47.774544	79.91	0.64	2.57	0.02	49.83	0.17	34.61	1.26	25.24	0.90	18.07	0.79
SF04	2009	THOC	0.69	ABBA	0.20	-92.469192	47.752932	168.19	0.66	1.41	0.02	50.08	0.11	41.15	0.53	26.03	0.38	16.66	0.29
SF05	2009	PIBA	0.76	ABBA	0.12	-91.637658	47.837013	176.82	0.80	1.56	0.01	50.64	0.06	50.23	0.50	28.02	0.45	22.10	0.28
Savage River SF, MD																			
SR01	2009	TSCA	0.40	ACSM	0.25	-79.083811	39.611706	86.50	4.71	2.08	0.05	49.53	0.15	35.82	1.01	20.56	0.84	15.49	0.39
SR02	2009	ACSM	0.44	TIAM	0.25	-79.085443	39.611926	65.07	4.61	2.69	0.08	48.86	0.31	34.17	0.92	19.91	0.75	14.90	0.47
SR03	2009	NYSY	0.29	QUPR	0.24	-79.209825	39.557244	76.76	4.51	2.47	0.05	49.76	0.19	32.41	0.73	18.32	0.71	14.40	0.40
SR04	2009	ACRU	0.48	ACSM	0.19	-79.200382	39.569988	69.12	7.84	2.24	0.07	50.27	0.34	32.31	1.01	18.14	1.01	14.18	0.68
SR05	2009	ACSM	0.50	HAVI	0.18	-79.200167	39.575785	62.90	4.88	2.36	0.09	49.30	0.24	32.61	1.11	18.71	0.82	14.75	0.56
SR07	2009	LITU	0.28	ACRU	0.21	-79.183152	39.592356	71.45	6.12	2.56	0.06	48.87	0.20	34.46	1.06	20.67	0.96	14.50	0.44
SR09	2009	ACRU	0.24	NYSY	0.24	-79.143510	39.634571	73.04	4.76	2.55	0.06	49.51	0.20	33.08	0.83	18.86	0.74	14.49	0.42
SR10	2009	PIST	0.81	ACRU	0.16	-79.085739	39.575589	134.38	13.12	1.47	0.05	50.88	0.30	44.87	1.39	27.75	1.22	17.08	0.88
SR13	2009	PIST	0.87	FRAM	0.09	-79.067071	39.536977	139.22	14.56	1.47	0.05	50.59	0.33	47.28	1.53	29.58	1.43	17.93	0.98
SR15	2009	ACRU	0.29	ACSM	0.25	-79.142303	39.532904	62.44	4.82	2.31	0.06	49.64	0.23	32.46	0.85	18.68	0.74	14.63	0.46

S4: Means of PLSR regression coefficients (and their uncertainties) for predicting foliar traits using AVIRIS imagery obtained from 500 jackknife models built using 50/50 calibration/validation split samples. Cells without numbers indicate water absorption bands that dropped after the atmospheric correction of AVIRIS imagery.

	M_{area}		N%		C%		ADF%		ADL%		Cellulose%	
Wavelength	Mean	S.D	Mean	S.D	Mean	S.D	Mean	S.D	Mean	S.D	Mean	S.D
Intercept	126.426186	32.269803	1.729643	0.412606	49.003116	0.761999	39.034803	5.588969	23.220173	4.101151	18.207460	2.486722
366	-	-	-	-	-	-	-	-	-	-	-	-
376	-	-	-	-	-	-	-	-	-	-	-	-
385	-	-	-	-	-	-	-	-	-	-	-	-
395	-	-	-	-	-	-	-	-	-	-	-	-
405	-	-	-	-	-	-	-	-	-	-	-	-
414	0.009842	0.033900	-0.000390	0.000342	0.000823	0.000775	-0.000457	0.009195	-0.001454	0.005459	-0.000393	0.003422
424	0.001031	0.020909	-0.000128	0.000227	0.000372	0.000472	0.002551	0.005078	0.000415	0.003585	0.000602	0.002036
434	-0.003641	0.014912	-0.000206	0.000179	0.000366	0.000375	0.002670	0.003795	0.000152	0.002868	0.000894	0.001531
443	0.003171	0.012630	-0.000260	0.000143	0.000355	0.000285	0.005475	0.003024	0.002932	0.002208	0.001091	0.001082
453	0.002966	0.016263	-0.000173	0.000159	0.000110	0.000315	0.005802	0.003897	0.004352	0.002392	0.001558	0.001274
463	-0.005699	0.019482	-0.000149	0.000182	0.000026	0.000305	0.005810	0.004440	0.004284	0.002506	0.002022	0.001328
472	-0.006232	0.015278	-0.000091	0.000147	-0.000079	0.000267	0.004879	0.003607	0.002898	0.002265	0.002124	0.001138
482	0.002245	0.014952	-0.000004	0.000142	0.000061	0.000251	0.006292	0.003683	0.004484	0.002195	0.002361	0.001240
492	-0.000358	0.016197	0.000036	0.000140	0.000094	0.000257	0.005887	0.003377	0.004173	0.002169	0.002241	0.001261
502	0.008244	0.012141	0.000026	0.000120	0.000177	0.000236	0.006337	0.002986	0.004343	0.001958	0.002424	0.001206
511	0.023242	0.014794	-0.000054	0.000122	0.000168	0.000212	0.005052	0.002735	0.003589	0.001863	0.001913	0.001064
521	0.016947	0.015156	-0.000073	0.000121	0.000059	0.000261	0.003336	0.002969	0.002832	0.002191	0.000637	0.001006
531	0.009256	0.014663	-0.000025	0.000131	-0.000196	0.000277	-0.000644	0.003033	0.000319	0.002528	-0.000752	0.001086
541	0.003596	0.018214	0.000008	0.000177	-0.000471	0.000338	-0.003973	0.003939	-0.001860	0.003193	-0.001801	0.001528
550	-0.003039	0.018765	-0.000035	0.000193	-0.000604	0.000357	-0.006255	0.004332	-0.003461	0.003362	-0.002654	0.001595
560	-0.020237	0.019735	0.000034	0.000211	-0.000838	0.000395	-0.008816	0.004648	-0.005107	0.003440	-0.003030	0.001765
570	-0.017118	0.016542	0.000007	0.000169	-0.000782	0.000357	-0.008372	0.003800	-0.004969	0.002851	-0.002957	0.001504

	M_{area}		N%		C%		ADF%		ADL%		Cellulose%	
Wavelength	Mean	S.D	Mean	S.D	Mean	S.D	Mean	S.D	Mean	S.D	Mean	S.D
580	-0.019610	0.015211	0.000121	0.000151	-0.000669	0.000314	-0.008420	0.003221	-0.004312	0.002323	-0.002852	0.001322
589	-0.016792	0.014228	0.000125	0.000147	-0.000586	0.000312	-0.007569	0.003008	-0.003706	0.002185	-0.002430	0.001238
599	-0.016469	0.013653	0.000149	0.000146	-0.000560	0.000311	-0.007405	0.002905	-0.003288	0.002146	-0.002392	0.001195
609	-0.013923	0.012425	0.000247	0.000128	-0.000454	0.000295	-0.007112	0.002542	-0.003128	0.001964	-0.002167	0.001100
619	-0.010277	0.013444	0.000262	0.000130	-0.000363	0.000287	-0.005947	0.002494	-0.002268	0.001883	-0.001617	0.001112
628	-0.011646	0.012189	0.000308	0.000122	-0.000311	0.000279	-0.005040	0.002516	-0.001958	0.001818	-0.001276	0.001066
638	-0.009284	0.012806	0.000367	0.000121	-0.000312	0.000288	-0.005292	0.002480	-0.002332	0.001782	-0.001277	0.001076
648	-0.009182	0.014101	0.000482	0.000131	-0.000288	0.000300	-0.004176	0.002609	-0.001627	0.001807	-0.000650	0.001124
655	-0.007735	0.016358	0.000530	0.000162	-0.000001	0.000351	-0.003105	0.003728	-0.001084	0.002534	-0.000344	0.001386
658	-0.003623	0.016805	0.000579	0.000148	0.000011	0.000333	-0.001469	0.003361	0.000299	0.002176	0.000160	0.001305
665	-0.013797	0.016276	0.000551	0.000138	-0.000039	0.000322	-0.002579	0.003030	-0.000216	0.002217	-0.000256	0.001272
668	-0.006656	0.016127	0.000587	0.000147	0.000056	0.000344	-0.000679	0.003348	0.000748	0.002221	0.000435	0.001386
675	0.000484	0.017007	0.000615	0.000167	0.000141	0.000384	0.000728	0.004108	0.001522	0.002688	0.000587	0.001573
685	-0.009857	0.017444	0.000675	0.000171	0.000008	0.000386	-0.001857	0.003747	-0.000674	0.002492	0.000479	0.001536
694	-0.019901	0.018483	0.000272	0.000167	-0.000409	0.000368	-0.005368	0.003649	-0.003948	0.002603	-0.000962	0.001267
704	-0.032551	0.021834	-0.000355	0.000228	-0.001156	0.000590	-0.012651	0.004495	-0.012914	0.003686	-0.004215	0.001825
714	-0.017426	0.021145	-0.000714	0.000235	-0.001101	0.000643	-0.010572	0.004089	-0.013955	0.003807	-0.004574	0.002008
724	0.043392	0.019012	-0.000809	0.000204	0.000481	0.000527	0.005950	0.004376	0.001358	0.003279	0.000880	0.001726
734	0.065809	0.025981	-0.000468	0.000285	0.001772	0.000828	0.017674	0.006035	0.015724	0.004454	0.005089	0.002574
743	0.036525	0.021299	0.000027	0.000256	0.001415	0.000672	0.012193	0.004941	0.013318	0.003891	0.003896	0.002217
753	0.005849	0.018929	0.000048	0.000229	0.000936	0.000488	0.009708	0.004924	0.008672	0.003819	0.003783	0.001792
763	0.009270	0.035643	0.000181	0.000437	0.000717	0.001008	-0.002401	0.009355	-0.004623	0.006924	0.000887	0.003910
773	-0.013998	0.021613	0.000043	0.000180	-0.000141	0.000423	0.000802	0.004344	-0.001949	0.003112	0.000379	0.001415
782	-0.019378	0.015758	0.000098	0.000162	-0.000256	0.000355	-0.003710	0.003909	-0.003433	0.002777	-0.001067	0.001342
792	-0.006982	0.015152	0.000029	0.000166	-0.000257	0.000342	-0.001754	0.003975	-0.001985	0.002720	-0.000695	0.001286
802	-0.010084	0.013984	-0.000001	0.000150	-0.000240	0.000328	-0.001786	0.003412	-0.001942	0.002295	-0.000675	0.001128
812	-0.014275	0.013183	0.000035	0.000149	0.000001	0.000309	-0.001090	0.003299	-0.000666	0.002372	-0.000465	0.001107

	M_{area}		N%		C%		ADF%		ADL%		Cellulose%	
Wavelength	Mean	S.D	Mean	S.D	Mean	S.D	Mean	S.D	Mean	S.D	Mean	S.D
821	0.007653	0.017447	-0.000064	0.000178	-0.000185	0.000361	-0.002278	0.003287	-0.001113	0.002630	-0.000475	0.001197
831	0.003832	0.014760	-0.000012	0.000152	-0.000262	0.000284	-0.002719	0.002902	-0.001574	0.002065	-0.000647	0.001140
841	-0.006172	0.011951	-0.000007	0.000137	-0.000216	0.000294	-0.002678	0.002775	-0.001518	0.002091	0.000180	0.001125
850	-0.009802	0.012162	0.000001	0.000122	-0.000257	0.000305	-0.002527	0.002815	-0.000598	0.002008	0.000007	0.001094
860	-0.008768	0.014983	0.000048	0.000155	-0.000168	0.000283	-0.002805	0.003197	-0.000919	0.002497	-0.000488	0.001109
870	-0.011678	0.015063	0.000042	0.000176	-0.000165	0.000297	-0.001766	0.003611	-0.000341	0.002791	-0.000206	0.001260
880	-0.018516	0.016890	0.000068	0.000183	0.000015	0.000299	-0.002389	0.003943	0.000070	0.002827	0.000074	0.001304
889	-0.014811	0.017439	-0.000014	0.000184	0.000075	0.000274	0.003197	0.003919	0.003595	0.002905	0.001299	0.001436
899	0.005024	0.011458	-0.000153	0.000142	0.000373	0.000260	0.002082	0.003304	0.002873	0.002601	0.000359	0.001119
909	0.002039	0.016544	-0.000215	0.000175	0.000108	0.000315	0.004006	0.003909	0.002955	0.002863	0.000962	0.001357
918	0.017181	0.019325	-0.000282	0.000254	0.000020	0.000348	0.004268	0.004853	0.003540	0.003542	0.001803	0.001761
928	-0.042293	0.027739	0.000109	0.000276	0.000314	0.000496	0.006441	0.005993	0.005120	0.004267	0.002532	0.002330
938	0.073559	0.039516	-0.000265	0.000374	-0.000756	0.000818	-0.000129	0.008179	-0.000520	0.006167	-0.003676	0.003019
947	-0.027420	0.021732	0.000110	0.000183	-0.000248	0.000447	-0.004477	0.004165	-0.005618	0.003536	-0.001420	0.001529
957	-0.010438	0.017445	0.000113	0.000222	-0.000434	0.000428	-0.002490	0.004550	-0.003471	0.003637	-0.000435	0.001794
967	-0.017632	0.017678	0.000217	0.000195	-0.000776	0.000360	-0.006210	0.004529	-0.005501	0.003205	-0.001365	0.001734
976	-0.040389	0.018728	0.000498	0.000204	-0.000714	0.000422	-0.008106	0.004211	-0.004943	0.003330	-0.002333	0.001698
986	-0.028267	0.015032	0.000437	0.000165	-0.000845	0.000392	-0.008660	0.003705	-0.005619	0.002779	-0.002225	0.001496
995	-0.050717	0.014698	0.000585	0.000191	-0.000993	0.000440	-0.012802	0.003943	-0.007804	0.002891	-0.003369	0.001554
1005	-0.027978	0.014104	0.000450	0.000154	-0.000891	0.000375	-0.007856	0.003194	-0.004421	0.002538	-0.001997	0.001309
1015	-0.021815	0.013148	0.000375	0.000143	-0.000801	0.000329	-0.007470	0.002796	-0.004850	0.002256	-0.002015	0.001159
1024	-0.007015	0.009345	0.000146	0.000109	-0.000638	0.000275	-0.003607	0.002374	-0.003486	0.001979	-0.001016	0.000932
1034	0.008064	0.008837	0.000002	0.000106	-0.000262	0.000227	0.001586	0.002381	0.000926	0.001722	0.000002	0.000940
1044	0.017981	0.008574	0.000023	0.000106	-0.000198	0.000250	0.000563	0.002096	0.000513	0.001546	-0.000164	0.000885
1053	0.032806	0.010614	-0.000121	0.000122	0.000221	0.000376	0.002795	0.002650	0.001481	0.001708	-0.000268	0.001197
1063	0.037863	0.012331	-0.000330	0.000138	0.000592	0.000445	0.008305	0.002984	0.004226	0.001929	0.001710	0.001318
1072	0.042104	0.011537	-0.000337	0.000145	0.000820	0.000466	0.009112	0.002968	0.006078	0.002177	0.001816	0.001336

	M_{area}		N%		C%		ADF%		ADL%		Cellulose%	
Wavelength	Mean	S.D	Mean	S.D	Mean	S.D	Mean	S.D	Mean	S.D	Mean	S.D
1082	0.047258	0.010954	-0.000404	0.000151	0.000689	0.000365	0.009044	0.002583	0.005804	0.002072	0.002193	0.001181
1091	0.053241	0.014302	-0.000479	0.000199	0.000624	0.000359	0.010310	0.003461	0.006093	0.002834	0.002765	0.001444
1101	0.034543	0.020003	-0.000394	0.000217	0.000836	0.000442	0.008278	0.004547	0.004587	0.003662	0.002299	0.001680
1111	0.029645	0.025402	-0.000183	0.000259	0.001374	0.000520	0.005185	0.005228	0.003311	0.004165	0.001711	0.001854
1120	-0.010853	0.027507	0.000197	0.000324	-0.000536	0.000608	-0.010538	0.005906	-0.007533	0.004331	-0.004049	0.002405
1130	0.030417	0.028280	-0.000067	0.000251	-0.000626	0.000543	0.000082	0.005000	-0.000844	0.003649	-0.000780	0.002056
1139	0.002299	0.021321	0.000111	0.000218	0.000049	0.000396	-0.003744	0.004348	-0.002102	0.003251	-0.001886	0.001567
1149	-0.028872	0.021295	0.000246	0.000267	-0.000485	0.000378	-0.005385	0.004604	-0.002523	0.003673	-0.001981	0.001397
1158	-0.000876	0.026061	0.000031	0.000269	0.000254	0.000485	0.000867	0.005466	0.001497	0.004356	0.000673	0.001846
1168	-0.046736	0.023541	0.000346	0.000248	-0.000189	0.000506	-0.002988	0.003868	-0.000865	0.003477	-0.000029	0.001651
1177	-0.062528	0.016700	0.000492	0.000227	-0.000608	0.000507	-0.006867	0.003725	-0.003021	0.002793	-0.001637	0.001561
1187	-0.070240	0.017355	0.000444	0.000208	-0.000944	0.000505	-0.010564	0.003659	-0.006342	0.002627	-0.002927	0.001525
1196	-0.086101	0.021535	0.000488	0.000233	-0.001024	0.000573	-0.010256	0.004028	-0.007072	0.002917	-0.002591	0.001674
1206	-0.066429	0.017389	0.000290	0.000198	-0.001110	0.000552	-0.009711	0.003632	-0.008486	0.002727	-0.003424	0.001603
1215	-0.047466	0.015624	0.000116	0.000189	-0.001047	0.000523	-0.007555	0.003481	-0.008535	0.003001	-0.002641	0.001461
1225	-0.044057	0.018352	0.000080	0.000150	-0.000608	0.000401	-0.005307	0.003274	-0.005456	0.002412	-0.001961	0.001304
1235	-0.013937	0.010301	-0.000036	0.000117	-0.000028	0.000288	-0.000054	0.002744	0.000010	0.002158	-0.000349	0.000979
1244	-0.002976	0.014937	-0.000136	0.000144	0.000305	0.000295	0.000269	0.003091	0.000961	0.002427	-0.000127	0.001123
1253	0.011465	0.013078	-0.000189	0.000145	0.000641	0.000314	0.004304	0.003258	0.003412	0.002398	0.001291	0.001239
1253	0.037632	0.021931	-0.000385	0.000222	0.001511	0.000621	0.009556	0.005845	0.006820	0.004402	0.002387	0.002205
1263	0.014071	0.013625	-0.000236	0.000159	0.000579	0.000334	0.005708	0.003281	0.004729	0.002767	0.002061	0.001358
1263	0.035047	0.026369	-0.000307	0.000269	0.001253	0.000568	0.005481	0.006895	0.002299	0.004612	0.002921	0.002291
1273	0.049950	0.037861	-0.000507	0.000264	0.001450	0.000615	0.007375	0.006494	0.003942	0.004816	0.002576	0.002227
1283	0.060033	0.028687	-0.000304	0.000267	0.001211	0.000499	0.007853	0.005503	0.005791	0.004420	0.002188	0.001928
1293	0.041609	0.028370	-0.000229	0.000351	0.001148	0.000636	0.004246	0.006506	0.003612	0.004877	0.001831	0.002403
1303	0.039784	0.027631	-0.000373	0.000390	0.001205	0.000639	0.005240	0.006830	0.002015	0.004970	0.002947	0.002311
1313	-	-	-	-	-	-	-	-	-	-	-	-

	M_{area}		N%		C%		ADF%		ADL%		Cellulose%	
Wavelength	Mean	S.D	Mean	S.D	Mean	S.D	Mean	S.D	Mean	S.D	Mean	S.D
1323	-	-	-	-	-	-	-	-	-	-	-	-
1333	-	-	-	-	-	-	-	-	-	-	-	-
1343	-	-	-	-	-	-	-	-	-	-	-	-
1353	-	-	-	-	-	-	-	-	-	-	-	-
1363	-	-	-	-	-	-	-	-	-	-	-	-
1373	-	-	-	-	-	-	-	-	-	-	-	-
1383	-	-	-	-	-	-	-	-	-	-	-	-
1393	-	-	-	-	-	-	-	-	-	-	-	-
1403	-	-	-	-	-	-	-	-	-	-	-	-
1413	-	-	-	-	-	-	-	-	-	-	-	-
1423	-	-	-	-	-	-	-	-	-	-	-	-
1433	-	-	-	-	-	-	-	-	-	-	-	-
1443	-	-	-	-	-	-	-	-	-	-	-	-
1453	-	-	-	-	-	-	-	-	-	-	-	-
1463	0.005810	0.031975	-0.000133	0.000373	0.000158	0.000793	-0.000024	0.007934	-0.002620	0.005827	-0.000841	0.002966
1473	0.029001	0.037795	-0.000221	0.000382	0.000165	0.000766	-0.003426	0.007679	-0.001354	0.005738	-0.001429	0.003007
1483	0.041916	0.026740	-0.000646	0.000284	0.000665	0.000630	0.006918	0.006199	0.002716	0.004146	0.002012	0.002283
1493	0.047061	0.026633	-0.000770	0.000264	0.001295	0.000479	0.010093	0.005243	0.004975	0.003748	0.003604	0.001807
1503	0.049876	0.018126	-0.000903	0.000205	0.001128	0.000480	0.011828	0.004753	0.006289	0.003580	0.003632	0.001724
1513	0.041430	0.015199	-0.000848	0.000189	0.001212	0.000495	0.009698	0.004121	0.005059	0.003046	0.002762	0.001618
1523	0.031056	0.014439	-0.000708	0.000168	0.001069	0.000513	0.007367	0.003594	0.002659	0.002715	0.002535	0.001523
1533	0.023841	0.013746	-0.000630	0.000160	0.000826	0.000471	0.006695	0.003838	0.003374	0.002703	0.001607	0.001366
1542	0.022918	0.013946	-0.000569	0.000173	0.000683	0.000514	0.003522	0.003845	0.001881	0.002642	0.000825	0.001387
1552	0.015082	0.010725	-0.000461	0.000145	0.000621	0.000390	0.001592	0.003373	0.000601	0.002216	0.000095	0.001288
1562	0.009784	0.011344	-0.000357	0.000138	0.000489	0.000390	-0.000744	0.003005	-0.000495	0.002095	-0.000840	0.001296
1572	0.005540	0.011965	-0.000187	0.000141	0.000404	0.000362	-0.002983	0.002942	-0.001342	0.002049	-0.000984	0.001178
1582	-0.006020	0.010161	-0.000100	0.000122	0.000150	0.000332	-0.003681	0.002850	-0.001976	0.001966	-0.000932	0.001014

	M_{area}		N%		C%		ADF%		ADL%		Cellulose%	
Wavelength	Mean	S.D	Mean	S.D	Mean	S.D	Mean	S.D	Mean	S.D	Mean	S.D
1592	-0.003114	0.010878	-0.000030	0.000111	0.000148	0.000294	-0.004094	0.002632	-0.002097	0.001893	-0.001551	0.001029
1602	0.002527	0.009991	0.000074	0.000117	0.000235	0.000319	-0.002604	0.002677	-0.000162	0.001947	-0.000776	0.001000
1612	0.007982	0.010065	0.000015	0.000137	0.000166	0.000353	-0.000999	0.003078	0.000856	0.002273	-0.000427	0.001046
1622	0.003618	0.010194	0.000151	0.000115	0.000131	0.000307	-0.001151	0.002773	0.001132	0.002065	-0.000559	0.000969
1632	-0.003388	0.011025	0.000261	0.000139	0.000047	0.000273	-0.003498	0.002952	-0.001643	0.002093	-0.001163	0.000895
1642	-0.001476	0.013032	0.000418	0.000163	-0.000443	0.000366	-0.000490	0.003415	0.001705	0.002471	0.000564	0.001297
1652	-0.001956	0.016358	0.000559	0.000193	-0.000686	0.000361	0.000373	0.004483	0.001812	0.002910	0.000968	0.001638
1662	-0.013515	0.015715	0.000663	0.000207	-0.000880	0.000397	-0.001561	0.004311	0.000932	0.002852	-0.000153	0.001558
1672	-0.002150	0.015773	0.000495	0.000165	-0.000484	0.000326	-0.004375	0.003631	-0.000903	0.002608	-0.001775	0.001375
1682	-0.004460	0.011468	0.000388	0.000126	-0.000407	0.000277	-0.003591	0.002947	-0.000377	0.002037	-0.000974	0.001022
1692	-0.008712	0.013501	0.000369	0.000136	-0.000614	0.000299	0.000661	0.002774	0.002316	0.001824	-0.000160	0.001118
1702	-0.019024	0.014660	0.000305	0.000164	-0.000927	0.000337	0.002214	0.003488	0.002949	0.002295	0.000857	0.001458
1712	-0.027303	0.014604	0.000449	0.000175	-0.001065	0.000402	-0.002046	0.003584	-0.000964	0.002634	-0.000265	0.001433
1722	-0.023552	0.017510	0.000193	0.000185	-0.001183	0.000431	0.001277	0.003915	-0.001280	0.002728	-0.000197	0.001532
1732	-0.020496	0.016656	0.000080	0.000214	-0.001260	0.000444	-0.000416	0.003928	-0.005138	0.002878	-0.000806	0.001512
1742	-0.021594	0.019723	0.000233	0.000222	-0.000520	0.000470	0.000402	0.004741	-0.001573	0.003122	-0.000781	0.001621
1752	-0.007890	0.015227	0.000170	0.000185	-0.000457	0.000317	-0.001258	0.003837	-0.001086	0.002641	-0.000042	0.001277
1762	-0.005088	0.016031	0.000239	0.000194	-0.000374	0.000319	-0.000597	0.003636	-0.001922	0.002646	-0.000249	0.001232
1772	0.017272	0.026114	0.000215	0.000252	-0.000072	0.000399	0.000643	0.005132	-0.000269	0.003586	0.000690	0.001591
1782	-	-	-	-	-	-	-	-	-	-	-	-
1792	-	-	-	-	-	-	-	-	-	-	-	-
1802	-	-	-	-	-	-	-	-	-	-	-	-
1811	-	-	-	-	-	-	-	-	-	-	-	-
1821	-	-	-	-	-	-	-	-	-	-	-	-
1831	-	-	-	-	-	-	-	-	-	-	-	-
1841	-	-	-	-	-	-	-	-	-	-	-	-
1851	-	-	-	-	-	-	-	-	-	-	-	-

	M_{area}		N%		C%		ADF%		ADL%		Cellulose%	
Wavelength	Mean	S.D	Mean	S.D	Mean	S.D	Mean	S.D	Mean	S.D	Mean	S.D
1861	-	-	-	-	-	-	-	-	-	-	-	-
1868	-	-	-	-	-	-	-	-	-	-	-	-
1871	-	-	-	-	-	-	-	-	-	-	-	-
1873	-	-	-	-	-	-	-	-	-	-	-	-
1878	-	-	-	-	-	-	-	-	-	-	-	-
1888	-	-	-	-	-	-	-	-	-	-	-	-
1898	-	-	-	-	-	-	-	-	-	-	-	-
1908	-	-	-	-	-	-	-	-	-	-	-	-
1918	-	-	-	-	-	-	-	-	-	-	-	-
1928	-	-	-	-	-	-	-	-	-	-	-	-
1938	-	-	-	-	-	-	-	-	-	-	-	-
1948	-	-	-	-	-	-	-	-	-	-	-	-
1958	-	-	-	-	-	-	-	-	-	-	-	-
1968	-	-	-	-	-	-	-	-	-	-	-	-
1978	-	-	-	-	-	-	-	-	-	-	-	-
1988	-	-	-	-	-	-	-	-	-	-	-	-
1998	-	-	-	-	-	-	-	-	-	-	-	-
2008	-	-	-	-	-	-	-	-	-	-	-	-
2018	-	-	-	-	-	-	-	-	-	-	-	-
2028	0.030522	0.024357	-0.000207	0.000249	0.001412	0.000511	0.007302	0.005509	0.003228	0.003536	0.001956	0.001913
2038	0.023825	0.018524	-0.000224	0.000203	0.001171	0.000381	0.006555	0.004386	0.002428	0.003004	0.002555	0.001523
2048	0.021020	0.018173	-0.000227	0.000205	0.001310	0.000412	0.004096	0.004610	0.000842	0.003432	0.002056	0.001598
2058	-0.004981	0.024276	0.000090	0.000259	0.001154	0.000556	-0.001543	0.005859	-0.003039	0.004257	-0.000335	0.002272
2068	-0.007846	0.019962	0.000062	0.000227	0.001045	0.000451	-0.001055	0.004503	-0.003125	0.003447	-0.000344	0.001793
2078	0.011623	0.012153	-0.000125	0.000145	0.000845	0.000233	0.000588	0.002792	-0.000762	0.002336	0.000253	0.001032
2088	0.009500	0.009460	-0.000187	0.000106	0.000768	0.000255	0.000571	0.002569	-0.000245	0.002009	-0.000300	0.000905
2099	0.000265	0.011830	0.000041	0.000136	0.000514	0.000221	-0.003319	0.003071	-0.003240	0.002414	-0.000843	0.000934

	M_{area}		N%		C%		ADF%		ADL%		Cellulose%	
Wavelength	Mean	S.D	Mean	S.D	Mean	S.D	Mean	S.D	Mean	S.D	Mean	S.D
2109	-0.001568	0.012008	0.000111	0.000157	0.000242	0.000214	-0.003959	0.003317	-0.002723	0.002415	-0.001244	0.001015
2119	-0.001276	0.013965	0.000068	0.000132	0.000121	0.000218	-0.001902	0.002972	-0.000888	0.002221	-0.000556	0.000856
2129	-0.009478	0.013851	0.000267	0.000136	-0.000081	0.000225	-0.003154	0.002726	-0.001345	0.002165	-0.001190	0.000841
2139	0.000715	0.012194	0.000204	0.000132	-0.000286	0.000233	-0.001664	0.002749	-0.000918	0.002143	-0.000256	0.000841
2149	-0.002838	0.009239	0.000225	0.000101	-0.000277	0.000241	-0.001564	0.002474	0.000020	0.001780	-0.000192	0.000736
2159	-0.001612	0.013535	0.000146	0.000114	-0.000274	0.000295	0.000761	0.002444	0.001050	0.001904	-0.000125	0.000904
2169	-0.006181	0.011048	0.000214	0.000120	-0.000389	0.000334	-0.002447	0.002611	-0.000042	0.002107	-0.000863	0.000988
2178	0.006201	0.012318	0.000168	0.000143	-0.000306	0.000297	0.001268	0.002781	0.001999	0.002355	0.000081	0.000938
2188	0.003992	0.012582	0.000191	0.000125	-0.000229	0.000306	0.002166	0.002946	0.003189	0.002411	-0.000257	0.000965
2198	0.009248	0.012470	0.000122	0.000126	-0.000342	0.000306	0.002656	0.002854	0.003109	0.002094	0.000559	0.000991
2208	0.001441	0.017818	0.000162	0.000153	-0.000422	0.000333	0.004269	0.003500	0.004816	0.002858	0.000778	0.001153
2218	-0.000692	0.013236	0.000155	0.000133	-0.000599	0.000373	0.004068	0.003548	0.005239	0.002825	0.001098	0.001336
2228	-0.003005	0.012046	0.000108	0.000130	-0.000471	0.000367	0.001681	0.003036	0.003565	0.002320	0.000859	0.001196
2238	0.002856	0.015296	-0.000016	0.000128	-0.000385	0.000321	0.003862	0.003684	0.004137	0.002652	0.000581	0.001076
2248	-0.015084	0.011967	0.000160	0.000124	-0.000339	0.000377	-0.000764	0.002786	0.002600	0.002119	0.000198	0.000973
2258	-0.007410	0.012800	-0.000059	0.000115	-0.000202	0.000269	0.000365	0.002664	0.000941	0.001857	0.000105	0.000939
2268	-0.016508	0.015062	0.000086	0.000147	-0.000109	0.000332	-0.002728	0.003010	0.000040	0.002090	-0.000975	0.001058
2278	-0.016034	0.014065	-0.000031	0.000154	-0.000088	0.000305	-0.004069	0.003358	-0.001298	0.002218	-0.000938	0.001128
2288	-0.022011	0.013135	-0.000017	0.000123	-0.000264	0.000288	-0.001236	0.003035	-0.001064	0.002027	-0.000323	0.000978
2298	-0.002488	0.014286	-0.000181	0.000144	0.000069	0.000314	0.001023	0.003255	0.000383	0.002252	0.000172	0.001031
2308	-0.017610	0.013893	-0.000149	0.000164	-0.000525	0.000349	-0.000406	0.003389	-0.002662	0.002604	-0.000181	0.001204
2318	0.002259	0.015139	-0.000185	0.000149	-0.000308	0.000318	-0.000103	0.003640	-0.002323	0.002800	0.000204	0.001107
2328	-0.013515	0.015056	-0.000008	0.000140	-0.000149	0.000285	-0.002772	0.003438	-0.002270	0.002620	-0.000270	0.000989
2338	0.006827	0.018302	-0.000201	0.000165	-0.000025	0.000292	0.000356	0.003745	-0.000906	0.002691	0.000982	0.001276
2348	-0.019973	0.025350	-0.000130	0.000189	-0.000322	0.000358	-0.002071	0.003753	-0.002362	0.002849	0.000514	0.001511
2358	-0.009124	0.022048	-0.000281	0.000190	-0.000146	0.000338	0.002697	0.004034	-0.000213	0.003330	0.000785	0.001128
2368	-0.016187	0.020951	-0.000259	0.000195	-0.000130	0.000366	-0.000401	0.004236	-0.002417	0.003540	0.001634	0.001393

	M_{area}		N%		C%		ADF%		ADL%		Cellulose%	
Wavelength	Mean	S.D	Mean	S.D	Mean	S.D	Mean	S.D	Mean	S.D	Mean	S.D
2378	-0.009220	0.042832	-0.000059	0.000238	0.000239	0.000349	0.000379	0.005131	0.000507	0.003861	0.000209	0.001835
2388	0.004007	0.033365	-0.000282	0.000234	-0.000063	0.000391	0.002051	0.005721	0.000124	0.004131	0.001157	0.001578
2398	0.018157	0.023733	-0.000269	0.000195	0.000047	0.000355	0.004217	0.005215	0.001717	0.003874	0.001157	0.001704
2408	0.000648	0.032982	-0.000296	0.000264	0.000415	0.000529	0.007294	0.006012	0.004231	0.004648	0.002610	0.002110
2418	-	-	-	-	-	-	-	-	-	-	-	-
2428	-	-	-	-	-	-	-	-	-	-	-	-
2437	-	-	-	-	-	-	-	-	-	-	-	-
2447	-	-	-	-	-	-	-	-	-	-	-	-
2457	-	-	-	-	-	-	-	-	-	-	-	-
2467	-	-	-	-	-	-	-	-	-	-	-	-
2477	-	-	-	-	-	-	-	-	-	-	-	-
2487	-	-	-	-	-	-	-	-	-	-	-	-
2497	-	-	-	-	-	-	-	-	-	-	-	-

S5 Legend from the National Land Cover Database 2006 (www.mrlc.gov/nlcd06_leg.php).

Chapter 4: Relative influence of foliar biochemical traits, watershed characteristics and land use on stream water quality in the Upper Midwestern United States

Abstract

The relationship between nutrient cycling processes and water quality in mixed-use ecosystems is driven by complex interactions among biotic and abiotic processes. In many cases, these processes cannot be directly observed or modeled at broad spatial scales. Numerous empirical studies have employed land use patterns, variations in watershed physiography or disturbance regimes to characterize nutrient export from mixed-use watersheds, but simultaneously disentangling the effects of such factors has been difficult. Here we use structural equation modeling (SEM) to assess the relative influence of foliar biochemistry (derived from imaging spectroscopy), watershed physiography and human land use patterns on the water quality (concentration of summer baseflow nitrate-N and soluble reactive phosphorus) in watersheds across the Upper Midwestern United States. Specifically, we propose a SEM linking water quality (stream nitrate-nitrogen and dissolved phosphorus) to foliar retention (AVIRIS-derived foliar traits related to recalcitrance), watershed retention (wetland proportion, MODIS Tasseled Cap Wetness), runoff (agricultural and urban land use), and watershed leakiness (AVIRIS foliar nitrogen, nitrogen deposition). The SEMs confirmed that variables associated with foliar retention derived from AVIRIS imaging spectroscopy are related negatively to watershed leakiness (standardized path coefficient = -0.892) and positively to watershed retention (standardized path coefficient = 0.705), with features related to watershed retention and runoff exerting

the strongest controls on water quality (standardized path coefficients of -0.270 and 0.331 respectively). Comparing forested and agricultural watersheds, we found significantly increased importance of foliar retention to watershed leakiness in forests compared to agriculture (standardized coefficients of -1.004 and -0.764 respectively), with measures of watershed retention more important to runoff and water quality in agricultural watersheds. The results illustrate the capacity of imaging spectroscopy to provide measures of foliar traits that influence nutrient cycling in watersheds. Ultimately, the results may help focus development and restoration policies towards building more resilient landscapes that take into consideration associations among functional traits of vegetation, physiography and climate.

Introduction

Stream water quality in mixed-use watersheds is a function of the interacting biotic and abiotic factors that control ecosystem-level nutrient cycling (Griffith et al. 2002, Meador and Goldstein 2003, Buck et al. 2004, Srivastava et al. 2007). The forested and agricultural components of landscapes display inherently different nutrient cycling regimes, especially as consequence of anthropogenically mediated changes in ecosystem processes (e.g., nitrogen deposition, fertilizer use), soil properties (tillage, and type), moisture regimes (irrigation) and broad-scale environmental changes related to climate (Schindler and Bayley 1993, Vitousek et al. 1997a, Mosier 1998, Compton and Boone 2000). Nutrient management in mixed-use landscapes is important to the reduction of high nitrogen (N) and phosphorus (P) concentrations in streams that contribute to eutrophication and acidification of receiving waters and the loss of biological diversity and estuarine productivity, and present a public health concern (Vitousek et al. 1997b). Agricultural fertilization is the primary nonpoint source of nitrate-nitrogen (NO_3-N) to receiving waters, but forest functional properties and disturbances to forests can also affect nutrient export, especially of nitrate-N (Townsend et al. 2004, Eshleman et al. 2009; Chapters 1 and 2). Like nitrate, streamwater phosphorus originates from a variety of sources, but in general is derived from nonpoint sources associated with agricultural and urban land use, and point sources associated with urbanization. Phosphorus is best predicted by urban and industrial activity in most cases and in some cases agriculture (Pieterse et al. 2003, Zampella et al. 2007, Coskun et al. 2008).

The functional properties of vegetation affect nutrient dynamics at the watershed scale, even when decoupled from environmental factors such as N deposition and soil C: N ratios (Huang et al. 2011b). The response of plants to nutrient availability depends on their physiology (Huang et al. 2011a) and climatic constraints on seasonal N availability (Arain et al. 2006). Plant N availability and subsequent variations in local N cycling rates are also functions of competition within local species assemblages and the attendant differences in physiological trait adaptations (Reich et al. 1999, Reich et al. 2003, Rennenberg et al. 2009, Huang et al. 2011a). Therefore, it is notable that even within forested ecosystems, nutrient cycling rates can differ between deciduous and conifer-dominated ecosystems (Aber and Driscoll 1997), and may vary considerably within landscapes dominated by a single functional type (Goodale et al. 2002). This is partly because of differences in foliar nitrogen and lignin/cellulose concentrations that characterize leaf lifespan (Wright et al. 2005, Shipley et al. 2006, Santiago 2007), influence soil C:N ratios (Ollinger et al. 2002) and, in combination with disturbance events (Eshleman 2000, McNeil et al. 2007a), may be strong controllers of nutrient cycling (Aber et al. 1991, Fortunel et al. 2009, de Bello et al. 2010). Further, N output (or "leakage") from forested ecosystems has also been linked to disturbance and land use legacies (Aber et al. 1997, Chen et al. 2004, McNeil et al. 2008). For example, McNeil et al. (2007b) demonstrated that N leakage from watersheds may be mediated by insect-related defoliation and could maintain N limitation in temperate forest ecosystems. Similar results have been obtained in the Hubbard Brook Experimental forest (Li et al. 2004) and the Chesapeake Bay watersheds (Eshleman et al. 1998, Eshleman 2000, Townsend et al. 2004, Eshleman et al. 2009).

In most mixed-landcover watersheds, agriculture forms the strongest source of nutrients to receiving waters (Howarth et al. 1996, Carpenter et al. 1998, Howarth 1998, Hutchins et al. 2010, Roberts and Prince 2010). The major underlying factors are fertilizer application and land management practices (Mattikalli and Richards 1996, Cicek et al. 2010, Hutchins et al. 2010, Roberts and Prince 2010) and resultant direct nutrient runoff during rainfall events (Reay et al. 1992, McCarty et al. 2008, Morari et al. 2012). For pasture-dominated landscapes, N and P export has also been linked to subsidies from animal waste (Worrall and Burt 1999, Pieterse et al. 2003, Buck et al. 2004). Agricultural nutrient management thus forms an important part of water resources protection strategies (Shepard 2005) and it has been shown that even small improvements in agricultural practices can result in significant improvements in water quality indicators (Diebel et al. 2008, Diebel et al. 2009).

Numerous studies have shown landscape-scale variables to be good predictors of aquatic habitat quality (Lyons et al. 1996, Fitzpatrick et al. 2001, Rooney and Bayley 2011, Daniel and Brown 2013) and have provided evidence of the importance of riparian zones for sustaining diverse fish communities in streams (Fennessy and Cronk 1997, Lowrance et al. 1997, Fitzpatrick et al. 2001, Meador and Goldstein 2003). A growing body of literature has empirically linked water quality in receiving waters with landcover associations (Johnson et al. 1997, Basnyat et al. 2000, Griffith et al. 2002, Buck et al. 2004, Stanley and Maxted 2008, Singh et al. 2013), but disentangling the relative influence of vegetation traits (as opposed to cover type), climate, disturbance and watershed physiography remains

to be explored due to the possibly complex and nonlinear interactions between these factors.

Multispectral and hypertemporal satellite sensors have long been employed to generate land use and land cover maps, create spatially explicit estimates of forest disturbance (Kennedy et al. 2010, Townsend et al. 2012), and derive parameters describing vegetation phenology (Reed et al. 1994, Stockli et al. 2008, Schleip et al. 2009) that we hypothesize are related to water quality. Recent research has shown that spectroscopic methods can be used to characterize key plant functional traits such as foliar nitrogen (Townsend et al. 2003, Majeke et al. 2008, Martin et al. 2008), specific leaf area (SLA), foliar lignin and cellulose (Wright et al. 2002, Majeke et al. 2008, Kokaly et al. 2009, Dybzinski et al. 2013) and potentially $\delta^{15}N$ concentrations (Kleinebecker et al. 2009, Elmore and Craine 2011), making it possible for these functional traits to be incorporated into models of water quality. However, the interactions among these potential drivers have not been comprehensively evaluated, especially given the complexity of existing process models and the absence of data needed to characterize these traits across most regions. So, while a large body of research has linked the role of physiological trait associations (Santiago et al. 2004, Shipley et al. 2006, Fortunel et al. 2009, de Bello et al. 2010), climatic factors (Fausey et al. 1995, Krysanova et al. 1998, Hall et al. 1999, Hu and Ou 2013), land use patterns (Basnyat et al. 2000, Griffith 2002, Griffith et al. 2002, Chen et al. 2007) and disturbance (Eshleman 2000, Eshleman et al. 2000, Townsend et al. 2004, Eshleman et al. 2009) to nutrient cycling rates ranging from the stand to the watershed scale, the relative role of canopy foliar biochemical and structural traits remain to be

explored due to lack of concurrent spatially explicit data. A major objective of this research was to test how measurements of foliar traits derived from NASA's Airborne Visible / Infrared Imaging Spectrometer (AVIRIS) relate to export of stream water nutrients.

This study utilizes a structural equation modeling approach to assess the relative influences of foliar biochemistry, watershed physiography and human land use patterns on water quality in watersheds across the Upper Midwestern United States (Fig. 1). We explore the influence of four broad groups of variables on streamwater quality. These are: 1) nutrient retention due to foliar biochemistry, 2) nutrient retention due to watershed physiography, 3) an index of human activity (landscape composition dominated with urban and agricultural land use), and 4) indicators of watershed-scale nutrient 'leakiness'. We predict that: A) higher foliar recalcitrance has a direct positive effect on nutrient retention in watersheds and indirectly with overall water quality (i.e., lesser nutrient export), and is negatively correlated with indicators of watershed leakiness and indicators of human activity; B) indicators of watershed leakiness and high human activity have negative direct influences on water quality (i.e., high nutrient export), as moderated indirectly by retention in watersheds and foliar recalcitrance. The structural model proposed is shown in Fig. 2 with arrows pointing in the direction of hypothesized influence. Variables constituting the latent factors in Fig. 2 are described in detail in the methods section.

Materials and methods

Watershed data

Watersheds for this study were identified within series of 53 swaths that were imaged by AVIRIS between 2008 and 2011 in the upper Midwestern United States (Fig. 1). Watersheds were selected to reflect the diversity in forest functional associations, landscape physiognomy and landcover composition. We selected first- through third-order watersheds from the NHD-plus database (NHDPlus 2010) that fell more than 90% within the AVIRIS swaths. NHD-plus stream layers as intersected with the selected watersheds were overlaid with TIGER (TIGER/Line 2011) road networks to identify a total of 216 potential sampling locations, after screening for safe access and presence of water in the channel. Streams were sampled in 2010 and 2011, always within one year of AVIRIS acquisition, with 28 watersheds sampled in both years (Fig. 1). Watershed sizes ranged from 9.83 ha to 7,684.65 ha with a median of 724.65 ha and mean of 1,122.68 ha (S.D. 1,329.49).

Water quality sampling

A total of 216 water samples from wadeable streams were obtained in the late summer (August-September) of 2010 and 2011, 5-50 m upstream from culverts depending on local accessibility. Streamwater samples were filtered on-site using 0.45 micron glass-fiber filters (Whatman Plc Piscataway, NJ), stored on ice in 60ml Nalgene bottles (Nalge Nunc International Corporation, Rochester NY), and frozen until the chemical analyses were performed. Samples were analyzed for nitrate-N (NO_3-N) and soluble reactive phosphorus (SRP) using protocols described in the Manual of analytical methods (WSLH 1993).

Nitrate-N concentrations averaged 0.042mg/L (0.04 – 4.97mg/L) and SRP concentrations averaged 0.0045mg/L (0.00027 - 0.179mg/L).

Watershed characteristics

Broad indicators of watershed physiography (stream length, stream density) were obtained from NHD-plus stream network data (NHDPlus 2010) clipped to watershed boundaries obtained by terrain analysis of the National Elevation Dataset (NED: Gesch et al. 2002) at field sampled locations. Average soil infiltration capacities for delineated watersheds were derived from the STATSGO database (Schwarz and Alexander 1995) by identifying major hydrologic soil groups, linking the hydrologic soil groups with infiltration capacities (NRCS 2007) and weighting by area within the respective watersheds. Contribution of groundwater to baseflow was obtained from Wolock (2003) and averaged within watersheds.

Climate and vegetation phenology

Daily precipitation and maximum and minimum temperatures were obtained from the DayMet database (Thornton et al. 2012) and averaged annually within each watershed to characterize an average climatologic record for each watershed. Mean parameters of vegetation phenology for each watershed for the year sampled were obtained by fitting a double logistic model (Eqn. 1) to NDVI time series obtained from the MODIS MOD09A1 product (500m, 8-day NDVI composites: USGS 2001). Phenological parameters were obtained for each year and averaged over all pixels contained in each watershed. Mathematically:

$$NDVI_t = a + b \cdot \left\{\left(\frac{1}{1+\exp\left(r_i \cdot (SOS - t)\right)}\right) + \left(\frac{1}{1+\exp\left(r_d \cdot (SOS + LGS - t)\right)}\right) - 1\right\} \quad \text{Eqn. 1}$$

Where: a = minimum NDVI, b = max-min NDVI, r_i = maximum rate of NDVI increase at start of season, SOS = start of season date (first inflection point), r_d = maximum rate of NDVI decline at end of season, EOS = end of season date (second inflection point).

Landcover and foliar traits

Data on proportional landcover for each watershed were obtained from the National Land Cover Database (NLCD 2006 : Fry et al. 2011). Maps of predicted foliar traits characterizing canopy biochemical (%N, %C, Lignin, Cellulose) and structural parameters (leaf mass per area, LMA) were obtained from results of concurrent AVIRIS campaigns (for details see Chapter 3) and averaged for each watershed.

Direct inputs and disturbance

In the absence of a continuous data record from the Landsat mission (45% of all Landsat 5 and Landsat ETM+ imagery was found cloud contaminated in summer months), we employed disturbance indices (following Healey et al. 2005) derived from the MOD09A1 product to characterize disturbance between the year of sampling and the previous year. Similar to other spatial products, averaged values of disturbance indices were assigned to each watershed for each year. Data on atmospheric nitrogen inputs to watersheds were obtained from the North American Nitrogen Deposition program (NADP 2007) for years corresponding to the sampling year and averaged within watershed boundaries.

Statistical methods

PLS path models

Structural equation models (SEMs) are a set of statistical methods that aim to estimate a network of causal relationships (Vinzi et al. 2010a). Structural relationships are constructed as recursive linkages between (unmeasured) latent complex concepts, each measured through observable indicators. Overall, the intent is to study the complexity of a system using a causality concept among latent constructs (latent variables, LVs) while describing each LV by measured observations called manifest variables (MVs). The partial least squares (PLS) approach to SEMs, also known as path modeling (PLS-PM), represents an intersection of path analysis (Tukey 1964, Alwin and Hauser 1985, Vinzi et al. 2010a) and confirmatory factor analysis (Thurstone 1931). Proposed as a component-based alternative to covariance based structural equation modeling (CB-SEM) estimation procedures by Wold (1966), the PLS-PM technique iteratively solves for blocks of the measurement model in the first step (the relation of LVs to MVs), and proceeds with the estimation of the structural model (the interrelationships between LVs) in the second step. These steps are iterated until the aggregated residual error is minimized (Dijkstra 2010). The PLS-PM approach attempts to, at best, explain the residual variance of the latent and manifest variables rather than modeling the sample covariance matrix. As such, the PLS-PM approach relaxes strict distributional and sample size requirements of data when compared to covariance-based SEMs (Lohmoller 1989). In contrast to CB-SEM analyses, the PLS-PM approach allows for formative indicator constructs to be identified, i.e. situations when the manifest variables are supposed to cause changes in latent variables (as

opposed to reflective indicators, in which the relationship is reversed). Confidence intervals for parameter estimates are finally obtained empirically by bootstrapping techniques. Details of PLS-PM are described in Vinzi et al. (2010a).

We defined five latent constructs (Fig. 2) that represent a conceptual description of watershed function. These were: 1) nutrient retention due to foliar recalcitrance (RETENF), characterized by: carbon to nitrogen ratio, lignin to nitrogen ratio, fiber to cellulose ratio and leaf mass per unit area; 2) nutrient retention in wetlands (RETENW), characterized by: MODIS tasseled cap wetness index, percentage wetland landcover, percentage water area, stream length, groundwater contribution to baseflow, and soil infiltration capacity and mean phenological start of season date; 3) watershed nutrient 'leakiness' (LEAKGE) , characterized by: foliar N concentration, stream density, MODIS tasseled cap brightness index, total atmospheric N deposition, MODIS disturbance index, index of aridity (ratio of precipitation to potential evapotranspiration), proportion of area under coniferous forest and the composite terrain index derived from a digital elevation model (Gesch et al. 2002); 4) nutrient runoff from human dominated landcover (RUNOFF), characterized by: proportion of urban built up area, proportion of area under agriculture and pasture, and finally 5) water quality (WTQUAL), characterized by measured streamwater concentration of nitrate-N (NO_3-N) and soluble reactive phosphorus (SRP). Table 1 lists basic statistical information on all variables, and presents the expected associated with each. We specified RETENF, RETENW and LEAKGE as formative constructs (i.e. latent variables defined as being 'caused' by manifest variables), and RUNOFF and WTQUAL as reflective constructs (i.e., latent variables that 'cause'

increases in manifest variables). We bootstrapped the model 500 times to obtain uncertainty estimates on all path coefficients. All analyses were conducted using the plspm package (Sanchez 2013) of the R statistical analysis system (R 2008).

Initial models were evaluated for specification appropriateness by inspecting measures of unidimensionality of the latent blocks. This ensures satisfaction of the implicit assumption that manifest variables are better related to their own latent variable than others, and Kaiser's rule that the first Eigenvalue of the correlation matrix should be higher than 1 while others are smaller. We used the Dillon-Goldstein's Rho (Chin 1998) and principal components analysis of each block to check for unidimensionalty following Vinzi et al. (2010b) and Sanchez (2013). We also report the classical Cronbach's alpha for each model construct. The model was termed suboptimal if it failed unidimensionality tests, namely if 1) the Dillon-Goldstein's Rho was less than 0.7, and 2) if the first and second Eigenvectors were both higher than 1.0 (Kaiser's rule). Model fits were further considered suboptimal if 3) the average communality index of a construct was less than 0.5 and 4) if the goodness-of-fit was less than 0.5. In brief, the communality index measures how much of the variability in a manifest variable is explained by the variability in its latent variable score (Vinzi et al. 2010b). The average communality of all MVs in a latent variable should be at least greater than 0.5. The goodness-of-fit statistic is simply the geometric mean of the average communality index and the average R^2 of each latent variable.

To optimize the SEM, we 1) inspected the model outer correlation matrix to identify the manifest variables having higher correlations with latent constructs other than the ones they were initially assigned to, and 2) evaluated bootstrap confidence intervals of

weights of under-performing manifest variables. We dropped those manifest variables that had low predictive power (non-significant path weights) and loaded highly on latent variables outside of their construct (high cross-loadings that did not make ecological sense, for example, if stream length were to load highly on foliar traits.) We report both the fully-specified model and the final reduced model from this iterative process.

We conducted bootstrap tests with replacement to test whether nutrient cycling mechanisms differed between watersheds that were predominantly forested (>70% forest) and ones that weren't. Path coefficients were calculated in each resampling iteration and the standard error estimates were compared via a parametric *t*-test (Sanchez 2013).

Results

Unidimensionality tests indicated suboptimal fits in the fully-specified model (Table 3A). Inspection of the outer correlation matrix revealed that multiple MVs loaded higher on other variables than the proposed construct indicating some amount of model miss-specification (Supplemental Table 1) and bootstrapped estimates of path weights (Supplemental Table 2) revealed that most, if not all, such MVs did not have significant path weights (i.e. P-value < 0.05). We iteratively dropped each non-significant MV and refit the model until all unidimensionality measures were satisfied (Table 3B). After iteratively dropping non-significant manifest variables, we were left with two manifest variables in each construct (Table 4). The reduced model indicated an adequate fit with the Dillon-Goldstein's Rho > 0.7 for both reflective LVs (RUNOFF, WTQUAL, Table 3B). The reduced model also satisfied Kaiser's rule (i.e. second Eigenvectors of all LVs less

than 1.0; Table 3B) and inspection of the outer correlation matrix confirmed the unidimensionality of the construct with every MV loading highly on its own LV (Table 4). Average communalities for all LVs were also greater than 0.5 (RETENF: 0.939, RETENW: 0.539, RUNOFF: 0.922, LEAKGE: 0.866, WTQUAL: 0.656).The reduced model had a higher goodness-of-fit (0.697) as compared with the fully-specified model (0.536) (Table 3).

The reduced model contained two manifest variables per each latent variable (Table 5). Nutrient retention due to foliar recalcitrance (RETENF) was best explained by foliar C: N ratios followed by foliar Lignin: N ratios. Retention in watersheds (RETENW) was best explained by the tasseled cap wetness index followed by proportional landcover under lakes. Runoff from human-dominated land use (RUNOFF) was equally well explained by proportional area under agriculture and pasture. Watershed 'leakiness' (LEAKGE) was best explained by foliar nitrogen concentration and atmospheric N deposition.

Individual inner model path coefficients estimated from the final model revealed that almost all our hypotheses were supported by the proposed model (Table 6). The model indicated that foliar recalcitrance increased retention of nutrients in watersheds (RETENF → ↑RETENW; $P < 0.0001$) and decreased watershed leakiness (RETENF → ↓LEAKGE; $P < 0.0001$). Nutrient retention in watersheds reduced watershed-scale nutrient export (RETENW → ↓WTQUAL; $P < 0.0001$), runoff from human-dominated landcover (RETENW → ↓RUNOFF; $P < 0.0001$) and watershed leakiness (RETENW → ↓LEAKGE; $P = 0.018$). Runoff from human-dominated landcover increased watershed-scale nutrient export (RUNOFF → ↑WTQUAL; $P < 0.0001$). Direct loadings between

other proposed linkages (Fig 3) had directions in agreement to proposed hypotheses but were not significant (all $P > 0.05$).

When paths were aggregated over all possible linkages (i.e. Total effects, Table 7), the model indicates that nutrient retention due to foliar retention had a significant effect on reducing watershed-scale nutrient export (RETENF → ↓WTQUAL; $P < 0.0001$), and reducing nutrient export from human-dominated landcover (RETENF → ↓RUNOFF; $P < 0.0001$). The model did not exhibit significant linkages between human-dominated land use patterns and watershed nutrient leakiness, or between watershed leakiness and water quality.

Comparing path coefficients between mostly forested (>70%) and other watersheds (Table 9, Fig 4), we found that nutrient retention due to foliar recalcitrance was the predominant factor mitigating nutrient leakage in forested watersheds (RETENF → ↓LEAKGE; $P = 0.002$). However, in mostly agricultural watersheds, wetland retention played in more prominent role in ameliorating water quality directly (RETENW → ↓WTQUAL; $P = 0.034$) as well as through reduction of runoff (RETENW → ↓RUNOFF; $P < 0.0001$) and leakage (RETENW → ↓LEAKGE; $P = 0.022$).

Latent variable scores exhibited strong latitudinal gradients; foliar and watershed retention increased with latitude (RETENF*Latitude $r = 0.83$, RETENW*Latitude $r = 0.74$; both $P < 0.0001$) and runoff and watershed leakage declined (RUNOFF*Latitude $r = -0.71$, LEAKGE*Latitude = -0.91 respectively; both $P < 0.0001$), consequently translating to a large latitudinal gradient in water quality indices (WTQUAL*Latitude $r = -0.71$, $P < 0.0001$) that parallels agricultural land use patterns in the Upper Midwest (%[Agriculture +

Pasture]*Latitude r = -0.72, $P < 0.0001$). Interestingly, this pattern is independent of the gradient in forest cover in surveyed watersheds (%Forest*Latitude r = 0.065, P = 0.387). These results show that foliar retention as derived from AVIRIS has a stronger relationship to ecosystem processes than traditionally used landscape variables such as percent land cover. Maps of latent variable scores derived from applying path weights to manifest variables show large amounts of spatial variation in projected litter recalcitrance between predominantly human dominated agriculture-woodlot landscapes (predicted low foliar recalcitrance Fig. 5A), mixed-hardwood and wetland dominated forests (predicted moderate foliar recalcitrance Fig 5B) and mixed-coniferous wetland dominated landscapes (predicted high foliar recalcitrance Fig. 5C) across the Midwest.

Discussion

The intent of this study was to explore the relative influence of canopy foliar traits, watershed physiography, and human land use patterns on measures of water quality in first- through third-order streams in the Upper Midwest, United states. We employed structural equation modeling to relate water quality measures (nitrate-N and soluble reactive phosphorus in stream water) with four broad latent variables: 1) nutrient retention due to foliar biochemistry, 2) nutrient retention due to watershed physiography, 3) an index of human activity (landscape composition dominated with urban and agricultural land use), and 4) indicators of watershed-scale nutrient ‘leakiness’. We found that: A) Higher foliar recalcitrance, as derived from AVIRIS-estimated C:N and lignin, had a direct positive effect on nutrient retention in watersheds and indirectly with overall water quality (i.e.

lesser nutrient export), and was negatively correlated with indicators of watershed leakiness and indicators of human activity; and B) indicators of watershed leakiness, as derived from NADP deposition and AVIRIS-estimated %N, and high human activity (derived from NLCD land cover) had negative, direct, influences on water quality (i.e. high nutrient export) which could be moderated indirectly by retention in watersheds (Tasseled Cap wetness and water body cover) and foliar recalcitrance.

The comparison of structural models for mostly forested watersheds with agricultural watersheds showed that nutrient retention due to foliar recalcitrance was the major factor determining watershed nutrient leakiness in forested ecosystems (Table 9, Fig. 4). This finding agrees with earlier studies that have associated recalcitrant foliar traits reducing litter decomposability and affecting eventual nitrogen cycling rates in several ecosystems (Aber et al. 1991, Verchot et al. 2001, Ayres et al. 2009, Fortunel et al. 2009, Kazakou et al. 2009), especially ones with high rates of N deposition and disturbance.

Similarly, we found that indicators of wetland landcover mitigated nutrient export to streams. Importantly, the comparison of agricultural and forested watersheds (Table 9, Fig. 4) revealed that watershed retention formed the most important factor mitigating runoff, leakage and eventual water quality in agricultural watersheds. Natural wetlands are known to be important sinks of nutrients (Howardwilliams 1985, Johnston 1991, Jansson et al. 1994, Saunders and Kalff 2001, Zedler 2003), and have led to the proliferation of constructed wetlands for ameliorating water quality issues (Mitsch et al. 1995, Uusi-Kamppa et al. 2000, Mitsch et al. 2005, Vymazal 2007). While the MODIS wetness index was a strong predictor of nutrient retention in watersheds, proportional area under wetlands

(from NLCD 2006: Fry et al. 2011) was not. Indicators of human dominated land use also behaved as expected with higher proportional areas under agriculture and pastures indicating higher nutrient export to watersheds. Intensive agricultural (Allan et al. 1997, Johnes and Heathwaite 1997, Howarth 1998, Boesch et al. 2001, Hutchins et al. 2010) and animal feeding operations (Carpenter et al. 1998, Pieterse et al. 2003, Buck et al. 2004, Elmore and Craine 2011) have long been identified as detrimental to the water quality of receiving waters, and have attracted considerable attention for targeted management and establishment of total maximum daily loads (Reckhow et al. 2005, Migliaccio and Srivastava 2007, Srivastava et al. 2007, USEPA 2010). Indicators of nutrient leakage from watersheds, however, were not significant predictors of water quality (Table 6, 7). The leakage latent variable consisted of measures of foliar N concentration (possibly an indicator of fertilizer application and/or differential nutrient uptake by vegetation) and N deposition (direct inputs), both ostensibly strong predictors of nitrogen export (Aber et al. 1997, Fenn and Poth 1999, Aber et al. 2002, Paerl et al. 2002). These effects may have been better captured by the latent vector for human land use (RUNOFF), which explicitly coded for patterns of agricultural cover types. Post-hoc tests revealed that this might also be an effect of the strong correlation of spatial N deposition patterns in the Upper Midwest with agricultural land use intensity ($r = 0.66$, $P < 0.0001$) and proportional land use under pasture ($r = 0.55$, $P < 0.0001$). As such, the results do not suggest that foliar N and N deposition are unrelated to water quality, only that patterns in these variables are weaker predictors than measures of land use.

Our findings are in general agreement with other studies conducted in the Upper Midwest in general and Wisconsin in particular (Fitzpatrick et al. 2001, Robertson et al. 2006, Diebel et al. 2008, Stanley and Maxted 2008, Edlund et al. 2009, Rogers et al. 2009, Singh et al. 2013), but our work builds on these studies by incorporating measures related to the role of vegetation functional traits in watershed nutrient export. Our effort was made possible by recent developments in imaging spectroscopy technology (Asner et al. 2004b, Ustin et al. 2004, Ollinger and Smith 2005, Kokaly et al. 2009, Asner et al. 2011) that enable landscape-scale estimation of foliar biochemical and morphological traits known to be strong drivers of ecosystem function and nutrient cycling (Reich et al. 1992, Shipley and Lechowicz 2000, Wright et al. 2004, Shipley et al. 2005, Shipley et al. 2006). High foliar lignin to nitrogen ratios (Robinson and Jolidon 2005, Hobbie et al. 2007, Johnson et al. 2007) and leaf dry matter content (Garnier et al. 2004, Kazakou et al. 2006, Quested et al. 2007, Fortunel et al. 2009, Kazakou et al. 2009) slow litter decomposition rates, but linking measures of litter recalcitrance with landscape-scale processes has remained difficult. We demonstrate that information obtained from imaging spectrometry can be used to simultaneously link ecosystem characteristics such as foliar biochemistry with anthropogenic stressors such as land use patterns to assess landscape-scale responses of ecosystem to perturbations. Indeed, information obtained from imaging spectrometers is increasingly being used for assessing ecosystem attributes such as foliar biochemistry (Asner et al. 2007, Huber et al. 2008, Majeke et al. 2008, Kokaly et al. 2009), nutrient cycling (Martin and Aber 1997, Asner et al. 2004a, Martin et al. 2008, Kokaly et al. 2009), invasive species (Glenn et al. 2005, Lawrence et al. 2006, Underwood et al. 2006, Asner et

al. 2008, Andrew and Ustin 2009, He et al. 2011) and mapping canopy fuels (Ha et al. 2006, Jia et al. 2006), and will be increasingly available to scientists and managers with the launch of the HysPIRI mission (Middleton et al. 2013), the National Ecological Observatory Network's Airborne Observation Platform (Kampe et al. 2010) and the European Space Agency's EnMAP platform (Stuffler et al. 2007).

Land use and ecosystems link in a variety of ways that influence water quality, although the connections may be indirect (Maloney and Weller 2011). Whereas it is relatively easy to monitor human-driven ecosystem stressors such as land use patterns as a basis to infer fertilizer application rates, the assessment of the role of landscape-scale, apparently unobservable determinants (e.g. decomposition rates) can be difficult. Our study provides a methodology that explicitly links measures of human land use, watershed physiography, ecosystem-wide nutrient subsidies and foliar biochemistry. This could facilitate a spatially explicit approach to targeting management interventions across large regions. We leverage the power of structural equation models to allow the formation of latent constructs that, although 'unobservable' in the strict sense, are based on measurements of ecosystem and anthropogenic indicators that have found wide empirical support in previous research and are used in guiding watershed management efforts worldwide.

Conclusions

Overall, we found that canopy foliar chemical and structural traits affected nutrient export across a broad region. These findings are made possible by the use of imaging

spectroscopy data. Once such imagery become widely available, they will provide the basis for much more comprehensive assessments of the drivers of water quality at landscape and broader scales. Our results provide a potential framework to guide landscape management decisions such as designing nutrient conserving landscapes (Diebel et al. 2009). For example, 'high leakage' watersheds could be amended with strategically located wetlands or riparian buffers (Mitsch et al. 1995, Diebel et al. 2009, de Souza et al. 2013) when topographic modifications (e.g. grading) are not possible. Management agencies could target watersheds with varying amounts of disturbance regimes, soil properties and/or physiography (Smith et al. 1997, Brakebill and Preston 2003, Brakebill et al. 2010) by focusing on those factors that are controllable by either natural or management interventions in specific landscapes. For example, the comparisons in Figure 4 suggest that foliar traits play a larger role in mediating nutrient runoff and mitigating effects of N deposition in forests than in largely agricultural watersheds. In contrast, watershed retention (i.e. wetlands) may play a larger role in mitigating runoff and ameliorating effects of N deposition in agricultural compared to forested watersheds. Managing and monitoring ecosystems to ensure balanced delivery of multiple ecosystem services is a key challenge for applied ecology (de Bello et al. 2010). Our study is a small step in this direction: by identifying ecological associations in addition to landscape-scale physiographic and climatologic variables, we provide insights into a range of drivers of water quality that may help focus development and restoration policies towards building more resilient landscapes. At the same time, utilizing recent advances in satellite and airborne imaging

technologies may make this process more standardized and available to broader audience of managers and stakeholders.

Literature cited

Aber, J. D., and C. T. Driscoll. 1997. Effects of land use, climate variation, and N deposition on N cycling and C storage in northern hardwood forests. Global Biogeochemical Cycles **11**:639-648.

Aber, J. D., J. M. Melillo, K. J. Nadelhoffer, J. Pastor, and R. D. Boone. 1991. Factors Controlling Nitrogen Cycling and Nitrogen Saturation in Northern Temperate Forest Ecosystems. Ecological Applications **1**:303-315.

Aber, J. D., S. V. Ollinger, and C. T. Driscoll. 1997. Modeling nitrogen saturation in forest ecosystems in response to land use and atmospheric deposition. Ecological Modelling **101**:61-78.

Aber, J. D., S. V. Ollinger, C. T. Driscoll, G. E. Likens, R. T. Holmes, R. J. Freuder, and C. L. Goodale. 2002. Inorganic nitrogen losses from a forested ecosystem in response to physical, chemical, biotic, and climatic perturbations. Ecosystems **5**:648-658.

Allan, J. D., D. L. Erickson, and J. Fay. 1997. The influence of catchment land use on stream integrity across multiple spatial scales. Freshwater Biology **37**:149-161.

Alwin, D. F., and R. M. Hauser. 1985. The decomposition of effects in path-analysis. Current Contents/Life Sciences:20-20.

Andrew, M. E., and S. L. Ustin. 2009. Habitat suitability modelling of an invasive plant with advanced remote sensing data. Diversity and Distributions **15**:627-640.

Arain, M. A., F. M. Yuan, and T. A. Black. 2006. Soil-plant nitrogen cycling modulated carbon exchanges in a western temperate conifer forest in Canada. Agricultural and Forest Meteorology **140**:171-192.

Asner, G. P., M. O. Jones, R. E. Martin, D. E. Knapp, and R. F. Hughes. 2008. Remote sensing of native and invasive species in Hawaiian forests. Remote Sensing of Environment **112**:1912-1926.

Asner, G. P., D. E. Knapp, T. Kennedy-Bowdoin, M. O. Jones, R. E. Martin, J. Boardman, and C. B. Field. 2007. Carnegie Airborne Observatory: in-flight fusion of hyperspectral imaging and waveform light detection and ranging (wLiDAR) for three-dimensional studies of ecosystems. Journal of Applied Remote Sensing **1**.

Asner, G. P., R. E. Martin, D. E. Knapp, R. Tupayachi, C. Anderson, L. Carranza, P. Martinez, M. Houcheime, F. Sinca, and P. Weiss. 2011. Spectroscopy of canopy chemicals in humid tropical forests. Remote Sensing of Environment **115**:3587-3598.

Asner, G. P., D. Nepstad, G. Cardinot, and D. Ray. 2004a. Drought stress and carbon uptake in an Amazon forest measured with spaceborne imaging spectroscopy.

Proceedings of the National Academy of Sciences of the United States of America **101**:6039-6044.

Asner, G. P., A. R. Townsend, M. M. C. Bustamante, G. B. Nardoto, and L. P. Olander. 2004b. Pasture degradation in the central Amazon: linking changes in carbon and nutrient cycling with remote sensing. Global Change Biology **10**:844-862.

Ayres, E., H. Steltzer, S. Berg, M. D. Wallenstein, B. L. Simmons, and D. H. Wall. 2009. Tree species traits influence soil physical, chemical, and biological properties in high elevation forests. PLoS ONE:e5964-e5964.

Basnyat, P., L. D. Teeter, B. G. Lockaby, and K. M. Flynn. 2000. The use of remote sensing and GIS in watershed level analyses of non-point source pollution problems. Forest Ecology and Management **128**:65-73.

Boesch, D. F., R. B. Brinsfield, and R. E. Magnien. 2001. Chesapeake Bay eutrophication: Scientific understanding, ecosystem restoration, and challenges for agriculture. Journal of Environmental Quality **30**:303-320.

Brakebill, J. W., S. W. Ator, and G. E. Schwarz. 2010. Sources of Suspended-Sediment Flux in Streams of the Chesapeake Bay Watershed: A Regional Application of the SPARROW Model1. Journal of the American Water Resources Association **46**:757-776.

Brakebill, J. W., and S. D. Preston. 2003. A hydrologic network supporting spatially referenced regression modeling in the Chesapeake Bay watershed. Environmental Monitoring and Assessment **81**:73-84.

Buck, O., D. K. Niyogi, and C. R. Townsend. 2004. Scale-dependence of land use effects on water quality of streams in agricultural catchments. Environmental Pollution **130**:287-299.

Carpenter, S. R., N. F. Caraco, D. L. Correll, R. W. Howarth, A. N. Sharpley, and V. H. Smith. 1998. Nonpoint pollution of surface waters with phosphorus and nitrogen. Ecological Applications **8**:559-568.

Chen, L. M., C. T. Driscoll, S. Gbondo-Tugbawa, M. J. Mitchell, and P. S. Murdoch. 2004. The application of an integrated biogeochemical model (PnET-BGC) to five forested watersheds in the Adirondack and Catskill regions of New York. Hydrological Processes **18**:2631-2650.

Chen, Z. Q., C. M. Hu, and F. Muller-Karger. 2007. Monitoring turbidity in Tampa Bay using MODIS/Aqua 250-m imagery. Remote Sensing of Environment **109**:207-220.

Chin, W. W. 1998. The partial least squares approach for structural equation modeling. Pages 295-236 *in* G. A. Marcoulides, editor. Modern methods for business research. Lawrence Erlbaum Associates, London.

Cicek, H., M. Sunohara, G. Wilkes, B. McNairn, F. Pick, E. Topp, and D. R. Lapen. 2010. Using vegetation indices from satellite remote sensing to assess corn and soybean response to controlled tile drainage. Agricultural Water Management **98**:261-270.

Compton, J. E., and R. D. Boone. 2000. Long-term impacts of agriculture on soil carbon and nitrogen in New England forests. Ecology **81**:2314-2330.

Coskun, H. G., A. Tanik, U. Alganci, and H. K. Cigizoglu. 2008. Determination of environmental quality of a drinking water reservoir by remote sensing, GIS and regression analysis. Water Air and Soil Pollution **194**:275-285.

Daniel, W. M., and K. M. Brown. 2013. Multifactorial model of habitat, host fish, and landscape effects on Louisiana freshwater mussels. Freshwater Science **32**:193-203.

de Bello, F., S. Lavorel, S. Diaz, R. Harrington, J. H. C. Cornelissen, R. D. Bardgett, M. P. Berg, P. Cipriotti, C. K. Feld, D. Hering, P. M. da Silva, S. G. Potts, L. Sandin, J. P. Sousa, J. Storkey, D. A. Wardle, and P. A. Harrison. 2010. Towards an assessment of multiple ecosystem processes and services via functional traits. Biodiversity and Conservation **19**:2873-2893.

de Souza, A. L. T., D. G. Fonseca, R. A. Liborio, and M. O. Tanaka. 2013. Influence of riparian vegetation and forest structure on the water quality of rural low-order streams in SE Brazil. Forest Ecology and Management **298**:12-18.

Diebel, M., J. Maxted, D. Robertson, S. Han, and M. Vander Zanden. 2009. Landscape Planning for Agricultural Nonpoint Source Pollution Reduction III: Assessing Phosphorus and Sediment Reduction Potential. Environmental Management **43**:69-83.

Diebel, M. W., J. T. Maxted, P. J. Nowak, and M. J. Vander Zanden. 2008. Landscape Planning for Agricultural Nonpoint Source Pollution Reduction I: A Geographical Allocation Framework. Environmental Management **42**:789-802.

Dijkstra, T. K. 2010. Latent variables and indices: Herman Wold's basic design and Partial Least Squares. Pages 23-46 *in* V. E. Vinzi, W. W. Chin, J. Henseler, and H. Wang, editors. Handbook of partial least squares. Springer-Verlag, Berlin, Germany.

Dybzinski, R., C. E. Farrior, S. Ollinger, and S. W. Pacala. 2013. Interspecific vs intraspecific patterns in leaf nitrogen of forest trees across nitrogen availability gradients. New Phytologist **200**:112-121.

Edlund, M. B., L. D. Triplett, M. D. Tomasek, and K. Bartilson. 2009. From paleo to policy: partitioning the historical point and nonpoint phosphorus loads to the St. Croix River, Minnesota-Wisconsin, USA. Journal of Paleolimnology **41**:679-689.

Elmore, A. J., and J. M. Craine. 2011. Spectroscopic Analysis of Canopy Nitrogen and Nitrogen Isotopes in Managed Pastures and Hay Land. Ieee Transactions on Geoscience and Remote Sensing **49**:2491-2498.

Eshleman, K. N. 2000. A linear model of the effects of disturbance on dissolved nitrogen leakage from forested watersheds. Water Resources Research **36**:3325-3335.

Eshleman, K. N., R. H. Gardner, S. W. Seagle, N. M. Castro, D. A. Fiscus, J. R. Webb, J. N. Galloway, F. A. Deviney, and A. T. Herlihy. 2000. Effects of disturbance on nitrogen export from forested lands of the Chesapeake Bay watershed. Environmental Monitoring and Assessment **63**:187-197.

Eshleman, K. N., B. E. McNeil, and P. A. Townsend. 2009. Validation of a remote sensing based index of forest disturbance using streamwater nitrogen data. Ecological Indicators **9**:476-484.

Eshleman, K. N., R. P. Morgan, J. R. Webb, F. A. Deviney, and J. N. Galloway. 1998. Temporal patterns of nitrogen leakage from mid-Appalachian forested watersheds: Role of insect defoliation. Water Resources Research **34**:2005-2016.

Fausey, N. R., L. C. Brown, H. W. Belcher, and R. S. Kanwar. 1995. Drainage and water-quality in Great-Lakes and corn-belt states. Journal of Irrigation and Drainage Engineering-Asce **121**:283-288.

Fenn, M. E., and M. A. Poth. 1999. Temporal and spatial trends in streamwater nitrate concentrations in the San Bernardino Mountains, southern California. Journal of Environmental Quality **28**:822-836.

Fennessy, M. S., and J. K. Cronk. 1997. The effectiveness and restoration potential of riparian ecotones for the management of nonpoint source pollution, particularly nitrate. Critical Reviews in Environmental Science and Technology **27**:285-317.

Fitzpatrick, F. A., B. C. Scudder, B. N. Lenz, and D. J. Sullivan. 2001. Effects of multi-scale environmental characteristics on agricultural stream biota in eastern Wisconsin. Journal of the American Water Resources Association **37**:1489-1507.

Fortunel, C., E. Garnier, R. Joffre, E. Kazakou, H. Quested, K. Grigulis, S. Lavorel, P. Ansquer, H. Castro, P. Cruz, J. Dolezal, O. Eriksson, H. Freitas, C. Golodets, C. Jouany, J. Kigel, M. Kleyer, V. Lehsten, J. Leps, T. Meier, R. Pakeman, M. Papadimitriou, V. P. Papanastasis, F. Quetier, M. Robson, M. Sternberg, J. P. Theau, A. Thebault, and M. Zarovali. 2009. Leaf traits capture the effects of land use changes and climate on litter decomposability of grasslands across Europe. Ecology **90**:598-611.

Fry, J., G. Xian, S. Jin, J. Dewitz, C. Homer, L. Yang, C. Barnes, N. Herold, and J. Wickham. 2011. Completion of the 2006 National Land Cover Database for the Conterminous United States. PE&RS **77**:858-864.

Garnier, E., J. Cortez, G. Billes, M. L. Navas, C. Roumet, M. Debussche, G. Laurent, A. Blanchard, D. Aubry, A. Bellmann, C. Neill, and J. P. Toussaint. 2004. Plant functional markers capture ecosystem properties during secondary succession. Ecology **85**:2630-2637.

Gesch, D., M. Oimoen, S. Greenlee, C. Nelson, M. Steuck, and D. Tyler. 2002. The National Elevation Dataset. Photogrammetric Engineering and Remote Sensing **68**:5-+.

Glenn, N. F., J. T. Mundt, K. T. Weber, T. S. Prather, L. W. Lass, and J. Pettingill. 2005. Hyperspectral data processing for repeat detection of small infestations of leafy spurge. Remote Sensing of Environment **95**:399-412.

Goodale, C. L., K. Lajtha, K. J. Nadelhoffer, E. W. Boyer, and N. A. Jaworski. 2002. Forest nitrogen sinks in large eastern US watersheds: estimates from forest inventory and an ecosystem model. Biogeochemistry **57**:239-266.

Griffith, J. A. 2002. Geographic techniques and recent applications of remote sensing to landscape-water quality studies. Water Air and Soil Pollution **138**:181-197.

Griffith, J. A., E. A. Martinko, J. L. Whistler, and K. P. Price. 2002. Interrelationships among landscapes, NDVI, and stream water quality in the US central plains. Ecological Applications **12**:1702-1718.

Ha, G. S. J., I. C. Burke, M. R. Kaufmann, A. F. H. Goetz, B. C. Kindel, and Y. F. Pu. 2006. Estimates of forest canopy fuel attributes using hyperspectral data. Forest Ecology and Management **229**:27-38.

Hall, R. I., P. R. Leavitt, R. Quinlan, A. S. Dixit, and J. P. Smol. 1999. Effects of agriculture, urbanization, and climate on water quality in the northern Great Plains. Limnology and Oceanography **44**:739-756.

He, K. S., D. Rocchini, M. Neteler, and H. Nagendra. 2011. Benefits of hyperspectral remote sensing for tracking plant invasions. Diversity and Distributions **17**:381-392.

Healey, S. P., W. B. Cohen, Z. Q. Yang, and O. N. Krankina. 2005. Comparison of Tasseled Cap-based Landsat data structures for use in forest disturbance detection. Remote Sensing of Environment **97**:301-310.

Hobbie, S. E., M. Ogdahl, J. Chorover, O. A. Chadwick, J. Oleksyn, R. Zytkowiak, and P. B. Reich. 2007. Tree species effects on soil organic matter dynamics: The role of soil cation composition. Ecosystems **10**:999-1018.

Howardwilliams, C. 1985. Cycling and retention of nitrogen and phosphorus in wetlands - a theoretical and applied perspective. Freshwater Biology **15**:391-431.

Howarth, R. W. 1998. An assessment of human influences on fluxes of nitrogen from the terrestrial landscape to the estuaries and continental shelves of the North Atlantic Ocean. Nutrient Cycling in Agroecosystems **52**:213-223.

Howarth, R. W., G. Billen, D. Swaney, A. Townsend, N. Jaworski, K. Lajtha, J. A. Downing, R. Elmgren, N. Caraco, T. Jordan, F. Berendse, J. Freney, V. Kudeyarov, P. Murdoch, and Z. L. Zhu. 1996. Regional nitrogen budgets and riverine N&P fluxes for the drainages to the North Atlantic Ocean: Natural and human influences. Biogeochemistry **35**:75-139.

Hu, X., and Y. Ou. 2013. Translating lake nutrient reference levels into nutrient criteria. Fresenius Environmental Bulletin **22**:400-403.

Huang, S., M. A. Arain, V. K. Arora, F. M. Yuan, J. Brodeur, and M. Peichl. 2011a. Analysis of nitrogen controls on carbon and water exchanges in a conifer forest using the CLASS-CTEM(N+) model. Ecological Modelling **222**:3743-3760.

Huang, S., M. A. Arain, V. K. Arora, F. M. Yuan, J. Brodeur, and M. Peichl. 2011b. Analysis of nitrogen controls on carbon and water exchanges in a conifer forest using the CLASS-CTEMN+ model. Ecological Modelling **222**:3743-3760.

Huber, S., M. Kneubuhler, A. Psomas, K. Itten, and N. E. Zimmermann. 2008. Estimating foliar biochemistry from hyperspectral data in mixed forest canopy. Forest Ecology and Management **256**:491-501.

Hutchins, M. G., A. Deflandre-Vlandas, P. E. Posen, H. N. Davies, and C. Neal. 2010. How do river Nitrate concentrations respond to changes in land-use? A modelling case study of headwaters in the river Derwent catchment, North Yorkshire, UK. Environmental Modeling & Assessment **15**:93-109.

Jansson, M., R. Andersson, H. Berggren, and L. Leonardson. 1994. Wetlands and lakes as nitrogen traps. Ambio **23**:320-325.

Jia, G. J., I. C. Burke, A. F. H. Goetz, M. R. Kaufmann, and B. C. Kindel. 2006. Assessing spatial patterns of forest fuel using AVIRIS data. Remote Sensing of Environment **102**:318-327.

Johnes, P. J., and A. L. Heathwaite. 1997. Modelling the impact of land use change on water quality in agricultural catchments. Hydrological Processes **11**:269-286.

Johnson, J. M. F., N. W. Barbour, and S. L. Weyers. 2007. Chemical composition of crop biomass impacts its decomposition. Soil Science Society of America Journal **71**:155-162.

Johnson, L. B., C. Richards, G. E. Host, and J. W. Arthur. 1997. Landscape influences on water chemistry in Midwestern stream ecosystems. Freshwater Biology **37**:193-+.

Johnston, C. A. 1991. Sediment and nutrient retention by fresh-water wetlands - effects on surface-water quality. Critical Reviews in Environmental Control **21**:491-565.

Kampe, T. U., B. R. Johnson, M. Kuester, and M. Keller. 2010. NEON: the first continental-scale ecological observatory with airborne remote sensing of vegetation canopy biochemistry and structure. Journal of Applied Remote Sensing **4**.

Kazakou, E., D. Vile, B. Shipley, C. Gallet, and E. Garnier. 2006. Co-variations in litter decomposition, leaf traits and plant growth in species from a Mediterranean old-field succession. Functional Ecology **20**:21-30.

Kazakou, E., C. Violle, C. Roumet, C. Pintor, O. Gimenez, and E. Garnier. 2009. Litter quality and decomposability of species from a Mediterranean succession depend on leaf traits but not on nitrogen supply. Annals of Botany **104**:1151-1161.

Kennedy, R. E., Z. G. Yang, and W. B. Cohen. 2010. Detecting trends in forest disturbance and recovery using yearly Landsat time series: 1. LandTrendr - Temporal segmentation algorithms. Remote Sensing of Environment **114**:2897-2910.

Kleinebecker, T., S. R. Schmidt, C. Fritz, A. J. P. Smolders, and N. Holzel. 2009. Prediction of delta 13C and delta 15N in plant tissues with near-infrared reflectance spectroscopy. New Phytologist **184**:732-739.

Kokaly, R. F., G. P. Asner, S. V. Ollinger, M. E. Martin, and C. A. Wessman. 2009. Characterizing canopy biochemistry from imaging spectroscopy and its application to ecosystem studies. Remote Sensing of Environment **113**:S78-S91.

Krysanova, V., D. I. Muller-Wohlfeil, and A. Becker. 1998. Development and test of a spatially distributed hydrological water quality model for mesoscale watersheds. Ecological Modelling **106**:261-289.

Lawrence, R. L., S. D. Wood, and R. L. Sheley. 2006. Mapping invasive plants using hyperspectral imagery and Breiman Cutler classifications (RandomForest). Remote Sensing of Environment **100**:356-362.

Li, X., R. B. Ambrose, and R. Araujo. 2004. Modeling mineral nitrogen export from a forest terrestrial ecosystem to streams. Transactions of the Asae **47**:727-739.

Lobser, S. E., and W. B. Cohen. 2007. MODIS tasselled cap: land cover characteristics expressed through transformed MODIS data. International Journal of Remote Sensing **28**:5079-5101.

Lohmoller, J. B. 1989. Latent Variable Path Modeling with Partial Least Squares. Physica, Heidelberg.

Lowrance, R., L. S. Altier, J. D. Newbold, R. R. Schnabel, P. M. Groffman, J. M. Denver, D. L. Correll, J. W. Gilliam, J. L. Robinson, R. B. Brinsfield, K. W. Staver, W. Lucas, and A. H. Todd. 1997. Water quality functions of Riparian forest buffers in Chesapeake Bay watersheds. Environmental Management **21**:687-712.

Lyons, J., L. Wang, and T. D. Simonson. 1996. Development and validation of an index of biotic integrity for coldwater streams in Wisconsin. North American Journal of Fisheries Management **16**:241-256.

Majeke, B., J. A. N. van Aardt, and M. A. Cho. 2008. Imaging spectroscopy of foliar biochemistry in forestry environments. Southern Forests **70**:275-285.

Maloney, K. O., and D. E. Weller. 2011. Anthropogenic disturbance and streams: land use and land-use change affect stream ecosystems via multiple pathways. Freshwater Biology **56**:611-626.

Martin, M. E., and J. D. Aber. 1997. High spectral resolution remote sensing of forest canopy lignin, nitrogen, and ecosystem processes. Ecological Applications **7**:431-443.

Martin, M. E., L. C. Plourde, S. V. Ollinger, M. L. Smith, and B. E. McNeil. 2008. A generalizable method for remote sensing of canopy nitrogen across a wide range of forest ecosystems. Remote Sensing of Environment **112**:3511-3519.

Mattikalli, N. M., and K. S. Richards. 1996. Estimation of surface water quality changes in response to land use change: Application of the export coefficient model using remote sensing and geographical information system. Journal of Environmental Management **48**:263-282.

McCarty, G. W., L. L. McConnell, C. J. Hapernan, A. Sadeghi, C. Graff, W. D. Hively, M. W. Lang, T. R. Fisher, T. Jordan, C. P. Rice, E. E. Codling, D. Whitall, A. Lynn, J. Keppler, and M. L. Fogel. 2008. Water quality and conservation practice effects in the Choptank River watershed. Journal of Soil and Water Conservation **63**:461-474.

McNeil, B. E., K. M. de Beurs, K. N. Eshleman, J. R. Foster, and P. A. Townsend. 2007a. Maintenance of ecosystem nitrogen limitation by ephemeral forest disturbance: An assessment using MODIS, Hyperion, and Landsat ETM. Geophysical Research Letters **34**:-.

McNeil, B. E., K. M. de Beurs, K. N. Eshleman, J. R. Foster, and P. A. Townsend. 2007b. Maintenance of ecosystem nitrogen limitation by ephemeral forest disturbance: An assessment using MODIS, Hyperion, and Landsat ETM. Geophysical Research Letters **34**.

McNeil, B. E., J. M. Read, T. J. Sullivan, T. C. McDonnell, I. J. Fernandez, and C. T. Driscoll. 2008. The spatial pattern of nitrogen cycling in the Adirondack Park, New York. Ecological Applications **18**:438-452.

Meador, M. R., and R. M. Goldstein. 2003. Assessing water quality at large geographic scales: Relations among land use, water physicochemistry, riparian condition, and fish community structure. Environmental Management **31**:504-517.

Middleton, E. M., S. G. Ungar, D. J. Mandl, L. Ong, S. W. Frye, P. E. Campbell, D. R. Landis, J. P. Young, and N. H. Pollack. 2013. The Earth Observing One (EO-1)

Satellite Mission: Over a Decade in Space. Ieee Journal of Selected Topics in Applied Earth Observations and Remote Sensing **6**:243-256.
Migliaccio, K. W., and P. Srivastava. 2007. Hydrologic components of watershed-scale models. Transactions of the Asabe **50**:1695-1703.
Mitsch, W. J., J. K. Cronk, X. Y. Wu, R. W. Nairn, and D. L. Hey. 1995. Phosphorus retention in constructed fresh-water riparian marshes. Ecological Applications **5**:830-845.
Mitsch, W. J., L. Zhang, C. J. Anderson, A. E. Altor, and M. E. Hernandez. 2005. Creating riverine wetlands: Ecological succession, nutrient retention, and pulsing effects. Ecological Engineering **25**:510-527.
Morari, F., E. Lugato, R. Polese, A. Berti, and L. Giardini. 2012. Nitrate concentrations in groundwater under contrasting agricultural management practices in the low plains of Italy. Agriculture Ecosystems & Environment **147**:47-56.
Mosier, A. R. 1998. Soil processes and global change. Biology and Fertility of Soils **27**:221-229.
Mu, Q., F. A. Heinsch, M. Zhao, and S. W. Running. 2007. Development of a global evapotranspiration algorithm based on MODIS and global meteorology data. Remote Sensing of Environment **111**:519-536.
NADP. 2007. National Atmospheric Deposition Program (NRSP-3). Illinois State Water Survey, 2204 Griffith Dr., Champaign, IL 61820.
NHDPlus. 2010. Horizon Systems, NHDPlus documentation, version1, available online at http://www.horizon-systems.com/nhdplus/documentation.php.
NRCS. 2007. Hydrologic Soil Groups. Page 14 Part 630 hydrology National Engineering Handbook. US Department of Agriculture, Natural Resources Conservation Service.
Ollinger, S. V., and M. L. Smith. 2005. Net primary production and canopy nitrogen in a temperate forest landscape: An analysis using imaging spectroscopy, modeling and field data. Ecosystems **8**:760-778.
Ollinger, S. V., M. L. Smith, M. E. Martin, R. A. Hallett, C. L. Goodale, and J. D. Aber. 2002. Regional variation in foliar chemistry and N cycling among forests of diverse history and composition. Ecology **83**:339-355.
Paerl, H. W., R. L. Dennis, and D. R. Whitall. 2002. Atmospheric deposition of nitrogen: Implications for nutrient over-enrichment of coastal waters. Estuaries **25**:677-693.
Pieterse, N. M., W. Bleuten, and S. E. Jorgensen. 2003. Contribution of point sources and diffuse sources to nitrogen and phosphorus loads in lowland river tributaries. Journal of Hydrology **271**:213-225.
Quested, H., O. Eriksson, C. Fortunel, and E. Garnier. 2007. Plant traits relate to whole-community litter quality and decomposition following land use change. Functional Ecology **21**:1016-1026.
R. 2008. R: A language and environment for statistical computing. R Foundation for Statistical Computing.*in* R. D. C. Team, editor., Vienna, Austria.

Reay, W. G., D. L. Gallagher, and G. M. Simmons. 1992. Groundwater discharge and its impact on surface-water quality in a Chesapeake Bay inlet. Water Resources Bulletin **28**:1121-1134.

Reckhow, K. H., G. B. Arhonditsis, M. A. Kenney, L. Hauser, J. Tribo, C. Wu, K. J. Elcock, L. J. Steinberg, C. A. Stow, and S. J. McBride. 2005. A predictive approach to nutrient criteria. Environmental Science & Technology **39**:2913-2919.

Reed, B. C., J. F. Brown, D. Vanderzee, T. R. Loveland, J. W. Merchant, and D. O. Ohlen. 1994. Measuring phenological variability from satellite imagery. Journal of Vegetation Science **5**:703-714.

Reich, P. B., D. S. Ellsworth, M. B. Walters, J. M. Vose, C. Gresham, J. C. Volin, and W. D. Bowman. 1999. Generality of leaf trait relationships: A test across six biomes. Ecology **80**:1955-1969.

Reich, P. B., M. B. Walters, and D. S. Ellsworth. 1992. Leaf life-span in relation to leaf, plant, and stand characteristics among diverse ecosystems Ecological Monographs **62**:365-392.

Reich, P. B., I. J. Wright, J. Cavender-Bares, J. M. Craine, J. Oleksyn, M. Westoby, and M. B. Walters. 2003. The evolution of plant functional variation: Traits, spectra, and strategies. International Journal of Plant Sciences **164**:S143-S164.

Rennenberg, H., M. Dannenmann, A. Gessler, J. Kreuzwieser, J. Simon, and H. Papen. 2009. Nitrogen balance in forest soils: nutritional limitation of plants under climate change stresses. Plant Biology **11**:4-23.

Roberts, A. D., and S. D. Prince. 2010. Effects of urban and non-urban land cover on nitrogen and phosphorus runoff to Chesapeake Bay. Ecological Indicators **10**:459-474.

Robertson, D. M., D. J. Graczyk, P. J. Garrison, L. Wang, G. Laliberte, and R. Bannerman. 2006. Nutrient concentrations and their relations to biotic integrity of wadeable streams in Wisconsin. Page 156 United Sates Geological Survey Professional Paper 1722. USGS Wisconsin Water Science Center, Middleton, WI.

Robinson, C. T., and C. Jolidon. 2005. Leaf breakdown and the ecosystem functioning of alpine streams. Journal of the North American Benthological Society **24**:495-507.

Rogers, J. S., K. W. Potter, A. R. Hoffman, J. A. Hoopes, C. H. Wu, and D. E. Armstrong. 2009. Hydrologic and Water Quality Functions of a Disturbed Wetland in an Agricultural Setting. Journal of the American Water Resources Association **45**:628-640.

Rooney, R. C., and S. E. Bayley. 2011. Relative influence of local- and landscape-level habitat quality on aquatic plant diversity in shallow open-water wetlands in Alberta's boreal zone: direct and indirect effects. Landscape Ecology **26**:1023-1034.

Sanchez, G. 2013. PLS path modeling with R. Berkeley, CA.

Santiago, L. S. 2007. Extending the leaf economics spectrum to decomposition: Evidence from a tropical forest. Ecology **88**:1126-1131.

Santiago, L. S., K. Kitajima, S. J. Wright, and S. S. Mulkey. 2004. Coordinated changes in photosynthesis, water relations and leaf nutritional traits of canopy trees along a precipitation gradient in lowland tropical forest. Oecologia **139**:495-502.

Saunders, D. L., and J. Kalff. 2001. Nitrogen retention in wetlands, lakes and rivers. Hydrobiologia **443**:205-212.

Schindler, D. W., and S. E. Bayley. 1993. The biosphere as an increasing sink for atmospheric carbon - estimates from increased nitrogen deposition. Global Biogeochemical Cycles **7**:717-733.

Schleip, C., T. H. Sparks, N. Estrella, and A. Menzel. 2009. Spatial variation in onset dates and trends in phenology across Europe. Climate Research **39**:249-260.

Schwarz, G. E., and R. B. Alexander. 1995. Soils data for the Conterminous United States Derived from the NRCS State Soil Geographic (STATSGO) Data Base. U.S. Geological Survey, Reston, VA.

Shepard, R. 2005. Nutrient management planning: Is it the answer to better management? Journal of Soil and Water Conservation **60**:171-176.

Shipley, B., and M. J. Lechowicz. 2000. The functional co-ordination of leaf morphology, nitrogen concentration, and gas exchange in 40 wetland species. Ecoscience **7**:183-194.

Shipley, B., M. J. Lechowicz, I. Wright, and P. B. Reich. 2006. Fundamental trade-offs generating the worldwide leaf economics spectrum. Ecology **87**:535-541.

Shipley, B., D. Vile, E. Garnier, I. J. Wright, and H. Poorter. 2005. Functional linkages between leaf traits and net photosynthetic rate: reconciling empirical and mechanistic models. Functional Ecology **19**:602-615.

Singh, A., A. R. Jakubowski, I. Chidister, and P. A. Townsend. 2013. A MODIS approach to predicting stream water quality in Wisconsin. Remote Sensing of Environment **128**:74-86.

Smith, R. A., G. E. Schwarz, and R. B. Alexander. 1997. Regional interpretation of water-quality monitoring data. Water Resources Research **33**:2781-2798.

Srivastava, P., K. W. Migliaccio, and J. Simunek. 2007. Landscape models for simulating water quality at point, field, and watershed scales. Transactions of the Asabe **50**:1683-1693.

Stanley, E. H., and J. T. Maxted. 2008. Changes in the dissolved nitrogen pool across land cover gradients in Wisconsin streams. Ecological Applications **18**:1579-1590.

Stockli, R., T. Rutishauser, D. Dragoni, J. O'Keefe, P. E. Thornton, M. Jolly, L. Lu, and A. S. Denning. 2008. Remote sensing data assimilation for a prognostic phenology model. Journal of Geophysical Research-Biogeosciences **113**.

Stuffler, T., C. Kaufmann, S. Hofer, K. P. Forster, G. Schreier, A. Mueller, A. Eckardt, H. Bach, B. Penne, U. Benz, and R. Haydn. 2007. The EnMAP hyperspectral imager-An advanced optical payload for future applications in Earth observation programmes. Acta Astronautica **61**:115-120.

Tarboton, D. G. 1997. A new method for the determination of flow directions and upslope areas in grid digital elevation models. Water Resources Research **33**:309-319.

Thornton, P. E., M. M. Thornton, B. W. Mayer, N. Wilhelmi, Y. Wei, and R. B. Cook. 2012. Daymet:Daily surface weather on a 1 km grid for North America,1980-2012. Oak Ridge National Laboratory Distributed Active Archive Center, Oak Ridge, Tennessee, U.S.A. .

Thurstone, L. L. 1931. The theory of multiple factors. Edwards Brothers, Ann Arbor, MI.

TIGER/Line. 2011. TIGER/Line Shapefiles: Technical documentation. US Department of Commerce.

Townsend, P. A., K. N. Eshleman, and C. Welcker. 2004. Remote sensing of gypsy moth defoliation to assess variations in stream nitrogen concentrations. Ecological Applications **14**:504-516.

Townsend, P. A., J. R. Foster, R. A. Chastain, and W. S. Currie. 2003. Application of imaging spectroscopy to mapping canopy nitrogen in the forests of the central Appalachian Mountains using Hyperion and AVIRIS. Ieee Transactions on Geoscience and Remote Sensing **41**:1347-1354.

Townsend, P. A., A. Singh, J. R. Foster, N. J. Rehberg, C. C. Kingdon, K. N. Eshleman, and S. W. Seagle. 2012. A general Landsat model to predict canopy defoliation in broadleaf deciduous forests. Remote Sensing of Environment **119**:255-265.

Tukey, J. W. 1964. Causation, regression and path analysis. Statistics and mathematics in biology. Hafner, Ne York.

Underwood, E. C., M. J. Mulitsch, J. A. Greenberg, M. L. Whiting, S. L. Ustin, and S. C. Kefauver. 2006. Mapping invasive aquatic vegetation in the Sacramento-San Joaquin Delta using hyperspectral imagery. Environmental Monitoring and Assessment **121**:47-64.

USEPA. 2010. Chesapeake Bay total maximum daily load for nitrogen, phosphorus and sediment: Sources of nutrients and sediment to the Chesapeake Bay. United States Environment Protection Agency, Philadelphia, Pennsylvania.

USGS. 2001. The MOD09A1 data product. NASA, Land Processes Distributed Active Archive Center (LP DAAC), Sioux Falls, South Dakota.

Ustin, S. L., D. A. Roberts, J. A. Gamon, G. P. Asner, and R. O. Green. 2004. Using imaging spectroscopy to study ecosystem processes and properties. Bioscience **54**:523-534.

Uusi-Kamppa, J., B. Braskerud, H. Jansson, N. Syversen, and R. Uusitalo. 2000. Buffer zones and constructed wetlands as filters for agricultural phosphorus. Journal of Environmental Quality **29**:151-158.

Verchot, L. V., Z. Holmes, L. Mulon, P. M. Groffman, and G. M. Lovett. 2001. Gross vs net rates of N mineralization and nitrification as indicators of functional differences between forest types. Soil Biology & Biochemistry **33**:1889-1901.

Vinzi, V. E., W. W. Chin, J. Henseler, and H. Wang, editors. 2010a. Handbook of Partial Least Squares: concepts, methods and applications. Springer-Verlag, Berlin, Germany.

Vinzi, V. E., L. Trinchera, and S. Amato. 2010b. PLS Path Modeling: from foundations to recent developments and open issues for model assessment and improvement.

Pages 47-82 *in* V. E. Vinzi, W. W. Chin, J. Henseler, and H. Wang, editors. Handbook of partial least squares. Springer-Verlag, Berlin.

Vitousek, P. M., J. D. Aber, R. W. Howarth, G. E. Likens, P. A. Matson, D. W. Schindler, W. H. Schlesinger, and D. Tilman. 1997a. Human alteration of the global nitrogen cycle: Sources and consequences. Ecological Applications **7**:737-750.

Vitousek, P. M., J. D. Aber, R. W. Howarth, G. E. Likens, P. A. Matson, D. W. Schindler, W. H. Schlesinger, and G. D. Tilman. 1997b. Human alteration of the global nitrogen cycle: Sources and consequences. Ecological Applications **7**:737-750.

Vymazal, J. 2007. Removal of nutrients in various types of constructed wetlands. Science of the Total Environment **380**:48-65.

Wold, H. 1966. Estimation of principal component and related models by iterative least squares. Pages 391-420 *in* P. R. Krishnaiah, editor. Multivariate analysis. Academic Press, New York.

Wolock, D. M. 2003. Base-flow index grid for the conterminous United States. U.S. Geological Survey, Reston, Virginia.

Worrall, F., and T. P. Burt. 1999. The impact of land-use change on water quality at the catchment scale: the use of export coefficient and structural models. Journal of Hydrology **221**:75-90.

Wright, I. J., P. B. Reich, J. H. C. Cornelissen, D. S. Falster, E. Garnier, K. Hikosaka, B. B. Lamont, W. Lee, J. Oleksyn, N. Osada, H. Poorter, R. Villar, D. I. Warton, and M. Westoby. 2005. Assessing the generality of global leaf trait relationships. New Phytologist **166**:485-496.

Wright, I. J., P. B. Reich, M. Westoby, D. D. Ackerly, Z. Baruch, F. Bongers, J. Cavender-Bares, T. Chapin, J. H. C. Cornelissen, M. Diemer, J. Flexas, E. Garnier, P. K. Groom, J. Gulias, K. Hikosaka, B. B. Lamont, T. Lee, W. Lee, C. Lusk, J. J. Midgley, M. L. Navas, U. Niinemets, J. Oleksyn, N. Osada, H. Poorter, P. Poot, L. Prior, V. I. Pyankov, C. Roumet, S. C. Thomas, M. G. Tjoelker, E. J. Veneklaas, and R. Villar. 2004. The worldwide leaf economics spectrum. Nature **428**:821-827.

Wright, I. J., M. Westoby, and P. B. Reich. 2002. Convergence towards higher leaf mass per area in dry and nutrient-poor habitats has different consequences for leaf life span. Journal of Ecology **90**:534-543.

WSLH. 1993. Manual of analytical methods, inorganic chemistry unit. Wisconsin State Laboratory of Hygiene, Environmental Sciences Section:[variously paged].

Zampella, R. A., N. A. Procopio, R. G. Lathrop, and C. L. Dow. 2007. Relationship of land-use/land-cover patterns and surface-water quality in the Mullica River basin. Journal of the American Water Resources Association **43**:594-604.

Zedler, J. B. 2003. Wetlands at your service: reducing impacts of agriculture at the watershed scale. Frontiers in Ecology and the Environment **1**:65-72.

Tables

Table 1: Variables used in the study, sources, and basic hypotheses (± effect) associated with each; we consider an effect negative when it mitigates water quality indicators (i.e. reduces export), vice-versa for positive.

Latent variable	Manifest variable	Source	Indicator	Assumed effect
Foliar retention (RETENF)	C:N Ratio	AVIRIS	Litter recalcitrance	-
	Lignin:N Ratio	AVIRIS	Litter recalcitrance	-
	Fiber:Cellulose Ratio	AVIRIS	Litter recalcitrance	-
	Leaf mass per area	AVIRIS	Litter recalcitrance	-
Retention in watersheds (RETENW)	Tasseled cap Wetness index	MODIS, Lobser and Cohen (2007)	Indicator of wetlands	-
	% Wetland (landcover)	NLCD 2006, Fry et al. (2011)	Indicator of wetlands	-
	% Water (landcover)	NLCD 2006, Fry et al. (2011)	Longer residence time	-
	Stream length	NHDplus (2010)	Longer in-stream processing	-
	Baseflow index	Wolock (2003)	Groundwater contribution	+/-
	Soil infiltration capacity	STATSGO, Schwarz and Alexander (1995)	Faster infiltration, more leaching	-
	Phenological start of season	MODIS	Longer uptake period	-
Runoff from human dominated landcover (RUNOFF)	% Urban (Landcover)	NLCD 2006, Fry et al. (2011)	Urban flushing	+
	% Agriculture (Landcover)	NLCD 2006, Fry et al. (2011)	Agricultural flushing	+
	% Pasture (Landcover)	NLCD 2006, Fry et al. (2011)	Pasture flushing	+
Watershed leakiness (LEAKGE)	Foliar N %	AVIRIS	Foliar decomposability	+
	Stream density	NHDplus (2010)	Longer in-stream processing	+
	Tasseled cap Brightness index	MODIS, Lobser and Cohen (2007)	Exposed soil	+
	MODIS Disturbance index	MODIS, Healey et al.(2005)	Disturbance flushing	+
	Aridity Index (Precipitation/PET)	DayMet Thornton et al. (2012)MODIS, Mu et al.(2007)	Warmer ecosystem	+
	NADP Nitrogen deposition	NADP (2007)	Direct input	+
	% Coniferous forest (Landcover)	NLCD 2006 (Fry et al. 2011)	Foliar recalcitrance	-
	Composite terrain index	NED Gesch et al.,(2002), Tarboton (1997)	Sediment accumulation	-
Water quality (WTQUAL)	log(NO_3-N)	Field collected		
	log(SRP)	Field collected		

Table 2: Basic statistics of the variables used in the study; units, means, standard deviations and ranges are presented.

Latent variable	Manifest variable	Unit	Mean	S.D	Minimum	Maximum
Foliar retention (RETENF)	C : N Ratio	-	21.886	3.189	16.302	30.280
	Lignin : N Ratio	-	9.447	2.014	6.227	15.399
	Fiber : Cellulose Ratio	-	2.271	0.112	2.024	2.565
	Leaf mass per area	gm/cm^2	101.250	21.302	66.703	150.300
Watershed retention (RETENW)	Tasseled cap Wetness index	%	-0.148	0.020	-0.219	-0.110
	% Wetland (landcover)	%	21.357	21.769	0.054	90.584
	% Water (landcover)	%	2.903	5.978	0.005	49.863
	Stream length	Km	6.445	7.866	0.000	52.743
	Baseflow index	%	59.233	5.124	46.916	69.898
	Soil infiltration capacity	mm/hr	0.236	0.084	0.057	0.420
	Phenological start of season	Day-of-year	128.592	8.795	104.905	144.597
Runoff from human dominated landcover (RUNOFF)	% Urban (Landcover)	%	0.345	0.692	0.000	4.419
	% Agriculture (Landcover)	%	6.340	11.325	0.000	43.464
	% Pasture (Landcover)	%	3.628	7.279	0.000	35.659
Watershed leakiness (LEAKGE)	Foliar N %	%	2.302	0.315	1.668	2.960
	Stream density	Km/Km2	0.827	0.786	0.000	5.551
	Tasseled cap Brightness index	-	0.440	0.050	0.272	0.523
	MODIS Disturbance index	-	0.000	0.000	0.000	0.000
	Aridity Index (Precipitation/PET)	mm/mm	0.658	0.210	0.347	1.096
	NADP Nitrogen deposition	kg/ha	7.040	1.636	3.576	10.427
	% Coniferous forest (Landcover)	%	4.737	7.859	0.000	57.336
	Composite terrain index	-	7.422	0.350	6.304	8.263
Water quality (WTQUAL)	log(NO3-N)	Log(mg/L)	3.736	2.170	-0.106	8.513
	log(SRP)	Log(mg/L)	1.510	1.461	-1.307	5.187

Table 3A: Unidimensionality measures of the fully-specified PLS path model. The model had a goodness-of-fit of 0.536.

Latent variable	Type of measure	MVs	Cronbach's alpha	Dillon-Goldstein's rho	1st Eigenvalue	2nd Eigen value
RETENF#	Formative	4	-	-	3.103	0.718
RETENW	Formative	7	-	-	2.667	1.489
RUNOFF	Reflective	3	0.676	0.828	1.925	0.921
LEAKGE	Formative	8	-	-	2.940	1.540
WTQUAL	Reflective	2	0.507	0.802	1.340	0.660

#RETENF: Retention due to foliar recalcitrance, RETENW: Watershed retention, RUNOFF: Runoff from human-dominated landcover, LEAKGE: Watershed 'leakiness', WTQUAL: Water quality.

Table 3B: Unidimensionality measures of the reduced-variable PLS path model. The model had a goodness-of-fit of 0.697.

Latent variable	Type of measure	MVs	Cronbach's alpha	Dillon-Goldstein's rho	1st Eigenvalue	2nd Eigen value
RETENF#	Formative	2	-	-	1.902	0.098
RETENW	Formative	2	-	-	1.482	0.518
RUNOFF	Reflective	2	0.916	0.960	1.844	0.156
LEAKGE	Formative	2	-	-	1.802	0.198
WTQUAL	Reflective	2	0.507	0.802	1.340	0.660

Table 4: Outer correlation matrix (correlations of manifest variables with latent variables) of the reduced variable model; shaded cells indicate latent variable blocks (in columns) associated with each manifest variable (in rows), numbers in bold typeface represent the maximum row-wise correlation of the manifest variable with latent variables.

Latent variable	Manifest variable	RETENF	RETENW	RUNOFF	LEAKGE	WTQUAL
Foliar retention (RETENF)	C : N Ratio	**0.994**	0.681	-0.604	-0.981	-0.614
	Lignin : N Ratio	**0.943**	0.730	-0.591	-0.878	-0.547
Watershed retention (RETENW)	Tasseled cap Wetness index	0.701	**0.986**	-0.790	-0.720	-0.679
	% Water (landcover)	0.264	**0.327**	-0.233	-0.280	-0.185
Runoff from human dominated landcover (RUNOFF)	% Agriculture (Landcover)	-0.602	-0.799	**0.963**	0.652	0.692
	% Pasture (Landcover)	-0.572	-0.750	**0.958**	0.617	0.643
Watershed leakiness (LEAKGE)	Foliar N %	-0.979	-0.701	0.648	**0.994**	0.660
	NADP Nitrogen deposition	-0.787	-0.706	0.613	**0.863**	0.650
Water quality (WTQUAL)	log(NO3-N)	-0.591	-0.665	0.709	0.665	**0.915**
	log(SRP)	-0.359	-0.432	0.350	0.387	**0.690**

Table 5: Bootstrapped outer path weights (standardized coefficients of manifest variables on latent variables) for final reduced variable model. Path weights are presented as estimates from 500 bootstrap estimates, accompanied by interquartile confidence intervals (LCI, UCI), associated *T* statistics and *P*- values. All effects are significant at $P < 0.05$.

Block	Variable	Estimate	S.E.	LCI	UCI	*T*	*P*
Foliar retention (RETENF)	C : N Ratio	0.768	0.097	0.557	0.938	7.932	<0.0001
	Lignin : N Ratio	0.249	0.101	0.068	0.466	2.460	0.020
Wetland retention (RETENW)	Tasseled cap Wetness index (MODIS)	1.086	0.026	1.042	1.149	41.031	<0.0001
	% Water (Landcover)	-0.204	0.053	-0.325	-0.107	-3.831	<0.0001
Runoff, human dominated landcover (RUNOFF)	% Agriculture (Landcover)	0.537	0.010	0.517	0.558	52.113	<0.0001
	% Pasture (Landcover)	0.504	0.009	0.488	0.526	53.553	<0.0001
Watershed leakiness (LEAKGE)	Foliar N %	0.844	0.061	0.723	0.956	13.923	<0.0001
	Nitrogen deposition	0.186	0.069	0.053	0.317	2.674	0.012
Water quality (WTQUAL)	$\log(NO_3\text{-}N)$	0.766	0.056	0.668	0.887	13.711	<0.0001
	log(SRP)	0.430	0.048	0.326	0.498	8.920	<0.0001

Table 6: Inner path coefficients of the final (reduced variable) model, estimates denote whether an antecedent latent variable ('From' column) positively or negatively affects the descendent variable ('To' column). Path weights are presented as estimates from 500 bootstrap estimates, accompanied by interquartile confidence intervals (LCI, UCI), associated *T* statistics and *P*-values. Effects that are not significant ($P < 0.05$) grayed out for clarity.

From	Block	To	Estimate	Boot. mean	S.E.	LCI	UCI	*T*	*P*
RETENF	→	RETENW	0.705	0.708	0.038	0.630	0.781	18.598	<0.0001
RETENF	→	RUNOFF	-0.084	-0.076	0.062	-0.188	0.055	-1.224	0.223
RETENF	→	LEAKGE	-0.892	-0.887	0.031	-0.940	-0.827	-28.642	<0.0001
RETENF	→	WTQUAL	-0.050	-0.022	0.082	-0.094	0.115	-0.272	0.786
RETENW	→	RUNOFF	-0.748	-0.754	0.053	-0.859	-0.650	-14.231	<0.0001
RETENW	→	LEAKGE	-0.096	-0.100	0.042	-0.181	-0.019	-2.386	0.018
RETENW	→	WTQUAL	-0.270	-0.265	0.072	-0.392	-0.122	-3.700	<0.0001
RUNOFF	→	LEAKGE	0.020	0.019	0.030	-0.037	0.077	0.641	0.523
RUNOFF	→	WTQUAL	0.331	0.341	0.062	0.227	0.459	5.521	<0.0001
LEAKGE	→	WTQUAL	0.186	0.208	0.119	0.079	0.422	1.753	0.081

Table 7: Total effects of the final (reduced variable) model, estimates denote whether an antecedent latent variable ('From' column) positively or negatively affects the descendent variable ('To' column) while accounting for all paths connected through other latent variables (i.e. direct + indirect effects). Path weights are presented as estimates from 500 bootstrap estimates, accompanied by interquartile confidence intervals (LCI, UCI), associated *T* statistics and *P*- values. Effects that are not significant ($P < 0.05$) grayed out for clarity.

Latent variable									
From		To	Estimate	Boot. mean	S.E.	LCI	UCI	*T*	*P*
RETENF	→	RETENW	0.705	0.708	0.038	0.630	0.781	18.598	<0.0001
RETENF	→	RUNOFF	-0.612	-0.611	0.034	-0.678	-0.546	-17.777	<0.0001
RETENF	→	LEAKGE	-0.972	-0.970	0.007	-0.982	-0.954	-135.624	<0.0001
RETENF	→	WTQUAL	-0.623	-0.620	0.046	-0.702	-0.519	-13.435	<0.0001
RETENW	→	RUNOFF	-0.748	-0.754	0.053	-0.859	-0.650	-14.231	<0.0001
RETENW	→	LEAKGE	-0.111	-0.114	0.036	-0.181	-0.050	-3.156	0.002
RETENW	→	WTQUAL	-0.538	-0.547	0.060	-0.653	-0.435	-9.191	<0.0001
RUNOFF	→	LEAKGE	0.020	0.019	0.030	-0.037	0.077	0.641	0.523
RUNOFF	→	WTQUAL	0.335	0.345	0.059	0.237	0.466	5.815	<0.0001
LEAKGE	→	WTQUAL	0.186	0.208	0.119	0.079	0.422	1.753	0.081

Table 8: Inner model fits. Coefficients of determination (R^2) representing how well variation in latent variable is described by all antecedent latent variables. Bootstrap standard error estimates (S.E.), and associated interquartile confidence intervals (LCI, UCI) are also presented. Note that RETENF does not have any antecedent latent variables.

	R^2	Boot. Mean	S.E.	LCI	UCI
RETENF	-	-	-	-	-
RETENW	0.497	0.502	0.054	0.397	0.609
RUNOFF	0.611	0.611	0.040	0.527	0.689
LEAKGE	0.816	0.815	0.019	0.777	0.855
WTQUAL	0.558	0.560	0.049	0.454	0.646

Table 9: Comparison of path coefficients between predominantly forested (>70% forested) and more agricultural watersheds. Estimates of Global path coefficients ('Estimate' column in Table 6) are presented along with differences, the bootstrap T-statistic of the difference (*T*), the degrees of freedom and the associated *P*-value. Comparisons that were not significant grayed out for clarity.

Path			Global	Agriculture	Forested	Difference	*T*	*d.f.*	*P*
RETENF	→	RETENW	0.705	0.744	0.672	0.072	0.860	171	0.196
RETENF	→	RUNOFF	-0.084	-0.105	-0.340	0.235	2.189	171	0.015
RETENF	→	LEAKGE	-0.892	-0.764	-1.004	0.240	2.875	171	0.002
RETENF	→	WTQUAL	-0.050	0.003	-0.187	0.190	1.487	171	0.069
RETENW	→	RUNOFF	-0.748	-0.791	-0.421	0.371	3.558	171	<0.0001
RETENW	→	LEAKGE	-0.096	-0.166	0.007	0.174	2.031	171	0.022
RETENW	→	WTQUAL	-0.270	-0.356	0.025	0.380	1.841	171	0.034
RUNOFF	→	LEAKGE	0.021	0.091	-0.014	0.105	1.059	171	0.146
RUNOFF	→	WTQUAL	0.331	0.321	0.334	0.013	0.132	171	0.447
LEAKGE	→	WTQUAL	0.186	0.179	0.267	0.089	0.843	171	0.200

Figures

Figure 1: Study area. Sampled watersheds are overlaid on AVIRIS flightlines. Letters refer to locations of maps in Figure 5.

Figure 2: Proposed structural model. Arrows denote directions of hypothesized influences.

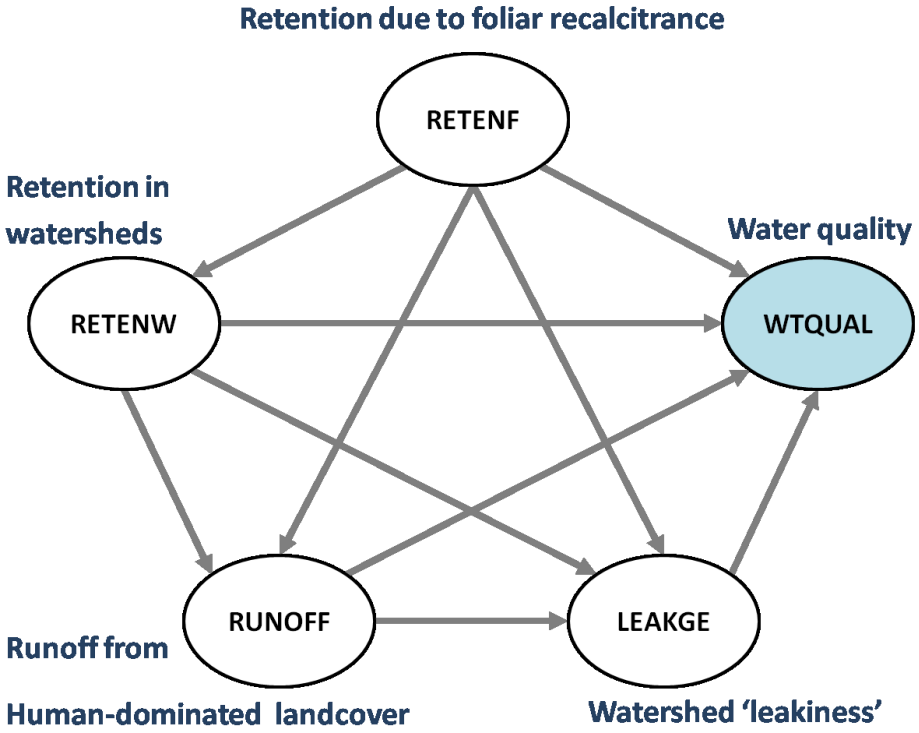

Figure 3: Fitted (reduced-variable) structural model. Path colors denote whether the antecedent latent variable positively (blue) or negatively (red) effects the descendent latent variable, line thickness is proportional to path weight. For example, RETENF increases RETENW, but decreases LEAKGE. Numbers adjacent to links denote standardized coefficient sizes. *$P < 0.05$, **$P < 0.01$, ***$P < 0.001$.

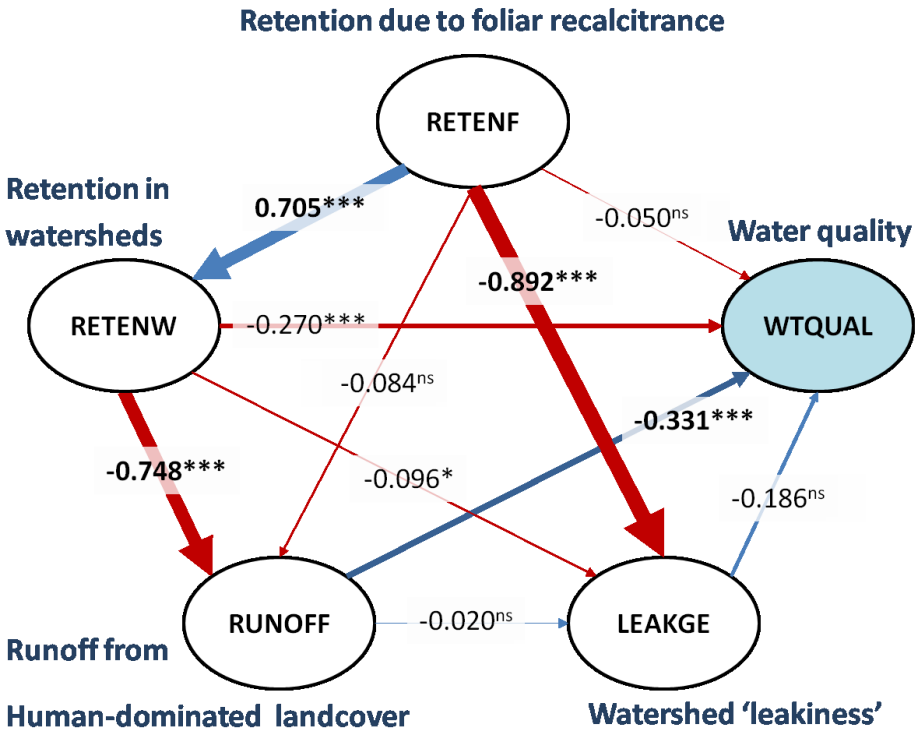

Figure 4: Comparison of inner path coefficients of models built for predominantly forested watersheds (>70% forested, green) vs. more agricultural ones (red). *$P < 0.05$, **$P < 0.01$, ***$P < 0.001$.

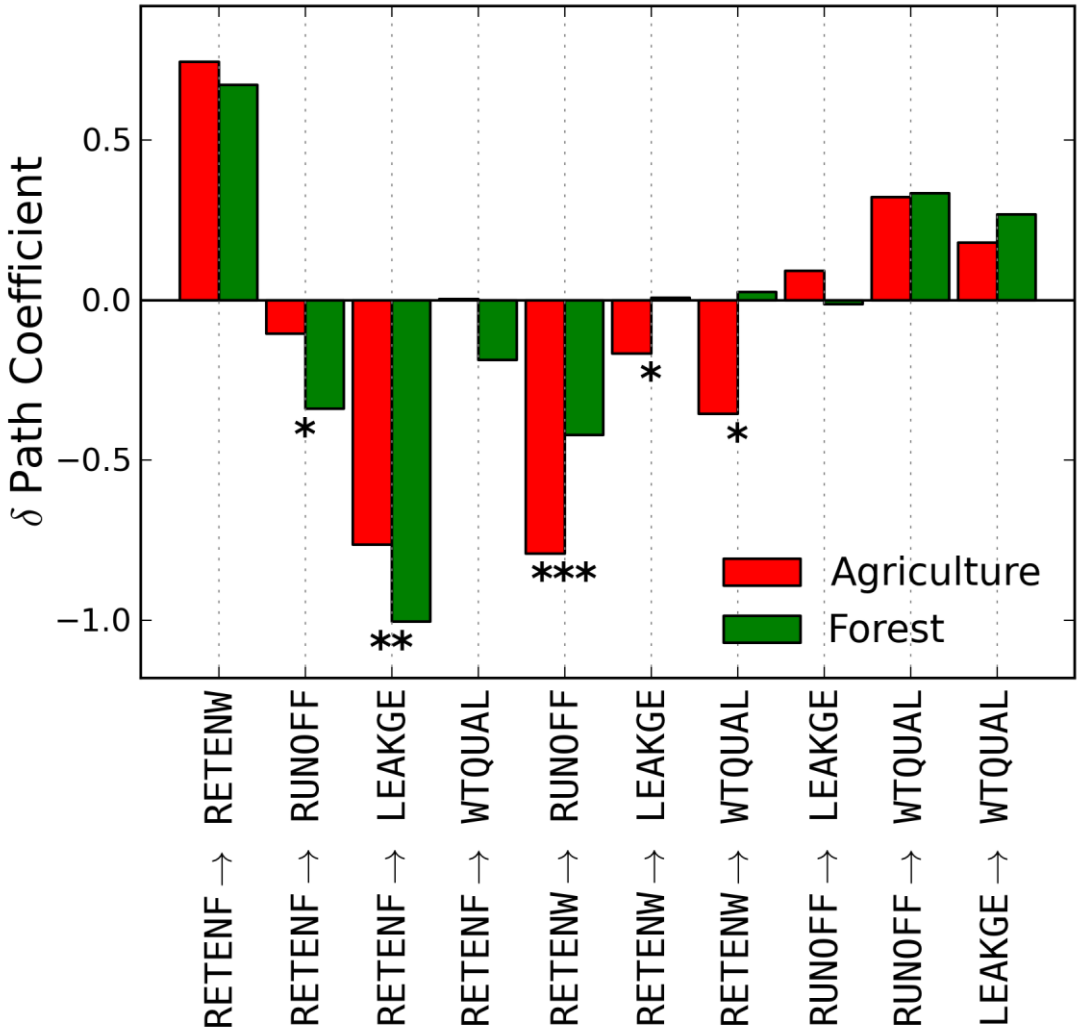

Figure 5: Maps of latent variable RETENF (nutrient retention due to foliar recalcitrance) derived by applying path weights (Estimate column, Table 5) to AVIRIS-derived maps of C:N ratio and lignin:N ratio. Brighter colors indicate projected low litter recalcitrance due to high litter quality. Panels on the right are land cover maps derived from NLCD 2006. Letters refer to location of sites in Figure 1. Black polygons indicate watersheds used in the study.

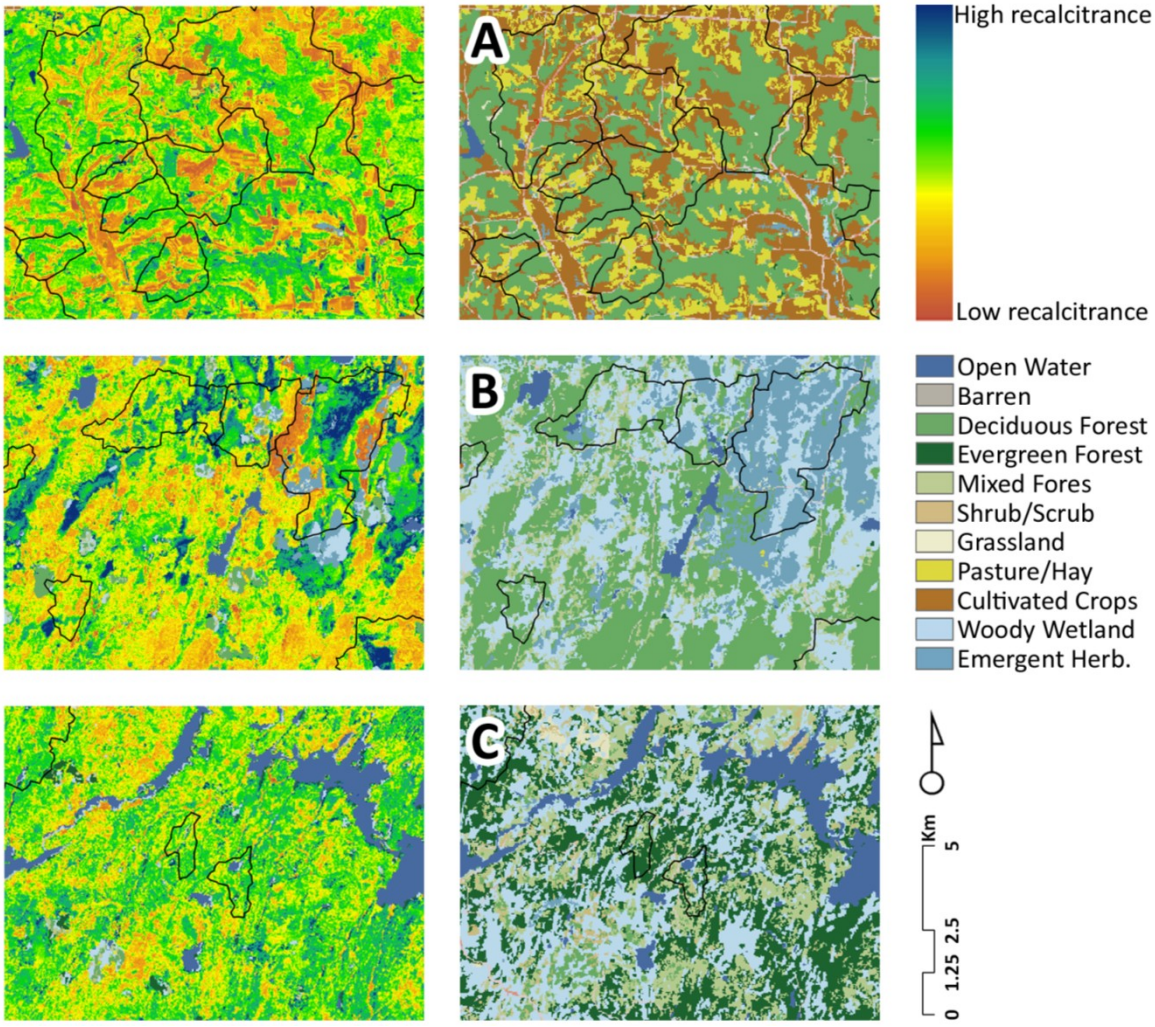

Supplementary material

Supplemental Table 1: Correlations of manifest variables with latent variables; shaded cells indicate latent variable blocks (in columns) associated with each manifest variable (in rows), numbers in bold typeface represent the maximum row-wise correlation of the manifest variable with latent variables.

Latent variable	Manifest variable	RETENF	RETENW	RUNOFF	LEAKGE	WTQUAL
Foliar retention	C : N Ratio	**0.985**	0.764	-0.602	-0.953	-0.614
(RETENF)	Lignin : N Ratio	**0.949**	0.798	-0.590	-0.890	-0.548
	Fiber : Cellulose Ratio	**0.443**	0.368	-0.327	-0.376	-0.271
	Leaf mass per area	**0.801**	0.701	-0.485	-0.759	-0.429
Watershed retention	Tasseled cap Wetness index	0.700	**0.939**	-0.783	-0.780	-0.679
(RETENW)	% Wetland (landcover)	0.465	**0.588**	-0.488	-0.508	-0.374
	% Water (landcover)	0.258	**0.309**	-0.230	-0.288	-0.185
	Stream length	0.018	-0.002	**0.052**	-0.027	0.002
	Baseflow index	**-0.336**	-0.278	0.076	0.274	0.179
	Soil infiltration capacity	0.001	0.094	**-0.213**	-0.055	-0.024
	Phenological start of season	0.520	**0.672**	-0.574	-0.603	-0.396
Runoff from human	% Urban (Landcover)	-0.174	-0.147	**0.305**	0.158	0.150
dominated landcover	% Agriculture (Landcover)	-0.617	-0.789	**0.961**	0.724	0.692
(RUNOFF)	% Pasture (Landcover)	-0.578	-0.732	**0.949**	0.680	0.643
Watershed leakiness	Foliar N %	-0.972	-0.774	0.647	**0.971**	0.660
(LEAKGE)	Stream density	0.020	**-0.111**	0.096	0.009	-0.005
	Tasseled cap Brightness index	-0.727	-0.755	0.555	**0.739**	0.467
	MODIS Disturbance index	-0.004	-0.028	0.019	0.040	**0.068**
	Aridity Index (Precipitation/PET)	0.022	**-0.140**	0.087	**0.035**	0.046
	NADP Nitrogen deposition	-0.785	-0.777	0.613	**0.867**	0.650
	% Coniferous forest (Landcover)	**0.686**	0.553	-0.272	-0.587	-0.304
	Composite terrain index	0.204	0.253	**-0.404**	-0.329	-0.318
Water quality	log(NO3-N)	-0.598	-0.661	0.707	0.697	**0.916**
(WTQUAL)	log(SRP)	-0.372	-0.457	0.346	0.399	**0.689**

Supplemental Table 2: Bootstrapped outer path weights (standardized coefficients of manifest variables on latent variables) for initial model. Path weights are presented as estimates from 500 bootstrap estimates, accompanied by interquartile confidence intervals (LCI, UCI), associated *T* statistics and *P*- values. Effects that are not significant ($P < 0.05$) grayed out for clarity.

Block	Variable	Estimate	S.E.	LCI	UCI	*T*	*P*
Foliar retention (RETENF)	C : N Ratio	0.660	0.141	0.384	0.920	4.690	<0.0001
	Lignin : N Ratio	0.566	0.232	0.143	1.063	2.440	0.021
	Fiber : Cellulose Ratio	0.113	0.095	-0.068	0.293	1.189	0.196
	Leaf mass per area	-0.304	0.176	-0.652	0.035	-1.732	0.089
Watershed retention (RETENW)	Tasseled cap Wetness index (MODIS)	0.835	0.065	0.714	0.951	12.894	<0.0001
	% Wetland (Landcover)	0.207	0.080	0.059	0.362	2.598	0.014
	% Water (Landcover)	-0.121	0.042	-0.200	-0.037	-2.859	0.007
	Stream length	0.054	0.045	-0.046	0.138	1.196	0.195
	Baseflow index	-0.276	0.070	-0.421	-0.155	-3.971	<0.0001
	Soil infiltration capacity	-0.025	0.060	-0.144	0.093	-0.420	0.365
	Phenological start of season	0.081	0.075	-0.062	0.244	1.084	0.221
Runoff from human dominated landcover (RUNOFF)	% Urban (Landcover)	0.113	0.063	-0.014	0.221	1.786	0.081
	% Agriculture (Landcover)	0.521	0.018	0.481	0.551	28.200	<0.0001
	% Pasture (Landcover)	0.484	0.016	0.451	0.513	29.936	<0.0001
Watershed leakiness (LEAKGE)	Foliar N %	0.669	0.098	0.463	0.845	6.817	<0.0001
	Stream density	0.078	0.057	-0.026	0.187	1.375	0.155
	Tasseled cap Brightness index (MODIS)	0.155	0.083	0.010	0.332	1.863	0.071
	Disturbance index (MODIS)	0.020	0.030	-0.037	0.078	0.664	0.319
	Aridity Index (Precipitation/PET)	0.060	0.046	-0.029	0.156	1.292	0.173
	Nitrogen deposition	0.230	0.090	0.054	0.413	2.545	0.016
	% Coniferous forest (Landcover)	0.053	0.041	-0.022	0.132	1.281	0.175
	Composite terrain index	-0.168	0.047	-0.255	-0.078	-3.576	0.001
Water quality (WTQUAL)	log(NO_3-N)	0.765	0.061	0.656	0.896	12.460	<0.0001
	log(SRP)	0.429	0.055	0.299	0.511	7.756	<0.0001

Overall conclusions

My primary focus was to develop models using hypertemporal satellite data and imaging spectroscopy to predict streamwater nutrient concentrations across large regions. The goal was the development of generalizable techniques that would facilitate prediction of stream water nutrient levels based on data obtained on a variety of spatial and temporal resolutions. By identifying ecological associations in addition to landscape-scale physiographic and climatologic variables, this research provides insights into a range of drivers of water quality that may help focus development and restoration policies towards building more resilient landscapes.

In general, a major goal of remote sensing, and imaging spectroscopy in particular, is the development of generalizable algorithms to repeatedly and accurately map ecosystem properties across space and time. In this regard, key objectives of my research were the development and application of generalizable algorithms to repeatedly and accurately map ecosystem properties such as foliar traits across space and time. This study illustrates the utility of imaging spectroscopy for providing rapid and accurate estimates key properties of forest canopies for a range of species and growth environments. A number of important results have come from this research; I summarize the findings from the four chapters below.

1. Remote sensing data from MODIS facilitated prediction of inter-annual stream water nutrient concentrations. Not only can predictions be made on per pixel and watershed scale basis, but I also showed that water quality impacts lag the

landscape dynamics that I hypothesized were drivers. This is consistent with a range of studies showing that water quality impacts of disturbance usually peak a year or more following the disturbance (Likens et al. 1970, Eshleman et al. 1998, Eshleman et al. 2000) These means that remotely sensed measures of landscape dynamics can be used to make predictions of expected impacts on water quality using imagery from one year in advance. Water quality indicators obtained from techniques developed from this research may therefore facilitate timely management responses if necessary.

2. Importantly, the predictive models developed in this research can be applied to any watersheds or watershed delineations for which the MODIS data exist. Annually derived, spatially explicit models developed here offer great promise for both monitoring and targeting the management of stream water quality at the watershed scale.
3. While MODIS-based inter-annual water quality measures were fairly accurate for Wisconsin, MODIS data also facilitated the formulation of models to explain intra-annual variations in water quality for the Chesapeake Bay. Spatial predictions obtained from the functional linear concurrent models (FLCMs) from this study may be instrumental in targeting management efforts and for better representing forests in process-based models such as BASINS-HSPF. In particular, FLCMs can be utilized in many other ecological applications that involve time series in both response and predictor variables. FLCMs also facilitate identification of the relative

importance in both the magnitude and timing of hypothesized drivers of intra-annual variations in drivers of ecosystem processes.

4. Using spectroscopic imagery and partial least squares regression (PLSR) models, I developed a start-to-finish processing stream that allows the mapping of six forest functional traits (leaf mass per area [LMA] as well as percent nitrogen, carbon, fiber, lignin and cellulose) across a range of images. The method is generalizable and yields accurate, repeatable results, with best model performance being for LMA and nitrogen, two of the most important variables for measuring ecosystem function and estimating photosynthetic capacity (Wright et al. 2004).
5. This research represents the first time both leaf and canopy (i.e., image) level spectra have been used to map functional traits at all stages of analysis, from the leaf to plot to image level. Also, I developed and demonstrated an approach to characterizing and mapping uncertainty based on measurement and prediction uncertainty at all stages of the analysis and identified the processing steps required to ensure consistent results.
6. Information obtained from imaging spectrometry can be used to link ecosystem characteristics such as foliar biochemistry with anthropogenic stressors such as land use patterns to assess landscape-scale responses of ecosystem to perturbations. This is made possible by the ability of imaging spectroscopy to provide measures of foliar traits that influence nutrient cycling and water quality in watersheds.
7. Using structural equation models, I found significant differences in the processes that control that control nutrient export from mixed use landscapes. Nutrient

retention due to foliar recalcitrance was the major factor determining nutrient leakiness in forested ecosystems, while retention in watersheds (likely due to wetland distribution) was the major driver in agricultural areas.

Overall, my research provides a suite of methodologies that explicitly link measures of human land use, disturbance, watershed physiography, ecosystem-wide nutrient subsidies and foliar biochemistry to regional-scale measures of ecosystem functioning in general and water quality in particular. Although the applications presented here are specific to the areas of study, the methodologies presented in this research provide a template for landscape scale monitoring that can be implemented using a range of existing and proposed remote sensing instruments. My results may therefore guide future studies and provide information that will enable resource managers to identify the development and restoration policies needed to ensure clean water. The novelty of the work is the utilization of a range of data sources at multiple temporal, spatial and spectral scales needed to fully characterize the influence of vegetation functional traits on water quality.

Literature cited

Eshleman, K. N., R. H. Gardner, S. W. Seagle, N. M. Castro, D. A. Fiscus, J. R. Webb, J. N. Galloway, F. A. Deviney, and A. T. Herlihy. 2000. Effects of disturbance on nitrogen export from forested lands of the Chesapeake Bay watershed. Environmental Monitoring and Assessment **63**:187-197.

Eshleman, K. N., R. P. Morgan, J. R. Webb, F. A. Deviney, and J. N. Galloway. 1998. Temporal patterns of nitrogen leakage from mid-Appalachian forested watersheds: Role of insect defoliation. Water Resources Research **34**:2005-2016.

Likens, G. E., F. H. Bormann, N. M. Johnson, D. W. Fisher, and R. S. Pierce. 1970. Effects of forest cutting and herbicide treatment on nutrient budgets in Hubbard Brook watershed-ecosystem. Ecological Monographs **40**:23-&.

Wright, I. J., P. B. Reich, M. Westoby, D. D. Ackerly, Z. Baruch, F. Bongers, J. Cavender-Bares, T. Chapin, J. H. C. Cornelissen, M. Diemer, J. Flexas, E. Garnier, P. K. Groom, J. Gulias, K. Hikosaka, B. B. Lamont, T. Lee, W. Lee, C. Lusk, J. J. Midgley, M. L. Navas, U. Niinemets, J. Oleksyn, N. Osada, H. Poorter, P. Poot, L. Prior, V. I. Pyankov, C. Roumet, S. C. Thomas, M. G. Tjoelker, E. J. Veneklaas, and R. Villar. 2004. The worldwide leaf economics spectrum. Nature **428**:821-827.